Functional Characterisation of the Cumulus Oocyte Matrix during Maturation of Oocytes

Kylie Renee Dunning

School of Paediatrics and Reproductive Health

Research Centre for Reproductive Health

Discipline of Obstetrics and Gynaecology

University of Adelaide, Adelaide

Australia

Thesis submitted to the University of Adelaide in fulfilment of the requirements for admission to the degree Doctor of Philosophy

October 2008

THE UNIVERSITY OF ADELAIDE
AUSTRALIA

“The majority of people meet with failure because of their lack of persistence in creating new plans to take the place of those which fail. “

Napoleon Hill

“Results! Why, man, I have gotten a lot of results. I know several thousand things that won't work.“

Thomas A. Edison

Opportunity is missed by most people because it is dressed in overalls and looks like work.

Thomas A. Edison

Abstract

Female gametes, or oocytes grow and mature in a niche environment maintained by the somatic cells of the ovarian follicle. At ovulation ovarian follicle cells respond to the luteinising hormone (LH) surge coordinating the final maturation, meiotic resumption and release of oocytes. Simultaneously, production of a unique "mucified" extracellular matrix surrounding the oocyte through synthesis of Hyaluronan (HA) and HA cross-linking proteins produces an "expanded" and stabilised cumulus oocyte matrix with a specific composition, structure and function.

In vitro maturation (IVM) of oocytes is a procedure by which cumulus oocyte complexes (COCs) are stimulated to produce cumulus matrix and undergo oocyte maturation *ex* vivo. *In vitro* maturation is a useful procedure for studying oocyte competence as well as offering health benefits for patients undergoing assisted reproduction. Oocytes derived from IVM have much lower developmental competence than *in vivo* matured oocytes, likely as a result of altered environmental conditions and gene expression leading to suboptimal maturation and/or inappropriate metabolic control in oocytes. Cumulus matrix expansion is widely used as an indicator of good oocyte developmental potential, however, the mechanism(s) that endow oocyte quality and how these may be influenced by the cumulus matrix are poorly understood.

To better understand the process by which cumulus matrix is linked to the final stages of oocyte maturation, I undertook investigation of mouse COC matrix composition and function after *in vivo* maturation in comparison to IVM. The gene responsible for Hyaluronan synthesis, *Has2*, was not impaired under IVM conditions. In contrast, two key extracellular matrix proteins; Versican and Adamts1, which are normally selectively incorporated into periovulatory COCs *in vivo*, were greater than 10-fold reduced in IVM whether stimulated with Egf and/or FSH. This work is the first to show that commonly used IVM conditions result in altered gene expression in cumulus cells. Furthermore, the absence of Adamts1 and Versican suggest that COC matrix may be functionally insufficient.

Although associated with good developmental potential, the function of the COC matrix in oocyte maturation is unknown. I assessed the properties of COC matrix that control metabolite supply to oocytes by examining transport of fluorescently labelled glucose and cholesterol across mouse COCs. Profound differences in the control of metabolite supply to oocytes in IVM were observed. *In vivo*

matured complexes were capable of excluding glucose from the entire COC and cholesterol was excluded from oocytes. Conversely IVM COCs were more permissive to rapid equilibration of glucose and cholesterol concentrations across the complex and in oocytes. In fact both metabolites accumulated rapidly in IVM oocytes resulting in inverse gradient patterns of glucose and cholesterol abundance with highest concentrations accumulating in the oocyte after IVM vs highest concentrations surrounding the COC after *in vivo* maturation conditions. As oocytes are highly sensitive to high glucose my results indicate that metabolic balance in IVM may be disrupted due to impaired molecular filtration properties of the mucified COC matrix that controls supply of hydrophilic and lipophylic substrates. Importantly these novel findings can explain the glucose sensitivity of IVM oocytes and identifies a mechanism by which IVM may lead to poorer oocyte developmental competence.

To translate these findings into the improvement of IVM I generated recombinant expression plasmid constructs for several *Adamts1* and *Versican* functional domains. The efficacy of Versican as an IVM supplement that activates cumulus cell signal transduction was proved in principle, by showing enhanced COC matrix expansion when added to mouse IVM cultures. Similar mechanisms are likely to be functional in human COCs since I demonstrated *VERSICAN* and *ADAMTS1* expression in human *in vivo* matured cumulus and granulosa cells. This work has advanced our understanding of oocyte maturation and will lead to improvements in IVM and healthier outcomes from reproductive therapies.

Declaration

This work contains no material which has been accepted for the award of any other degree or diploma in any university or other tertiary institution and, to the best of my knowledge and belief, contains no material previously published or written by another person, except where due reference has been made in the text.

I give consent to this copy of my thesis when deposited in the University Library, being made available for loan and photocopying, subject to the provisions of the Copyright Act 1968.

The author acknowledges that copyright of published works contained within this thesis (as listed below) resides with the copyright holder(s) of those works.

Kylie Renee Dunning

October 2008

Dunning KR, Lane M, Brown HM, Yeo C, Robker RL, Russell DL (2007) Altered composition of the cumulus-oocyte complex matrix during in vitro maturation of oocytes. Hum Reprod 22, 2842-50.

Acknowledgements

I first have to thank my supervisors, Dr Darryl Russell and Dr Rebecca Robker for providing me the opportunity to pursue my PhD with them and learn so much. Also, for their encouragement, support and guidance through the learning curve required to write a thesis and to Darryl for his encouragement and guidance throughout the last four years.

Thank you to all the staff in the Discipline of Obstetrics and Gynaecology and the Research Centre for Reproductive Health for your friendly, smiling faces. To all the members of the lab, for offering to read sections of this thesis and for your friendship, thank you! And to Lyn, Stephanie, Pat and Hannah for technical assistance, morning tea debriefings and being great friends, I don't know how I would have got through the first year without you.

These studies were financially supported with grant funding from the National Health and Medical Research Council. I would like to acknowledge financial support of the Faculty of Health Sciences, University of Adelaide, the Discipline of Obstetrics and Gynaecology and the Research Centre for Reproductive Health for international and domestic travel opportunities and my postgraduate scholarship.

Thank you to my parents and family for all you help and support, particularly in the last 12 months. Lastly I wish to thank my fiancé, Matthew White to whom I am indebted for many household duties, meals, moral support and love. Thank you so very much!

Publications arising from this thesis

1. Dunning KR, Lane M, Brown HM, Yeo C, Robker RL, Russell DL (2007) Altered composition of the cumulus-oocyte complex matrix during in vitro maturation of oocytes. Hum Reprod 22, 2842-50.
2. Dunning KR, Brown HM, Thompson JG, Robker RL, Russell DL. Cumulus Oocyte Matrix Function during Oocyte Maturation and Ovulation. *In preparation*

Abstracts arising from this thesis

2007

1. **Dunning KR**, Lane M, Brown HM, Yeo C, Thompson JG, Robker RL and Russell DL. *Functional Characterisation of the Cumulus Oocyte Matrix During Maturation of Oocytes .* Australian Society for Reproductive Biology, National Conference, Christchurch New Zealand, September 2007.
2. **Dunning KR,** Lane M, Brown HM, Yeo C, Thompson JG, Robker RL and Russell DL. *Altered Composition of the Cumulus Oocyte Complex Matrix During in vitro Maturation of Oocytes.* Podium presentation at the 2007 Society for the Study of Reproduction, International Conference, July, Texas, USA.
3. **Dunning KR**, Lane M, Brown HM, Yeo C, Thompson JG, Robker RL and Russell DL. *Functional Characterisation of the Cumulus Oocyte Matrix During Maturation of Oocytes.* Australian Society for Medical Research, SA conference, Adelaide SA, June 2007.

2006

4. Russell DL, Brown HM, **Dunning KR**, Pritchard M and Robker RL. Ovarian Folliculogenesis and Lymphangiogenesis are dependent on ECM remodelling by the protease Adamts1. Biology of Reproduction Supp 2006
5. Ricciardelli C, Ween WP, **Dunning K** & Russell DL. *ADAMTS processing of Versican induces pericellular sheath formation and motility of cancer cells.* Australian Health and Medical Research Congress, Matrix Biology Society of Australia and New Zealand, Melbourne, November 2006.
6. Ricciardelli C, Ween MP, **Dunning K** & Russell DL. *ADAMTS processing of Versican induces pericellular sheath formation and motility of cancer cells.* 3rd Pacific Rim International Breast and Prostate cancer meeting, Fraser Island, October 2006.
7. Ween MP, **Dunning K**, Russell DL & Ricciardelli C. *ADAMTS processing of Versican induces pericellular sheath formation by cancer cells.* Australian Society for Medical Research, SA Meeting, Adelaide, June 2006.

2005

8. **Dunning KR**, Yeo CX and Russell DL *Altered Matrix Composition of Cumulus Oocyte Complexes Following In vitro Maturation.* Australian Society for Medical Research, SA Meeting, Adelaide, June 2005.
9. **Dunning KR**, Yeo CX and Russell DL *Altered Matrix Composition of Cumulus Oocyte Complexes Following In vitro Maturation.* Australian Society for Reproductive Biology, National Conference, Perth WA, September 2005.

Table of Contents

List of Figures

List of Tables

Abbreviations

αMEM	Minimum Essential Medium alpha
ADAM	A Disintegrin and Metalloprotease
Adamts1	a disintegrin-like and metallopeptidase (reprolysin type) with thrombospondin type 1 motifs
Ambp	alpha 1 microglobulin/bikunin
ANOVA	analysis of variance
Ar	Androgen receptor
ART	artificial reproductive technology
bp	base pairs
BSA	bovine serum albumin
CBP	complement binding protein
cDNA	Complementary DNA
CEI	cumulus expansion index
CIP	Calf Intestinal Alkaline Phosphatase
COC	Cumulus Oocyte Complex
CRP	complementary regulatory protein
CS	chondroitin sulphate
DMEM	Dulbecco's Modified Eagle Medium
DNA	Deoxyribonucleic acid
E. coli	Escherichia coli
eCG	Equine chorionic gonadotropin
ECM	extracellular matrix
Egf	Epidermal growth factor
Egf-L	Egf-like peptide
EgfR	Egf receptor
ErbB2	erythroblastic leukemia viral oncogene homolog 2
ERK	Extracellular signal-regulated kinase
F1	first filial
FAK	focal adhesion kinase
FCS	fetal calf serum

FF-MAS	Follicular fluid-meiosis-activating sterol
FSH	Follicle Stimulating Hormone
G	globular
G1	globular domain 1
G2	globular domain 3
GAG	glycosaminoglycan
GC	granulosa cell
GEC	glomerular endothelial cell
GLUT	glucose transporter
GREM1	gremlin
GV	germinal vesicle
h	hour
HA	Hyaluronan
Has1	Hyaluronan synthase 1
Has2	Hyaluronan synthase 2
Has3	Hyaluronan synthase 3
HC	heavy chain
hCG	human Chorionic Gonadotropin
HS	heparin sulphate
HSPG	heparin sulphate proteoglycans
IαI	inter-α trypsin inhibitor
i.p.	intraperitoneal
ITS	insulin transferrin selenium
IU	international units
IVM	*in vitro* maturation
kDa	kilodalton
KO	knock out
LB	luria broth
LH	Luteinizing hormone
Lhcgr	luteinizing hormone/choriogonadotropin receptor
mGC	mural granulosa cell

MI	metaphase I
MII	metaphase II
min	minute
MMP	Matrix Metalloproteinase
mRNA	Messenger RNA
Nrip1	Nuclear receptor interacting protein 1
^{o}C	degrees Celsius
OHSS	ovarian hyperstimulation syndrome
PB	polar body
PBS	Phosphate Buffered Saline
PCOS	polycystic ovarian syndrome
PCR	Polymerase Chain Reaction
Pgr	Progesterone receptor
PRKO	Progesterone receptor knockout
Ptger2	prostaglandin E receptor 2, subtype EP2
Ptgs2	prostaglandin-endoperoxide synthase 2
Ptx3	Pentraxin 3
PVDF	polyvinylidene difluoride
Rac	RAS-related C3 botulinum substrate 1
RHAMM	receptor for HA-mediated motility
RhoA	ras homolog gene family, member A
RNA	ribonucleic acid
ROI	region of interest
ROS	reactive oxygen species
Rpm	revolutions per minute
RT	reverse transcription
RT-PCR	realtime reverse transcription polymerase chain reaction
S.E.M.	standard error of the mean
SDS	Sodium Dodecyl sulphate
SDS-PAGE	Sodium Dodecyl sulphate - polyacrylamide gel electrophoresis
Tnfaip6	Tumor necrosis factor alpha-induced protein 6
TSP-1	thrombospondin type I

VEGF	Vascular endothelial growth factor
VEGFR	Vascular endothelial growth factor receptor
ZP	zona pellucida

Chapter 1

Introduction

1.1 BACKGROUND

Reproductive success is dependent on the appropriate maturation and expulsion of mature oocytes from follicles of the ovary, in a process known as ovulation. The growth of ovarian follicles, or folliculogenesis, and oocyte development and maturation are highly coordinated and mutually dependent processes (Eppig 2001) (Figure 1.1). In the mature antral follicle, specialised somatic cells known as cumulus cells encapsulate the oocyte. Each oocyte is surrounded by several layers of cumulus cells which in the mouse equates to approximately 1000-3000 cells per oocyte (Salustri *et al.* 1992). Collectively the oocyte and cumulus cells are referred to as the cumulus oocyte complex (COC, Figure 1.1). The cumulus cells are attached to the oocyte and to each other via gap junctions, which allow the transfer of small molecules (<1-2kDa) such as metabolites, ions and signalling molecules, a process that is critical for oocyte growth and subsequent embryo development (Buccione *et al.* 1990; Gershon *et al.* 2008). Gap junctions between the oocyte and cumulus cells require transzonal cumulus cell projections that pass through the zona pellucida (ZP) into the oocyte. These transzonal projections provide additional communication through endocytic uptake of factors by the oocyte and the innermost layers of cumulus cells (Albertini *et al.* 2001). Adjacent to the COC is a layer of stratified epithelial cells known as mural granulosa cells. The cumulus and mural granulosa cells differ in their responsiveness to hormone stimulation resulting in diverse gene expression profiles and differing functional roles within the follicle.

In all mammals, the luteinizing hormone (LH) surge initiates processes in ovarian follicles that are required for ovulation (Richards *et al.* 2002). The LH surge activates complex gene expression changes in mural granulosa and cumulus cells. Numerous extracellular matrix (ECM) remodelling events ensue including the degradation of the connective matrix and cellular layers at the apex of the ovarian follicle, which is required for ovulation of the oocyte. The LH surge also initiates the process of cumulus expansion through an increase in the production of Hyaluronan (HA)-rich matrix by the cumulus cells (Salustri *et al.* 1992). This results in an enlargement of a visco-elastic matrix between the cumulus cells and surrounding the oocyte. At the completion of cumulus expansion, the COC is 20-fold its initial volume and fills most of the follicular antrum in rodents (Salustri *et al.* 1992) (Figure 1.2, c). Cumulus expansion is concomitant with the resumption of meiosis and nuclear maturation to metaphase II. Following cumulus expansion, the COC detaches from the mural granulosa cells on the basal side of

NOTE: This figure is included on page 43 in the print copy of the thesis held in the University of Adelaide Library.

Figure 1.1 Schematic of folliculogenesis, cumulus oocyte complex (COC) expansion and oocytematuration.

Folliculogenesis from the primary to the antral stage, whereupon follicles are able to respond to the luteinising hormone (LH) surge, involves granulosa cell proliferation, formation of a fluid filled antral cavity and divergence of the mural granulosa and cumulus cell lineages. Cumulus cells immediately surround the oocyte and mural granulosa cells line the follicle wall. Oocytes remain arrested in prophase I of meiosis during folliculogenesis until the endogenous LH surge or administration of the exogenous LH-analogue, human chorionic gonadotropin (hCG), induce resumption of meiosis and expansion of the cumulus oocyte complex (COC). Following completion of COC expansion the oocyte has extruded the first polar body and reached metaphase II, the COC is ovulated and is capable of being fertilised. Figure modified from (Kimura *et al.* 2007).

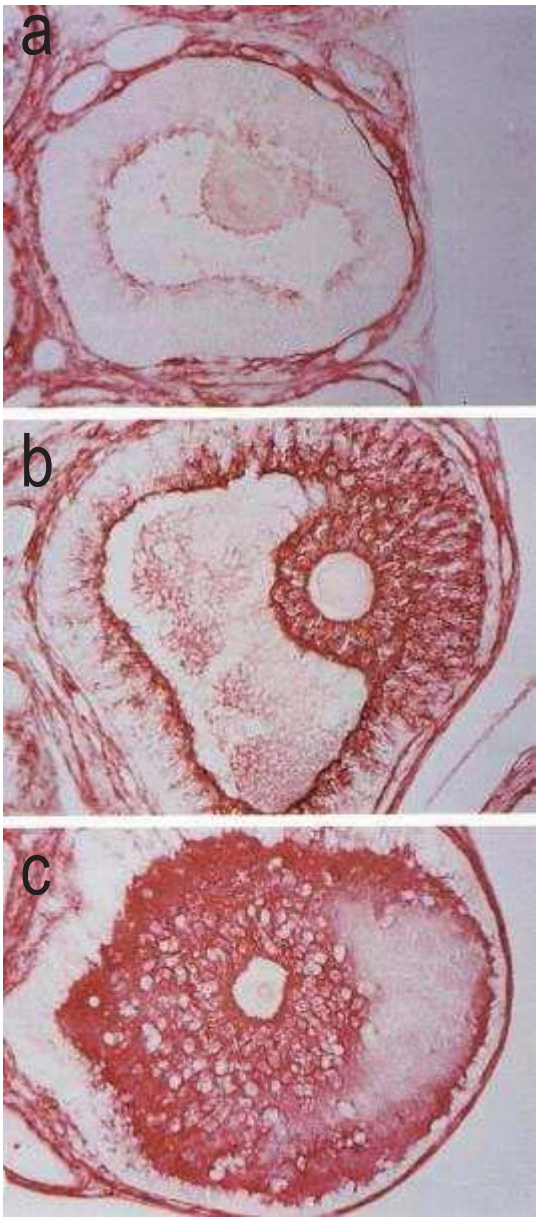

Figure 1.2 Immunolocalisation of Hyaluronan in the expanding COC of preovulatory mouse follicle.

Micrographs of mouse follicle sections showing localisation of Hyaluronan (brown staining) during cumulus expansion of mouse preovulatory follicles before (a, unexpanded COC), or after 5 hours (b) and 10 hours (c, expanded COC) administration of hCG to induce expansion and ovulation. Figure from (Salustri *et al.* 1992).

the follicle and is ovulated at the apical side (nearest the ovarian surface) where connective tissue has been degraded and there is a thinning in the layers of cells. The ovulated expanded COC then attaches to the oviductal ampulla where it can be transferred to the site of fertilisation. The production of this mucified matrix is not a passive or insignificant biological process occurring alongside oocyte maturation, in fact the production and correct formation of this matrix is critical for successful ovulation, fertilisation and subsequent embryo development (Russell and Robker 2007).

1.2 COMPONENTS OF CUMULUS MATRIX

1.2.1 Hyaluronan

In all species examined thus far, the major component of COC matrix is Hyaluronan (HA; syn., Hyaluronic acid, hyaluronate). Synthesis of HA occurs following both the LH surge *in vivo* and *in vitro* after stimulation of isolated cumulus oocyte complexes with follicle stimulating hormone (FSH) (Eppig 1979b; Eppig 1980; Salustri *et al.* 1992) or epidermal growth factor (Egf)(Tirone *et al.* 1997) and is dependent on the secretion of oocyte factors that stimulate cumulus specific gene expression (Eppig 1979a; Eppig 1980; Salustri *et al.* 1989; Salustri *et al.* 1992). Five hours post hCG administration *in vivo*, HA synthesis and deposition is evident amongst the cumulus cells and the oocyte of the COC, and in those mural granulosa cells adjacent to the antrum (Figure 1.2 b). Nearing the completion of expansion, HA is interdispersed between the cells of the expanded COC and present in the antral fluid (Figure 1.2 c).

Hyaluronan is an unsulphated glycosaminoglycan (GAG) with a repeating disaccharide structure of alternating D-glucuronic acid and N-acetylglucosamine, and is not covalently attached to a core protein as occurs with all other GAGs such as chondroitin or heparin sulphates (Meyer and Palmer 1934; Weissman and Meyer 1954; Laurent and Fraser 1992).

Hyaluronan is synthesised in the cytoplasm by a membrane bound enzyme, Hyaluronan synthase, which adds alternating monosaccharide units to the chain on the cytoplasmic side of the membrane and secretes the polymerised HA chain through the membrane into the intercellular space (Philipson and Schwartz 1984; Weigel *et al.* 1997). There are three mammalian Hyaluronan synthase genes; *HAS1*, *HAS2* and *HAS3* (Itano and Kimata 1996; Shyjan *et al.* 1996; Spicer *et al.* 1997). They show high

protein sequence similarity, but have differential tissue expression patterns (Itano and Kimata 1996; Shyjan *et al.* 1996; Spicer and McDonald 1998; Recklies *et al.* 2001) and synthesise Hyaluronan chains of varying masses (Itano *et al.* 1999). Has2 is responsible for the synthesis of HA in cumulus cells and shows strong induction following LH stimulation both *in vivo* and *in vitro* in mouse, porcine and bovine cumulus cells (Fulop *et al.* 1997b; Kimura *et al.* 2002; Schoenfelder and Einspanier 2003). Hyaluronan synthase 2 produces HA chains with a mass exceeding 2 x 10^6 daltons, larger than that produced by Has1 or Has3 (Itano *et al.* 1999).

Functionally HA is recognised as the backbone around which the expanded COC matrix assembles but more specifically its role in expanded COC function has yet to be elucidated. Known actions of HA in other tissues and systems have been extrapolated to describe the potential role(s) of HA in the COC (Russell and Salustri 2006). Hyaluronan is able to regulate several cellular properties and functions by binding to cell surface receptors CD44 and RHAMM (receptor for HA-mediated motility), leading to altered cell shape and behaviour which can result in altered adhesion, migration, proliferation, differentiation, cell death and anchorage (Knudson and Knudson 1993). The interaction of HA with CD44 has been shown to promote anchorage independent growth and cell survival through the activation of ErbB2 receptor. This mechanism is thought to similarly occur in cumulus cells since the induction of CD44 and HA occurs simultaneously in cumulus cells in the human, porcine and bovine (Ohta *et al.* 1999; Yokoo *et al.* 2002; Schoenfelder and Einspanier 2003). In addition, culture of human cumulus cells in vitro with HA decreases the rate of apoptosis (Kaneko *et al.* 2000; Saito *et al.* 2000). In further support of the potential importance of HA promoting cumulus cell survival in the COC, cumulus cell apoptosis in both the human and bovine correlates negatively with oocyte developmental competence (Lee *et al.* 2001; Host *et al.* 2002; Yuan *et al.* 2005). However a mechanism by which HA promotes cumulus cell survival through binding to CD44 is probably not essential to COC function *in vivo*, as mice with a null mutation in CD44 display normal fertility (Schmits *et al.* 1997; Protin *et al.* 1999). The binding of HA to the other characterised HA receptor RHAMM, may elicit a different response. In one cell system, the binding of HA to these receptors resulted in activation of different signal transduction pathways where HA bound RHAMM activated the small GTPase signal transducer Rac while binding of HA to CD44 resulted in activation of the RhoA pathway (Goueffic *et al.* 2006). The constitutive expression of RHAMM has been detected in bovine cumulus cells throughout the maturation process however the functional significance of RHAMM in the COC has not been determined (Schoenfelder and Einspanier 2003). It has been shown that RHAMM and CD44 can act together, in

conjunction with HA, to increase activation of the ERK1/2 signalling pathway and increase CD44 expression (Tolg *et al.* 2006; Hamilton *et al.* 2007). Very recently it was shown that HA fragments generated during sperm penetration of the COC were able to stimulate the production and secretion of chemokines, which in turn led to sperm capacitation and enhanced fertilisation *in vitro*, demonstrating a role for cumulus matrix in promoting fertilisation (Shimada *et al.* 2008).

Hyaluronan is a major component of all extracellular matrices and exists as a random coil structure that upon interaction with water molecules forms a hydrated gel complex that acts as an extracellular space filler (Fraser *et al.* 1997). This property is central to the deformable, but highly elastic capacity of cartilage matrix. The hydrated HA-rich COC matrix demonstrates viscoelastic properties, allowing the expanded COC to become misshapen as it passes through the rupture pore during ovulation, but restoring its shape afterwards. This property may be important for protection of the oocyte during ovulation. The COC matrix is described as interconnecting fibrils that generate a mesh with 'pores' (Yudin *et al.* 1988). Protease treatment of expanded COCs leads to instability and reduced elasticity suggesting a critical role for extracellular proteins in stabilising and organising COC matrix (Cherr *et al.* 1990).

1.2.2 Proteoglycans and HA-associated proteins

Appropriate formation and expansion of the COC requires not only the synthesis of HA by cumulus cells but also the incorporation of proteins derived both from serum and secreted from mural granulosa and cumulus cells of the preovulatory follicle. These proteins are critical for the correct formation and stabilization of COC matrix and include the heavy chains of inter-α trypsin inhibitor (IαI), tumor necrosis factor alpha-induced protein-6 (Tnfaip-6), pentraxin 3 (Ptx3) and Versican that are reviewed in detail below.

1.2.2.1 Inter-α trypsin inhibitor (IαI)

The inter-α trypsin inhibitor (IαI) family of molecules are synthesised and assembled into a dimer or trimer complex in the liver, which are secreted and circulate in blood plasma (Salier *et al.* 1996). The IαI

complex contains two proteins known as heavy chains (HCs), which are attached to a chondroitin sulphate (CS) chain of the proteoglycan bikunin (Salier *et al.* 1996). During cumulus expansion *in vivo* Iαl diffuses from the blood vasculature into the follicular fluid, due to increased permeability of the vasculature following the LH surge, and incorporates into the COC matrix (Chen *et al.* 1992; Powers *et al.* 1995; Hess *et al.* 1998). The incorporation of Iαl into the HA-rich cumulus matrix involves the transfer of the HCs from Iαl to HA by a transesterification of the HC bond from the CS of bikunin to HA (Zhao *et al.* 1995; Chen *et al.* 1996; Nagyova *et al.* 2004). Bikunin is released during this reaction and does not appear to play a role in the formation or stabilisation of the expanded cumulus matrix (Zhuo *et al.* 2001). Iαl is a critical component of the COC matrix such that when COC expansion is carried out *in vitro*, in the absence of serum or a purified source of Iαl, HA is labile and readily lost into the media, resulting in the dispersion of cumulus cells and loss of normal COC morphology despite normal synthesis of HA (Eppig 1979b; Salustri *et al.* 1989; Chen *et al.* 1992; Castillo and Templeton 1993; Chen *et al.* 1994).

1.2.2.2 Tumor necrosis factor alpha-induced protein 6 (Tnfaip6, TSG6)

Tumor necrosis factor alpha-induced protein 6 (Tnfaip6, previously termed TSG6) is also an essential component required for successful cumulus expansion (Fulop *et al.* 2003). Tnfaip6 is synthesised by cumulus and granulosa cells following the LH surge *in vivo* and is dependant on secretion of factors from the oocyte (Fulop *et al.* 1997a; Yoshioka *et al.* 2000; Mukhopadhyay *et al.* 2001; Varani *et al.* 2002). Tnfaip6 binds HA directly through its link domain (Kahmann *et al.* 2000) and is required for the transesterification reaction between Iαl HCs and HA where it acts as a catalyst cofactor (Fulop *et al.* 2003; Jessen and Odum 2003; Rugg *et al.* 2005; Sanggaard *et al.* 2005). The ability of Tnfaip6 to bind HA in addition to the HCs of Iαl has previously been thought to maintain the structure of the COC matrix (Carrette *et al.* 2001). However, work demonstrating that short oligosaccharide fragments of HA, capable of inhibiting binding of Tnfaip6 to HA (Lesley *et al.* 2002), do not impair COC expansion (Mukhopadhyay *et al.* 2004) and that hyaluronidase treatment of COCs to remove HA does not abolish Tnfaip6 detection, indicates that Tnfaip6 it is not covalently linked to HA (Ochsner *et al.* 2003; Scarchilli *et al.* 2007). Additionally, once the HCs of Iαl are transferred to HA, Tnfaip6 reforms a complex with new HCs of Iαl (Rugg *et al.* 2005) and during cumulus expansion *in vivo* is found in a complex with HCs only until just prior to ovulation (Ochsner *et al.* 2003). This evidence indicates that while Tnfaip6 is not

directly involved in the cross linking of HA (Scarchilli *et al.* 2007), it is a critical component of the COC matrix, bound to IαI, functioning as a catalyst for the transfer of HCs to HA. Additionally, Tnfaip6 may be required for the incorporation of pentraxin 3 into the cumulus matrix (Scarchilli *et al.* 2007) as is discussed below.

1.2.2.3 Pentraxin 3 (Ptx3)

Pentraxin 3 (Ptx3) exists as a high molecular weight multimer composed of approximately 10 individual Ptx3 proteins (each approximately 45kDa in size) joined by interchain disulphide bonds (Bottazzi *et al.* 1997). Induction of *Ptx3* expression in cumulus cells occurs following the LH-surge and is dependant on the secretion of oocyte growth factors (Varani *et al.* 2002). Prior to ovulation, Ptx3 co-localises with HA in the expanding COC matrix (Varani *et al.* 2002; Salustri *et al.* 2004). While Ptx3 does not bind HA directly, it does play an important role in the formation of the cumulus matrix as ablation of the Ptx3 gene results in cumulus matrix instability (Varani *et al.* 2002; Salustri *et al.* 2004). Recent evidence shows that Ptx3 interacts directly with the HCs of IαI and that this interaction is critical for the organisation and stability of the COC matrix (Scarchilli *et al.* 2007). The binding of Ptx3 to Tnfaip6 may act in cross linking several Hyaluronan strands and subsequent stabilisation of the matrix (Scarchilli *et al.* 2007) (Figure 1.3 a). The interaction of Ptx3 with HCs, and subsequent integration of Ptx3 into the COC matrix, may first occur through interaction of Ptx3 with Tnfaip6 forming a large multimeric complex at the time of HC transfer from Tnfaip6 to HA (Scarchilli *et al.* 2007).

1.2.2.4 Versican

Versican is a HA-binding proteoglycan with numerous chondroitin sulphate (CS) attachments. *Versican* mRNA has been localised to mouse and rat mural granulosa cells (mGCs) after LH stimulation while the secreted protein localises both to the mGCs and the ECM of expanding COCs (Russell *et al.* 2003b) (Figure 1.4 b). Due to the predominant expression of Versican in mural granulosa cells *in vivo*, it has been proposed that this COC matrix component is derived mainly from the follicle wall (Russell *et al.* 2003b). Versican is structurally similar to aggrecan which functions in cartilage as a crosslinker of HA and is important in hydration and elasticity of the matrix. Structurally Versican contains N- and C-

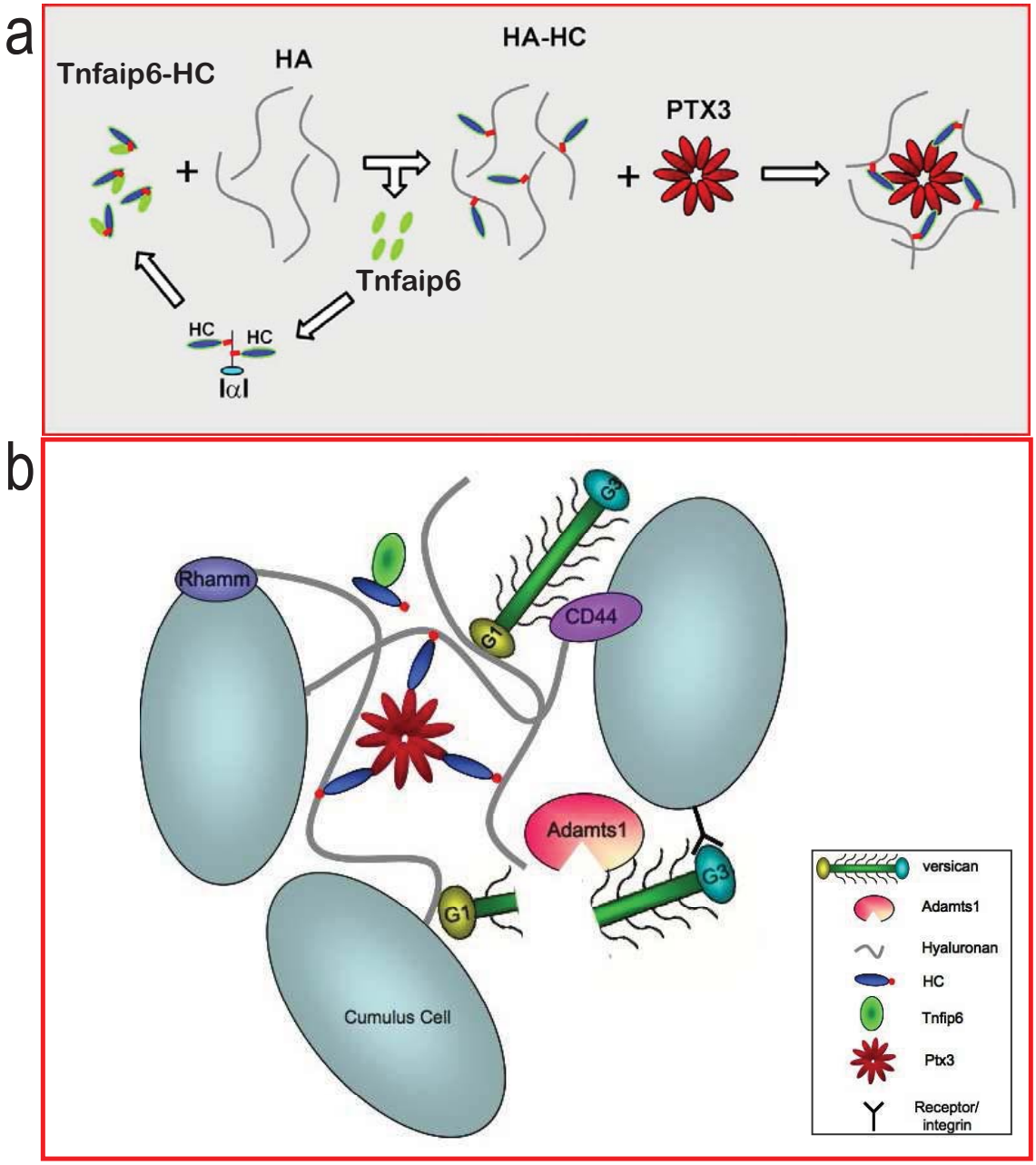

Figure 1.3 Interaction of Hyaluronan with extracellular proteins of the cumulus oocyte matrix.

(a) Schematic of the transfer of heavy chains (HC) from IαI to Hyaluronan (HA), which is catalysed by Tumor necrosis factor alpha-induced protein 6 (Tnfaip6). The HCs bound to HA are thought to cross-link and stabilise the cumulus matrix through binding to pentraxin 3 (Ptx3). Figure modified from (Scarchilli *et al.* 2007).

(b) Schematic depicts the structure of the expanded COC matrix. Hyaluronan is the major component of the cumulus matrix, able to bind CD44 and Rhamm receptors and is organised by extracellular proteins. Ptx3, HCs of IαI and Versican bind HA directly. Ptx3 binds several HCs and is thought to link several HA strands. These interactions result in a highly organised matrix network. The G1 domain of Versican binds HA and the G3 domain binds cell surface integrins and receptors. Adamts1 cleaved Versican in the COC matrix, potentially modifies the structure of the matrix and may enhance the binding of Versicans G3 domain with cell surface integrins and Egf receptors. Figure modified from (Russell and Robker 2007).

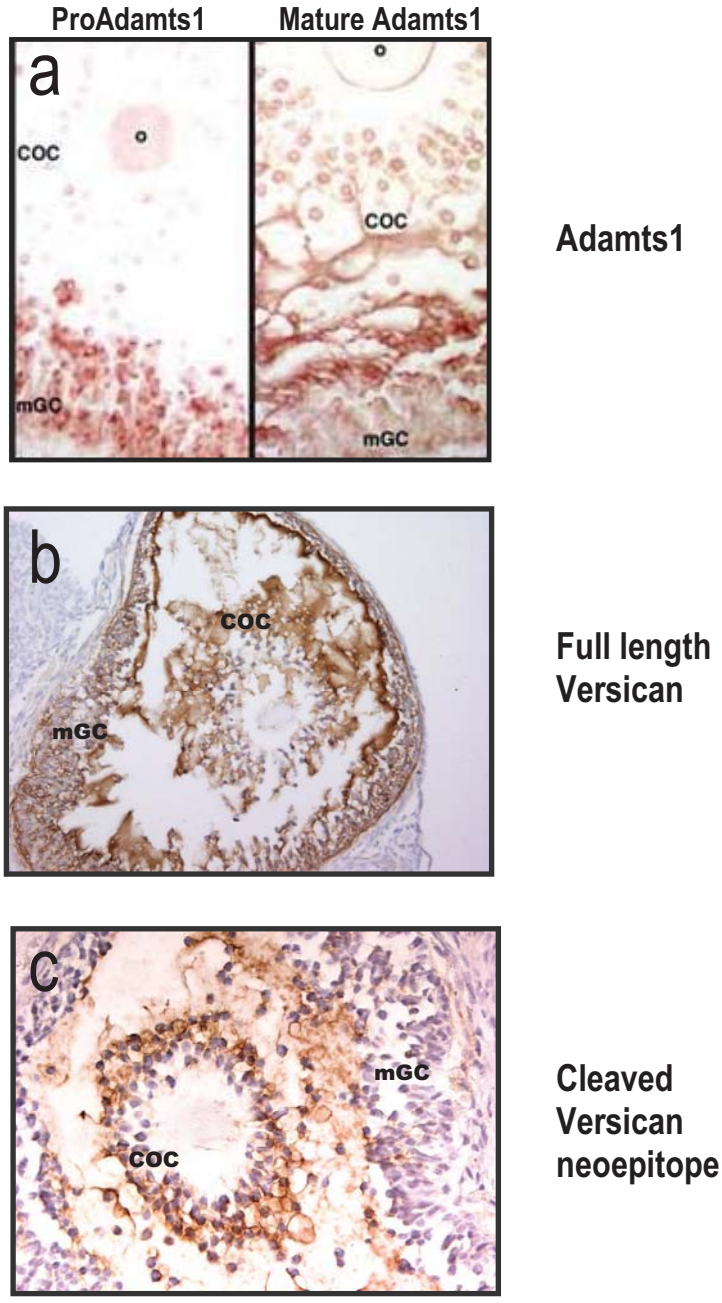

Figure 1.4 Versican, Adamts1 and Adamts1 cleaved Versican localise to the matrix of the expanding COC

Localisation of Versican and Adamts1 proteins in periovulatory mouse follicles 12 h following hCG administration to induce cumulus expansion and ovulation. Images show immunohistochemistry of (a) pro and mature Adamts1 (Russell *et al.* 2003a) (b) full length Versican and (c) neoepitope generated by Adamts1 cleavage of Versican (cleaved Versican neoepitope). ProAdamts1 localises to the mural granulosa cells and the mature form to the cumulus matrix and surfaces of the oocyte and cumulus cells (a). Intense staining of full length Versican is seen in the granulosa cell layer and in the expanded COC (b). Adamts1 cleaved Versican is found predominantly in the COC matrix and antral cavity demonstrating similar spatial distribution to active Adamts1 (c). COC, cumulus oocyte complex; mGC, mural granulosa cell.

terminal globular (G) domains termed G1 and G3 respectively, which are separated by a CS attachment region. The G1 domain contains an immunoglobulin-like loop region and binds HA via two link protein-like tandem repeats (LeBaron *et al.* 1992). The Versican G3 domain shares a high sequence homology with the selectin adhesion receptors and contains two epidermal growth factor (Egf) domains, a carbohydrate recognition domain and a complement regulatory protein (CRP) region (Shinomura *et al.* 1993). The G3 domain is known to interact with cell surface proteins including sulphated glycolipids (Miura *et al.* 1999), heparan sulphate proteoglycans (Ujita *et al.* 1994), growth factor receptors (Xiang *et al.* 2006) and integrins (Wu *et al.* 2002). The chondroitin sulphate attachments of Versican are able to interact with the link module of CD44 (Kawashima *et al.* 2000). Versican may therefore cross link the HA rich matrix of the expanding COC with cumulus cells, or other matrix components, or induce cell signalling pathways through binding to CD44. In addition to matrix interaction, Versican is involved in a range of cellular functions including proliferation (Zhang *et al.* 1998; Yang *et al.* 1999), cell migration (Evanko *et al.* 1999), and apoptosis (Wu *et al.* 2005a; Sheng *et al.* 2005). The function of Versican may be modulated by cleavage in the CS domain to disassociate the two globular domains (Zhang *et al.* 1998; Wu *et al.* 2001; Xiang *et al.* 2006).(Yang *et al.* 1999)

1.2.2.5 Adamts1

The protease Adamts1 (a disintegrin-like and metallopeptidase (reprolysin type) with thrombospondin type 1 motifs) cleaves Versican in the CS attachment domain (Sandy *et al.* 2001), and Adamts1-mediated Versican cleavage has been shown to occur in ovulating mouse COCs (Russell *et al.* 2003a) (Figure 1.4 c). The expression of *Adamts1* is induced in mGCs in response to the LH-surge in periovulatory ovaries of mouse (Robker *et al.* 2000), rat (Espey *et al.* 2000), cow (Madan *et al.* 2003) and mare (Boerboom *et al.* 2003) and is strongly expressed in normal human ovaries (Jansen *et al.* 2004). Regulation in human is not known, but in mice *Adamts1* expression is specific to mGCs and dependent on progesterone receptor (PgR) expression (Robker *et al.* 2000; Russell *et al.* 2003a; Doyle *et al.* 2004a). Similar to Versican, the production of Adamts1 is thought to occur predominantly in the mural granulosa cells with the mature protease localising to the COC matrix, possibly through binding to its substrate (Russell *et al.* 2003a) (Figure 1.4 a). In addition to a metalloprotease domain, Adamts1 comprises a domain distantly related to disintegrin domains of ECM molecules and three type-1

thrombospondin-like domains at the C-terminus. The functional importance of Versican processing by Adamts1 in the COC, as characterised by null mutant mouse lines, is discussed below (Section 1.3).

1.2.2.6 Other COC matrix proteins

Cartilage link protein has been detected in both rat (Kobayashi *et al.* 1999; Sun *et al.* 2003) and human cumulus matrix (Familiari *et al.* 1996; Relucenti *et al.* 2005), and in the rat was shown to increase the degree of COC expansion (Sun *et al.* 2002). The link module of Versican binds link protein and this interaction promotes increased binding of HA to Versican and may further enhance the stability of the COC matrix (Matsumoto *et al.* 2003). Additionally, fibronectin, tenascin-C and laminin have been identified in human cumulus matrix (Familiari *et al.* 1996; Relucenti *et al.* 2005) with tenascin-C also present in mouse cumulus oocyte complexes (Hernandez-Gonzalez *et al.* 2006). An interaction between tenascin-C, Versican and HA is functionally important in the formation of matrices that surround neuronal cells (Aspberg *et al.* 1997). These perineuronal net matrices that are compositionally analogous to the COC matrix act to regulate cell-cell contact and communication, which may potentially be one role of the cumulus matrix also.

1.3 CUMULUS MATRIX AND FERTILITY

1.3.1 Role of cumulus matrix in ovulation and fertilisation

While the formation of the expanded cumulus oocyte complex (COC) matrix has been described in detail in many species, the function of this matrix is not well understood. What is understood of its functional importance is restricted to the period immediately following ovulation and during fertilisation when the COC must adhere to the infundibulum and be transported through the oviduct to the site of fertilisation. The matrix of an expanded COC is able to adhere to the ciliated infundibular epithelial cells to be transported through the oviduct but denuded oocytes cannot (Odor and Blandau 1973; Lam *et al.* 2000). Prior to fertilisation, the sperm must first traverse the layers of cumulus cells and extracellular matrix of the expanded COC. Studies have shown that the cumulus matrix binds sperm directly (Salustri *et al.* 2004). Additionally the COC matrix may act as a sperm chemoattractant (Eisenbach and Tur-

Kaspa 1999), be involved in sperm capacitation (Van Soom *et al.* 2002) and potentially act as a barrier, allowing penetration only by sperm capable of fertilisation (Hong *et al.* 2004). Thus the COC matrix may act in the attraction and capacitation of sperm. Prior to its role in oviductal transport and fertilisation however, the formation and correct organisation of the cumulus matrix is an obligatory requirement for successful ovulation. In fact, even mild disruptions in COC matrix composition and expansion have a marked negative effect on ovulation as well as subsequent fertilisation rates of any oocytes that do ovulate. This is exemplified in mice by gene ablation of proteins or enzymes involved in the production of COC matrix (Table 1.1) These mice display a range of phenotypes stemming from impaired cumulus expansion (Davis *et al.* 1999; Hizaki *et al.* 1999; White *et al.* 2000; Zhuo *et al.* 2001; Varani *et al.* 2002; Fulop *et al.* 2003), including anovulation (Robker *et al.* 2000; White *et al.* 2000) and decreased fertilisation rates (Lim *et al.* 1997; Hizaki *et al.* 1999; Zhuo *et al.* 2001; Varani *et al.* 2002; Salustri *et al.* 2004). The decreased fecundity in these various mouse models clearly demonstrates the functional importance of the cumulus matrix in fertility.

1.3.1.1 Cumulus matrix components essential for fertility

Mutant mouse models lacking COC matrix proteins exhibit impaired cumulus expansion or abnormal organisation of cumulus matrix, which is associated with reduced fecundity (Table 1.1). Ablation of bikunin (*Ambp*), *Tnfaip6* or *Ptx3*, which form part of the cumulus matrix, as discussed previously, results in severe subfertility or sterility due to decreased ovulation rates and a failure to fertilise (Table 1.1) (Sato *et al.* 2001; Zhuo *et al.* 2001; Varani *et al.* 2002; Fulop *et al.* 2003; Salustri *et al.* 2004). Following ovulation in the *Ptx3* null mouse, the cumulus cells of the COC disperse and are lost from the complex due to a failure to organise and retain HA within the COC (Varani *et al.* 2002; Fulop *et al.* 2003; Salustri *et al.* 2004). A similar phenotype is observed in mice lacking Tnfaip6 where ovulated oocytes are denuded or attached to few sparsely arranged cumulus cells (Fulop *et al.* 2003). Similarly, generation of bikunin KO mice, where IαI does not circulate and thus transfer of HCs to HA cannot occur, resulted in a phenotype whereby COC expansion occurs, due to HA synthesis, but rapid dispersion and degeneration eventuates prior to and following ovulation (Sato *et al.* 2001; Zhuo *et al.* 2001).

Analysis of cumulus matrix lacking in Versican, in relation to COC expansion and fertilisation, has not been performed in a null mouse model, as mice homozygous for a mutation in the Versican gene die in

Table 1.1 Phenotypes of mouse models with null mutations in genes that express or regulate expression of cumulus matrix components

		Gene Name (synonym(s))	Gene symbol	Ovulation Rate (% Compared to control)	*In vivo* Fertilisation rate (%)	Cumulus expansion & matrix morphology	Reference
Function of gene product	Transcription regulation	progesterone receptor	*Pgr*	0	-	expansion observed	(Lydon *et al.* 1995; Robker *et al.* 2000)
		androgen receptor	*Ar*	62	N/D	disrupted expansion	(Hu *et al.* 2004)
		Nuclear receptor interacting protein 1 (RIP140)	*Nrip1*	0	-	disrupted expansion	(White *et al.* 2000)
		prostaglandin E receptor 2, subtype EP2 (EP2, EP2 receptor, Ptgerep2)	*Ptger2*	67	8.5	disrupted expansion	(Hizaki *et al.* 1999)
		prostaglandin-endoperoxide synthase 2 (COX2, cyclooxygenase 2)	*Ptgs2*	40	0% natural cycle 2% superovulation	Not reported	(Lim *et al.* 1997)
				5	N/D	disrupted expansion	(Davis *et al.* 1999)
	Extracellular matrix proteins or organisers of matrix	a disintegrin-like and metallopeptidase (reprolysin type) with thrombospondin type 1 motif (ADAMTS-1, METH1)	*Adamts1*	33	N/D	expansion observed	(Mittaz *et al.* 2004)
				23% natural cycle 32% superovulation	27	expansion observed abnormal matrix distribution	(Russell *et al.* 2005)
		tumor necrosis factor alpha induced protein 6 (Tnfaip6, TSG-6, Tsg6)	*Tnfaip6*	48	0	disrupted expansion	(Fulop *et al.* 2003)
		alpha 1 microglobulin/bikunin (ASPI, HI-30, Intin4, Itil, Urinary Trypsin Inhibitor, UTI)	*Ambp*	43	<10	disrupted expansion	(Zhuo *et al.* 2001)
		pentraxin related gene (pentraxin 3, TSG-14)	*Ptx3*	45	2	disrupted expansion	(Varani *et al.* 2002)
				Not different*	0	disrupted expansion	(Salustri *et al.* 2004)

*Oocytes harvested at 14 h (Varani *et al.* 2002) vs 20 h (Salustri *et al.* 2004) post hCG may account for differences in ovulation reported in *Ptx3* null mouse model.
Table modified from (Russell and Robker 2007).

utero by embryonic day 10.5 as a result of a heart defect (Mjaatvedt *et al.* 1998). However, the phenotype resulting from reduced cleavage of Versican in COC matrix has been characterised in both the *Adamts1* and progesterone receptor (*Pgr*) knockout mice. *Adamts1* gene disruption results in a reduction in the number of ovulations (Shindo *et al.* 2000; Mittaz *et al.* 2004) and a significant reduction in fertilisation and on-time embryo development rates (Russell *et al.* 2005) (Table 1.1). While morphological cumulus expansion in the *Adamts1* null mouse was first reported as normal (Mittaz *et al.* 2004), closer characterisation of the COC matrix by immunolocalisation of HA and Versican reveals matrix that is abnormally distributed amongst cumulus cells and the oocyte both prior to and following ovulation (Russell *et al.* 2005). This abnormal matrix containing uncleaved Versican continues to surround the oocyte and cumulus cells when in the oviduct, well beyond the normal period of time. The reduction in fertilisation rates is likely due to the abnormal organisation of COC matrix in the *Adamts1* null mice, however the lack of properly organized matrix may also affect aspects of oocyte quality or maturation. Female mice lacking progesterone receptor (Pgr) have decreased abundance of Adamts1 and a 50% reduction in the cleavage of Versican in the expanding COC (Russell *et al.* 2003a). These mice fail to ovulate which may, in part be due to reduced processing of Versican during cumulus expansion *in vivo* (Russell *et al.* 2003a) (Table 1.1).

1.3.1.2 Essential regulators of cumulus matrix production

The receptor for the hormone progesterone, Pgr is critically important for the induction of ovulation as Pgr antagonists effectively block ovulation in both humans and rodents (Gaytan *et al.* 2003; Baird *et al.* 2003). As discussed above, female mice lacking the progesterone receptor ($Pgr^{-/-}$) display an anovulatory phenotype and fail to induce expression of *Adamts1* in the periovulatory period (Lydon *et al.* 1995; Robker *et al.* 2000) (Table 1.1). The absence of this cumulus matrix component is thought to be a contributing factor to ovulatory failure (Robker *et al.* 2000; Russell *et al.* 2003a).

Ablation of the androgen receptor (*Ar*) has provided information regarding the potential role of androgens in cumulus expansion and ovulation. Expression of the *Ar* has been detected in both rat (Pelletier 2000; Szoltys *et al.* 2003) and human (Hickey *et al.* 2005) cumulus cells. Androgen receptor (Ar) knockout mice fail to induce *Pgr* and COC matrix components *Has2* and *Tnfaip6*, resulting in disrupted cumulus expansion and significantly reduced ovulation rate (Hu *et al.* 2004) (Table 1.1).

Similarly, targeted deletion of the nuclear receptor interacting protein 1 (*Nrip1*, previously termed RIP140), a transcriptional regulator present in preovulatory granulosa cells, display an anovulatory phenotype, disrupted COC expansion (White *et al.* 2000) and aberrant expression of cumulus matrix components and regulators of matrix production including, *Adamts1*, *Has2*, *Ptx3, Tnfaip6,* prostaglandin-endoperoxide synthase 2 (*Ptgs2*), epiregulin, amphireulin and betacellulin (Tullet *et al.* 2005).

Cumulus expansion is also dependent on expression of prostaglandin-endoperoxide synthase 2 (*Ptgs2*), the rate-limiting enzyme in prostaglandin production (Wong and Richards 1992; Sirois and Richards 1992). *Ptgs2* expression is rapidly induced following the LH surge in cumulus and mural granulosa cells (Sirois and Richards 1992). Female mice lacking Ptgs2 have impaired fertility with defective cumulus expansion and reduced ovulation rates (Lim *et al.* 1997; Davis *et al.* 1999), which may be attributed to a reduction in the expression of *Tnfaip6* (Ochsner *et al.* 2003). Mice with a null mutation for the Ptgs2 receptor, prostaglandin E receptor 2 (*Ptger2*, synonym; EP-2), additionally display abnormal cumulus expansion, impaired fertility and a reduction in abundance of Tnfaip6 in the COC matrix (Ochsner *et al.* 2003).

In mice, gene ablation of cumulus matrix components or regulators of their expression demonstrate the functional importance of the formation and correct organisation of the cumulus matrix for female fertility (Table 1.1). The impaired fertility observed in mice with altered cumulus matrix is thought to be due to a failure to ovulate, impaired fertilisation or a combination of these factors. However the mechanism whereby altered cumulus matrix results in reduced fertility is unknown. The impaired fertility observed in mice with altered cumulus matrix may partially be attributable to a reduction in oocyte quality.

1.3.2 Role in oocyte quality and developmental capacity

Following fertilisation, the on-time development of an embryo to the blastocyst stage and ultimately, production of healthy live offspring is thought to be dependant on the developmental competence, or quality, of the oocyte. This theory stems from *in vitro* production of embryos where oocyte maturation, fertilisation and embryo development occur *in vitro* (Gosden 2002; Krisher 2004; Sirard *et al.* 2006). There are conflicting views on the use of oocyte morphology as a means of predicting oocyte quality

(Hamamah 2005; Wang and Sun 2007; Rienzi *et al.* 2008). Cumulus expansion and the expression of cumulus genes have been correlated with oocyte quality and the degree of COC expansion has been used as an indicator of good oocyte quality for some time (Ball *et al.* 1983; Somfai *et al.* 2004). In human studies, increased expression of *CD44* by cumulus cells (Ohta *et al.* 1999) and HA concentration in follicular fluid (Saito *et al.* 2000) correlate with greater developmental competence. It has been reported that *PTX3* expression in cumulus cells correlates with oocyte quality (Zhang *et al.* 2005). However, this correlation was not supported in two other studies (McKenzie *et al.* 2004; Cillo *et al.* 2007). The expression of *HAS2* and *PTGS2* was higher in human cumulus cells isolated from oocytes that developed into embryos of a higher quality when compared to embryos of a lesser quality (McKenzie *et al.* 2004; Cillo *et al.* 2007). Such correlations are also seen in the cow with high expression of *HAS2*, *PTGS2* and *TNFAIP6* by cumulus cells being correlated with increased oocyte developmental competence (Assidi *et al.* 2008). Overall, this indicates that the expression of genes required for cumulus expansion, and subsequent ovulation, are good indicators of oocyte quality and subsequent embryo health. The correlation of cumulus matrix gene expression and greater oocyte developmental competence also demonstrates that the formation, composition and correct organisation of the COC matrix, plays a role in oocyte maturation.

1.4 OOCYTE MATURATION

1.4.1 Initiation of oocyte meiotic maturation *in vivo*

Within ovarian follicles, mammalian oocytes are arrested at the first prophase of meiosis, also known as the germinal vesicle (GV) stage. Resumption of meiosis occurs following the endogenous LH surge, or exogenously administered human chorionic gonadotropin (hCG) (Figure 1.1). This is characterised by GV breakdown followed by spindle formation, alignment of the chromosomes at the equator and the entry of the oocyte into metaphase I (MI), finishing with the extrusion of the first polar body. The oocyte then proceeds into meiosis II and arrests at the second metaphase (MII). This sequence occurs within the follicle and is known as nuclear or meiotic maturation. Mature oocytes are then ovulated and capable of fertilisation. Completion of metaphase II occurs at fertilisation.

As stated earlier, the process of COC expansion (or mucification) occurs concomitantly with oocyte maturation, occurring in response to the LH surge. However, cumulus cells do not express the LH

receptor (*Lhcgr*), as evidenced in the rat where periovulatory COCs express minimal or no *Lhcgr* mRNA (Peng *et al.* 1991) or protein (Bukovsky *et al.* 1993), while granulosa cells display high abundance. This preovulatory *Lhcgr* expression pattern has been confirmed in isolated COCs and granulosa cells from mouse, bovine and equine (Eppig *et al.* 1997; Goudet *et al.* 1999; Robert *et al.* 2003). Highly purified LH is unable to stimulate cumulus expansion in isolated COCs while FSH does (Eppig 1979a; Eppig 1979b). The ovulatory stimulus therefore does not act directly on the cumulus cells but acts on the mural granulosa cells of the follicle, which then transmit the signal to the COC to undergo expansion and oocyte maturation. This secondary signal is now thought to occur via the rapid induction after the LH surge (within 1-3 hours) of Egf-like (Egf-L) ligands, epiregulin, amphiregulin and betacellulin, which are secreted by granulosa cells and transmit the ovulatory signal to the COC (Park *et al.* 2004; Sekiguchi *et al.* 2004). These peptides individually are able to induce COC expansion and the resumption of meiosis and inhibitors of the Egf receptor effectively block cumulus cell responses to the LH surge in rodents (Park *et al.* 2004; Ashkenazi *et al.* 2005). Further to this, these Egf-L ligands are able to induce cumulus cell matrix gene expression *Has2*, *Tnfaip6* and *Ptgs2* in isolated follicles in culture (Ashkenazi *et al.* 2005). Both amphiregulin and epiregulin are induced in human granulosa cells by treatment with LH (Freimann *et al.* 2004a; Freimann *et al.* 2004b). These Egf-L peptides are assumed to be functionally redundant since mice with null mutations of individual genes display normal fertility (Luetteke *et al.* 1999; Lee *et al.* 2004). The Egf-L peptides are synthesised in latent form as a transmembrane protein that requires cleavage prior to activation of receptors on cumulus cells, as treatment with protease inhibitors is able to block the LH induced response in cumulus cells (Dong *et al.* 1999; Ashkenazi *et al.* 2005). In other systems, activation of Egf-L peptides has shown to be mediated by the ADAM (A Disintegrin and Metalloprotease) family of metalloproteases (Dong *et al.* 1999; Hinkle *et al.* 2004). Recent evidence has shown that Adamts1 is able to proteolytically activate latent Egf-L peptides in a cancer cell line enabling the activation of the Egf receptor ErbB-2 (Liu *et al.* 2005). The protease required for activation of the ovulatory Egf-L peptides in the ovary is currently unknown, but is clearly a member of the metalloprotease family. Due to their similar spatial and temporal synthesis in granulosa cells, it is possible that Adamts1 cleaves and activates the Egf-L peptides in follicles following the LH surge. Thus, successful induction of Adamts1 may be critical for the activation of Egf-L peptides and subsequent oocyte maturation *in vivo*.

1.4.2 In vitro maturation (IVM) of oocytes

The *in vitro* maturation of mammalian oocytes is a useful procedure for studying oocyte and early embryo development. Additionally, in human assisted reproductive therapies, *in vitro* maturation (IVM) of oocytes is an appealing alternative, which could reduce the expense and risks associated with current ovarian hyperstimulation by hormonal treatment of women (Wang and Gill 2004). In current practice, women are typically administered high doses of exogenous gonadotropins to stimulate increased follicle growth and maturation of numerous oocytes *in vivo* prior to retrieval for *in vitro* fertilisation. However gonadotropin administration frequently leads to the development of ovarian hyperstimulation syndrome (OHSS), considered to be one of the most serious complications associated with assisted reproduction technology (Papanikolaou *et al.* 2006). Symptoms associated with OHSS include abdominal pain, nausea, vomiting, diarrhoea, weight gain, liver dysfunction and formation of blood clots which have in some cases led to death (Delvigne and Rozenberg 2002). The risk of OHSS is increased in women younger than 30, who have been diagnosed with polycystic ovarian syndrome (PCOS) or have high serum estradiol levels prior to the administration of the ovulatory stimulus, human chorionic gonadotropin (hCG) (Delvigne and Rozenberg 2002). In patients requiring fertility treatment with one or more of these risk factors, avoidance of excessive gonadotropin administration would be a safer alternative. Additionally, for couples seeking fertility treatment where male factor infertility is determined, these women could be spared the risk and expense of hormone therapy. *In vitro* maturation of oocytes requires minimal or no exogenous gonadotropin as maturation is carried out in culture. *In vitro* maturation involves the removal of the immature, unexpanded COC from antral follicles and culturing until nuclear maturation (metaphase II) is reached. However, the use of IVM has limitations as oocytes matured *in vitro* are of poorer quality (Wang and Gill 2004). When compared to *in vivo* matured oocytes, embryos derived from IVM oocytes have decreased cleavage rates, increased levels of embryo growth retardation and poor implantation and pregnancy rates (Greve *et al.* 1987; Barnes *et al.* 1996; Goud *et al.* 1998; Kim *et al.* 2000; Trounson *et al.* 2001; Wang and Gill 2004). The *in vitro* maturation of oocytes is utilised routinely in domestic species to generate embryos from unstimulated ovaries (Gilchrist and Thompson 2007), despite the lower developmental competence of the resultant embryos (Thompson *et al.* 1995; Rizos *et al.* 2002). The use of this technology for treatment of human infertility is not common practice due to the low success rates. Further understanding of the normal follicular environment in which oocytes develop and how IVM is deficient may lead to improved culture conditions and to increased developmental competence of IVM oocytes.

Under standard IVM conditions of mouse COCs in the presence of FSH or Egf and in conjunction with growth factors secreted by the oocyte, the induction of genes required for cumulus matrix formation such as *Has2* (Eppig 1979a; Salustri *et al.* 1989; Elvin *et al.* 1999; Dragovic *et al.* 2005), *Tnfaip6* (Fulop *et al.* 1997a; Yoshioka *et al.* 2000), *Ptx3* (Varani *et al.* 2002; Salustri *et al.* 2004) and *Ptgs2* (Joyce *et al.* 2001; Park *et al.* 2004) occurs. The critical organiser of the cumulus matrix, Iαl, is derived from addition of serum, generally fetal calf serum, and is adequately incorporated into the matrix during IVM (Chen *et al.* 1992). That these cumulus matrix components are induced, or included in the maturation media, demonstrates that current IVM conditions are conducive to the synthesis and formation of a COC matrix containing at least some of the components known to be critical for expansion and fertility (Section 1.3). It has not yet been determined however, whether Adamts1 and Versican are present and/or functional in the cumulus matrix of IVM complexes.

The cumulus complex surrounding oocytes is important for oocyte maturation and embryogenesis (Goud *et al.* 1998; Atef *et al.* 2005). Embryo quality from IVF of *in vivo* matured oocytes is correlated with cumulus expression of several ECM genes (McKenzie *et al.* 2004; Zhang *et al.* 2005). Cumulus cells also control critical energy metabolites in the oocyte environment (Eppig 2005; Sugiura *et al.* 2005), and limit exposure to excessive glucose which is detrimental to oocyte quality (Hashimoto *et al.* 2000; Colton *et al.* 2002; Sutton *et al.* 2003). Thus, the microenvironment maintained by cumulus cells and the cumulus matrix must influence oocyte maturation during IVM. While the formation and correct organisation of the COC matrix has shown to be critical for fertility, the role it plays during maturation is unknown.

1.5 FUNCTIONS OF THE EXTRACELLULAR MATRIX

Known functional properties of cumulus matrix components in other tissues can provide insight into their key roles in the cumulus oocyte complex. Extracellular matrix (ECM) provides tissues with their elasticity or tensile strength as well as acting as a scaffold to which cells can adhere and migrate. The ECM is composed predominantly of protein and carbohydrate molecules that interact with each other and with adjoining cells. Functions of the ECM include important roles in cell growth, migration and differentiation,

enabling joints and tissues to absorb large changes in pressure, acting as biological filters and being organisers of tissue structure and size.

The extracellular matrix is organised such that it generates a mesh with 'pores' of differing sizes, with increasing matrix concentration resulting in a decrease in pore size (Ogston and Sherman 1961); this quality would also be dependent on the degree of hydration and cross-linking between matrix molecules. These properties would influence the degree to which molecules can diffuse through the matrix. In addition, electrostatic charge of the matrix influences permselectivity as demonstrated by the glomerular glycocalyx (Reitsma *et al.* 2007). Evidence from *in vitro* models also demonstrates the functional capacity of the ECM to act as a molecular sieve including decreased diffusion of caffeine and glucose through a matrix of Hyaluronan (Ogston and Sherman 1961; McCabe 1972). Similarly, compared to water, glucose diffusion is decreased by 50% through the nucleus pulposus (Paulson *et al.* 1951), a proteoglycan rich component of the invertebral disc responsible for absorbing changes in pressure.

This evidence poses the possibility that following expansion, the cumulus matrix may also act as a biological filter, potentially regulating the diffusion and exposure of molecules to the oocyte. Indeed, ultrastructural analysis of the cumulus matrix has shown that it also is organised into a mesh like network (Cherr *et al.* 1990). A fully hydrated HA-rich matrix such as the COC matrix can be conceptualised as a tortuous network of pores between the ECM components through which large molecules must traverse in order to difuse through the space occupied by matrix. The degree of retardation on molecules attempting to diffuse through the cumulus matrix or 'mesh', would be expected to increase with the increasing concentration and structural organisation (or rigidity) of matrix.

The putative ability of cumulus matrix to filter small molecules or metabolites would be important in regulating, or limiting, exposure of the oocyte to signalling molecules or harmful substances. An example of the potential physiological relevance of such a functional property is the disparate requirements for glucose by cumulus cells and oocytes. The rapid induction of HA synthesis by cumulus cells is concomitant with an increase in glucose uptake and glucose flux through the hexosamine pathway to generate HA subunits (Sutton-McDowall *et al.* 2004; Sutton-McDowall *et al.* 2005; Harris *et al.* 2007). However, increased activity of the hexosamine pathway, as would occur in the presence of high glucose concentrations that exceed the metabolic flux, leads to decreased oocyte developmental

competence (Hashimoto *et al.* 2000; Sutton-McDowall *et al.* 2006; Thompson *et al.* 2007). The high demand and consumption of glucose by cumulus cells for HA production demonstrates the importance of sufficient glucose supply to the COC during IVM. In fact, during spontaneous oocyte maturation *in vitro* it has been shown that the presence of glucose is necessary for the completion of meiosis (Hashimoto *et al.* 2000). However, the exposure of oocytes to physiologically high glucose concentrations produces detrimental effects on developmental competence (Hashimoto *et al.* 2000; Colton *et al.* 2002; Sutton *et al.* 2003). Furthermore, while they are sensitive to high glucose, the oocyte relies upon metabolites of glucose synthesised in cumulus cells as their substrates for energy production through oxidative phosphorylation (Biggers *et al.* 1967; Leese and Barton 1985). The divergent glucose demands of cumulus cells and oocytes during maturation may be met through a regulatory role of the COC. In this model, glucose is rapidly absorbed and metabolised by cumulus cells, while diffusion across the COC is retarded by the matrix resulting in a steep gradient of glucose concentrations between the fluid around the COC and the oocyte at the centre. In support of this concept, following cumulus expansion *in vivo* there is a reduction in glucose uptake by the oocyte, which was thought to be, and likely is in part, a result of a loss in gap junction communication between cumulus cells and the oocyte (Saito *et al.* 1994), which occurs following the LH surge (Gilula *et al.* 1978; Larsen *et al.* 1986; Granot and Dekel 1994; Sela-Abramovich *et al.* 2005). However, molecular filtration properties of the cumulus matrix may contribute to the control of glucose in the oocyte environment.

In addition to glucose, lipophilic molecules are known to modulate oocyte maturation. These include steroids, such as progesterone and androgens (Smith and Tenney 1980; Eppig *et al.* 1983; Borman *et al.* 2004; Gill *et al.* 2004), and mesiosis activating sterol (FF-MAS), which improves nuclear maturation in human patients with polycystic ovary syndrome (Grondahl *et al.* 2000) and increases oocyte developmental competence in both mouse and pig (Marin Bivens *et al.* 2004; Faerge *et al.* 2006; Cukurcam *et al.* 2007). A putative role of the COC matrix controlling the rate at which the oocyte is exposed to lipophilic signalling molecules could also importantly regulate oocyte maturation.

1.6 POTENTIAL FUNCTIONS OF ADAMTS1 AND VERSICAN IN THE CUMULUS MATRIX

The matrix proteins, Adamts1 and Versican are abundantly present in the cumulus matrix during oocyte maturation *in vivo* (Russell *et al.* 2003a; Russell *et al.* 2003b). However, their functional significance during oocyte maturation, ovulation and fertilisation is unknown. Both Adamts1 and Versican proteins contain numerous domains and functional motifs and their importance during cumulus matrix expansion and oocyte maturation can be predicted but has yet to be elucidated.

1.6.1 Adamts1

1.6.1.1 Role of Adamts1 in fertility

As discussed previously, ablation of *Adamts1* results in reduced fertility as a result of reduced ovulation, fertilisation and on-time embryo development rates (Shindo *et al.* 2000; Mittaz *et al.* 2004; Russell *et al.* 2005). Women with polycystic ovary syndrome (PCOS) are anovulatory and the mechanisms responsible for this syndrome are not well characterised. However, it has been proposed that an altered expression of ECM components, including *ADAMTS1*, which is down regulated in PCOS, leads to a thickening of the ovarian capsule that is involved in the anovulatory phenotype (Jansen *et al.* 2004). This evidence demonstrates that Adamts1 is essential for optimal fecundity and is involved in the ovarian tissue remodelling processes required during folliculogenesis, ovulation and fertilisation. Additionally or alternatively, the decreased fertility rates of the *Adamts1* null mice may be attributed, in part, to a decrease in oocyte quality resulting from structural and functional insufficiencies in the COC matrix during maturation.

1.6.1.2 Adamts1 structure, function and ovarian expression

Based on homology with proteins of known function, the domains of Adamts1 are predicted to have proteolytic, adhesive, anti-angiogenic and cell signalling properties. Proteolytic activation of Adamts1

requires cleavage of the prodomain by furin (Kuno *et al.* 1999; Rodriguez-Manzaneque *et al.* 2000). In the ovary, both the pro- and mature forms of Adamts1 are increased, greater than 10-fold, following the LH surge with mRNA confined predominantly to the granulosa cell layer (Russell *et al.* 2003a). Pro-Adamts1 protein localises to granulosa cell cytoplasmic secretory vehicles (Russell *et al.* 2003a), while secreted mature, Adamts1 becomes selectively localised to the expanding COC matrix where it cleaves Versican (Russell *et al.* 2003a) (Figure 1.4 a). Adamts1 mediated cleavage may be important in modulating Versican function and is discussed later (Section 1.6.2.1).

Additional functions of Adamts1 may occur via its disintegrin domain, conserved among members of the reprolysin family of metalloproteases, Adamts1 lacks the core RGD/X motif, but a conserved cysteine arrangement implicates this region in interaction with integrins (Pfaff *et al.* 1994; Usami *et al.* 1994). The C-terminal TSP-1 domain may be involved in anchoring Adamts1 to the ECM and possibly in anti-angiogenic actions of the protein (Kuno and Matsushima 1998; Vazquez *et al.* 1999; Iruela-Arispe *et al.* 2003).

The domains of Adamts1 suggest it may function in the ovarian follicle through its adhesive, cell signalling and anti-angiogenic properties. Interestingly, mature Adamts1 localises to the surface of oocytes indicating that Adamts1 may be involved in oocyte-sperm fusion or other aspects of oocyte function or zona pellucida remodelling (Russell *et al.* 2003a). However, this observation requires confirmation utilising a technique other than immunohistochemistry, such as recombinant labelled protein. Other potential functions are likely to include proteolytic processing of COC matrix molecules during expansion, modulation of matrix adhesive properties and regulation of signalling between cumulus cells and/or the oocyte, most probably linking each of these processes simultaneously.

1.6.2 Versican

1.6.2.1 Versican structure, isoforms and ovarian expression

As discussed previously, Versican is a chondroitin sulphate proteoglycan containing multiple functional motifs. Versican consists of two globular domains, G1 and G3, separated by a glycosaminoglycan (GAG) domain where chondroitin sulphate attachment occurs. Differential splicing of the GAG domains generates four different isoforms; V0, V1, V2 and V3 (Shinomura *et al.* 1993; Dours-Zimmermann and

Zimmermann 1994; Ito *et al.* 1995; Zako *et al.* 1995). All isoforms, with the exception of V2, are expressed in the ovary, with V0 and V1 being predominant (Russell *et al.* 2003b). In the ovary, Versican expression is significantly upregulated in mGCs following the LH surge with Versican protein localising selectively to the matrix of the expanded COCs (Russell *et al.* 2003b) (Figure 1.4 b).

1.6.2.2 Versican function

The presence of large chondroitin sulphate (CS) chains in the GAG domain of Versican attract water, and steric interactions between HA and CS cause HA to extend and fill the pericellular space (Evanko *et al.* 1999). The CS moities also introduce a negative charge, which is able to attract and bind growth factors, cytokines and chemokines (Spivak-Kroizman *et al.* 1994). Glycosaminoglycans are able to generate a reservoir of growth factors, which allows and often enhances their presentation to cell surface receptors (Ruoslahti and Yamaguchi 1991; Tanaka *et al.* 1993). Versican may function similarly in the COC matrix, generating a growth factor reservoir and potentially controlling the spatial distribution and/or the timing of growth factor signalling in the COC.

Versican has demonstrated antioxidant properties, able to inhibit free radical induced apoptosis (Wu *et al.* 2005a). Free radicals, or reactive oxygen species (ROS), are generated during ovulation as well as in culture conditions where high concentrations of glucose and oxygen are present. The presence of Versican in the COC matrix may protect cumulus cells and the oocyte from oxidant damage during *in vitro* maturation and in the inflammatory response associated with ovulation *in vivo*.

Versican has demonstrated roles in the adhesion, migration and proliferation of cells through an interaction between cell surfaces and other matrix proteins (Zimmermann and Ruoslahti 1989). Conflicting functions of Versican include the anti and pro-adhesive functions of the G1 and G3 domains respectively (Ang *et al.* 1999; Yang *et al.* 1999; Wu *et al.* 2002; LaPierre *et al.* 2007). Adamts1 mediated cleavage of Versican, as occurs in the COC matrix *in vivo* (Russell *et al.* 2003a), results in a dissociation of the matrix cross-linking properties of the G1 and G3 domains, which would lead to an alteration in the ability of Versican to interact with other cellular components due to differing functions of both domains, thus modifying matrix structure and function. Incorporation of cleaved Versican product into the cumulus matrix may have an anti-adhesive function in releasing the expanded COC from the follicular wall.

However, the mechanism by which cleavage of Versican by Adamts1 affects COC expansion and concomitant oocyte maturation and ovulation remain to be demonstrated.

The Egf-like motifs present in the G3 domain of Versican promote cell proliferation (Zhang *et al.* 1998) and activate the Egf receptor (EgfR) and downstream signalling pathways (Xiang *et al.* 2006). In the ovary, activation of the Egf pathway is required for the induction of cumulus expansion and ovulation *in vivo* in response to the LH surge. As Versicans G3 domain is known to activate EgfRs, Versican may be involved in the induction of cumulus expansion and/or oocyte maturation through the activation of cumulus cell EgfRs. Further, evidence from studies of heart morphogenesis indicate that Versican cleavage generates activities not seen with intact Versican (Kern *et al.* 2007), Adamts1 mediated cleavage of Versican in COC matrix may allow an enhanced interaction of the Egf-like motifs with cell surface receptors (Figure 1.3 b). Both Adamts1 and Versican are selectively and intensively incorporated into the COC matrix *in* vivo (Figure 1.4) and at least Adamts1 is obligatory for fertility. What is not yet known is their function in the COC, or the key functions of this matrix that require Adamts1 and Versican.

1.7 SUMMARY, HYPOTHESES AND AIMS

Matrix gene expression and COC expansion are correlated with increased developmental competence of human oocytes and ablation of cumulus matrix genes results in subfertility or infertility. The expression of *Adamts1* and *Versican* mRNA following the LH surge *in vivo* is confined, primarily to the mural granulosa cell layer with the proteins localising to the expanded COC, indicating that these matrix components are derived from the granulosa cell layer of the periovulatory follicle. Given that oocytes matured by IVM display poor developmental competence, further studies are required to determine whether insufficiencies in the normal microenvironment of the maturing oocyte arise through a lack of requisite COC functions when removed from the follicle.

My general hypothesis is that the cumulus cells and matrix co-ordinately establish a specialised microenvironment that promotes optimal oocyte maturation.

Further studies are required to elucidate the role of cumulus matrix during oocyte maturation. It has not been determined whether cumulus gene expression and expanded matrix composition are maintained under IVM conditions. Some matrix components are principally products of mural granulosa cells:

> ***I hypothesise that oocyte in vitro maturation systems are deficient in components secreted by mural granulosa cells, specifically Adamts1 and Versican, and that this significantly impacts the functional integrity of the cumulus matrix.***

Based on studies in other systems of ECM with similar composition, potential functions of the COC matrix may include:

1) Control of the oocytes microenvironment. Oocytes are sensitive to glucose and delegate aspects of their metabolic needs to cumulus cells indicating their important role in controlling metabolites in the oocyte microenvironment. Given that *in vitro* and *in vivo* matrices in other biological systems demonstrate filtration properties, regulating the diffusion of small molecules, it is reasonable to propose that the COC matrix acts similarly. Whether the COC matrix is able to function in this manner has not been investigated.

I hypothesise that the COC matrix exhibits specific filtration properties and is capable of regulating the exposure of the oocyte to metabolites, growth factors and other signalling molecules.

2) Signalling actions of matrix components. Egf-like ligands produced by granulosa cells transduce the LH surge signal to cumulus cells inducing expansion, facilitating ovulation and may be a distinct requisite for full oocyte developmental competence. Versican C-terminal Egf-like domains can activate Egf receptor signalling pathways in other systems. Further, during embryonic heart development, proteolyic cleavage of Versican by Adamts1, as occurs in the expanding COC *in vivo*, leads to activities of Versican differing to that of the full length protein. Whether Versican has Egf-like activity on the COC, and whether modification by Adamts1 cleavage is involved in this function has not been investigated.

I hypothesise that the Egf-like properties of Versican will promote cumulus expansion in vitro and proteolytic cleavage by Adamts1 will further enhance this action.

Further elucidation of the role that Adamts1 and Versican play in the cumulus matrix will yield a better understanding of the role of cumulus matrix expansion in oocyte competence, and development of improved *in vitro* maturation conditions for oocytes.

1.8 AIMS AND HYPOTHESES

SPECIFIC HYPOTHESES AND AIMS

Hypothesis 1: Oocyte *in vitro* maturation systems are deficient in components secreted by mural granulosa cells that normally promote full oocyte competence.

To address this hypothesis the following aims were completed:

- Determine whether Versican and Adamts1 mRNA and protein are deficient in the matrix of cumulus oocyte complexes following *in vitro* maturation in the mouse.

- Determine whether Adamts1 and Versican are normally present in human cumulus and mural granulosa cells following *in vivo* maturation.

Hypothesis 2: The matrix of the expanded COC regulates the passage and supply of metabolites to the oocyte and this function is disrupted in the matrix of IVM COCs.

To address this hypothesis the following aims were completed:

- Establish assays for determining the passage of biological metabolites through the cumulus oocyte complex.

- Determine whether COC matrix can act as a biological filter, modulating the passage of hydrophobic and hydrophilic metabolites to the oocyte.

- Determine whether the filtration properties of the COC matrix is disrupted following *in vitro* maturation.

Hypothesis 3: Versican is a signalling factor in the COC able to promote cumulus expansion *in vitro*, an effect that is enhanced following cleavage by Adamts1.

To address this hypothesis the following aims were completed:

- Generate novel expression constructs of Versican and Adamts1 and optimise their expression and purification in a mammalian cell culture system.

- Determine the effect of exogenous Versican on cumulus expansion during *in vitro* maturation.

- Determine the effect of co-supplementation of Versican and Adamts1 on cumulus expansion during *in vitro* maturation.

Chapter 2

Materials and Methods

2.1 MATERIALS

Equine chorionic gonadotropin (eCG/Gestyl) was purchased from Professional Compounding Centre of Australia, (Sydney, NSW). Human chorionic gonadotropin (hCG/Pregnyl) was purchased from Organon, Australia (Sydney, NSW). Chondroitinase ABC was from Seikagaku (East Falmouth, MA). Secondary antibody (horseradish peroxidise-labelled goat-anti-rabbit) was purchased from Millipore (North Ryde, NSW, Australia). Plastic culture dishes were purchased from SARSTEDT Australia Pty. Ltd. (Adelaide, SA). Culture media was purchased from GIBCO, Invitrogen Australia Pty. Ltd. (VIC, Australia). All other reagents were purchased from Sigma-Aldrich Pty. Ltd. (Castle Hill, NSW, Australia) unless stated otherwise.

2.2 METHODS

2.2.1 Animals

All mice (F1 C57Bl/6 X CBA and *Adamts1* null mutant mouse line) were maintained on a 12 h:12 h day/night cycle with rodent chow and water provided ad libitum. All murine experiments were approved by the University of Adelaide's ethics committee and were conducted in accordance with the Australian Code of Practice for the Care and Use of Animals for Scientific Purposes.

2.2.2 Assessment of cumulus expansion

The degree of cumulus expansion of *in vitro* matured oocytes was assessed in 20 h IVM cultures by two independent blinded assessors using a scale previously described (Vanderhyden *et al.* 1990; Dragovic *et al.* 2005). Briefly, a score of 0 indicates no expansion of cumulus cells, +1 the most outer layers of cumulus cells expand; +2 expansion of the outer half of cumulus cells; +3 all layers expanded except the corona radiata; +4 expansion of all layers of cumulus cells (Figure 2.1). For each treatment a mean cumulus expansion index (CEI) (0.0-4.0) was calculated.

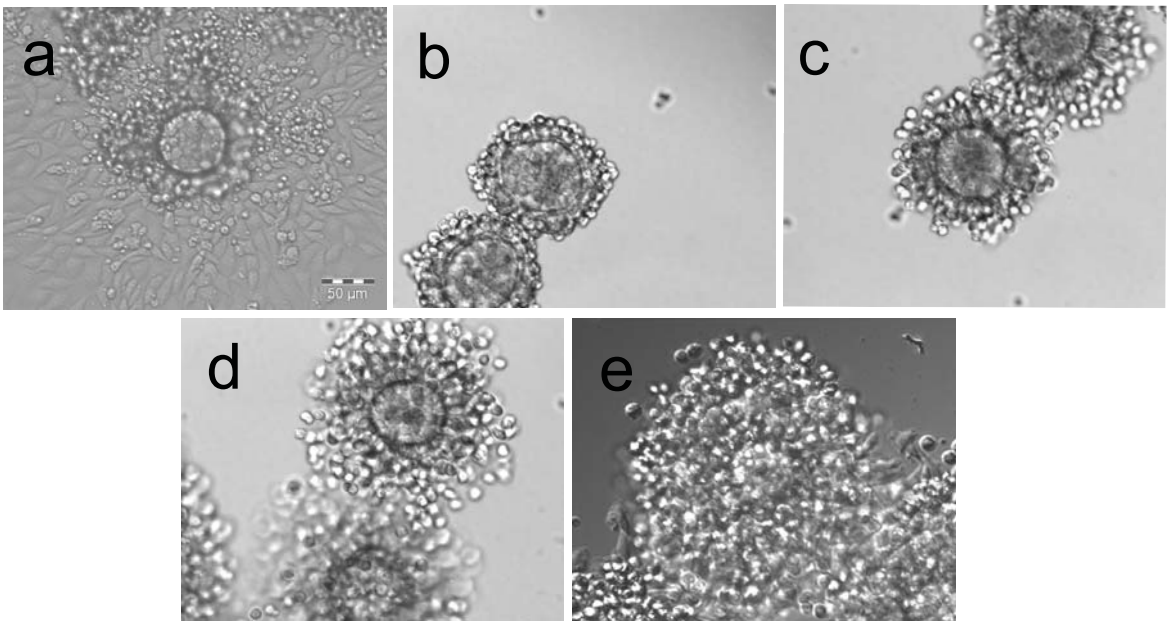

Figure 2.1 Example of scoring system used to assess cumulus expansion following *in* vitro maturation (IVM)

The degree of cumulus expansion of cumulus oocyte complexes (COCs) following 20 h of maturation was assessed by two independent blinded assessors using a scale previously described (Vanderhyden *et al.* 1990). Briefly, a score of 0 indicates no expansion with cumulus cells lost from the oocyte and adhering in a monolayer to the culture dish (a), +1 indicates no expansion however cumulus cells remain attached to the oocyte (b); +2 expansion of the outer half of cumulus cells (c); +3 all layers expanded except the corona radiata (d); +4 expansion of all layers of cumulus cells (e). For each treatment a mean cumulus expansion index (CEI) (0.0-4.0) was calculated. Scale bar = 50μm and all images captured at equivalent magnification.

2.2.3 Genotyping of *Adamts1* null mouse line

The *Adamts1* null mutant mouse line on a 129SvJ/C57Bl6 genetic background used in this study was described previously (Mittaz *et al.* 2004). Heterozygous female (*Adamts1*$^{-/+}$) and homozygous male (*Adamts1*$^{-/-}$) crosses were maintained on a 12 h:12 h day/night cycle with rodent chow and water provided *ad libitum*. All murine experiments were approved by The University of Adelaide's ethics committee and were conducted in accordance with the Australian Code of Practice for the Care and Use of Animals for Scientific Purposes. At days 19-22 of postnatal age, mice were weaned and tail tips were biopsied from anaesthetised mice. Genotyping of offspring was performed by PCR analysis of tail DNA. Genomic DNA was extracted from tail tip biopsies, by incubation at 55^{o}C for 1 hour (130rpm shaking) in buffer (10mM Tris-HCL pH 7.8, 75mM NaCl, 25mM EDTA, 1% (w/v) SDS) containing 0.16μg/μl Proteinase K. To the digested tails, 250μl of phenol chloroform was added and mixed followed by centrifugation at 13,000rpm for 10 minutes. Approximately 200μl of the upper, aqueous phase was transferred to a new tube and DNA was precipitated by adding 500μl of ice cold absolute ethanol. Precipitated DNA was pelleted by centrifugation at 13,000rpm for 20 minutes. The precipitated DNA was resuspended in 100μl of nuclease-free H_2O. The DNA was then used in two polymerase chain reactions using the oligonucleotide pairs shown in Table 2.1. The first PCR contained the primer pair 'Adamts1 ex2 (F)' and 'Adamts1 ex3 (R)' which spanned exons 2 and 3 (Figure 2.2 a). These primers amplified a product of 576bp from the wild type gene when exon 2 was present, indicating the progeny carried at least one wild-type allele (Figure 2.2 b, Lane 1). The second reaction contained the primer pairs 'Adamts1 KO (F)' and 'Adamts1 KO (R)', which spanned intron 1 and exon 3 (Figure 2.2 a). A product of 278bp was amplified when exon 2 was deleted (Figure 2.2 b, lanes 2 and 4), and an additional product of 1323bp was amplified in the presence of exon 2 (Figure 2.2 b, Lane 2). The amplification of the 278bp product from the primer pair 'Adamts1 KO (F)' and 'Adamts1 KO (R)' and no band in the reaction containing primer pair 'Adamts1 ex2 (F)' and 'Adamts1 ex2 (R)' indicated a homozygous *Adamts1*$^{-/-}$ progeny (Figure 2.2 b, Lanes 3 and 4). Genotyping PCRs contained 5μl 5X GoTaq Flexi® buffer (Promega Corporation, Annandale, NSW, Australia) 3mM $MgCl_2$, 0.5mM each dNTP, 5ng of each primer, 1.25 units of GoTaq® polymerase and H_2O to 25μl. Cycling conditions used were 94^{o}C, 5 minutes (1 cycle); 94^{o}C, 1 minute; 60^{o}C, 1 minute; 72^{o}C, 1 minute (35 cycles), 72^{o}C, 5 minutes (1 cycle). Amplified products were visualised by agarose gel electrophoresis (Section 2.2.4).

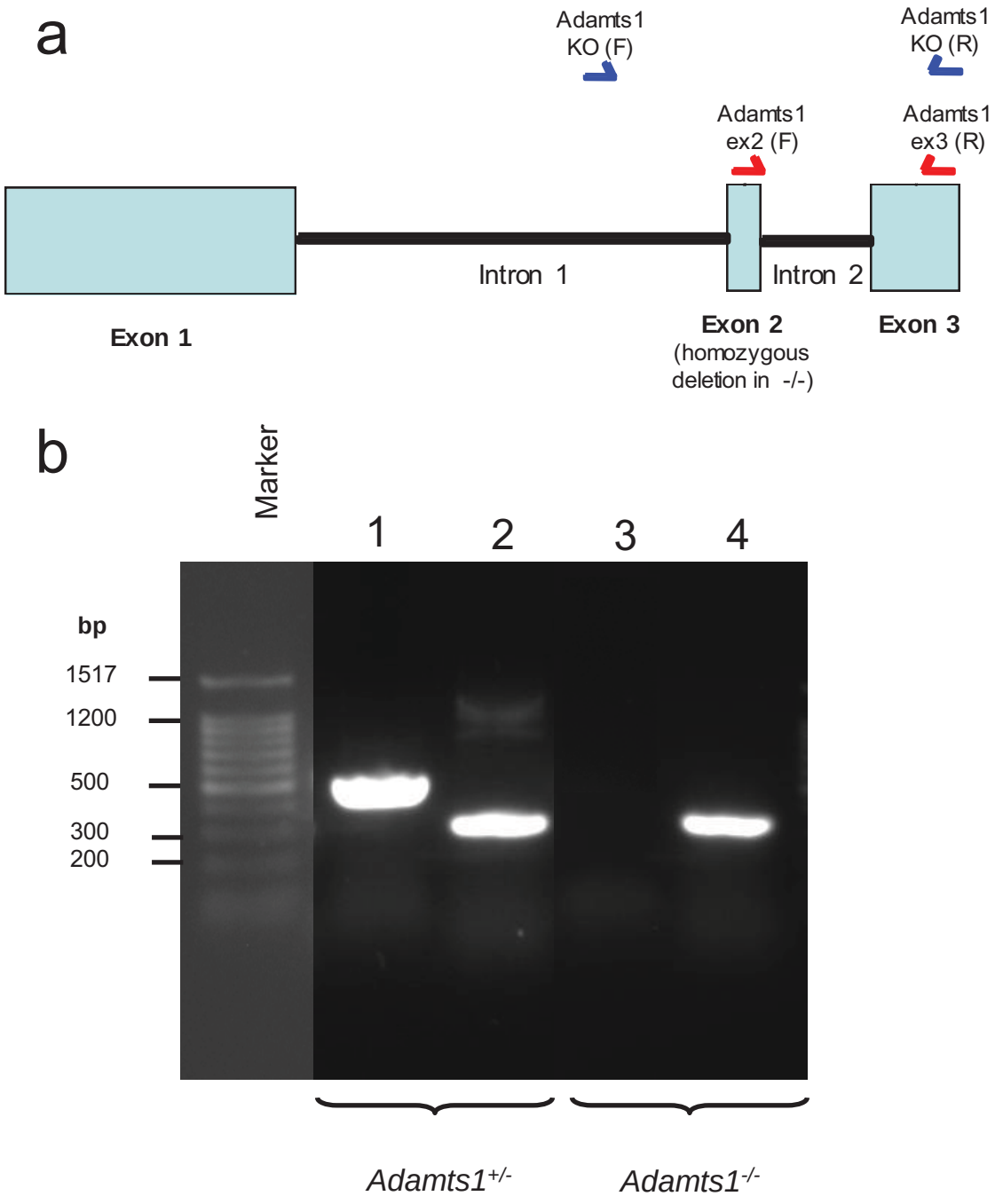

Figure 2.2 Genotyping of *Adamts1* mice.

(a) Schematic representation of the location of oligonucleotides utilised for genotyping in relation to 3 of the 9 coding exons of *Adamts1*. *Adamts1* null mice were generated by targeted deletion of exon 2 (Mittaz, *et al.* 2004). (b) Ethidium bromide stained 1% agarose / 0.5 X TBE gel showing PCR products generated using primer pairs Adamts1 ex2 (F) and Adamts1 ex3 (R) (lanes 1 and 3) and primer pairs Adamts1 KO (F) and Adamts1 KO (R) (lanes 2 and 4). Genotyping of a heterozygous offspring yielded PCR products as seen in lanes 1 and 2, while genotyping of an *Adamts1*$^{-/-}$ offspring produced the pattern seen in lanes 3 and 4.

Table 2.1 Oligonucleotide primers utilised for genotyping of *Adamts1* colony

Forward Primer	Sequence (5'-3')	Intron/Exon & nucleotide number (NC_000082.5)	Reverse Primer	Sequence (5'-3')	Intron/Exon & nucleotide number (NC_000082.5)	Predicted Product Size (bp)
Adamts1 ex2 (F)	AGTTACCTCCAATGCAGCTCTCA	Exon 2 (2893-2915)	Adamts1 ex3 (R)	ATCCCGAGAGTGTCACACGTG T	Exon 3 (3448-3469)	576
Adamts1 KO (F)	TCCTCAAGCCCCACCCCTTGG	Intron 1 (2181-2201)	Adamts1 KO (R)	TCCTGCTGGGGTCACATACAG	Exon 3 (3484-3504)	1323 (WT) 278 (KO)

2.2.4 Agarose gel electrophoresis

Restriction digests or PCR products were separated by agarose gel electrophoresis in a gel containing 1-2% (w/v) agarose (Promega Corporation, Annandale, NSW, Australia)/0.5X TBE (44.5mM Tris, 44.5mM Boric acid, 1mM EDTA pH8.0) and 2μg/ml Ethidium Bromide. Electrophoresis was performed in 0.5X TBE buffer at 100V. To each sample, 5X loading buffer (25% (v/v) glycerol, 50mM EDTA, 0.25% (w/v) bromophenol blue) was added to a final 1X concentration. To determine size and concentration of resolved DNA fragments the following DNA markers were utilised, SPP1/EcoRI and pUC19/HpaII (Geneworks, Adelaide Australia) and 100bp ladder (Promega Corporation, Annandale, NSW, Australia). Gels were visualised using a UV transilluminator and gel documentation system (Kodak DC120).

2.2.5 Western blotting

Proteins were separated on 4-15% Tris-HCl acrylamide gels (Bio-Rad Laboratories Pty. Ltd., Gladesville, NSW, Australia) and transferred to polyvinylidene difuoride (PVDF) membrane (Immobilon-P, Millipore, North Ryde, NSW, Australia). All Western gels included pre-stained protein molecular weight markers (Bio-Rad Laboratories Pty. Ltd., Gladesville, NSW, Australia).

2.2.6 Adamts1 and Versican immunoblotting

Membranes were blocked in TBST (10mM Tris (pH 7.5), 150mM NaCl and 0.05% Tween 20) containing 3% (w/v) non-fat milk for 1 h at room temperature. Membranes were then incubated with primary

antibodies for 1 h at room temperature in 3% milk/TBST. Primary antibodies were diluted at 1:5000 for α-Adamts1-MMP (Russell *et al.* 2003a) or 1:200 for α-JSCDPE (previously termed anti-DPEAAE) (Sandy *et al.* 2001). Blots were then washed in TBST and incubated with horseradish peroxidase-linked anti-rabbit IgG at 1:10000 (Millipore, North Ryde, NSW, Australia). Enhanced chemiluminescence detection was used as per manufacturer's instructions (Amersham Biosciences, GE Healthcare Life Sciences, Rydalmere NSW, Australia).

2.2.7 General methods for amplification and sub-cloning of *Adamts1* and *Versican* coding sequences

2.2.7.1 Polymerase Chain Reaction (PCR)

For PCR amplification of DNA for subcloning into recombinant expression vectors, the proof reading Platinum® Taq DNA Polymerase (Invitrogen Australia Pty. Ltd., Mt Waverley, VIC, Australia) was utilised. Typically, reactions were performed in a 50μl volume containing 1.0 unit of Platinum® Taq, 5μl 10X High Fidelity PCR Buffer, 0.2mM each dNTP, 2mM $MgSO_4$, 0.4μM each primer, 1-10ng of template DNA and adjusted to a total volume of 50μl with H_2O. Cycling conditions were as follows, 94°C 2 minutes (1 cycle), 94°C, 30 seconds; 55°C 30 seconds; 68°C, 1minute/per kb (25 cycles). PCR cycling was performed on a Gene Amp® ABI 9700 thermal cycler.

2.2.7.2 Restriction enzyme digests

Restriction enzymes were purchased from Promega Corporation (Annandale, NSW, Australia). Typically, restriction digests were performed in a 20μl reaction containing 200ng-1μg of DNA, 2-5U of the appropriate restriction enzyme, 2μl of the manufacturer's recommended 10X Buffer and sterile H_2O to 20μl. Digests were incubated in a dry block for 1-2 hours at 37°C and analysed by agarose gel electrophoresis (2.2.4) to verify restriction patterns or for gel extraction of appropriate fragment.

2.2.7.3 Removal of five prime phosphates

Five prime phosphates were removed from linearised plasmids to prevent re-circularisation during ligation. To a 20µl restriction digest reaction 10 units of Calf Intestinal Alkaline Phosphatase (CIP, New England Biolabs Inc., Ipswich, MA, USA) was added and incubated at 37°C for 30 minutes following the digest.

2.2.7.4 Precipitation of DNA

Impurities resulting from restriction digests were removed using phenol chloroform extraction followed by precipitation. This involved adjusting the volume to 100µl with H_20, to which an equal volume of phenol:chloroform:isoamyl (25:24:1) was added. This was mixed by vortexing and centrifuged at 13,000rpm for 10 minutes. The aqueous layer was removed to which a 1/10 volume of 3M Na Acetate pH5.2 and 3 volumes of ethanol was added and mixed by vortexing. The DNA was allowed to precipitate at room temperature for 1 hour then centrifuged at 13,000rpm for 1 hour. The supernatant was removed and the precipitated DNA resuspended in H_2O.

2.2.7.5 Ligations

Adamts1 and *Versican* coding sequences were PCR amplified and cloned into the p3xFLAG -CMV™-13 vector (Sigma-Aldrich Pty. Ltd, Castle Hill, NSW, Australia) as described in sections 5.2.1.1.1 and 5.2.1.1.2. Amplified PCR products were purified using the Wizard® Plus SV PCR Clean-Up System (Promega Corporation, Annandale, NSW, Australia), if a single product was visualised by agarose gel electrophoresis (2.2.4), the PCR insert was subjected to the appropriate restriction digest(s). The expression plasmid was subjected to the identical restriction digest procedure as the insert. Digested PCR products and plasmids were gel purified using the MinElute™ Gel extraction kit as per manufacturers' instructions (Roche Applied Science, Castle Hill, NSW, Australia). Ligations were performed by adding a 3:1 molecular ratio of insert:vector, 1 unit of T4 DNA ligase (Roche Applied Science, Castle Hill, NSW, Australia), 2µl 10X Ligation buffer (Roche Applied Science, Castle Hill,

NSW, Australia) and H_20 to 20μl and incubated at 16°C for 16 hours. Additionally, control ligations were performed containing vector only.

2.2.7.6 Transformation of E. coli

Plasmids were transformed into chemically competent E. coli XL1 – Blue Supercompetent cells (Stratagene, La Jolla, CA, USA) as per the manufacturers instructions. Briefly, sterile 1.5ml microfuge tubes were pre-chilled on ice. Chemically competent cells were thawed on ice and 10μl aliquoted into each tube followed by 0.2μl of (1.42M) β-mercaptoethanol. Following incubation on ice for 10 minutes, 0.1-50ng of plasmid DNA was added. The tubes were further incubated on ice for 30 minutes then heat-pulsed in a 42°C water bath for 45 seconds followed by incubation for two minutes on ice. The cells were resuspended in 900μl of 42°C SOC media (20g/L tryptone, 5g/L yeast extract, 0.5g/L NaCl, 10mM $MgCl_2$, 20mM glucose), transferred to 15ml sterile tubes and incubated at 37°C with aeration (230rpm) for 1 hour. The transformed E. coli were plated on LB-Agar plates (10g/L tryptone, 5g/L yeast extract, 5g/L NaCl, 15g/L agar) containing ampicillin (100μg/ml, Sigma-Aldrich Pty. Ltd, Castle Hill, NSW, Australia and incubated at 37°C for 16 hours.

2.2.7.7 Plasmid mini-preparations

Cells transformed with ligated plasmid-insert constructs were screened by performing small scale mini plasmid preparations using the Wizard® Plus SV Miniprep kit (Promega Corporation, Annandale, NSW, Australia). Single colonies were picked and inoculated into 2ml of Luria broth (LB, 10g/L tryptone, 5g/L yeast extract, 5g/L NaCl) containing 100μg/ml ampicillin (Sigma-Aldrich Pty. Ltd, Castle Hill, NSW, Australia) and incubated at 37°C with aeration for 16 hours (250rpm). From these cultures, 1.5ml was removed, bacteria were pelleted by centrifugation at 13,000rpm for 1 minute and the supernatant removed. The pellet was resuspended in 250μl of Cell Resuspension Solution followed by the addition of 250μl of Cell Lysis Solution and mixed by inversion. Alkaline Protease Solution (10μl) was added, mixed by inversion, incubated at room temperature for 5 minutes, followed by the addition of 350μl of Neutralization Solution and mixed by inversion. The bacterial lysate was centrifuged at 13,000rpm for 10 minutes. The supernatant was then added to the Spin Column, centrifuged at 13,000rpm and the flow through removed from the collection tube. The column was washed with 750μl of Column Wash

Solution, centrifuged again at 13,000rpm for 1 minute, followed by a second 250μl wash and centrifugation for 2 minutes. The spin column was transferred to a sterile 1.5ml microfuge tube and the plasmid DNA eluted using 30μl of sterile H_2O. Clones were subjected to diagnostic restriction digests followed by agarose gel electrophoresis to confirm the presence of ligated inserts. Positive colonies were sequenced to confirm error free and in-frame sequence of the expression constructs.

2.2.7.8 Plasmid midi-preparations

Single colonies containing expression constructs were grown on a large scale to produce ample amounts of high purity endotoxin-free plasmid DNA for transfection into mammalian cells. 2ml of inoculated Luria broth (LB, 10g/L tryptone, 5g/L yeast extract, 5g/L NaCl) containing 100μg/ml ampicillin (Sigma-Aldrich Pty. Ltd, Castle Hill, NSW, Australia) was incubated at 37°C with aeration for 8 hours (230rpm). From this 200μl was used to inoculate 100ml of LB (100μg/ml ampicillin) and incubated at incubated at 37°C with aeration (230rpm) for 16 hours. The bacteria were pelleted by centrifugation, 10,000xg 10 minutes and the supernatant discarded. Plasmids were purified using the Pureyield® Plasmid Midiprep System (Promega Corporation, Annandale, NSW, Australia) as per the manufacturers instructions. Briefly, the pelleted bacteria were resuspended in 3ml of Cell Resuspension Solution and 3ml of Cell Lysis Solution was added, mixed by inversion and incubated for 3 minutes at room temperature to allow for complete lysis of bacterial cells. Next, 5ml of Neutralization Solution was added and mixed by inversion and the solution centrifuged at 14,000xg for 30 minutes. The supernatant was then decanted onto a PureYield Binding Column and centrifuged at 1,500xg for 3 minutes. The Column was washed with 5ml of Endotoxin Removal wash and 20ml of Column Wash Solution with centrifugation between washes at 1,500xg for 5 minutes and removal of the flow though. A final centrifugation step was included, 1,500xg for 10 minutes to remove any residual ethanol from the washing solutions. The plasmid DNA was eluted with 200μl of sterile H_2O and centrifugation at 1,500xg for 5 minutes. The concentration and purity of plasmid preparations was determined using spectrophotometry, measuring the optical density of preparations at 260nm and 280nm.

2.2.7.9 Sequencing

Sequencing of plasmids was performed using BigDye Terminator 3.1 kit (Applied Biosystems, Scoresby, VIC, Australia). Sequencing reactions consisted of 190ng of plasmid DNA, 2.4pmol of designated primer, 0.4μl Terminator Ready Reaction Mix 3.1, 2μl of 5X Big Dye Sequencing Buffer and H_2O to 20μl. Cycling conditions used for sequencing were as follows, 96°C, 1 minute (1 cycle); 96°C, 10 seconds; 50°C, 5 seconds; 60°C 4 minutes (25 cycles). Sequencing products were precipitated by addition of 80μl of 75% isopropanol (v/v), brief vortexing and precipitation at room temperature for 15 minutes, followed by centrifugation at 13,000rpm for 20 minutes and removal of the supernatant. The pellets were washed with 250μl of 75% isopropanol (v/v) and re-centrifugated at 13,000rpm for 5 minutes. The supernatant was aspirated and residual isopropanol evaporated by incubating the tubes, with the lids open, in a 90°C heat block for 1 minute. Samples were analysed at the Molecular Pathology Sequencing Facility (Institute of Medical and Veterinary Science, IMVS, Adelaide Australia) by an ABI 3730 Capillary sequencer (Applied Biosystems, Scoresby, VIC, Australia). Resultant chromatograms were aligned and compared with published sequences for homology.

Chapter 3

Altered Composition of the Cumulus Oocyte Complex Matrix During *in vitro* Maturation of Oocytes

3.1 INTRODUCTION

In all mammals, the luteinizing hormone (LH)-surge initiates a sequence of events required to coordinate ovulation and maturation of the oocyte (Richards *et al.* 2002). Among these is cumulus expansion, whereby synthesis of Hyaluronan (HA) and several interacting extracellular matrix (ECM) proteins produces a unique visco-elastic matrix enveloping the cumulus oocyte complex (COC) (Russell and Salustri 2006). The cumulus cell matrix is essential for successful ovulation and fertilisation (Russell and Robker 2007) as exemplified by disruptions to these processes in response to null mutation of genes that either express or regulate expression of COC matrix components in mice (Lim *et al.* 1997; Robker *et al.* 2000; Zhuo *et al.* 2001; Varani *et al.* 2002; Ochsner *et al.* 2003). The degree of cumulus matrix expansion has also been correlated with oocyte developmental competence (Ball *et al.* 1983; Allworth and Albertini 1993; Chen *et al.* 1993; McKenzie *et al.* 2004).

Formation of the COC matrix requires cumulus cell expression of a number of matrix genes that are dependent on oocyte secreted growth factors in addition to induction by LH. Hyaluronan synthase 2 (*Has2*) is regulated in this way (Tirone *et al.* 1997; Su *et al.* 2004; Dragovic *et al.* 2005) and *Has2* expression has been correlated with developmental competence of the oocyte. Versican is a HA-binding proteoglycan that has distinct expression and regulation in the ovary. *Versican* mRNA has been localised to mouse mural granulosa cells (mGCs) after LH stimulation while the secreted protein localises to the ECM of the expanding COC (Russell *et al.* 2003b). Versican may function in the COC by binding HA via its N-terminal link protein-domain, while the C-terminal domains interact with cell surface proteins including sulphated glycolipids (Miura *et al.* 1999), heparan sulphate proteoglycans (Ujita *et al.* 1994), growth factor receptors (Xiang *et al.* 2006) and integrins (Wu *et al.* 2002).

Versican is a substrate for the protease Adamts1 (a disintegrin and metalloproteinase with thrombospondin motifs 1) (Sandy *et al.* 2001), and Adamts1 mediated Versican cleavage occurs in ovulating mouse COCs (Russell *et al.* 2003a). In the mouse COC Adamts1 accounts for more than 70% of all proteolytic activity against Versican (Russell *et al.* 2005) while Adamts4 may be responsible for the remaining cleavage (Russell *et al.* 2003a; Richards *et al.* 2005). The expression of *Adamts1* mRNA is induced in mGCs in response to the LH-surge in mice (Robker *et al.* 2000), rat (Espey *et al.* 2000), cow (Madan *et al.* 2003) and mare (Boerboom *et al.* 2003) and is strongly expressed in normal human ovaries (Jansen *et al.* 2004). Adamts1 deficient COCs also show significantly reduced rates of ovulation

(Mittaz *et al.* 2004) and fertilisation (Brown, Dunning, Russell, manuscript in preparation). Thus Versican in its intact and/or cleaved forms may alter the functional properties of the COC matrix during oocyte maturation, ovulation and/or fertilisation.

In human assisted reproductive therapies, *in vitro* maturation (IVM) of oocytes is an appealing alternative to exogenous gonadotrophin stimulation, as it reduces the expense and risks associated with infertility therapies (Wang and Gill 2004). However, the use of IVM has limitations as oocytes matured *in vitro* are of poorer quality (Wang and Gill 2004). When compared to *in vivo* matured oocytes, embryos derived from IVM oocytes have decreased cleavage rates, increased levels of embryo growth retardation and poor implantation and pregnancy rates (Greve *et al.* 1987; Barnes *et al.* 1996; Goud *et al.* 1998; Kim *et al.* 2000; Trounson *et al.* 2001; Wang and Gill 2004). The cumulus complex surrounding oocytes is important to oocyte maturation and embryogenesis (Goud *et al.* 1998; Atef *et al.* 2005). Embryo quality from IVF of *in vivo* matured oocytes is correlated with cumulus expression of several ECM genes (McKenzie *et al.* 2004; Zhang *et al.* 2005). Cumulus cells also control critical energy metabolites in the oocyte environment (Eppig 2005; Sugiura *et al.* 2005), and prevent exposure of the oocyte to glucose, which is detrimental to oocyte quality (Hashimoto *et al.* 2000; Colton *et al.* 2002; Sutton *et al.* 2003). Thus, the microenvironment maintained by cumulus cells and their ECM influences oocyte maturation during IVM.

I hypothesised that the IVM COC is deficient in components secreted from mGCs that normally form a part of the microenvironment of maturing oocytes, specifically Versican and Adamts1. To determine whether Versican and Adamts1 are deficient in IVM COCs we analysed the expression and protein levels both during *in vivo* and *in vitro* maturation of mouse COCs. Additionally, we determined whether these matrix components are normally present in human cumulus and mGCs following *in vivo* maturation.

3.2 MATERIALS AND METHODS

3.2.1 Isolation and culture of cumulus oocyte complexes

For IVM, COCs were isolated from pre-pubertal 23-day-old F1 C57Bl/6 X CBA mice 44-48 h after i.p. injection of 4IU eCG. COCs were washed in complete MEM (alpha MEM media supplemented with 5%

(v/v) fetal calf serum (FCS), 0.25 mM Sodium Pyruvate (GIBCO, Invitrogen Australia Pty Ltd, VIC, Australia) and penicillin G (100U/ml), streptomycin sulphate (100mg/ml)) and cultured in groups of 30 in 37^{o}C, 5%CO_2, 95% air for either 6 or 20 h in drops of 100μl of complete MEM media with suitable treatments and overlaid with sterile mineral oil (Sigma-Aldrich Pty. Ltd, Castle Hill, NSW, Australia). Culture treatments involved media supplemented with either 50mIU/ml recombinant human FSH (Sigma-Aldrich Pty. Ltd, Castle Hill, NSW, Australia) or 3ng/ml Egf (Sigma-Aldrich Pty. Ltd, Castle Hill, NSW, Australia) or both Egf and FSH at the same doses.

Expression analysis was performed following 6 h or 20 h of IVM culture. After 6 h the expression of *Adamts1*, *Versican* and *Has2* have previously been shown to be strongly upregulated in the ovary (Fulop *et al.* 1997b; Robker *et al.* 2000; Ochsner *et al.* 2003; Russell *et al.* 2003b), while 20 h IVM culture has previously been shown to be the time for completion of oocyte maturation *in vitro* (Eppig 1979b; Downs 1989). Groups of 30 COCs were harvested for RNA isolation after 6 h or 20 h of culture. Gene expression at these times was compared to *in vivo* matured COCs obtained following 6 h, 12 h (preovulatory) or 16 h (postovulatory) hCG treatment. *In vivo* matured COCs were obtained from pre-pubertal mice treated with i.p. administration of eCG (4IU) followed after 44 h by hCG (5IU) and collected after 6 h or 12 h (preovulatory) or 16 h (postovulatory). Preovulatory mGC and COCs were collected by puncture of large antral follicles with a 26-gauge needle to release cells. COCs were cleaned of large adherent masses of mGCs before collection for RNA or protein isolation. Ovulated COCs (16 h after hCG) were isolated by puncture of the ampulla of the oviduct. Corresponding mGCs were also collected for RNA or protein isolation by puncture of the large follicles, cell pellets were snap frozen and stored at -80ºC for later mRNA or protein extraction and PCR or Western blot analysis as described below.

3.2.2 Isolation of human cumulus and granulosa cells

Ethical approval for the use of human samples was obtained from the Women's and Children's Hospital Human Research Ethics Committee, Adelaide Australia. Informed written consent for the use of cumulus and mural granulosa cells was obtained from couples undergoing infertility treatment at Repromed, Dulwich, South Australia. Patients with clinical indications of polycystic ovarian syndrome were not included in this study. Of the 14 patients included in the study (average age 34.5±3.7 years),

infertility was attributed to male factor (n=5), tubal defects (n=4), or unexplained (n=5). When patients began their menstrual cycle, they were administered daily FSH (150-300IU, Gonal-F, Serono or Puregon, Organon, NSW, Australia) and following 8-14 days, patients with a minimum of 3 follicles of >18mm diameter observed by transvaginal ultrasound scans were scheduled for oocyte retrieval. Following this observation, women were administered 10,000IU hCG (Pregnyl, Organon, NSW, Australia), after 36 h follicles were aspirated transvaginally. Following this procedure all patients yielded 8-23 COCs. All patients had successful fertilisation, with average 60±30% of oocytes fertilised (76% for ICSI n=5, or 52% for IVF n=9). Fifty percent of patients achieved pregnancy from a single embryo transferred in this round of treatment, indicated by fetal heartbeat after 8-weeks. We obtained matched cumulus and mural granulosa cell pairs from follicular aspirates at the time of oocyte retrieval. Cumulus cells were isolated from COCs by either manual trimming of the outer cumulus cell mass before IVF (n=9), or hyaluronidase treatment of COCs before ICSI for the five patients with male factor infertility. These different cell collection regimens showed no significant differences in the expression of *VERSICAN*, *ADAMTS1* or *HAS2*. Mural and cumulus cells were stored as cell pellets at –80^{o}C until RNA isolation was performed.

3.2.3 Real time RT-PCR

Total RNA was isolated using Trizol (Invitrogen Australia Pty. Ltd., Mt Waverley, VIC, Australia), as per manufacturer's instructions, with the inclusion of 7.5μg Blue Glycogen (Ambion, Applied Biosystems, Scoresby, VIC, Australia) during precipitation. Total RNA was then treated with 1U of DNase as per manufacturer's instructions (Ambion, Applied Biosystems, Scoresby, VIC, Australia). First strand complimentary DNA (cDNA) was synthesised from total RNA (350 or 400ng) using random hexamer primers (Geneworks, Hindmarsh SA, Australia) and Superscript III reverse transcriptase (Invitrogen Australia Pty. Ltd., Mt Waverley, VIC, Australia).

Specific gene primers for real time RT-PCR were designed against published mRNA sequences (Table 3.1 and 3.2) using Primer Express software (PE Applied Biosystems, Scoresby, VIC, Australia) and synthesised by Sigma Genosys (Sigma-Aldrich Pty. Ltd, Castle Hill, NSW, Australia). Primer pairs and sequences for murine *Adamts1*, *Versican*, *Has2* and *RpL19*, and human *ADAMTS1*, *VERSICAN*, *HAS2* and *RPL19* are listed in Tables 3.1 and 3.2 respectively. Primer sequences that detect human V1

VERSICAN splice variant and human *ADAMTS1* were described previously (Corps *et al.* 2004; Cross *et al.* 2005). Real time RT-PCR was performed in triplicate for each sample on an ABI GeneAmp 5700 sequence detection system (PE Applied Biosystems, Scoresby, VIC, Australia). In each reaction, 2μl of cDNA (equivalent to 10ng of total RNA), 0.2μl of forward and reverse primers, 10μl of SYBR Green master mix were added and H_2O to a final volume of 25μl. All primers were used at a concentration of 50μM with the exception of human V1 *VERSICAN* primers, which were used at 25μM and human *ADAMTS1*, which were used at 6.25μM. PCR cycling conditions were 50°C for 2 min, 95°C for 10 min, followed by 40 amplification cycles of 95°C for 15 seconds and 60°C for 1 min. Controls included omission of the cDNA template or RT enzyme in otherwise complete reaction mixtures; each showed no evidence of product amplification or primer dimers. *Adamts1*, *Versican* and *Has2* gene expression were normalized to *RpL19*-internal control and *ADAMTS1*, *VERSICAN* and *HAS2* gene expression were normalized to *RPL19* all were then expressed relative to calibrator samples using the $2^{-(\Delta\Delta CT)}$ method (K. Livak PE-ABI, Sequence Detector User Bulletin 2) (Livak and Schmittgen 2001). Results for each PCR were normalized to the calibrator, which was given the arbitrary value of 1. For murine *Versican* and *Adamts1*, real time RT-PCR, the calibrator was RNA from mGCs after eCG + hCG 12 h *in vivo* treatment. For *Has2* the calibrator was COCs after eCG + hCG 6 h *in vivo* treatment. For human V1 *VERSICAN*, *ADAMTS1* and *HAS2* real time RT-PCR, the calibrator was RNA from the human cell line 293T. Following real time RT-PCR, analysis of the dissociation curves confirmed that a single product was amplified in all reactions.

Table 3.1 Murine Real Time Primer Sequences

Gene	Primer Name	Amplicon size (bp)	Sequence (5'-3')	Accession no.
Adamts1	ADAMTS1 F	148	TGATAAGTGTGGCGTTTGTGG	NM_009621
Adamts1	ADAMTS1 R		CCCCCTTTGATTCCGATGT	NM_009621
Cspg2	Versican F	143	CTTTGCTCATCGACGCACAT	XM_488510
Cspg2	Versican R		TGTCATTGAGGCCGATCCA	XM_488510
Has2	Has2 F	104	CAGACCTTCTCACATGCACAATGAG	NM_008216
Has2	Has2 R		TCAGTTACAGTTCGCCCATGTAAAC	NM_008216
Rpl19	L19 F	103	TTCCCGAGTACAGCACCTTTGAC	NM_009078
Rrpl19	L19 R		CACGGCTTTGGCTTCATTTTAAC	NM_009078

Table 3.2 Human Real Time Primer Sequences

Gene	Primer Name	Amplicon size (bp)	Sequence (5'-3')	Accession no.
ADAMTS1	hADAMTS1F	89	GCACTGCAAGGCGTAGGAC	NM_006988
ADAMTS1	hADAMTS1 R		AAGCATGGTTTCCACATAGCG	NM_006988
VERSICAN (V1)	hV1 F	122	TGAGAACCCTGTATCGTTTTGAGA	X15998
VERSICAN (V1)	hV1 R		CTGAATCTATTGGATGACCAATTACAC	X15998
RPL19	hL19 F	79	CATGCCAAATGGACCAATGTC	NM_014763
RPL19	hL19 R		TGCTCAGGTTCCATGCTCATTA	NM_014763

3.2.4 Western blot

In two replicate experiments, protein extracts from COCs and mGCs were prepared by homogenisation in 0.05M sodium acetate, 6M urea and 0.1% Triton buffer and protease inhibitors (0.1M EDTA, 5 mM benzamidine, 0.005M phenylmethylsufonyl fluoride, 10 IU/ml aprotinin and 10μl/ml Sigma protease inhibitor cocktail (Sigma-Aldrich Pty. Ltd, Castle Hill, NSW, Australia). Protein concentrations were determined by Bradford assay (Bio-Rad Laboratories Pty. Ltd., Gladesville, NSW, Australia). Samples were chondroitinase treated by diluting 1:5 in 0.4M sodium acetate, 0.1% BSA and 0.4M Tris-HCl, pH 8.0 containing 0.02U/ml chondroitinase ABC and incubated for 1hr at 37˚C. The equivalent of 21 COCs was loaded for each treatment. For granulosa cell extracts, collected at the same time as *in vivo* matured COCs, the protein quantity loaded was equalised to the respective COC sample to allow comparison of the relative abundance of Adamts1 and Versican in each tissue compartment. Proteins were separated by SDS-PAGE and immobilised on polyvinylidene difuoride (PVDF) membrane as per section 2.2.5 and immunoblotting performed using antibodies directed against Adamts1 and the neoepitope generated by Adamts1 cleavage of Versican (DPEAAE) (2.2.6). The bands detected by Western blot were quantitatively analysed using QuantityOne (BioRad, Regents Park, NSW, Australia) software and expressed arbitrarily as values of relative density.

3.2.5 Statistical analysis

Murine real time RT-PCR expression analysis and cumulus expansion experiments were performed in triplicate and analysed by performing a One-Way ANOVA and a Tukey *post hoc* test using SPSS version 13 (SPSS, Chicago, IL, USA). A p value <0.05 was considered statistically significant. For the human real time RT-PCR experiments, the expression of each gene was assessed between cumulus and mural granulosa cells using a t-test. Differences were considered significant at a P value less than 0.05.

3.3 RESULTS

3.3.1 Induction of *Adamts1* and *Versican* mRNA in IVM vs *in vivo* matured cumulus complexes.

The degree of cumulus expansion was assessed (Section 2.2.2) to determine whether IVM conditions were optimal. As expected, COCs cultured without Egf or FSH stimuli failed to undergo COC matrix expansion (mean CEI = 0.82, Figure 3.1) while consistently high cumulus expansion indices (CEI) were observed for COCs treated with EGF (3ng/ml, CEI = 3.6), FSH (50mIU/ml, CEI = 3.4) or EGF + FSH (3ng/ml +50mIU/ml, CEI = 3.4), with no significant differences in CEI between the stimulation regimens (Figure 3.1). These experiments demonstrate that our *in vitro* maturation conditions were optimal and able to replicate previous observations (Downs 1989; Vanderhyden *et al.* 1990; Park *et al.* 2004).

Expression of *Adamts1* and *Versican* mRNA were induced by 6 and 24-fold respectively in COCs after 6 h hCG treatment *in vivo* compared to COCs from eCG only treated mice (Figure 3.2, a and b). However, after IVM treatment for 6 h there was no significant induction of either *Adamts1* or *Versican* by FSH, Egf or their combination. The level of *Adamts1* or *Versican* expression in IVM COCs was 10 and 15-fold lower respectively after 6 h of culture than in COCs after 6 h *in vivo* hCG treatment. *In vivo* stimulated COCs had ~40% lower expression of *Adamts1* and *Versican* compared to mGCs collected at the same time, but this difference was not significant.

Robust cumulus expansion in response to all IVM stimuli indicates that the IVM conditions were optimal. However, to more quantitatively compare and confirm the response of cumulus cells to stimulation *Has2* expression was compared after IVM and *in vivo* treatments (Figure 3.2 c). As expected, culture of COCs

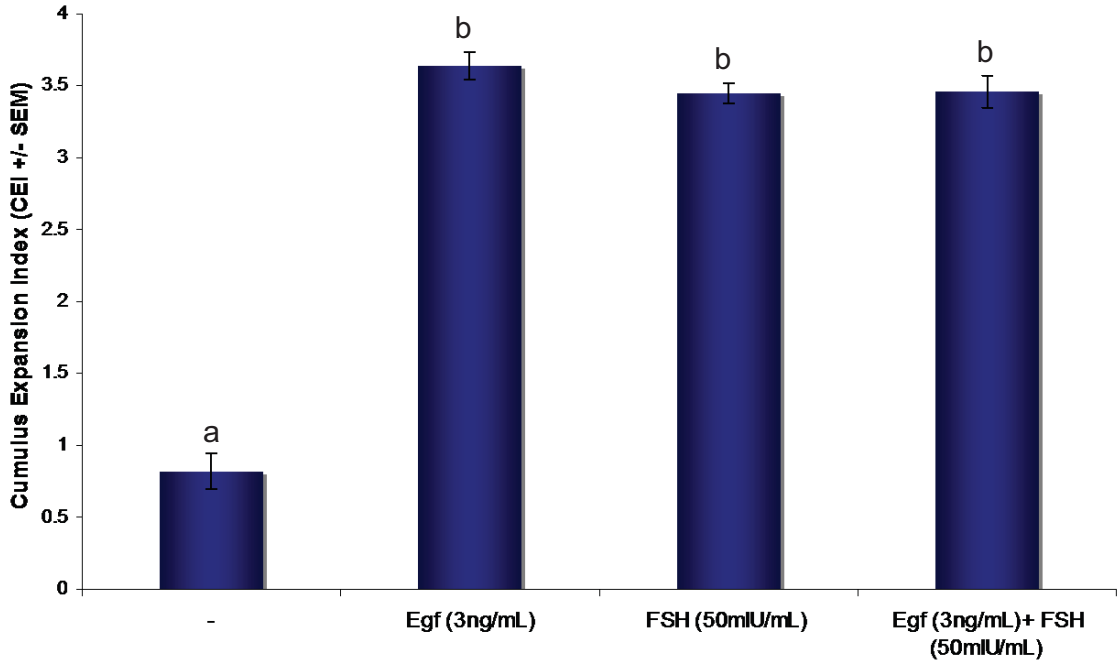

Figure 3.1 High degree of cumulus expansion was demonstrated with all treatment regimes.

Cumulus Oocyte Complexes (COCs) were cultured in the presence of Egf (3ng/mL), FSH (50mIU/mL), Egf (3ng/mL) + FSH (50mIU/mL) or no stimulus (-) at 37ºC/5%CO_2/95%air for 20 h. The data is expressed as mean +/-S.E.M. (n = 3 independent experiments).

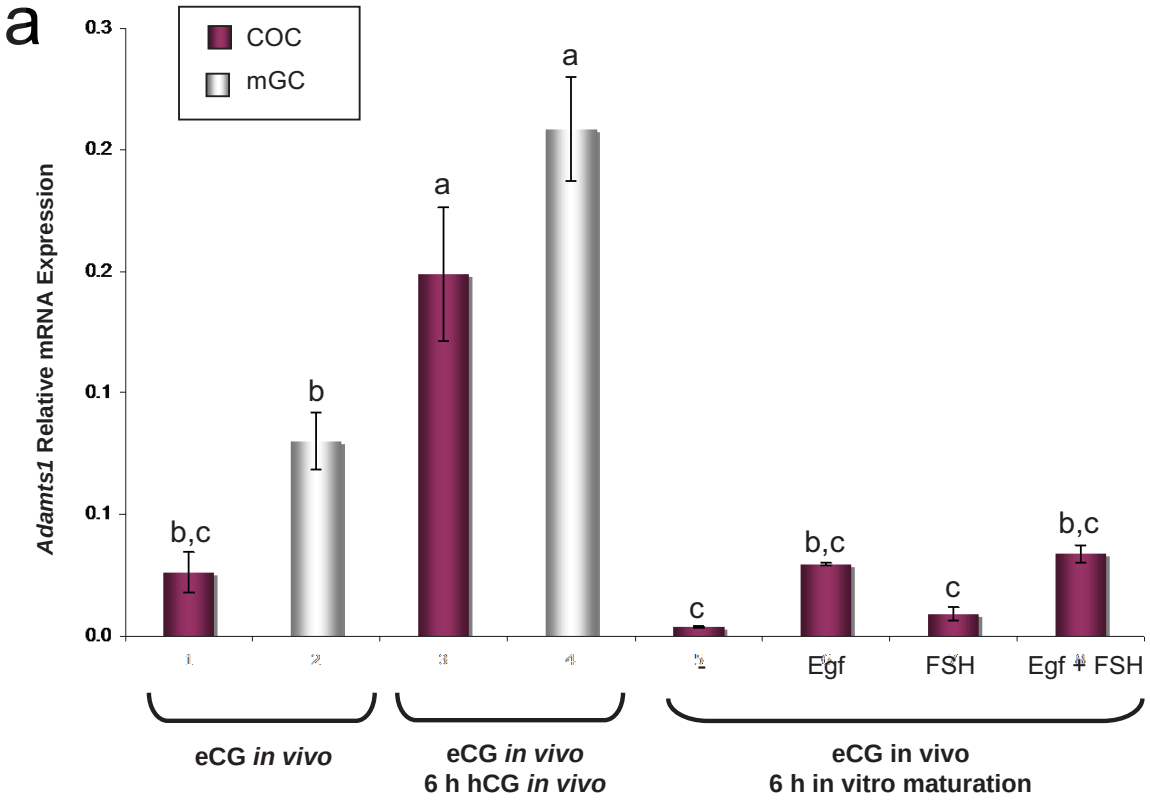
a
COC
mGC
Adamts1 Relative mRNA Expression
0.3
0.2
0.2
0.1
0.1
0.0
b,c
b
a
a
c
b,c
c
b,c
Egf
FSH
Egf + FSH
eCG in vivo
eCG in vivo
6 h hCG in vivo
eCG in vivo
6 h in vitro maturation

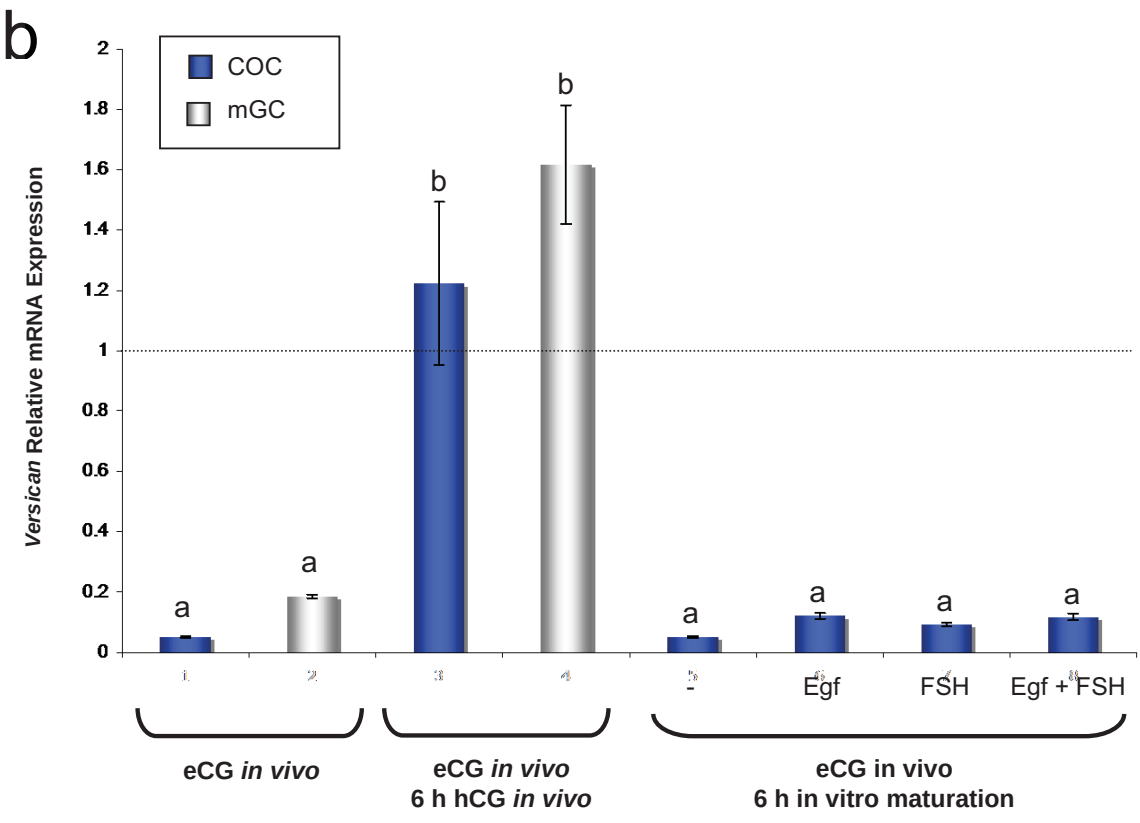
b
COC
mGC
Versican Relative mRNA Expression
2
1.8
1.6
1.4
1.2
1
0.8
0.6
0.4
0.2
0
a
a
b
b
a
a
a
a
Egf
FSH
Egf + FSH
eCG in vivo
eCG in vivo
6 h hCG in vivo
eCG in vivo
6 h in vitro maturation

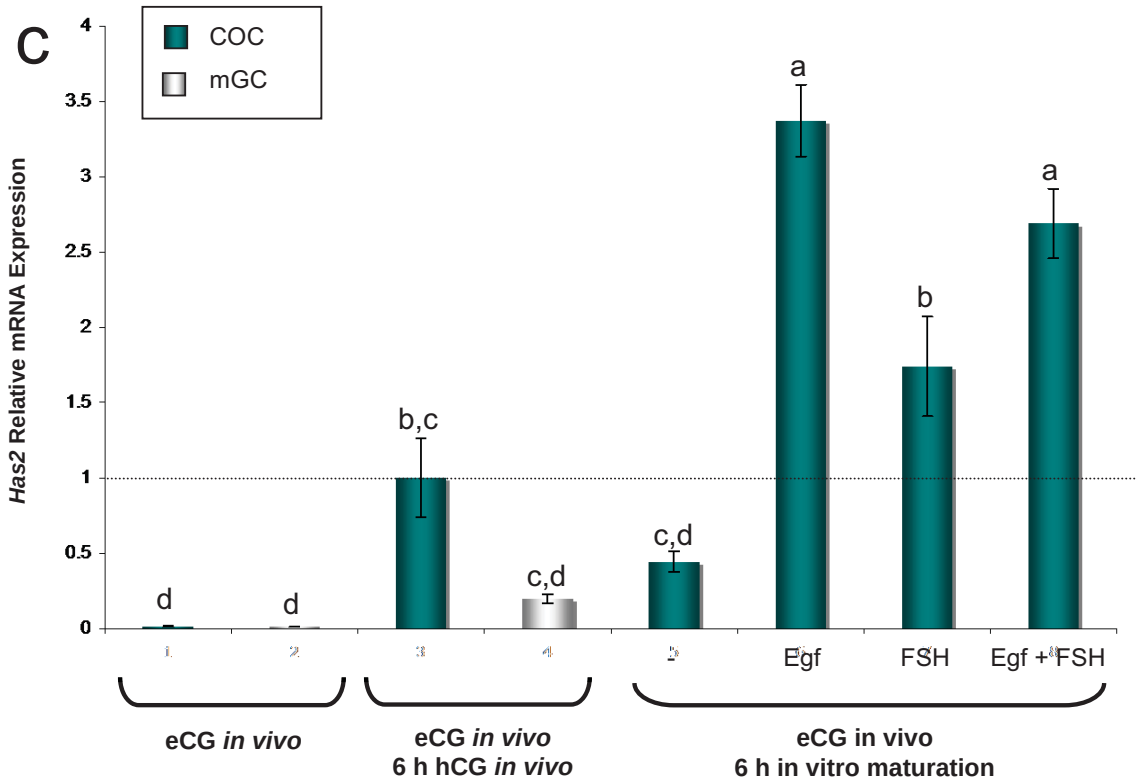

Figure 3.2 Induction of *Adamts1* and *Versican* mRNA *in vivo* but not *in vitro* in response to 6 h oocyte maturation stimuli.

Analysis of mRNA expression in mural granulosa cells (mGCs) or cumulus oocyte complexes (COCs) from equine chorionic gonadotrophin 44 h (eCG) stimulated mice after 6 h of maturation by *in vivo* hCG treatment or IVM culture with Egf, FSH or a combination of the two. The mRNA expression of (a) *Adamts1* (b) *Versican* and (c) *Has2* is normalized to the *Rpl19* internal control and presented as mean ± S.E.M. (n=3 independent experiments). (a) *Adamts1* and (b) *Versican* are expressed relative to the calibrator (mGCs treated *in vivo* with eCG + 12 h hCG), which was set at 1. (c) *Has2* is expressed relative to the calibrator (COCs treated *in vivo* with eCG + 6 h hCG), which was set at 1. Bars with different characters are significantly different ($P<0.05$).

for 6 h without stimuli caused a small, non significant induction of *Has2* expression when compared to COCs that were not cultured however, maturation of COCs *in vitro* through treatment with either Egf, FSH or Egf + FSH significantly increased *Has2* expression 8, 4 and 6-fold respectively over the untreated control and 240, 120 and 200-fold over the expression in COCs prior to culture. The *in vivo* induction of *Has2* mRNA after 6 h of hCG treatment was 70-fold increased over the non-cultured control COC, and was significantly lower than the induction in Egf treated IVM COC (Figure 3.2 c).

To determine whether *Adamts1* and *Versican* expression is simply delayed under IVM conditions, mRNA levels were examined in IVM cultures after 20 h, which is the accepted time required for complete expansion and maturation *in vitro* (Eppig 1979b; Downs 1989; De La Fuente *et al.* 1999) (Figure 3.3). Expression levels of both *Adamts1* and *Versican* in IVM COCs were negligible and similar to immature control COCs after eCG treatment alone (Figure 3.3). In contrast expression for both *Adamts1* and *Versican* were markedly induced in COCs matured *in vivo* for 12 h (21- and 16-fold respectively) or 16 h (3- and 5-fold respectively) compared to immature control COCs. The level of *Adamts1* and *Versican* mRNA in mGCs was significantly higher than in COCs from the same follicles after 12 h hCG (2 and 1.3-fold respectively).

3.3.2 *In vitro* matured cumulus oocyte complexes are deficient in Adamts1 protein, as well as intact and cleaved Versican.

To verify our observations of mRNA expression, we compared protein abundance of Adamts1, Versican and the 70kDa Versican cleavage product generated by Adamts1 action (Russell *et al.* 2003a). Western blot analysis was performed following 20 h of *in vitro* maturation as this has previously been shown to be sufficient time for complete matrix synthesis *in vitro* (Eppig 1979b; Downs 1989). This was compared to COCs and mGC obtained immediately pre- or post-ovulation (12 h or 16 h hCG respectively) as it has previously been shown that expanded COCs shortly following ovulation *in vivo* have the equivalent amount of Hyaluronan per cell as *in vitro* expanded COCs (Salustri *et al.* 1992). Abundant intact ~350kDa Versican was present in COC and mGC extracts after hCG 12 h treatment (Figure 3.4 a, Lanes 4 and 6) but not detectable in COCs from eCG treated mice (Figure 3.4 a, Lane 1). There was no detectable full length Versican in COCs cultured without stimulus (Lane 2) or treated for 20 h with Egf (Lane 3). The 70kDa cleavage product of Versican has been verified as predominantly an Adamts1

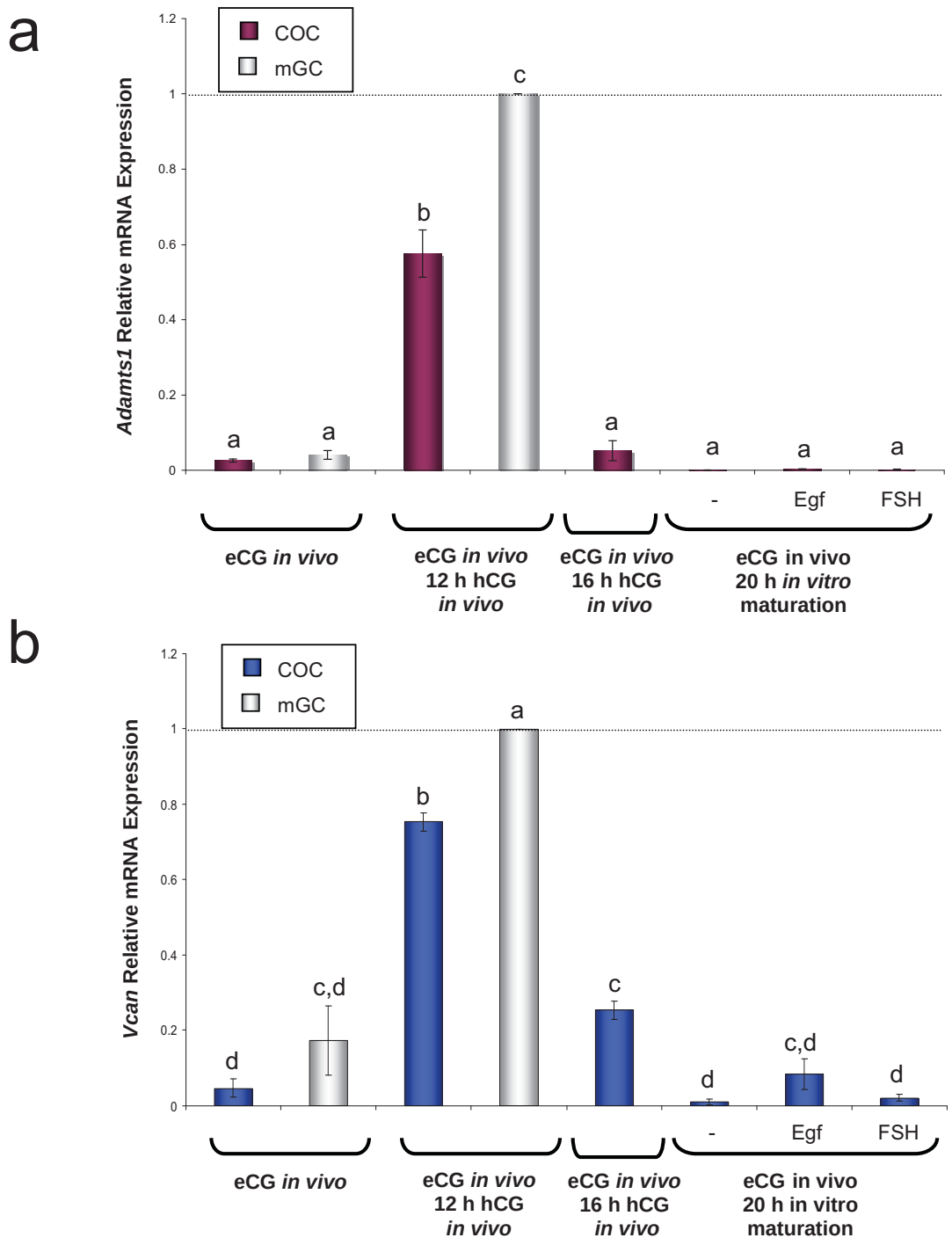

Figure 3.3 Induction of *Adamts1* and *Versican* mRNA *in vivo* but not *in vitro* in response to 20 h oocyte maturation stimuli.

Analysis of mRNA expression in murine mural granulosa cells (mGCs) or cumulus oocyte complexes (COCs) stimulated for 12 or 16 h *in vivo* by hCG treatment or in IVM culture with Egf or FSH for 20 h. The mRNA expression of (a) *Adamts1* and (b) *Versican* is normalized to the *Rpl19* internal control and presented as mean ± S.E.M. (n=3 independent experiments). (a) *Adamts1* and (b) *Versican* are expressed relative to the calibrator (mGCs treated *in vivo* with eCG + 12 h hCG), which was set at 1. Bars with different characters are significantly different ($P<0.05$).

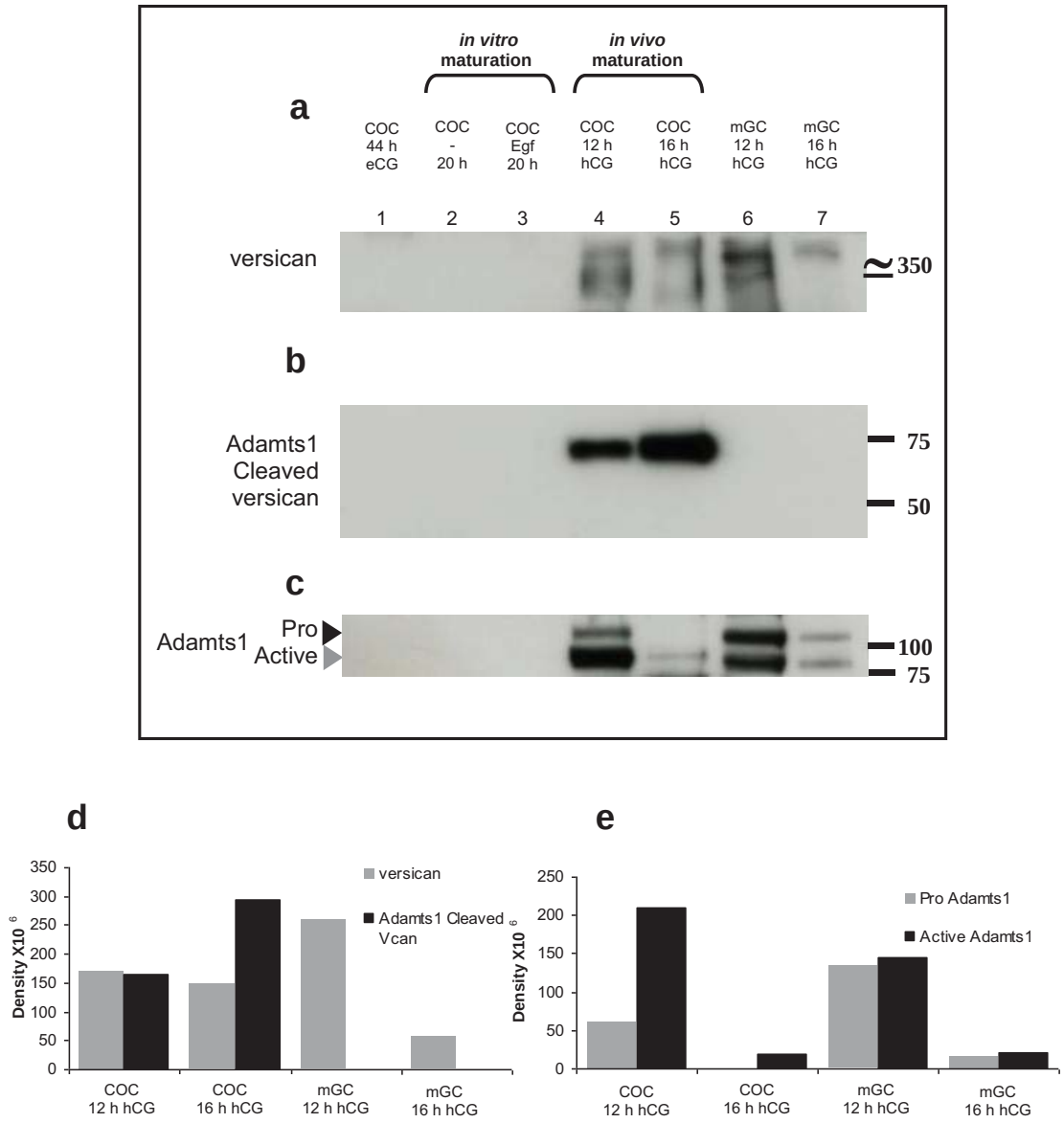

Figure 3.4 Protein abundance of Adamts1 and Versican after IVM or *in vivo* stimulation.

Adamts1 and versican protein were analyzed by Western blot in mural granulosa cells (mGCs) and cumulus oocyte complexes (COCs) after *in vitro* maturation (IVM) or *in vivo* stimulation**.** The equivalent of 21 COCs from 3 mice was loaded for each treatment. For mGCs the protein quantity loaded was equalized to the respective COC sample. The blot was probed with antibodies that detect full length versican (a), the ectodomain DPEAAE generated by Adamts1 cleavage of versican (b), or Adamts1 pro- and active isoforms (c) as described in *Materials and Methods*. Molecular weight marker sizes (kDa) are indicated to the right of the Western blot. Quantified intensities of each protein are shown in d and e. (d) shows relative intensities of full length and cleaved versican bands. (e) Relative intensity of pro- and active Adamts1. Data shown is from one representative of two replicate experiments with identical results.

generated cleavage product in COCs (Russell *et al.* 2003a) and was detected specifically in COCs after 12 and 16 h hCG treatment (Figure 3.4 b, Lanes 4 and 5). Adamts1 cleaved Versican was more abundant in COCs following ovulation (Figure 3.4 b, Lanes 4 and 5 and Figure 3.4 d), however this Versican fragment was undetectable in mGCs (Figure 3.4 b, Lanes 6 and 7). Likewise, the cleaved Versican fragment was undetectable in untreated COCs after culture or IVM COCs (Lanes 2 and 3 respectively, Figure 3.4 b). In accordance with the presence of cleaved Versican, active Adamts1 of 85kDa was most abundant in *in vivo* matured COCs (Figure 3.4 c, Lanes 4 and 5 and Figure 3.4 e). The active protease was 3.4-fold predominant over the pro-protein (110kDa) after 12 h hCG *in vivo* treated COCs (Figure 3.4, Lane 4 and Figure 3.4 e), and in COCs collected from oviducts 16 h after hCG, only active Adamts1 was detectable (Figure 3.4, Lane 5 and Figure 3.4 e). In mGCs from the same follicles pro- and active Adamts1 were present in equal abundance (Figure 3.4 c, Lanes 6 and 7 and Figure 3.4 e). Both the mature and precursor forms of Adamts1 were absent in COCs after eCG-treatment only. Importantly, COCs cultured either without stimulation or Egf stimulated IVM COCs contained no detectable Adamts1 protein (Lanes 1, 2 and 3, Figure 3.4 c).

3.3.3 *ADAMTS1* and *VERSICAN* mRNA in human cumulus and mural granulosa cells

Expression of *ADAMTS1* and *VERSICAN* mRNA was investigated in human cumulus and granulosa cells collected from women undergoing assisted reproduction. In matched cumulus and mural granulosa cell samples from 14 patients, *ADAMTS1*, *VERSICAN* and *HAS2* mRNA were abundantly present (Figure 3.5). The expression of *HAS2* mRNA was significantly 4.3-fold higher in cumulus cells than their matched mural granulosa cell pairs, confirming the purity of each isolated cell type. Interestingly, *VERSICAN* mRNA was also significantly 8.2-fold higher in cumulus cells than in the mural compartment (Figure 3.5). Expression of *ADAMTS1* at this time showed similar abundance of mRNA in both cell compartments.

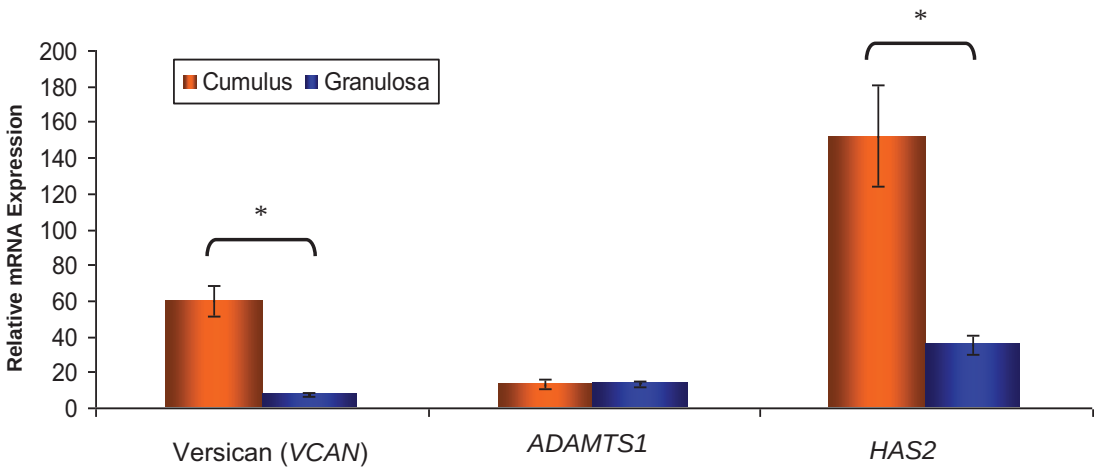

Figure 3.5 *ADAMTS1*, *VERSICAN* and *HAS2* mRNA are expressed in human cumulus and granulosa cells after *in vivo* stimulation.

Real Time RT-PCR analysis of mRNA for *ADAMTS1*, *VERSICN* (V1 isoform) and *HAS2* in paired human cumulus and mural granulosa cells. The data is expressed as mean ± S.E.M. and normalized to *RPL19* (n=14 patients). *ADAMTS1*, *VERSICAN* (V1 isoform) and *HAS2* are expressed relative to the calibrator (293T cells, human embryonic kidney), which was set at 1. Asterix indicate significant difference (P<0.0005).

3.4 DISCUSSION

Maturation of oocytes *in vitro* deprives them of the normal follicular environment, including potentially important secretions from the mGCs and results in reduced developmental potential when compared to *in vivo* maturation (Combelles *et al.* 2002; Wang and Gill 2004; Combelles *et al.* 2005). In the present study we have shown that murine COCs matured by IVM are deficient in the matrix components, Adamts1 and Versican, normally abundant in COCs *in vivo*.

The expression of *Adamts1* and *Versican* was upregulated within 6 h following hCG administration both in COCs and mGCs reaching maximal levels at 12 h and 6-12 h respectively as previously reported for mGCs (Robker *et al.* 2000; Russell *et al.* 2003b). However, mouse COCs undergoing IVM for either 6 or 20 h show no significant induction of *Adamts1* or *Versican* mRNA after FSH and/or Egf treatment compared to untreated cultures. These COCs had 10-500 fold lower expression compared to COCs from eCG/12 h hCG treated mice. This result demonstrates that *in vivo* there is a considerable cumulus cell induction of *Adamts1* and *Versican* while in IVM with FSH and/or Egf stimuli this normal gene induction is deficient. The same IVM COCs showed a strong and significant induction of *Has2* mRNA, as frequently reported (Dragovic *et al.* 2005). Has2 expression was even greater after 6h IVM than that seen after 6 h stimulation *in vivo* confirming that the signal transduction and cumulus gene induction pathways were activated under all IVM conditions. Previously it has been suggested that *Adamts1* and *Versican*, are predominantly expressed in the mGC layer and not the cumulus cells *in vivo* (Robker *et al.* 2000; Russell *et al.* 2003b). However, the *in situ* hybridisation technique used previously has a less sensitive threshold than the quantitative PCR of the current study in which both genes were strongly detected in COCs. We did however, confirm that at the peak of induction (eCG/12 h hCG) *Adamts1* and *Versican* expression were significantly greater in mGCs than COCs, consistent with reports that *Adamts1* gene promoter is responsive to LH as well as progesterone receptor mediated transactivation (Robker *et al.* 2000; Doyle *et al.* 2004b). These two pathways are also selectively mGC expressed genes in mouse preovulatory follicles (Eppig *et al.* 1997; Robker *et al.* 2000). Furthermore, a spatial pattern of pro-Adamts1 protein predominantly produced in mGCs and the secreted active protease predominant in COCs was confirmed here as previously reported (Russell *et al.* 2003a). This spatial pattern indicates that mGCs are the primary site of Adamts1 synthesis in mouse follicles *in vivo*. We conclude that both *Adamts1* and *Versican* are LH-responsive genes predominantly expressed in mGCs, but also induced in mouse COCs *in vivo*.

After 36 h hCG stimulation, human *VERSICAN* and *HAS2* were predominantly cumulus expressed genes. The pattern of human *VERSICAN* expression appears to vary slightly from that in mouse follicles, with a greater abundance of mRNA present in human cumulus than mural cells. This may be due to differences in collection time points following administration of ovulatory stimuli or may indicate intrinsic differences in the mechanisms of cumulus expansion between these species with Versican being predominantly cumulus expressed in human follicles. In contrast, *ADAMTS1* mRNA was equivalent in both cumulus cells and mGCs following stimulation, similar to the expression in mouse follicles. Overall, this evidence suggests that ADAMTS1 and VERSICAN are involved in human COC expansion and maturation as in mice, but whether cumulus *VERSICAN* and *ADAMTS1* expression are induced normally during human IVM needs further investigation.

That these gene products of the normal *in vivo* COC environment are absent in IVM indicates that full *in vivo* responsiveness of the COC in IVM is insufficient and the environment around the maturing oocyte may correspondingly be functionally inadequate. Whether Adamts1 and Versican play essential roles in the maturation of oocytes, either direct or indirect, is not yet known, but there are at least two potential mechanisms by which this may occur. Firstly, it is known that Versican can modulate growth factor receptor interactions (Wu *et al.* 2004), and that Versican and its cleavage products have Egf-like signaling activity (Xiang *et al.* 2006). Additionally, Adamts1 modulates activity of growth factors including VEGFs, FGFs and the Egf-like factors (Luque *et al.* 2003; Liu *et al.* 2006; Suga *et al.* 2006), and modulates Versican action in the developing heart (Kern *et al.* 2007). In maturing COCs Adamts1 cleaves Versican (Russell *et al.* 2003a) but may also act on heparin sulphate bound Egf and amphiregulin as demonstrated in cell lines (Liu *et al.* 2006). The action of Egf-like growth factors is emerging as critical to acquisition of full oocyte competence (see review by Russell and Robker 2007). Thus, alteration to the normal oocyte-somatic interactions mediated by growth factors in the absence of Adamts1 and/or Versican is likely to be detrimental to IVM oocyte quality. Secondly, Versican may modulate cellular responses to reactive oxygen species (ROS) associated with the inflammatory properties that occur during ovulation *in vivo,* and during IVM where culture conditions lead to an increase in ROS which in bovine IVM has a negative impact on embryo development (Luvoni *et al.* 1996; Hashimoto *et al.* 2000). The antioxidant properties of pericellular Versican, as described in other culture systems (Wu *et al.* 2005a), may protect cumulus cells and oocytes from exposure to free radicals.

Our findings show that mouse COCs matured *in vitro* are deficient in both Adamts1 and Versican mRNA and protein, unlike *in vivo* matured COCs. Human *in vivo* matured COCs normally express these factors also, although whether this expression is deficient in human IVM conditions remains to be empirically addressed. The dramatically altered matrix environment of IVM oocytes is likely to contribute to the poor health of embryos derived from IVM. The relationship between this expression as a marker of oocyte quality as well as the effects of supplementation of Adamts1 and Versican on IVM success is the subject of further investigation.

Chapter 4

Cumulus Oocyte Matrix Function during Oocyte Maturation and Ovulation

4.1 INTRODUCTION

While the formation of the expanded cumulus oocyte complex (COC) matrix is well described in many species, and commonly used in selection of the best quality oocytes in ART, the function of this matrix is not well understood. Our limited understanding of its functional roles suggest the COC matrix is important during ovulation, for transport through the oviduct and at fertilisation. However, the role it plays in oocyte maturation is relatively unknown. The cumulus matrix is clearly critical for fertility, as repeatedly observed in mice with null mutations in genes that express or regulate the expression of cumulus matrix components (Table 1.1) (Davis *et al.* 1999; Robker *et al.* 2000; Shindo *et al.* 2000; Sato *et al.* 2001; Zhuo *et al.* 2001; Varani *et al.* 2002; Mittaz *et al.* 2004; Salustri *et al.* 2004). Many of these null mouse models exhibit impaired or disrupted cumulus expansion (Davis *et al.* 1999; Hizaki *et al.* 1999; White *et al.* 2000; Zhuo *et al.* 2001; Varani *et al.* 2002; Fulop *et al.* 2003) as well as reduced ovulation rates indicating a key role in these processes (Table 1.1). Further to this, they exhibit significant reduction in fertilisation rates, due in some cases to the cumulus matrix being a critical participant in sperm interactions. Additionally, or alternatively, the reduced fecundity observed in these mice may be a result of decreased oocyte quality. The functional role of the cumulus oocyte matrix and the mechanism by which these null mutations in matrix genes result in impaired fertility is largely unknown.

The difference between *in vitro* (IVM) and *in vivo* matured COC matrix (Chapter 3), affords the opportunity to assess the functional consequences of the compositional insufficiency observed in IVM COCs. The abundance of the matrix proteins, Adamts1 and Versican in mouse COCs following *in vivo* maturation but their complete absence following IVM (Chapter 3), led to the investigation of potential functional properties of the COC matrix and the consequences of an altered IVM matrix.

Cumulus expansion requires rapid synthesis of HA by cumulus cells (Eppig 1979a; Salustri *et al.* 1989) that is sustained by an increase in glucose uptake and glucose flux through the hexosamine pathway to synthesise HA subunits (Sutton-McDowall *et al.* 2004; Sutton-McDowall *et al.* 2005; Harris *et al.* 2007). At the same time increased vasculature permeability around follicles allows a large influx of blood plasma components including glucose into the follicle (Koos 1995; Katayama *et al.* 2003). The high requirement and consumption of glucose by cumulus cells for the production of HA and subsequent

cumulus expansion demonstrates the importance of ample glucose supply to the COC. In addition, glucose is able to regulate the rate of meiotic resumption and progression and oocyte developmental competence (Hashimoto *et al.* 2000; Colton *et al.* 2002; Sutton-McDowall *et al.* 2005; Sutton-McDowall *et al.* 2006). However, the exposure of oocytes to high physiological glucose has detrimental effects on developmental competence (Hashimoto *et al.* 2000; Colton *et al.* 2002; Sutton *et al.* 2003).

The high requirement for glucose by cumulus cells and the negative effects it exerts on oocyte developmental competence led us to hypothesise that cumulus expansion, specifically the production of the highly organised cumulus oocyte matrix, has the capacity to regulate the exposure of the oocyte to small metabolites, both hydrophilic and lipophilic in nature. In support of this concept, following cumulus expansion *in vivo* there is a reduction in glucose uptake by the oocyte (Saito *et al.* 1994). This has previously been thought to occur due to the loss of gap junctions between cumulus cells and the oocyte (Saito *et al.* 1994), which occurs following the LH surge (Gilula *et al.* 1978; Larsen *et al.* 1986; Granot and Dekel 1994; Sela-Abramovich *et al.* 2005). We hypothesised that this observation is also modulated through the molecular filtration properties of the cumulus matrix and that permselectivity of the COC matrix extends to hydrophilic molecules such as glucose and lipophilic compounds including steroids and sterols. Lipophilic molecules with known functional roles in the oocyte include steroids, such as progesterone and androgens, which are known to modulate oocyte maturation (Smith and Tenney 1980; Eppig *et al.* 1983; Borman *et al.* 2004; Gill *et al.* 2004) and meiosis activating sterol (FF-MAS), which has been shown to improve nuclear maturation in human patients with polycystic ovary syndrome (Grondahl *et al.* 2000) and increase oocyte developmental competence in both mouse and pig (Marin Bivens *et al.* 2004; Faerge *et al.* 2006; Cukurcam *et al.* 2007). Limitation on the normally high diffusion of these compounds by the cumulus matrix may facilitate an organised pattern substrate supply important for function of the COC as a unit and for optimal oocyte maturation.

At the molecular level the extracellular matrix can be considered as actively moving rods generating a mesh. The higher the concentration of the matrix, the tighter the meshwork becomes (Ogston and Sherman 1961). The degree of cross-linking between matrix molecules would additionally influence rigidity and other functional qualities of the meshwork. Both these parameters will also determine the ability of small molecules to diffuse through the matrix, with the degree of retardation expected to increase with increasing concentration of matrix. Indeed, in an *in vitro* model system, it has been demonstrated that the diffusion rate of glucose through Hyaluronan decreased as the concentration of

the matrix increased (Ogston and Sherman 1961). Thus, extracellular matrix networks have a defined ability to hinder the passage of molecules through them, working as a molecular sieve (Laurent 1995). For example, the diffusion rate of caffeine, a hydrophilic low molecular weight molecule, is reduced by 50% in a matrix of hyaluronate at a concentration much lower than that present in some tissues (McCabe 1972). Another well established example is the nucleus pulposus of the vertebrae, a proteoglycan rich matrix containing Versican (Sztrolovics *et al.* 2002), which has jelly-like properties and functions to distribute pressure over the invertebral discs under compression (Humzah and Soames 1988). The diffusion of glucose through the nucleus pulposus is 50% slower than its diffusion rate through water (Paulson *et al.* 1951). These *in vitro* and *in vivo* matrices demonstrate the ability of matrix to dramatically hinder the passage of small metabolites, including glucose and caffeine. On the basis of its composition, I hypothesized that the expanded COC matrix also forms a meshwork with the capacity to modulate diffusion rates of small molecules. Furthermore, the disparate requirements for glucose in cumulus cells and oocytes suggest that appropriate cumulus and oocyte cell function may require fine spatial control on metabolite concentrations. The combination of restrained diffusion and disparate glucose consumption in cumulus cells and oocytes would result in a concentration gradient with highest solute concentrations on the COC exterior and lower concentrations on the interior. Thirdly, I hypothesized that the filtration properties of the matrix would be altered in IVM COCs, due to the lack of key ECM components.

I investigated the passage of; glucose and cholesterol, to the oocyte in immature and *in vivo* matured COCs by assessing uptake of fluorescently labelled analogues by cumulus and oocyte compartments of the COC. Cholesterol was used here as a simple marker for the transport of other lipophilic molecules known to influence meiotic progression and developmental competence such as progesterone, androgens, prostaglandins and FF-MAS. To determine whether altered matrix composition after IVM changes the filtration properties, glucose and cholesterol diffusion were compared in IVM versus *in vivo* matured COCs. Using COCs from *Adamts1* null mice the importance of Versican cleavage by Adamts1 on the molecular sieving property of the COC matrix was also investigated.

4.2 METHODS

4.2.1 Isolation and Culture of Cumulus Oocyte Complexes (COCs)

Progeny from the *Adamts1* null mutant mouse line were genotyped as described in section 2.2.3. *In vivo* matured COCs were obtained from female pre-pubertal 21-25-day-old *Adamts1*$^{-/+}$ and *Adamts1*$^{-/-}$ mice treated with i.p. administration of eCG (5IU) followed 48 h later by hCG (5IU). Mice were culled by cervical dislocation at 16 h post hCG, ovaries were removed, placed in complete MEM (αMEM media supplemented with 5% (v/v) fetal calf serum (FCS), 0.25 mM sodium pyruvate (GIBCO, Invitrogen Australia Pty. Ltd., Mt Waverley, VIC, Australia) and post-ovulatory COCs collected from oviducts by blunt dissection. For isolation of periovulatory COCs, mice were culled by cervical dislocation at 11 h post hCG, ovaries were removed, trimmed of adherent tissues and placed into complete MEM. Periovulatory COCs were isolated from antral follicles by puncturing using a 27-gauge needle. Immature unexpanded COCs were isolated in this same manner from mice 44 h after eCG administration and used immediately for metabolite uptake assays or subjected to IVM. For *in vitro* maturation, unexpanded immature COCs were washed in complete MEM and cultured in groups of 10 at 37^{o}C, 5%CO_2, 95% air for 16 h in 100μl drops of complete MEM media containing 50mIU/ml recombinant human FSH (Sigma-Aldrich Pty. Ltd, Castle Hill, NSW, Australia) and 3ng/ml Egf (Sigma-Aldrich Pty. Ltd, Castle Hill, NSW, Australia) overlaid with 3ml of mineral oil (Sigma-Aldrich Pty. Ltd, Castle Hill, NSW, Australia). After 16 h of culture, COC expansion was assessed (Section 2.2.2) and the complexes collected for metabolite uptake assays.

4.2.2 Metabolite Uptake Assay

Quantitative assays were developed and optimised to assess the rate of uptake and spatial distribution in COCs of metabolites with hydrophilic (glucose) and lipophilic (cholesterol) properties utilising fluorescently labelled analogues.

4.2.2.1 Glucose Uptake Assay

A nonhydrolyzable fluorescent glucose analogue (6-(N-(7-nitrobenz-2-oxa-1,3-diazol-4-yl)amino)-6-deoxyglucose; 6-NBD-Glucose, Invitrogen Australia Pty. Ltd., Mt Waverley, VIC, Australia) was used to ensure that glucose was not metabolised by cells which might result in either loss of fluorescence or

secretion from cells of secondary metabolites. 6-NBD-Glucose was reconstituted in complete MEM to a working concentration of 100μM.

A time course experiment was first performed in immature unexpanded COCs to establish the kinetics of uptake and determine a suitable length of time for labelling of immature unexpanded COCs and *in vitro* and *in vivo* matured and expanded COCs. COCs were placed in 250μL of prewarmed complete MEM containing 100μM 6-NBD-Glucose and incubated at 37°C for 0, 2, 7 or 15 minutes followed by transfer to 500μL of fresh warm complete MEM for 2 minutes. It is assumed that during the wash step labelled glucose is still able to be absorbed or transported between cells, thus this step is considered a wash that removes extracellular label, but also a chase period when the incorporated label can continue to flux into and out of cells. Optimal labelling conditions for 6-NBD-Glucose were fixed at a 15 minute pulse in the fluorescent label followed by a 2 minute wash/chase period. This time point was chosen as sufficient for readily measurable uptake of the substrate by oocytes that was linear with time elapsed, and had not reached saturation in either the cumulus cells nor the oocyte of *in vitro* or *in vivo* matured cumulus oocyte complexes (Figure 4.2).

4.2.2.2 Cholesterol Uptake Assay

Fluorescently labelled cholesterol (22-(N-(7-nitrobenz-2-oxa-1,3-diazol-4-yl)amino)-23,24-bisnor-5-cholen-3-ol; NBD-cholesterol, Invitrogen Australia Pty. Ltd., Mt Waverley, VIC, Australia) was reconstituted in absolute ethanol to a stock concentration of 5mg/ml. This was diluted to a working concentration of 5μg/ml in complete MEM.

As with glucose, a time course experiment was performed with cholesterol to establish the kinetics of uptake and determine a suitable length of time for labelling of unexpanded immature COCs and *in vitro* and *in vivo* matured and expanded COCs. COCs were placed in 250μL of prewarmed complete MEM containing 5μg/ml NBD-cholesterol and incubated at 37°C for 0, 1 or 2 minutes followed by transfer to 500μL of fresh warm complete MEM for 2 minutes.

As discussed with glucose, we assumed that during the wash step, labelled cholesterol is able to be absorbed or diffused between cells, thus this step is considered a wash that removes extracellular label,

but also a chase period when the incorporated label can continue to flux into and out of cells. Optimal labelling conditions for NBD-Cholesterol were fixed at a 2 minute pulse in the fluorescent label followed by a 2 minute wash/chase period. This time point was chosen as sufficient for readily measurable uptake of the substrate by oocytes that was linear with time elapsed, and had not reached saturation in either the cumulus cells nor the oocyte of *in vitro* or *in vivo* matured cumulus oocyte complexes (Figure 4.3).

4.2.2.3 Quantitation of Metabolite Uptake

Immediately after the wash period, COCs were mounted by transferring in 1μl of wash media to a 3μl drop of medium on a coverslip. Images of each COC were captured within 2 minutes following the wash/chase by confocal microscopy with fixed predetermined magnification, exposure and gain settings. The plane of focus in which the oocyte diameter was largest was assumed to be the centre of the complex and was selected for imaging and analysis. For each treatment group $n \geq 17$ COCs were sampled across 3 or more independent experiments. The amount of fluorescence in each COC was quantified using analySIS pro software (Olympus Australia Pty. Ltd., Mt Waverly, VIC, Australia). A region of interest (ROI), of fixed size, that encompassed the entire oocyte diameter and spanned across the COC including some external area outside the complex was placed over the image of the COC such that it centred on the geometric centre of the oocyte (Figure 4.1 a). An identical ROI was used for each COC in all experiments. The average fluorescence in each pixel column across the ROI is reported giving an average value for the relative fluorescence intensity at 1.22μM increments. For each treatment, the mean $\pm$ S.E.M. was calculated for all COCs across experiments and data represented graphically as intensity of fluorescence over distance (Figure 4.1 b).

To determine the intensity of fluorescent label immediately surrounding the COCs, the average (+/- S.E.M.) of the intensity values from the outermost 10μm of each end of the ROI was calculated. Similarly, to determine fluorescent uptake specifically in cumulus cells, the average (+/-S.E.M.) of fluorescence intensity was calculated for intensity values between 100-110μm and 240-250μm of the ROI, two regions either side of the oocyte that contained cumulus cells, for each COC.

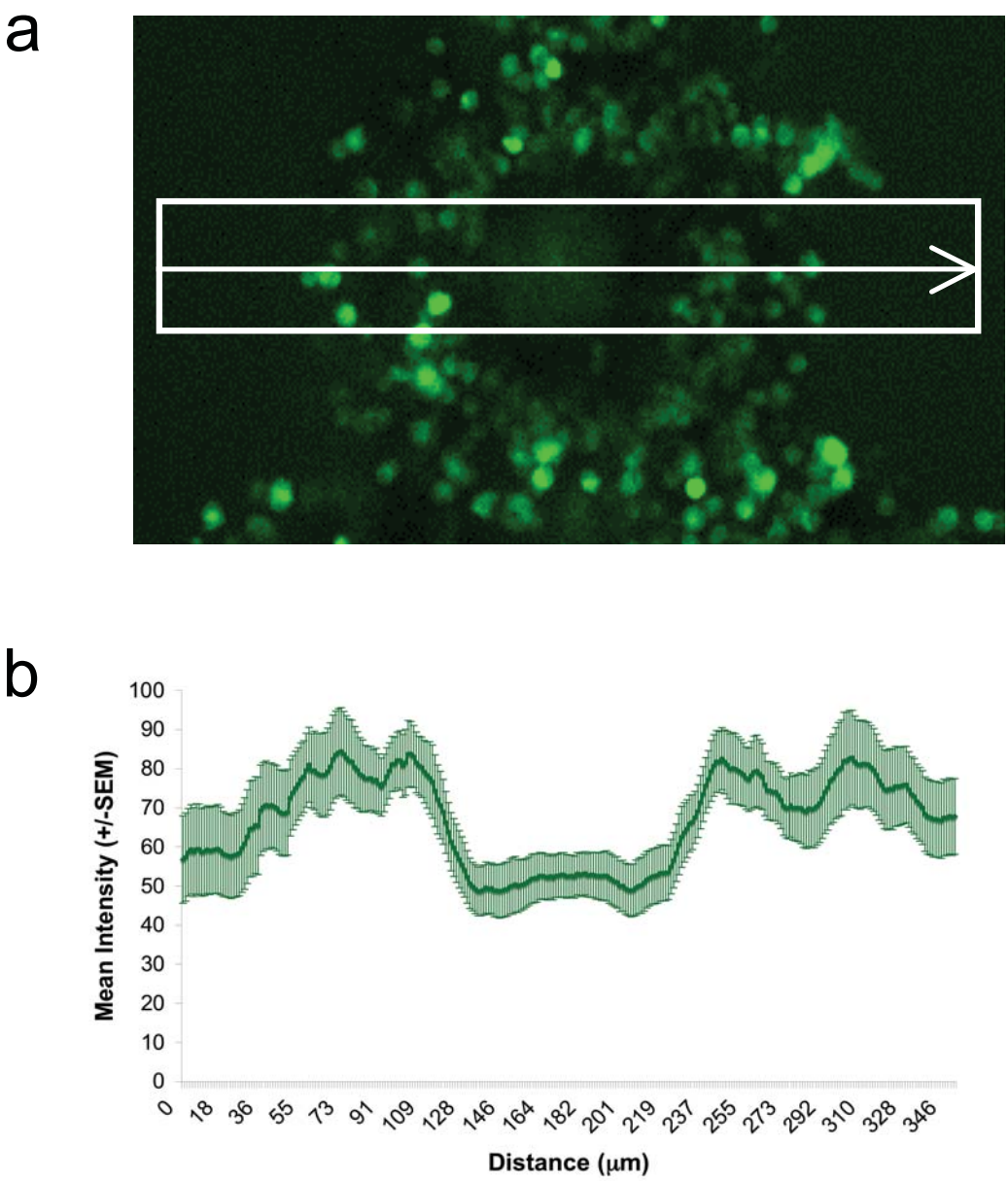

Figure 4.1 Example of quantification of fluorescence intensity across a cumulus oocyte complex (COC).

Oocyte and cumulus cell metabolite uptake was quantified using confocal images of COCs and Analysis Pro Software (Olympus). (a) Example of the quantification process, measuring the distribution of fluorescence intensity across a COC. The highlighted region of interest (ROI) was placed over the COC such that an equal distance was measured either side of the geometric centre of the oocyte. The average fluorescence in each column of pixels within the ROI is reported. (b) Example of the graphical output obtained using Analysis Pro Software where the data is expressed as mean intensity of fluorescence +/- S.E.M. (n=17 COCs, 4 independent experiments).

The uptake of label, specifically by oocytes, was determined by measuring the average pixel intensities in an ROI (50x50μM) placed over the geometric centre of oocytes then calculating the average (+/- S.E.M) of intensity for all oocytes in each treatment. In all experiments, parallel *in vitro* matured and *in vivo* matured COCs were harvested, labelled and imaged on the same day.

4.2.2.4 Statistical Analysis

Uptake of fluorescent label in oocytes, cumulus cells and surrounding media were analysed by performing a One-Way ANOVA and a Tukey *post hoc* test on mean fluorescence intensities using Prism version 5 (GraphPad Software Inc., San Diago, CA, United States). A *P* value <0.05 was considered statistically significant.

4.3 RESULTS

4.3.1 Glucose Uptake in Unexpanded Cumulus Oocyte Complexes (COCs)

The kinetics of 6-NBD-Glucose transport across the unexpanded cumulus oocyte complex (COC) and into oocytes after 0, 2, 7 or 15 minute exposure to the labelled substrate (Figure 4.2 a-d) showed that glucose permeates the cumulus complex to the oocyte rapidly. Significant glucose uptake was observed within the oocyte within a labelling period of 2 minutes (Figure 4.2 b, f). The accumulation of 6-NBD-Glucose label continued to increase both within cumulus cells and the oocyte with increasing duration of labelling incubation to 7 and 15 minutes (Figure 4.2 c and d respectively). Fluorescence intensity was greater in cumulus cells than the oocyte following a 2 or 7 minute incubation in fluorescent label, however following 15 minutes, glucose intensity within the oocyte reached similar levels to the cumulus cells (Figure 4.2 d and e). The mean intensity of fluorescence in oocytes increased significantly ($P<0.05$ at each interval) and in a linear fashion ($R^2= 0.9912$; $P<0.0001$) with labelling times of 2, 7 and 15 minutes (Figure 4.2 f and g). During the pulse periods chosen, the exogenous supply of fluorescent glucose was not depleted in the surrounding media as glucose uptake in the oocyte was linear and did not plateau (Figure 4.2 g). These observations indicate that this method can quantitatively measure the kinetics of glucose transport across the COC.

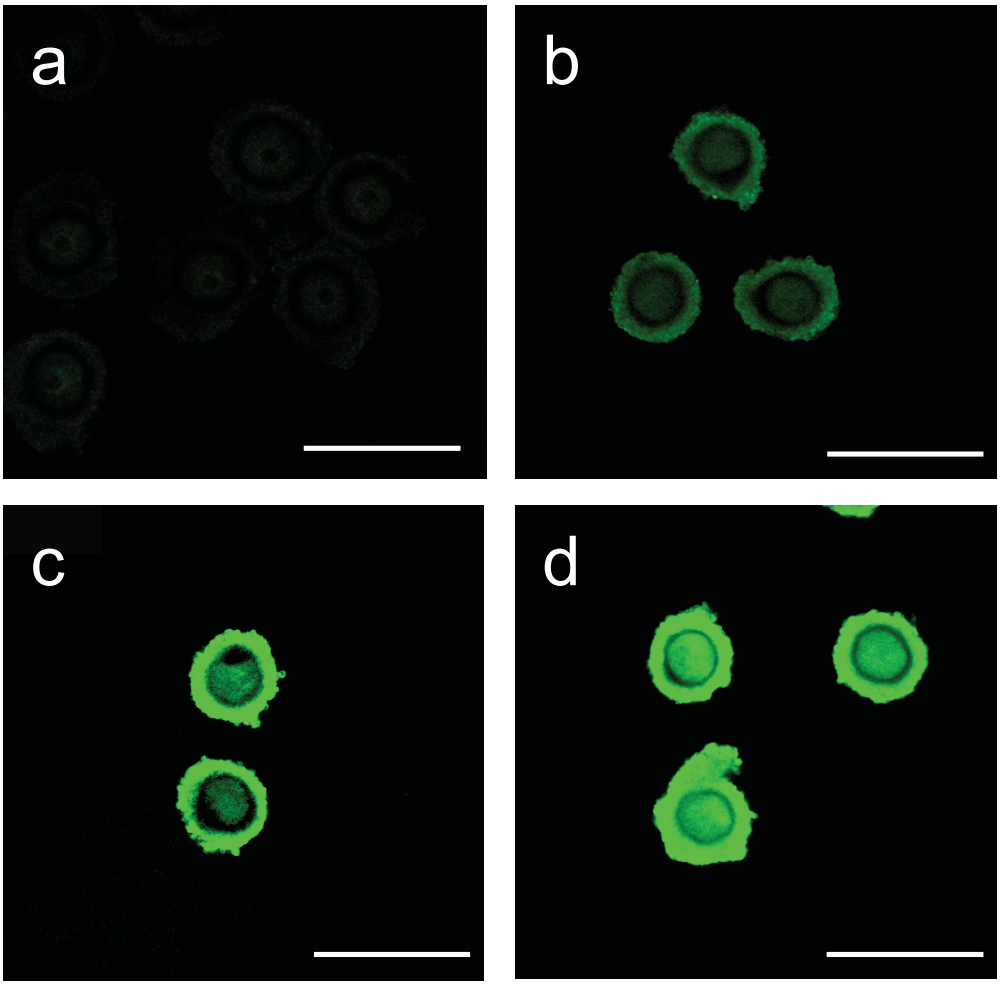
a
b
c
d

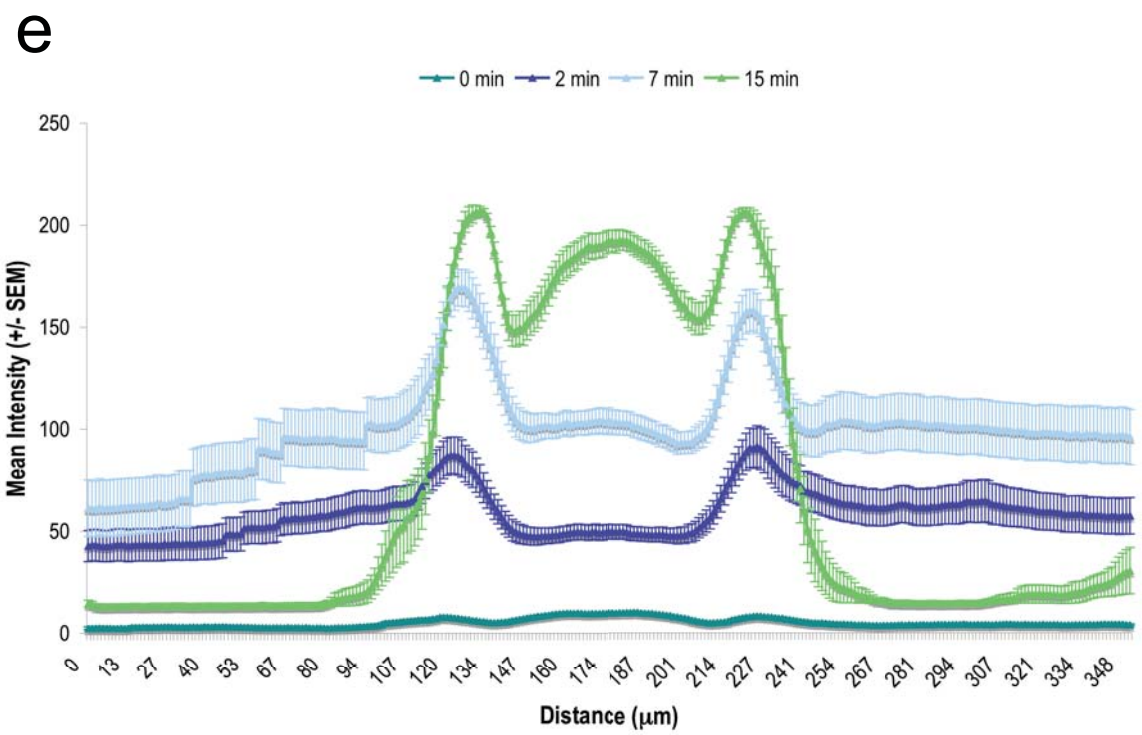
e
0 min
2 min
7 min
15 min
250
200
150
100
50
0
Mean Intensity (+/- SEM)
0
13
27
40
53
67
80
94
107
120
134
147
160
174
187
201
214
227
241
254
267
281
294
307
321
334
348
Distance (μm)

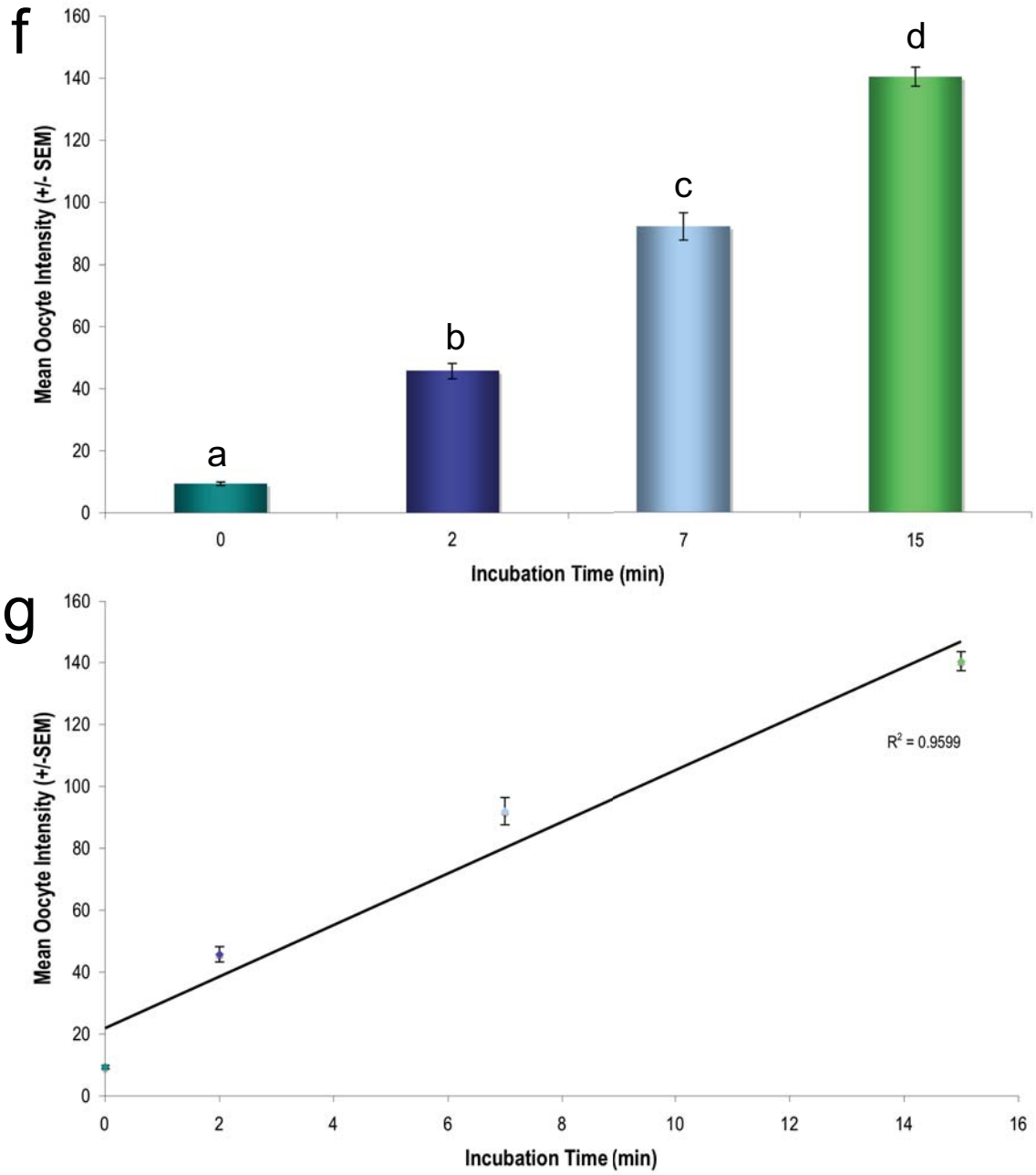

Figure 4.2 Glucose uptake in the unexpanded cumulus oocyte complex (COC) is proportional to duration of incubation.

Analysis of fluorescently labelled glucose uptake in unexpanded immature COCs from Adamts1$^{+/-}$ mice. Confocal images of unexpanded COCs incubated in 6-NBD-Glucose for 0 min (a), 2 min (b), 7 min (c) or 15 min (d) all followed by a 2 min wash. Quantified intensities of glucose uptake across the diameter of COCs for 0, 2, 7 and 15 min incubation periods is shown in e, data expressed as mean intensity of fluorescence +/- S.E.M. (n≥16 COCs, 3 independent experiments). Quantification of fluorescence intensity within oocytes was determined as described in Figure 4.1 with the region of interest encompassing the oocyte only. The average (+/-S.E.M) of intensity values was then calculated (f). Glucose uptake was proportional to time of exposure as shown in g. Bars with different characters are significantly different (P<0.05). Scale bar = 200μm.

4.3.2 Cholesterol Uptake in Unexpanded Cumulus Oocyte Complexes (COCs).

The kinetics of cholesterol diffusion across the unexpanded cumulus complex and uptake by oocytes was similar, but more rapid than glucose. Accumulation of cholesterol within oocytes was significant within a 1 minute labelling pulse (Figure 4.3 b and e). The accumulation of cholesterol within both oocytes and cumulus cells continued to increase with increasing duration of label exposure (Figure 4.3 d and e). Cholesterol uptake in cumulus cells was greater than that seen in oocytes following both a 1 and 2 minute pulse (Figure 4.3 d). The mean intensity of fluorescence in oocytes was linear (R^2= 0.9993, $p<0.0001$) and increased significantly ($p<0.05$) following durations of label exposure of 1 and 2 minutes (Figure 4.3 e and f). During the pulse periods chosen, the exogenous supply of fluorescent cholesterol was not depleted in the surrounding media as demonstrated by the linear increase in fluorescence intensity (Figure 4.3 f) thus validating that the assay was suitable for analysing the kinetics of cholesterol uptake across COCs.

4.3.3 Comparison of Glucose Uptake in Unexpanded and Expanded *in vivo* Matured Cumulus Oocyte Complexes (COCs).

A direct comparison was made between glucose uptake in COCs of unexpanded (44 h eCG) and *in vivo* matured and expanded COCs either periovulatory (11 h post hCG) or postovulatory (16 h hCG, section 4.2.2). The results showed that the expanded COC was markedly more resistant to 6-NBD-Glucose transport during a 15 min pulse than unexpanded COCs (Figure 4.4 a-c). Remarkably, the majority of the fluorescence was present in the media immediately surrounding the *in vivo* expanded COCs even after 2 min chase/wash in 500µl fresh MEM (Figure 4.4 b and c). This retention of the label in the surrounding media suggests that after COC expansion the extensive matrix resists glucose thus the label is retained in surrounding media. Glucose uptake in oocytes was significantly reduced in the expanded periovulatory and postovulatory COC compared to immature unexpanded COCs ($P<0.05$, Figure 4.4 d). This observation suggests that the matrix is resistant to glucose diffusion.

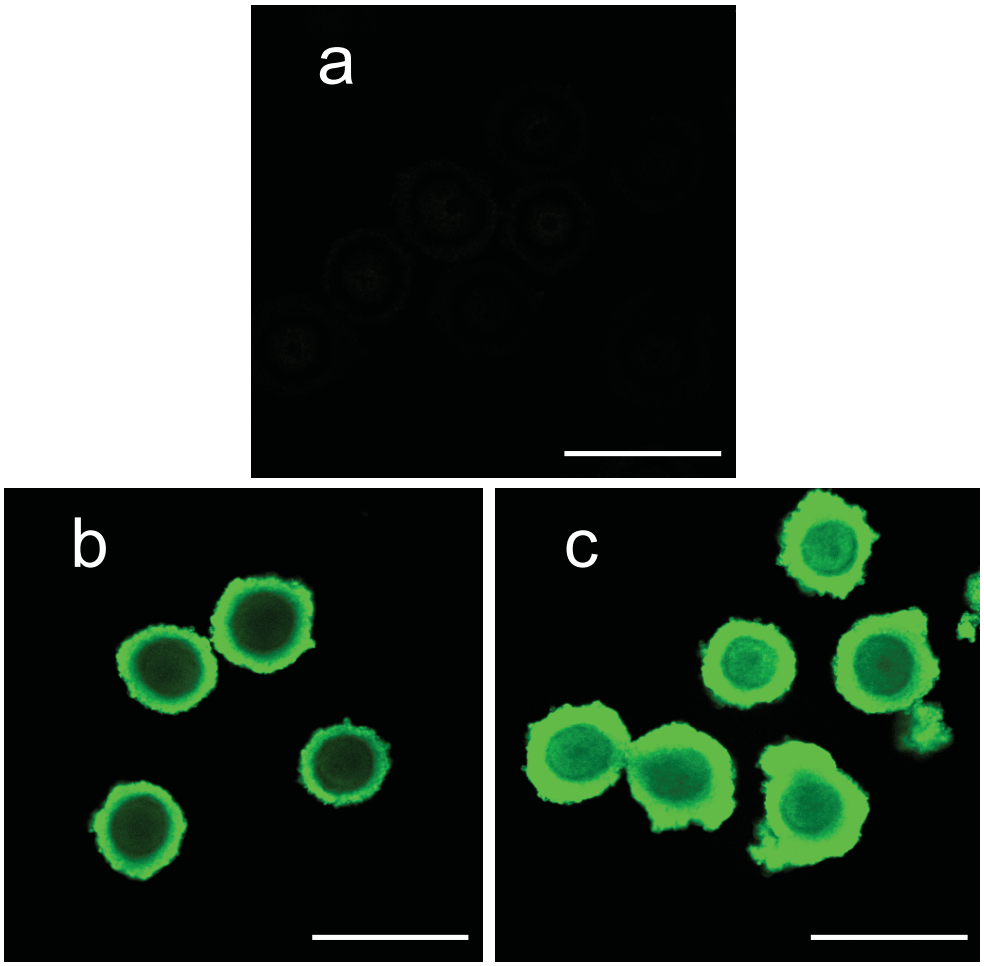
a
b
c

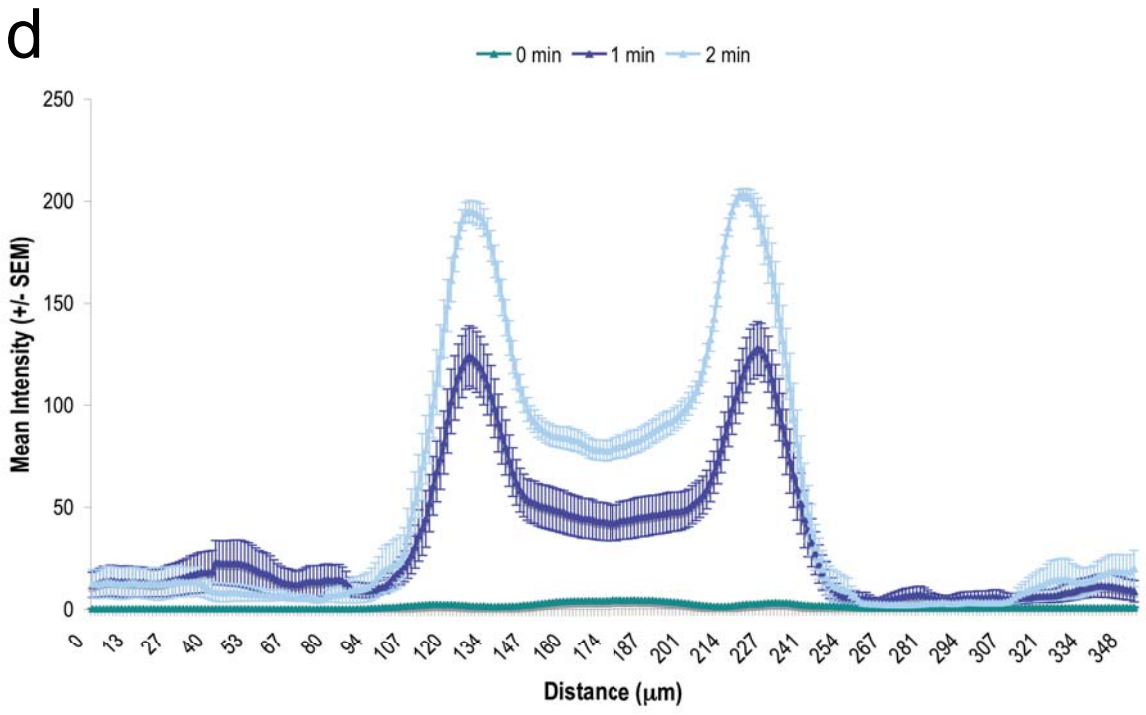
d
0 min
1 min
2 min
Mean Intensity (+/- SEM)
250
200
150
100
50
0
0
13
27
40
53
67
80
94
107
120
134
147
160
174
187
201
214
227
241
254
267
281
294
307
321
334
348
Distance (μm)

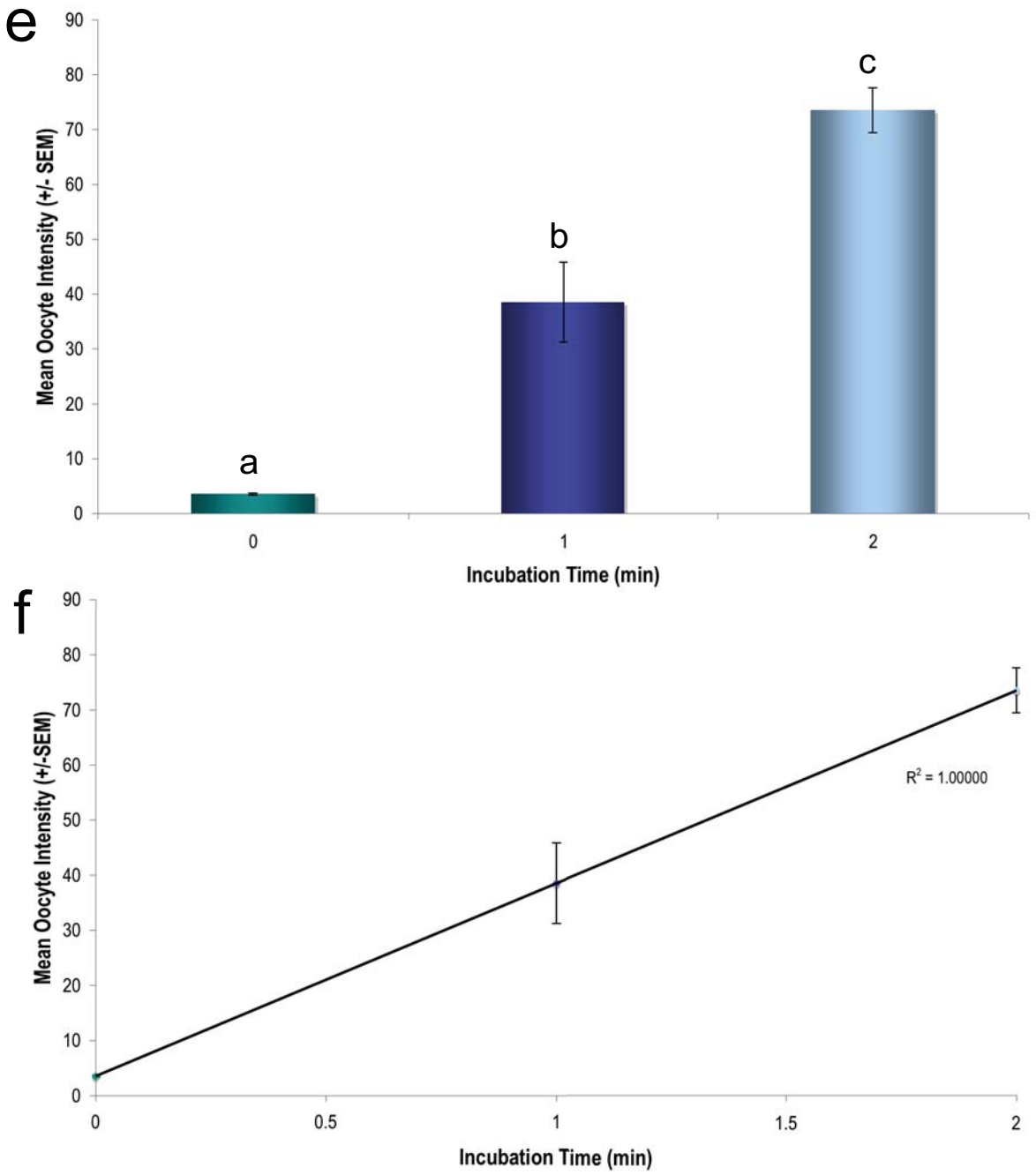

Figure 4.3 Cholesterol uptake in the unexpanded cumulus oocyte complex (COC) is proportional to duration of incubation.

Analysis of fluorescently labelled cholesterol uptake in unexpanded COCs from Adamts1$^{+/-}$ mice. Confocal images of unexpanded COCs incubated in NBD-Cholesterol for 0 min (a) 1 min (b) or 2 min (c) all followed by a 2 min chase wash. Quantified intensities of cholesterol uptake across the diameter of COCs for 0, 1 and 2 min incubation periods is shown in d, data expressed as mean intensity of fluorescence +/- S.E.M. (n≥19 COCs, 4 independent experiments). Quantification of fluorescence intensity within oocytes was determined as described in Figure 4.1 with the region of interest encompassing the oocyte only. The average (+/-S.E.M) of intensity values was then calculated (e). Cholesterol uptake was proportional to time as shown in f. Bars with different characters are significantly different ($P<0.05$). Scale bar = 200μm.

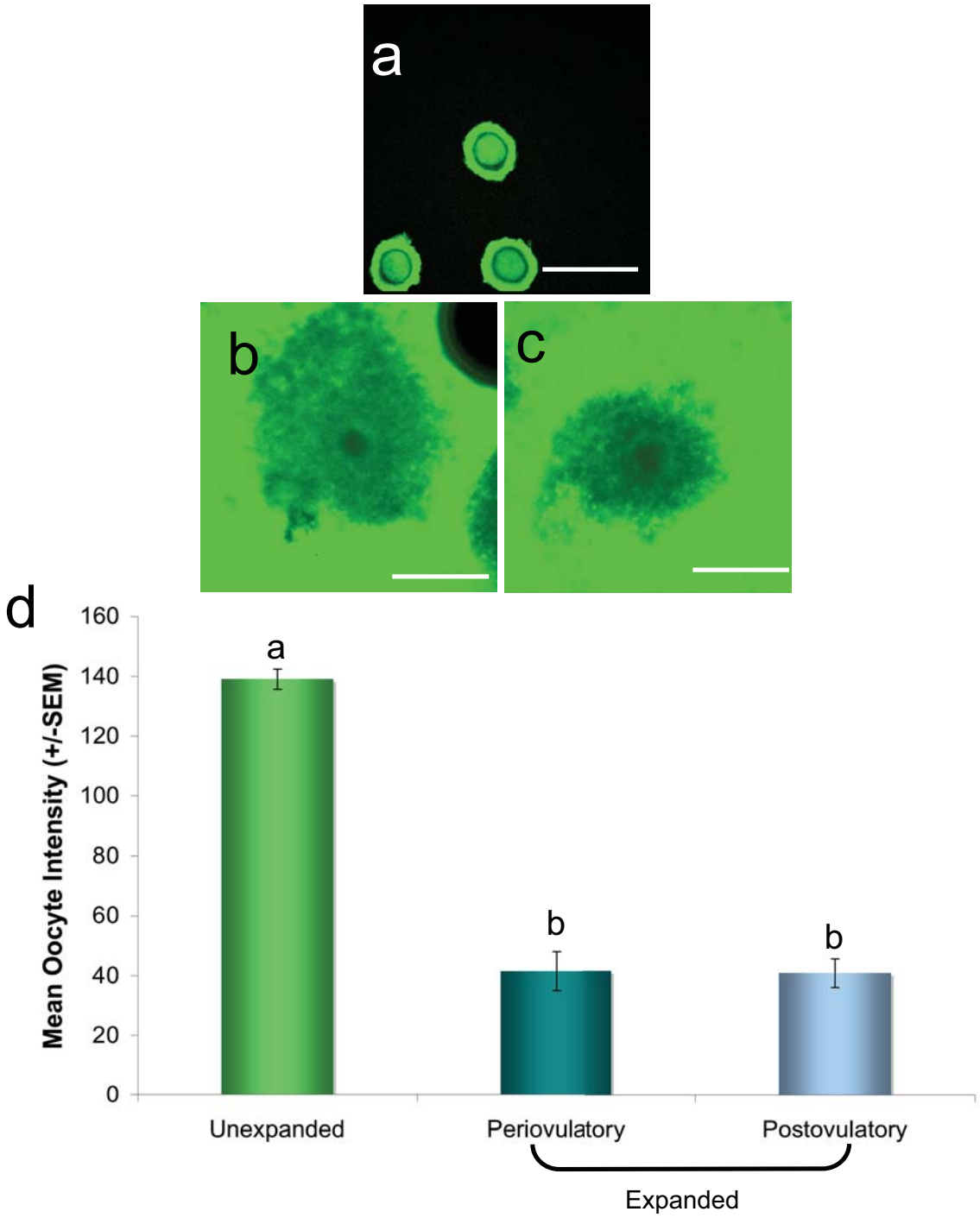

Figure 4.4 Glucose uptake in oocytes is significantly reduced following cumulus expansion.

Analysis of fluorescently labelled glucose uptake in unexpanded and expanded *in vivo* matured COCs from *Adamts1*$^{+/-}$ mice. Confocal images of (a) unexpanded, (b) periovulatory (11 h post hCG) expanded and (c) postovulatory (16 h hCG) expanded COCs incubated in 6-NBD-Glucose for 15 min followed by a 2 min chase wash. Quantification of glucose uptake in oocytes in shown in d. Quantification of glucose uptake within oocytes was determined as described in Materials and Methods (Section 4.2.2.3) with the region of interest encompassing the oocyte only. The average (+/-S.E.M) of intensity values was then calculated (n≥13 COCs). Bars with different characters are significantly different ($P<0.05$). Scale bar = 200μm.

4.3.4 Cholesterol Uptake in Unexpanded Immature and Expanded *in vivo* matured cumulus oocyte complexes (COCs).

Differences in cholesterol diffusion and uptake between unexpanded and *in vivo* expanded COCs was determined following a 2 minute pulse in NBD-Cholesterol and a 2 minute wash/chase (Section 4.2.2.2). Confocal images of the NBD-Cholesterol uptake in COCs showed that following expansion, COCs were resistant to cholesterol absorption when compared to unexpanded COCs (Figure 4.5 a and b). Individual cumulus cells at the outer edges of expanded COCs showed cholesterol uptake, but towards the middle of the complexes, cumulus cells and oocytes contained only minimal fluorescence. Quantitation of the accumulated cholesterol in oocytes showed a significant reduction (8-fold) following expansion (Figure 4.5 c; $p<0.05$). These observations suggest that, as with glucose, the expanded COC matrix presents a resistant barrier to cholesterol diffusion and exposure of the oocyte.

4.3.5 Comparison of Glucose Uptake in Expanded cumulus oocyte complexes (COCs) Following *in vivo* and *in vitro* Maturation.

In order to further demonstrate that the cumulus matrix regulates metabolite diffusion to the oocyte, two models in which key matrix components are lacking were employed. The first is the *in vitro* maturation model of cumulus expansion, which was previously demonstrated to be deficient in both Adamts1 and Versican (Chapter 3, Dunning *et al*., 2007). The second is the *Adamts1* null mouse model in which *in vivo* matured COCs are deficient in Adamts1 protein and cleaved Versican (Russell *et al.* 2005). For these experiments *in vitro* matured COCs and/or *Adamts1*$^{-/-}$ COCs were subjected to the metabolite uptake assays and compared to *in vivo* matured *Adamts1*$^{+/-}$ COCs.

Firstly, glucose uptake in expanded COCs following *in vivo* maturation and ovulation or IVM (Section 4.2.1) was compared using the same conditions as described above. For *in vivo* matured *Adamts1*$^{+/-}$ COCs, the majority of cumulus cells did not contain the fluorescent glucose (Figure 4.6 a), with only occasional sporadic cumulus cells on the outer edges of complexes showing fluorescence uptake and oocytes were consistently void of glucose (Figure 4.6 a). Intense fluorescence was repeatedly observed

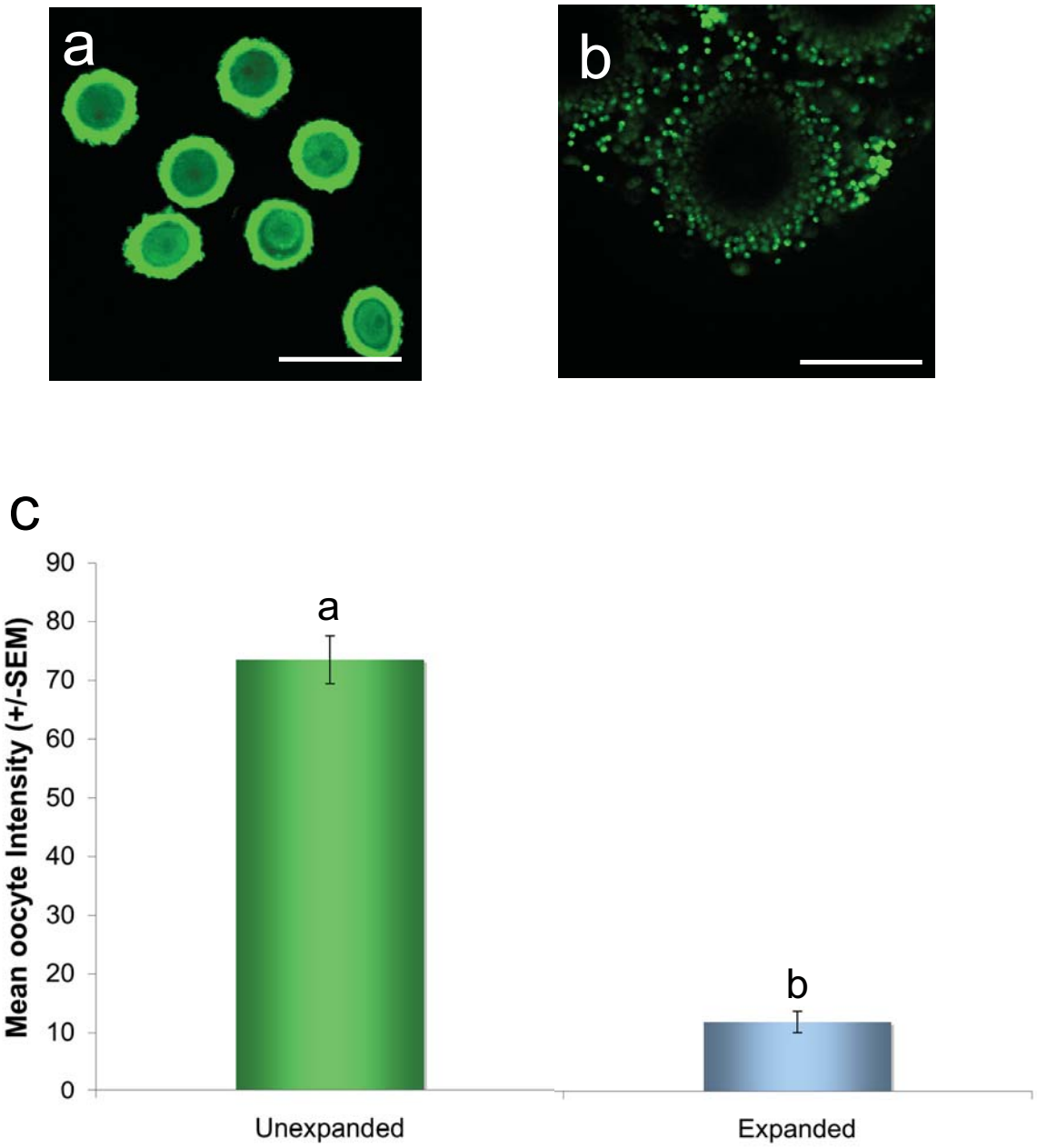

Figure 4.5 Cholesterol uptake in oocytes is significantly reduced following cumulus expansion.

Analysis of fluorescently labelled cholesterol uptake in unexpanded and expanded *in vivo* matured COCs from *Adamts1*$^{+/-}$ mice. Confocal images of (a) unexpanded and (b) postovulatory expanded COCs incubated in NBD-Cholesterol for 2 min followed by a 2 min chase wash. Quantification of cholesterol uptake in oocytes is seen in c. Quantification of cholesterol uptake within oocytes was determined as described in Materials and Methods (Section 4.2.2.3) with the region of interest encompassing the oocyte only. The average (+/-S.E.M) of intensity values was then calculated (n≥16 COCs, ≥ 3 independent experiments) Bars with different characters are significantly different ($P<0.05$). Scale bar = 200μm.

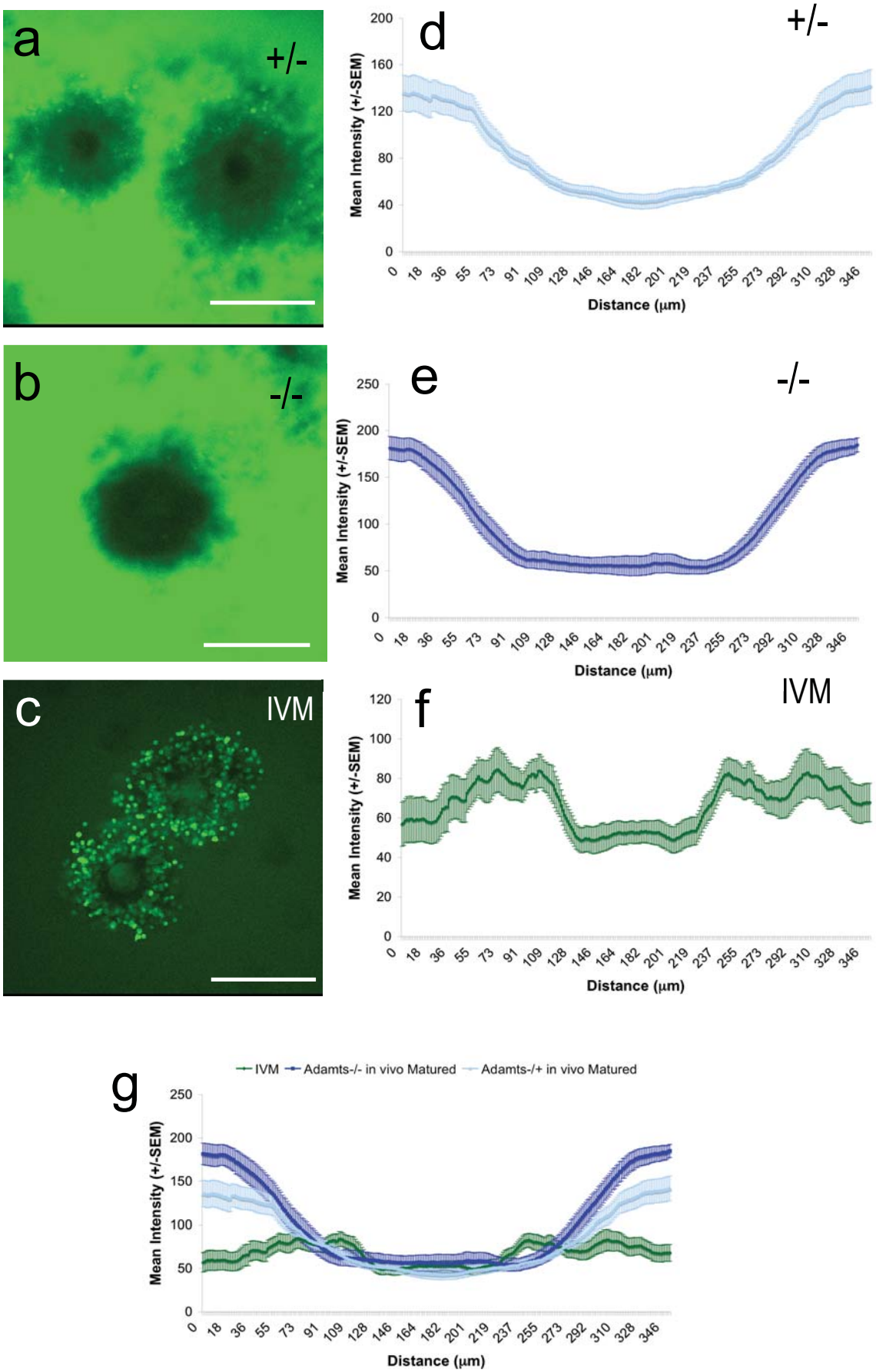
a
+/-
b
-/-
c
IVM
d
+/-
e
-/-
f
IVM
Mean Intensity (+/-SEM)
Distance (μm)
0 18 36 55 73 91 109 128 146 164 182 201 219 237 255 273 292 310 328 346
g
IVM
Adamts-/- in vivo Matured
Adamts-/+ in vivo Matured

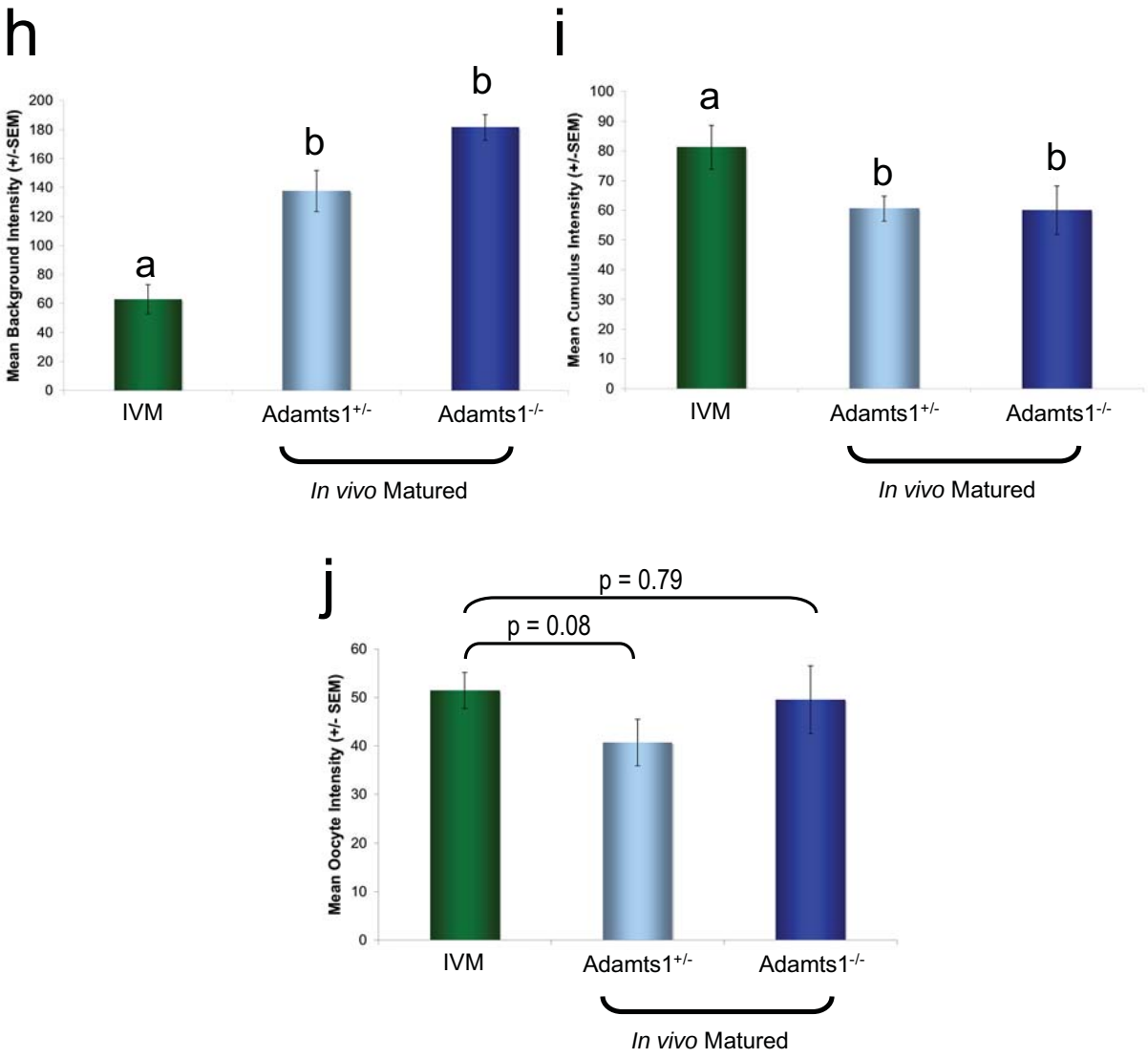

Figure 4.6 The accumulation of glucose is perturbed in the cumulus oocyte complex (COC) and its surrounding matrix following *in vitro* maturation.

Analysis of glucose accumulation in cumulus oocyte complexes (COCs) and their surrounding media following *in vivo* and *in vitro* maturation (IVM). Confocal images of 6-NBD-Glucose uptake in (a) *in vivo* matured *Adamts1*$^{+/-}$, (b) *in vivo* matured *Adamts1*$^{-/-}$ and (c) IVM COCs following an incubation period of 15 min followed by a 2 min wash. Quantified glucose uptake across *in vivo* matured *Adamts1*$^{+/-}$ and *Adamts1*$^{-/-}$ and IVM COC is shown in d, e and f respectively, data expressed as mean intensity of fluorescence +/- S.E.M. (n≥15 COCs, 4 independent experiments). Overlay of the graphical intensity profiles for all treatments is shown in g. Quantification of glucose accumulation in the surrounding matrix was determined by calculating the average (+/-S.E.M) of fluorescence intensity values from 10μm from each end of the region of interest (h). Similarly, for cumulus uptake, the average (+/-S.E.M) of fluorescence intensity values from 100-110μm and 240-250μm for each COC were used (i). Quantification of glucose uptake within oocytes was determined as described in Materials and Methods (Section 4.2.2.3) with the region of interest encompassing the oocyte only. The average (+/-S.E.M) of intensity values was then calculated (j, n≥15 COCs, 4 independent experiments) Bars with different characters are significantly different (P<0.05). Scale bar = 200μm.

outside the *in vivo* matured COC indicating that the extensive *in vivo* generated matrix is highly resistant to 6-NBD-Glucose permeation. Analysis of the mean intensity of glucose fluorescence across the *in vivo* matured *Adamts1*$^{+/-}$ complex showed a steep concentration gradient from very high concentrations seen outside the complex and rapidly declining with the least fluorescence observed within the oocyte (Figure 4.6 d).

A similar pattern of uptake was seen for *in vivo* matured *Adamts1*$^{-/-}$ COCs, oocytes and cumulus cells were void of glucose except for occasional outer cumulus cells that did contain fluorescent glucose (Figure 4.6 b). Again, quantitation of the fluorescence intensity across the complex revealed a gradient of glucose concentration decreasing from a high intensity outside, to a very low intensity within the oocyte (Figure 4.6 e).

A striking disparity in the uptake of glucose was seen between *in vivo* matured and IVM complexes (Figure 4.6 a and c respectively). Following IVM and label exposure, both cumulus cells and oocytes contained strong 6-NBD-Glucose fluorescence (Figure 4.6 c). The mean intensity of fluorescence quantified in IVM complexes (n= 17 COCs, 4 independent experiments), revealed that the greatest concentration of glucose was within the cumulus cell layer of the complex, with very low levels present on the outer edge (Figure 4.6 c and f) resulting in a reversed spatial gradient pattern of glucose accumulation across the cumulus cell compartment compared to that seen after *in vivo* maturation (Figure 4.6 d-f). The altered gradient pattern of glucose accumulation observed following IVM was similar to that seen with unexpanded COCs (Figure 4.2 e). When assessed in parallel, the combined quantitation of glucose uptake for *in vivo* matured *Adamts1*$^{+/-}$ and *Adamts1*$^{-/-}$ COCs and IVM COCs (Figure 4.6 g), shows dramatic differences in the gradient of glucose present across the complexes of *in vivo* compared to IVM COCs. The glucose uptake in each of the regions; the surrounding media; the cumulus cells and the oocyte, was compared between treatment groups.

Comparison of the difference in the background 6-NBD-Glucose fluorescence between *in vivo* and *in vitro* matured COCs (as described in section 4.2.2.3) showed there was significantly more fluorescent glucose in the surrounding media after labelling followed by washing, of *in vivo* matured complexes than IVM COCs ($P<0.05$, Figure 4.6 h).

The differences in cumulus cell uptake of glucose between *in vivo* matured and IVM COCs, quantified as per section 4.2.2.3 additionally showed significantly more fluorescent glucose in the cumulus compartment of IVM COCs compared to *in vivo* matured *Adamts1*$^{+/-}$ and *Adamts1*$^{-/-}$ COCs ($p<0.05$, Figure 4.6 i).

The mean intensity of glucose fluorescence present in oocytes was determined using a region of interest encompassing the oocyte only (Section 4.2.2.3) for the three experimental conditions and is shown in Figure 4.6 j. The fluorescence intensity representing glucose present in oocytes after IVM was greater than that seen for *in vivo* matured COCs however; this was not statistically different ($p=0.08$, Figure 4.6 j). Additionally, there was no difference in glucose intensity between IVM and *Adamts1*$^{-/-}$ *in vivo* matured oocytes ($p=0.79$, Figure 4.6 j).

4.3.6 Cholesterol Uptake in Expanded Cumulus Oocyte Complexes (COCs) Following *in vivo* and *in vitro* Maturation.

Cholesterol uptake by cumulus cells and oocytes in expanded COCs was also compared in *in vivo* matured *Adamts1*$^{+/-}$ and *Adamts1*$^{-/-}$ and IVM COCs as described in section 4.2.2.2. Following *in vivo* maturation and a 2 minute labelling pulse followed by a 2 minute wash/chase, cumulus cells and oocytes of *in vivo* matured *Adamts1*$^{+/-}$ and *Adamts1*$^{-/-}$ and IVM COCs absorbed moderate levels of cholesterol (Figure 4.7 a-c).

There was no significant difference in the abundance of cholesterol present in the surrounding media of IVM and *in vivo* matured *Adamts1*$^{+/-}$ COCs (Figure 4.7 h). There was however, a significant 2-fold increase in background fluorescence around *in vivo* matured *Adamts1*$^{-/-}$ COCs compared to their heterozygous counterparts (Figure 4.7 h).

The spatial gradient of cholesterol uptake was similar between IVM and *in vivo* matured COCs, with low background and consistently higher concentrations of cholesterol present within the cumulus layers and low abundance in oocytes after an identical 2 minute pulse and 2 minute wash/chase procedure (Figure 4.7 d-f). Importantly, the mean intensity of cholesterol fluorescence following IVM was increased in both the oocyte and cumulus cells compared to COCs matured *in vivo* (Figure 4.7 g). Significantly more

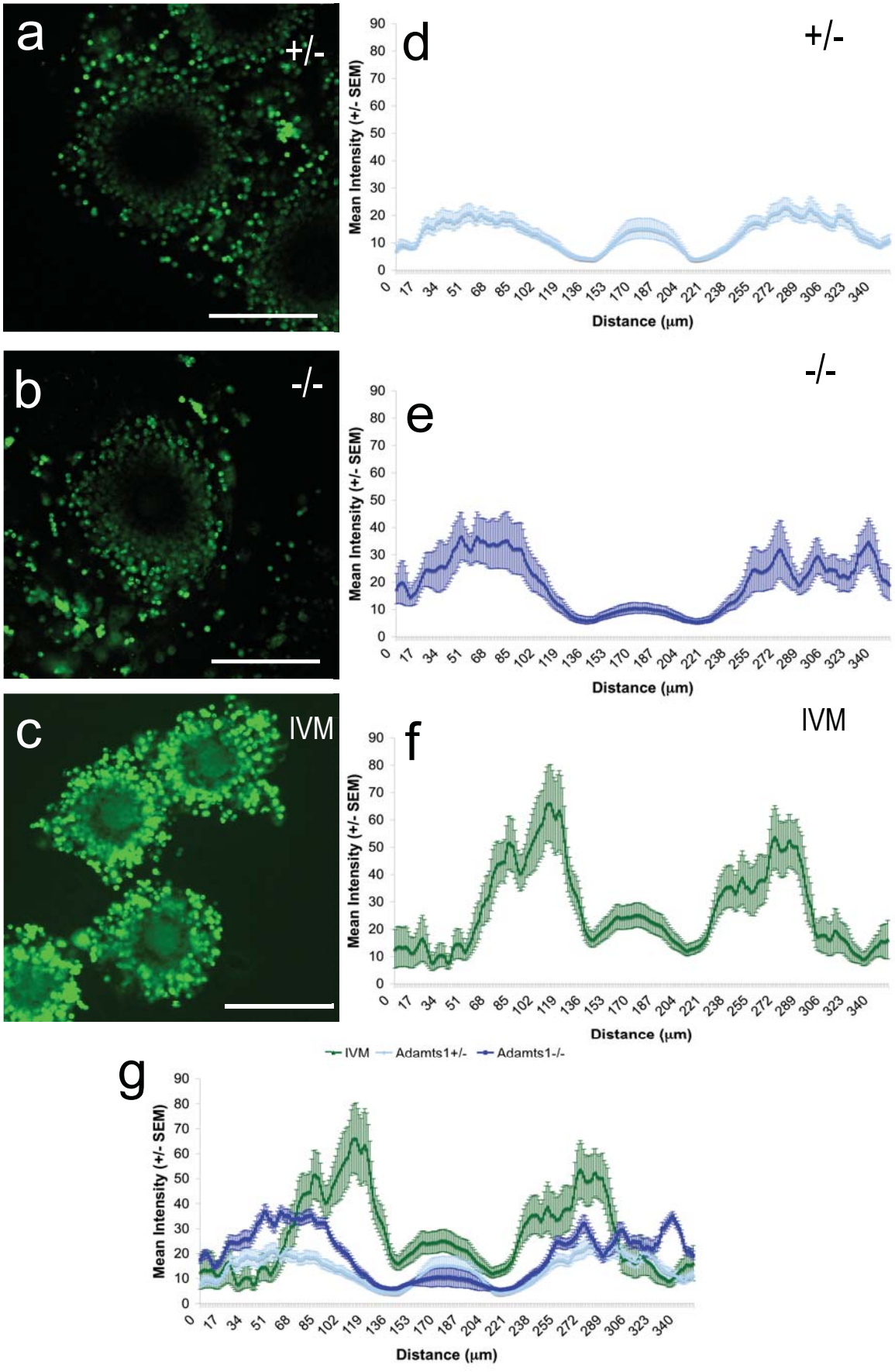
a
+/-
b
-/-
c
IVM
d
+/-
e
-/-
f
IVM
g
Mean Intensity (+/- SEM)
Distance (μm)
IVM
Adamts1+/-
Adamts1-/-

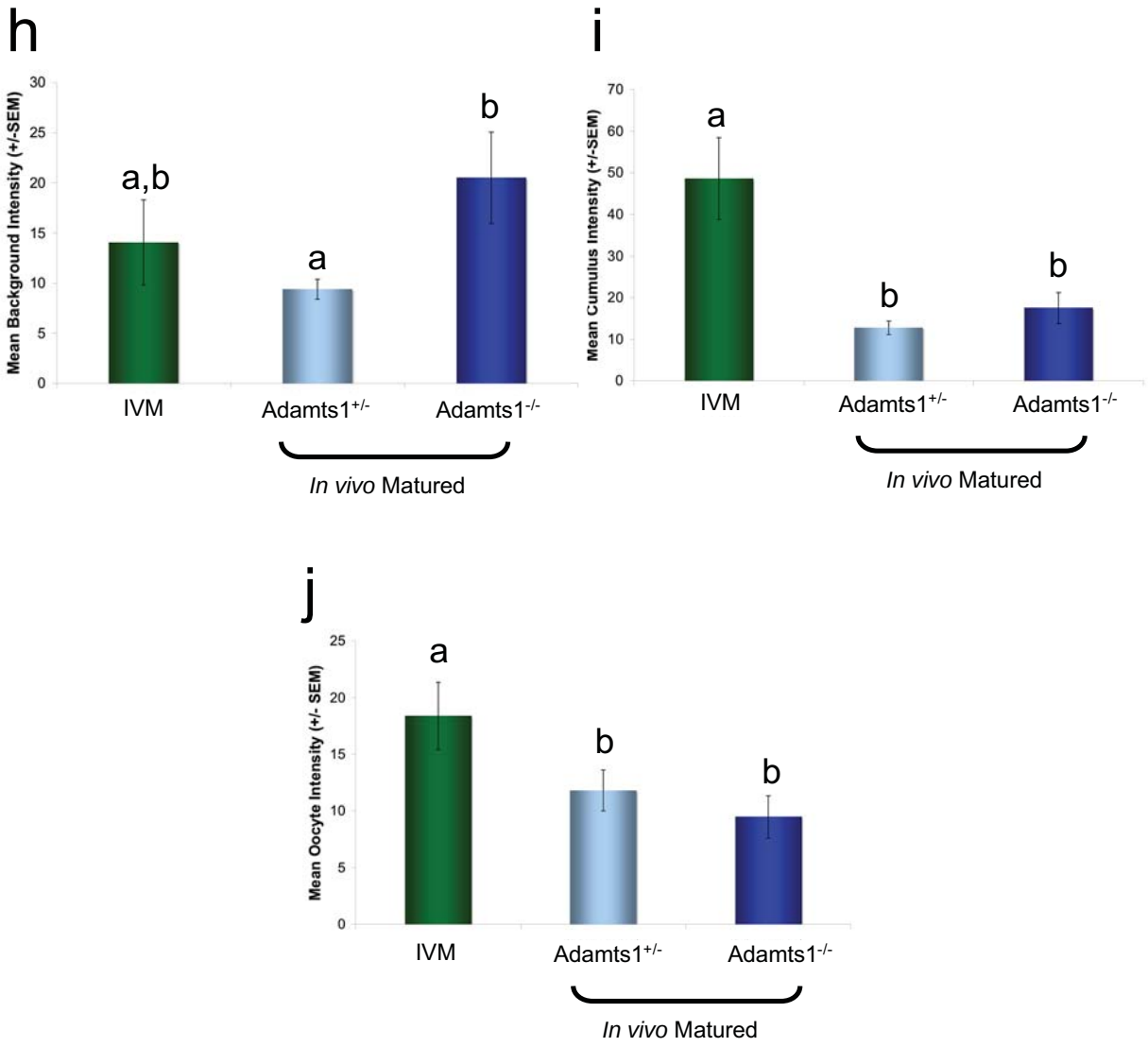

Figure 4.7 Cholesterol uptake is significantly increased in cumulus cells and oocytes following *in vitro* maturation.

Analysis of cholesterol uptake in cumulus oocyte complexes (COCs) following *in vivo* and *in vitro* maturation (IVM). Confocal images of NBD-Cholesterol uptake in (a) *in vivo* matured *Adamts1*$^{+/-}$, (b) *in vivo* matured *Adamts1*$^{-/-}$ and (c) IVM COCs, following an incubation period of 2 min followed by a 2 min wash. Quantified intensity profiles of cholesterol uptake across *in vivo* matured *Adamts1*$^{+/-}$ and *Adamts1*$^{-/-}$ COCs and IVM COCs, is shown in d, e and f respectively, data expressed as mean intensity of fluorescence +/-S.E.M. (n≥13 COCs, 4 independent experiments). Overlay of the graphical intensity profiles for all treatments is shown in g. Quantification of cholesterol accumulation in the surrounding matrix was determined by calculating the average (+/-S.E.M) of fluorescence intensity values from 10μm from each end of the region of interest (h). Similarly, for cumulus uptake, the average (+/-S.E.M) of fluorescence intensity values from 100-110μm and 240-250μm for each COC were used (i). Quantification of cholesterol uptake within oocytes was determined as described in Materials and Methods (Section 4.2.2.3) with the region of interest encompassing the oocyte only. The average (+/-S.E.M) of intensity values was then calculated (j, n≥16 COCs) Bars with different characters are significantly different (P<0.05). Scale bar = 200μm.

cholesterol was present in cumulus cells following IVM than cumulus cells of COCs that underwent *in vivo* maturation ($P<0.05$, Figure 4.7 i). Additionally, a significant increase in the uptake of cholesterol by oocytes was seen following IVM compared to *Adamts1*$^{+/-}$ and *Adamts1*$^{-/-}$ *in vivo* matured COCs (Figure 4.7 j).

4.4 DISCUSSION

The formation of the cumulus matrix is arguably one of the most striking events in biology however its functional significance is poorly understood. I hypothesised that it may play a role in controlling metabolite supply to the oocyte on the basis of recognised filtration properties of matrices and the known sensitivities of oocytes to their environmental conditions. The results of a series of experiments clearly demonstrate that the presence of cumulus matrix resulted in a dramatic difference in the absorption of both glucose and cholesterol.

Two metabolites were chosen that likely influence oocyte developmental potential but also have markedly different physicochemical properties. Glucose is a hydrophilic molecule that enters cells through facilitative receptor mediated transport via GLUTs (Mueckler 1994). Cholesterol is a hydrophobic molecule able to freely diffuse through lipid membranes. Interestingly, we found a clear difference in the absorption of glucose and cholesterol after COC expansion suggesting that the expanded COC matrix presents an active barrier to glucose and cholesterol uptake compared to unexpanded COCs and that this matrix does indeed have molecular filtration properties (Figure 4.4 and 4.5). Furthermore, enhanced resistance characteristics of *in vivo* expanded matrices compared to those matured by IVM indicates that these properties are not the result of HA alone, but are dependent on the composition of the matrix.

Prior to expansion, the transport of glucose across the compact cumulus layers to the oocyte was rapid, with uptake occurring in the oocyte within 2 min (Figure 4.2 b and e). Following a 15 minute incubation, the same incubation period used for the expanded COCs, glucose intensity within the oocyte reached similar levels to that seen in its surrounding cumulus cells (Figure 4.2 d and e). In contrast, there was a significant reduction of glucose uptake in the oocyte within this timeframe following expansion (Figure 4.4 d). In fact, it appears that glucose is actively excluded from this matrix with intense fluorescence

accumulation seen in the media surrounding the COCs (Figure 4.4 and Figure 4.6). The exclusion of glucose from the COC matrix and the absence of cellular uptake in either cumulus cells or the oocyte are less marked in IVM COC suggesting that changes in IVM COC matrix, possibly the absence of Adamts1 and Versican, alter exposure and uptake by the oocyte. Overall, these results show that oocyte exposure to glucose following COC expansion *in vivo* is significantly reduced. This function of the matrix may be important during the meiotic maturation and fertilisation of oocytes. The matrix generated during IVM expansion results in different metabolite exclusion characteristics and thus protection of oocytes from harmful environmental conditions may be reduced. This observation may help to explain the known sensitivity of oocytes to excessive glucose in IVM/IVF culture media.

Cholesterol uptake in unexpanded COCs was very rapid with fluorescence present in the oocyte within 1 min (Figure 4.3 b). Following *in vivo* maturation and expansion, cholesterol uptake was reduced in cumulus cells and was minimal in oocytes indicating that the COC matrix impedes cholesterol diffusion (Figure 4.5 b). Compared to *in vivo* maturation, cholesterol diffusion across the cumulus compartment and uptake in oocytes of IVM COCs was dramatically increased (Figure 4.7 g). These results indicate that characteristics unique to the *in vivo*-derived matrix are important in regulating the diffusion rate of cholesterol across the complex and uptake of cholesterol by the oocyte. Cholesterol is normally transported to cells via lipoprotein particles however we used cholesterol here as a simple marker of transport of a lipophilic molecule. Although serum (fetal calf serum) was present in all cultures, we expect that the cholesterol remained as free cholesterol since the formation of lipoproteins is a specific cell mediated event and the incorporation of exogenous lipids into lipoprotein particles requires complex manipulations (Blasiole *et al.* 2007). Cholesterol transport is expected to be analogous to that of other lipophilic molecules particularly steroids such as progesterone and androgens as well as sterols including the meiosis activating sterol that are clearly important in oocyte maturation (Smith and Tenney 1980; Eppig *et al.* 1983; Grondahl *et al.* 2000; Borman *et al.* 2004; Gill *et al.* 2004; Marin Bivens *et al.* 2004). Additionally, cumulus cells are responsible for de-novo synthesis of cholesterol (Su *et al.* 2008) and its appropriate supply to the oocyte may be important for the control of suitably timed meiotic progression (Sadler and Jacobs 2004). Thus the transport of cholesterol in the context of the expanded COC matrix is highly relevant to oocyte maturation both *in vivo* and *in vitro*.

Our finding that IVM COCs, which lack Versican and Adamts1, have reduced metabolite exclusion properties, which suggests that specific components of the cumulus matrix are responsible for the filtration properties of the *in vivo* expanded COC. Observations of matrices analogous to the expanded cumulus matrix support the idea that this matrix acts a molecular filter. The 'perineural net' that surrounds neurons consists of HA, chondroitin sulphate proteoglycans including Versican, as well as cross-linking proteins such as tenascins (Yamaguchi 2000; Bruckner *et al.* 2003). Much like the proposed role of COC matrix in protecting oocytes from environmental factors, the perineural net is widely thought to protect neurons from oxidative stress (Morawski *et al.* 2004). Versican has also been shown in other cellular systems to be protective for cells against oxidative damage (Wu *et al.* 2005a). Furthermore control of ion homeostasis in the neuronal local extracellular environment is maintained by the perineuronal net (Bruckner *et al.* 1993; Hartig *et al.* 1999).

The glycocalyx of kidney glomeruli is composed of proteoglycans and glycosaminoglycans very similar in composition to the matrix of the expanded COC. Versican and HA are proposed to play a role in the permeselectivity of the glomerulus with decreased abundance of Versican assocated with proteinuria (Jeansson and Haraldsson 2003; Jeansson *et al.* 2006). Likewise, the absence of veriscan from IVM COC matrix could be responsible for the impaired filtration properties observed in this study. The similarities in composition between the glycocalyx of the glomerular endothelial cells (GEC) with the matrix of the expanded COC support a functional equivalency whereby the cumulus matrix could also provide selectivity of molecules based on both charge and size. That depletion of verisican from the GEC glycocalyx functionally alters the charge selectivity of the barrier of the glomerulus (Jeansson *et al.* 2006), suggests that a lack of Versican may also impair filtration properties based on molecular charge and size in the *in vitro* matured COC.

The altered IVM matrix has functional consequences as shown here, resulting in aberrant metabolite supply to the oocyte following IVM. Oocyte energy supply is dependent on oxidative phosphorylation, in which carboxylic acids for oocyte use are provided from glucose metabolism by cumulus cells (Biggers *et al.* 1967; Leese and Barton 1985). Additionally, glucose metabolism in cumulus cells increases dramatically during COC expansion/oocyte maturation and is critical for optimal oocyte competence (Sutton-McDowall *et al.* 2006). We found that normally, following cumulus expansion *in vivo*, the supply of glucose to cumulus cells is limited. This would presumably result in a fixed rate of cumulus cell glucose metabolism dependent on the rate of substrate availability. As a result glucose is expected to

be depleted in the environment surrounding the oocyte due to the high demand by cumulus cells and limited rate of supply promoting supply of carboxylic acid metabolites to oocytes and meeting their unique metabolic requirements. The capacity of the COC matrix to control the oocyte microenvironment may facilitate the establishment of a cumulus to oocyte lactate/pyruvate shuttle, whereby cumulus cells with a high requirement and consumption for glucose, provide oocytes with pyruvate and lactate for its energy needs. Establishing a gradient of glucose diffusion to the oocyte by the cumulus matrix would allow for the cumulus cells to utilise glucose and convert it to the oocytes preferred substrates. In IVM COCs there is clearly an increased rate of glucose uptake within the cumulus mass and oocyte indicating a large deviation in the balance of metabolite supply and potentially explaining the sensitivity of oocytes to high glucose in IVM. Increased glucose availability in IVM cumulus cells and the oocyte is also likely to result in altered flux via the hexosamine biosynthesis pathway, which generates the substrates for Hyaluronan synthesis, and O-linked glycosylation of signalling molecules which, if altered results in decreased oocyte developmental competence (Sutton-McDowall *et al.* 2006; Thompson *et al.* 2007). This may particularly hold true for glucose diffusion and uptake in IVM oocytes as glucose exposure to maturing oocytes has detrimental effects on their developmental competence as discussed previously (Hashimoto *et al.* 2000; Sutton-McDowall *et al.* 2006; Thompson *et al.* 2007).

The COC matrix may also modulate exposure and hence responses of cumulus cells and oocytes to steroid and sterol signalling molecules and the increased diffusion rate and exposure of IVM oocytes to such factors may influence their response and account for the poor developmental competence of IVM oocytes. Several studies have shown that the addition of other lipophilic substrates to defined media such as meiosis activating sterol (FF-MAS), an intermediate in the cholesterol biosynthesis pathway, stimulates oocyte growth and improves oocyte competence (Cukurcam *et al.* 2007; Cavilla *et al.* 2008). In general, little is known about lipid signalling and cholesterol uptake by cumulus cells and the ability of the matrix to filter hydrophobic molecules means it is likely to regulate mechanisms that have yet to be identified.

This work demonstrates a novel function of the cumulus oocyte matrix. We have demonstrated that the expanded COC matrix has the capacity to act as a molecular filter that provides a unique extracellular environment to the maturing oocyte. Further, this function is alterd in IVM conditions and the extracellular matrix components, Versican, Hyaluronan and Adamts1 contribute. A greater understanding of the role that COC matrix components play in oocyte maturation could be translated to

optimise IVM conditions. Optimisation may include supplementation of current IVM media with recombinant Adamts1 and Versican proteins so they are incorporated into the matrix of expanding COCs, potentially improving the capacity of the IVM COC to regulate its own microenvironment. If the cumulus matrix produced *in vitro* can be improved to recapitulate the *in vivo* oocyte environment, including appropriate supply of energy metabolites and lipophilic molecules, IVM success rates and oocyte developmental competence may be improved leading to IVM becoming a viable option for patients requiring fertility treatment, especially those at risk of ovarian hyperstimulation syndrome (OHSS) (Le Du *et al.* 2005; Reinblatt and Buckett 2008).

Chapter 5

Adamts1 and Versican: Recombinant protein production and functional roles during *in vitro* oocyte maturation

5.1 INTRODUCTION

The matrix proteins, Adamts1 and Versican are abundantly present in the cumulus matrix during oocyte maturation *in vivo* (Russell *et al.* 2003a; Russell *et al.* 2003b; Dunning *et al.* 2007) and Chapter 3). However, their functional significance during oocyte maturation, ovulation and fertilisation is unknown. We have shown that the cumulus matrix of IVM COCs is deficient in these proteins (Chapter 3) and also has altered capacity to regulate the supply of small metabolites by the oocyte (Chapter 4). Both Adamts1 and Versican proteins contain numerous functional domains and motifs and their importance for cumulus matrix expansion and oocyte maturation can be predicted. Many of the known actions of Adamts1 and Versican could importantly influence COC and oocyte function but have yet to be investigated. The question of whether supplementation of IVM culture with recombinant Adamts1 and Versican proteins directly influences IVM COC was next addressed. Supplementation with recombinant proteins containing targeted mutations and deletions further provides the opportunity to elucidate the roles of the functional domains of Adamts1 and Versican in cumulus matrix function.

5.1.1 Adamts1

5.1.1.1 Regulation of expression in the ovary and role in fertility

The expression of *Adamts1* mRNA in granulosa cells (GCs) is induced in response to the LH surge in periovulatory ovaries in mice (Robker *et al.* 2000) rat (Espey *et al.* 2000), cow (Madan *et al.* 2003) and mare (Boerboom *et al.* 2003). Human *ADAMTS1* mRNA is strongly expressed in normal human ovaries (Jansen *et al.* 2004). Additionally, we have shown that 36 hours post hCG administration, human *ADAMTS1* mRNA is equally abundant in both cumulus and mural granulosa cells (Chapter 3), however, the regulation of *ADAMTS1* expression in human is not known.

Adamts1 is involved in folliculogenesis, ovulation and fertilisation and is essential for optimal fertility. In humans, reduced *ADAMTS1* expression was reported in the ovaries of patients with polycystic ovary syndrome (PCOS) (Jansen *et al.* 2004). Women with PCOS fail to ovulate and the etiology of this syndrome is not well understood; however, it is thought that the altered expression of ECM components, including *ADAMTS1*, contributes to the formation of cysts, the thickening of the ovarian capsule and/or

the anovulatory phenotype (Jansen *et al.* 2004). *Adamts1* gene disruption results in a reduction in the number of ovulations in mice (Shindo *et al.* 2000; Mittaz *et al.* 2004) and a significant decrease in the number of healthy growing follicles due to a failure to successfully remodel the ovarian ECM (Brown *et al.* 2006). Additionally, there is a significant reduction in fertilisation rates and on-time embryo development in *Adamts1* null COCs (Russell *et al.* 2005) which may, in part, be due to reduced oocyte developmental competence resulting from structural and functional insufficiencies in the COC matrix during maturation. Further supporting this concept, cumulus oocyte matrix of COCs matured *in vitro* which lack Adamts1 (Chapter 3) also have decreased developmental competence (Wang and Gill 2004). The absence of Adamts1 during oocyte maturation correlating with oocytes of lower developmental competence, led me to hypothesise that Adamts1 was involved in the process of oocyte maturation.

5.1.1.2 Adamts1 domain structure and function

The modular structure of Adamts1 includes domains with sequence homology to proteolytic, adhesive, anti-angiogenic and cell signalling proteins. The human and mouse sequences are highly conserved, exhibiting 83.4% sequence identity at the amino acid level (Vazquez *et al.* 1999). The Adamts1 protein is synthesised as an inactive protein and undergoes several processing events. Initially a signal peptidase cleaves the signal peptide during translation and transportation through the endoplasmic reticulum (Porter *et al.* 2005). This is followed by the removal of the prodomain, which is thought to be mediated by the protease furin (Kuno *et al.* 1999; Rodriguez-Manzaneque *et al.* 2000). It is thought that the presence of the pro-domain renders the protein proteolytically inactive; however it is possible that it is additionally required for correct folding of the protein and for secretion (Milla *et al.* 1999; Cao *et al.* 2000; Porter *et al.* 2005). Full length Adamts1, containing the Pro-domain, is 110kDa in size and reduced to 85kDa following proteolytic activation by the removal of the pro domain (Rodriguez-Manzaneque *et al.* 2000). In the ovary, both the pro- and mature forms of Adamts1 are increased, greater than 10-fold, following the LH surge (Russell *et al.* 2003a). The inactive, pro-Adamts1 protein (110 kDa) localises to granulosa cell cytoplasmic organelles thought to be secretory vehicles (Russell *et al.* 2003a). Mature, proteolytically active Adamts1 (85 kDa) is selectively localised to the matrix of the expanding COC (Russell *et al.* 2003a).

Secreted Adamts1 incorporates into the extracellular matrix via its C-terminal domain (Kuno and Matsushima 1998) likely through interaction with sulphated glycosaminoglycans in the ECM based on *in vitro* studies where the addition of soluble heparin releases Adamts1 protein into the media (Kuno *et al.* 1997). Adamts4 activation is mediated by a convertase, which is anchored to heparin sulphate proteoglycans (HSPG) at the plasma membrane (Mayer *et al.* 2008). Due to the high degree of homology shared between Adamts1 and -4, Adamts1 may also be anchored to HSPGs for proteolytic activation to occur.

Known functions of Adamts1 include its ability to cleave both Versican and aggrecan (Kuno *et al.* 2000; Sandy *et al.* 2001). Adamts1 cleaves Versican at the Glu^{441}-Ala^{442} within the sequence $DPEAAE^{441}$-A^{442} RRGQ generating a 70kDa cleavage product with the neoepitope of DPEAAE (Sandy *et al.* 2001). The proteolytic cleavage of Versican by Adamts1, as occurs in the expanding COC *in vivo (Russell et al. 2003a)*, may be important in modulating Versican function and is discussed later.

Adamts1 has been shown to possess antiangiogenic properties; a result of the TSP-1 domains of Adamts1 binding to VEGF-165, thus inhibiting binding to its receptor, VEGFR2 (Luque *et al.* 2003). Adamts1 additionally modulates the activity of the growth factors; FGF and Egf-like factors (Luque *et al.* 2003; Liu *et al.* 2006; Suga *et al.* 2006). The action of Egf-like growth factors is emerging as critical to acquisition of full oocyte competence (Russell and Robker 2007) thus this may be a key mechanism by which Adamts1 participates in ovulation and oocyte competence.

Additional functions of Adamts1 may occur via its disintegrin domain, which contains two disintegrin loops that are present in members of the reprolysin family of metalloproteases (Pfaff *et al.* 1994; Usami *et al.* 1994). The disintegrin conserved sequence is 13-15 amino acids in length and contains an RGD or RGX (where X is any negative amino acid). This motif has the ability to bind cell surface integrins and can act as a ligand itself or as an antagonist, preventing binding of other ligands (Wolfsberg and White 1996). Adamts1 lacks the core RGD/X motif, but a conserved cysteine arrangement implicates this region in interaction with integrins.

These modular functional domains of Adamts1 suggest it may exert adhesive, cell signalling and anti-angiogenic properties within the ovarian follicle. Interestingly, Adamts1 immunohistochemistry identified the mature protein on oocyte surfaces (Russell *et al.* 2003a). This observation needs to be confirmed

using an approach that does not depend on antibody recognition, such as recombinant labelled protein, but may indicate that Adamts1 participates in aspects of oocyte function or zona pellucida remodelling, or perhaps has roles in oocyte-sperm fusion. Other potential functions are likely to include proteolytic processing of matrix molecules during expansion, modulation of matrix adhesive properties and regulation of signalling between cumulus cells and/or the oocyte, most probably linking each of these processes simultaneously. As the domains of Adamts1 have both predicted and known diverse functions, we sought to demonstrate their functional importance in the establishment, integrity and function of the expanded COC matrix.

5.1.2 Versican

5.1.2.1 Domain organisation and isoforms

The chondroitin sulphate proteoglycan, Versican structure (Figure 5.3) includes the amino terminal globular domain (G1) containing an immunoglobulin-like loop region and tandem link protein-like motifs that bind HA (LeBaron *et al.* 1992). The carboxy terminal globular domain (G3) shows high sequence similarity to the selectin adhesion receptors and is comprised of two epidermal growth factor (Egf) domains, a carbohydrate recognition domain and a complement binding protein (CBP) region (Shinomura *et al.* 1993). The large GAG-attachment domain joining G1 and G3 is encoded by two alternatively spliced exons (GAGα or GAGβ) that encode motifs for chondroitin sulphate side attachments (LeBaron *et al.* 1992). Due to differential splicing within the GAG attachment domain, there exists four different isoforms of Versican; V0, V1, V2 and V3 (Shinomura *et al.* 1993; Dours-Zimmermann and Zimmermann 1994; Ito *et al.* 1995; Zako *et al.* 1995). These different forms of Versican differ in the length of the core protein and the number of GAG attachments (Dours-Zimmermann and Zimmermann 1994; Ito *et al.* 1995; Zako *et al.* 1995) The V0 isoform of Versican is the largest and contains both GAG-α and GAG-β domains (Ito *et al.* 1995; Shinomura *et al.* 1995). The V1 isoform encodes only the GAG-β domain and V2 only the GAG-α domain and V3 lacks both GAG attachment domains (Shinomura *et al.* 1995; Zako *et al.* 1995). All isoforms of Versican contain the G1-Hyaluronan binding domain and are therefore able to form different size aggregates with Hyaluronan which, to some extent, determines tissue volume (Wight and Merrilees 2004). The approximate molecular weights of core proteins are 370, 263, 180 and 74kDa for V0, V1, V2 and V3 respectively (Dours-Zimmermann and Zimmermann 1994; Ito *et al.* 1995; Shinomura *et al.* 1995; Zako *et al.* 1995).

5.1.2.2 Expression and function in the ovary and cumulus oocyte complex

Versican isoforms; V0, V1 and V3 are present throughout folliculogenesis with V0 and V1 being the predominant forms, expression is strongly induced in the granulosa cells following the LH surge *in vivo* (Russell *et al.* 2003b). Versican protein is localised near the basement membrane of the preovulatory follicle but predominantly in the matrix of the expanded COC after the LH surge indicating that Versican is required during follicle development and ovulation (Russell *et al.* 2003b). Mice homozygous for a mutation in the Versican gene die in utero by embryonic day 10.5 as a result of a heart defect (Mjaatvedt *et al.* 1998) and thus cannot be utilised for studies of the ovary or fertility.

Versican can bind HA through its N-terminal link protein domains and does so within the HA rich matrix of the expanding COC (LeBaron *et al.* 1992; Russell *et al.* 2003b). The C-terminal motifs of the G3 domain can interact with cell surface proteins including sulphated cell surface glycolipids (Miura *et al.* 1999), ECM glycoproteins, heparin sulphate proteoglycans (Ujita *et al.* 1994) and integrins (Wu *et al.* 2002). Versican may therefore have the ability to crosslink Hyaluronan of the expanding COC matrix with the cumulus cells or other matrix components and could also have cell signalling consequences.

The highly negatively charged chondroitin sulphate side chains of Versican attract and bind growth factors, cytokines and chemokines (Spivak-Kroizman *et al.* 1994) creating a reservoir of growth factors in the ECM or on the suface of cells where they can be presented to their receptors (Ruoslahti and Yamaguchi 1991; Tanaka *et al.* 1993). A growth factor reservoir within the matrix of the COC could regulate the timing and type of response to growth factors required for optimal oocyte maturation. Conversely, the absence of Versican and such a growth factor reservoir during IVM may contribute to the lower competence of *in vitro* matured oocytes.

Versican protein, present in the expanding COC matrix, is cleaved by Adamts1 yielding a 70kDa N-terminal fragment immunopositive for the neoepitope DPEAAE, (Russell *et al.* 2003a). This proteolytic cleavage in turn dissociates the matrix cross-linking properties of Versican's N- and C-terminal domains, thus altering Versicans interactions with other cellular components and modifying matrix structure (Wu *et al.* 2002). This processing may modulate the adhesion, migration and proliferation of cells through

interactions between Versican and cell surface and matrix proteins (Zimmermann and Ruoslahti 1989). Versican promotes cell adhesion through its G3, C-terminal domain, which has been shown to interact with β_1-integrin and activate focal adhesion kinase (FAK), thus promoting cell adhesion and preventing apoptosis (Wu *et al.* 2002; LaPierre *et al.* 2007). However, Versican is also considered to be an anti-adhesive molecule capable of impeding the attachment of embryonic fibroblasts to collagen type I, fibronectin and laminin (Yamagata *et al.* 1989; Yamagata *et al.* 1993). This anti-adhesive property of Versican is mediated via the G1 domain (Ang *et al.* 1999; Yang *et al.* 1999). The presence of cleaved Versican in the matrix of the COC *in vivo* may have an anti-adhesive function in releasing the expanded COC from the follicular wall during ovulation. However, the mechanism by which cleavage of Versican by Adamts1 affects COC expansion and concomitant oocyte maturation and ovulation remains to be demonstrated.

Cell proliferation is enhanced via the G3 Versican domain, which is thought to occur through the Egf-like motifs (Zhang *et al.* 1998). The Egf-like motifs of Versican do activate Egf receptors (EgfR) and downstream signal transduction pathways (Xiang *et al.* 2006). The induction of cumulus expansion *in vivo* requires activation of the Egf pathway and LH surge stimulation of granulosa cell expression of the Egf-like peptides amphiregulin, epiregulin and beta-cellulin (Park *et al.* 2004). These generate a paracrine signal from mural granulosa cells to the cumulus cells, which lack LH receptors, inducing cumulus expansion and ovulation. Null mutation of these factors individually does not impair COC expansion (Hsieh and Conti 2005) indicating that a number of similar signalling factors act co-ordinately in this response. As the Egf-like motifs of Versican are capable of activating EgfRs, I hypothesised that Versican was able to directly activate cumulus expansion and oocyte maturation through the activation of Egf receptors and that this response may be modulated by the cleavage of Versican by Adamts1.

To investigate the many potential mechanistic means by which Adamts1 and Versican, or their interaction could participate in COC function during ovulation and/or oocyte maturation I synthesised several recombinant forms of each protein and investigated their activity in IVM cultures.

5.2 METHODS

5.2.1 Recombinant Protein Production

5.2.1.1 Construction of plasmids

5.2.1.1.1 p3xFLAG*Ats*1, p3xFLAG-ΔPro*Ats*1, p3xFLAG-ΔDis*Ats*1 and Catalytically Inactive p3xFLAG E/A *Ats*1

Two catalytically active *Adamts1* constructs were generated; p3xFLAG-*Ats*1 containing the complete murine *Adamts1* sequence and p3xFLAG-ΔPro*Ats*1 containing the entire mature coding sequence with a truncation of the 5'- pro-region, which was designed to produce constitutively active recombinant protease (Figure 5.1).

The mature *Adamts1* coding sequence, ΔPro*Ats*1 (depicted in Figure 5.1), was amplified using cDNA synthesised from NIH3T3 cell line and ΔProAdamts1(F) and ΔProAdamts1(R) primers (Table 5.1). The gel purified PCR product was subcloned into NheI and HindIII sites of pcDNA®3.1/myc-His(-) A (Invitrogen Australia Pty. Ltd., Mt Waverley, VIC, Australia).

The ΔPro*Ats*1 sequence was subsequently subcloned from pcDNA®3.1/myc-His(-) A into p3xFLAG-CMV®-13 mammalian expression vector (Sigma-Aldrich Pty. Ltd, Castle Hill, NSW, Australia). The p3xFLAG-CMV®-13 contained an upstream Preprotrypsin sequence for the secretion of the recombinant protein into the culture media and a C-terminal 3XFLAG® fusion protein for detection of recombinant protein. The ΔPro*Ats*1 fragment was excised from pcDNA®3.1/myc-His(-) A by firstly digesting with ApaI. The resulting 5' overhangs were removed using 5 units of DNA Polymerase I, large (Klenow) Fragment (New England Biolabs Inc., Ipswich, MA, USA) and incubation at room temperature for 20 minutes. This fragment was gel purified and further digested with NotI. The resulting fragment was again gel purified and subcloned into NotI and EcoRV sites of p3xFLAG-CMV®-13. The cloned ΔPro*Ats*1 fragment was termed p3XFLAG-ΔPro*Ats*1. Cloned fragments were sequenced to confirm their homology to the published *Adamts1* sequence.

To amplify the Pro region of the *Adamts1* coding sequence, NIH3T3 cDNA and the primers ProAdamts1(F) and ProAdamts1(R) were utilised (Table 5.1). The resulting ProAdamts1 PCR product

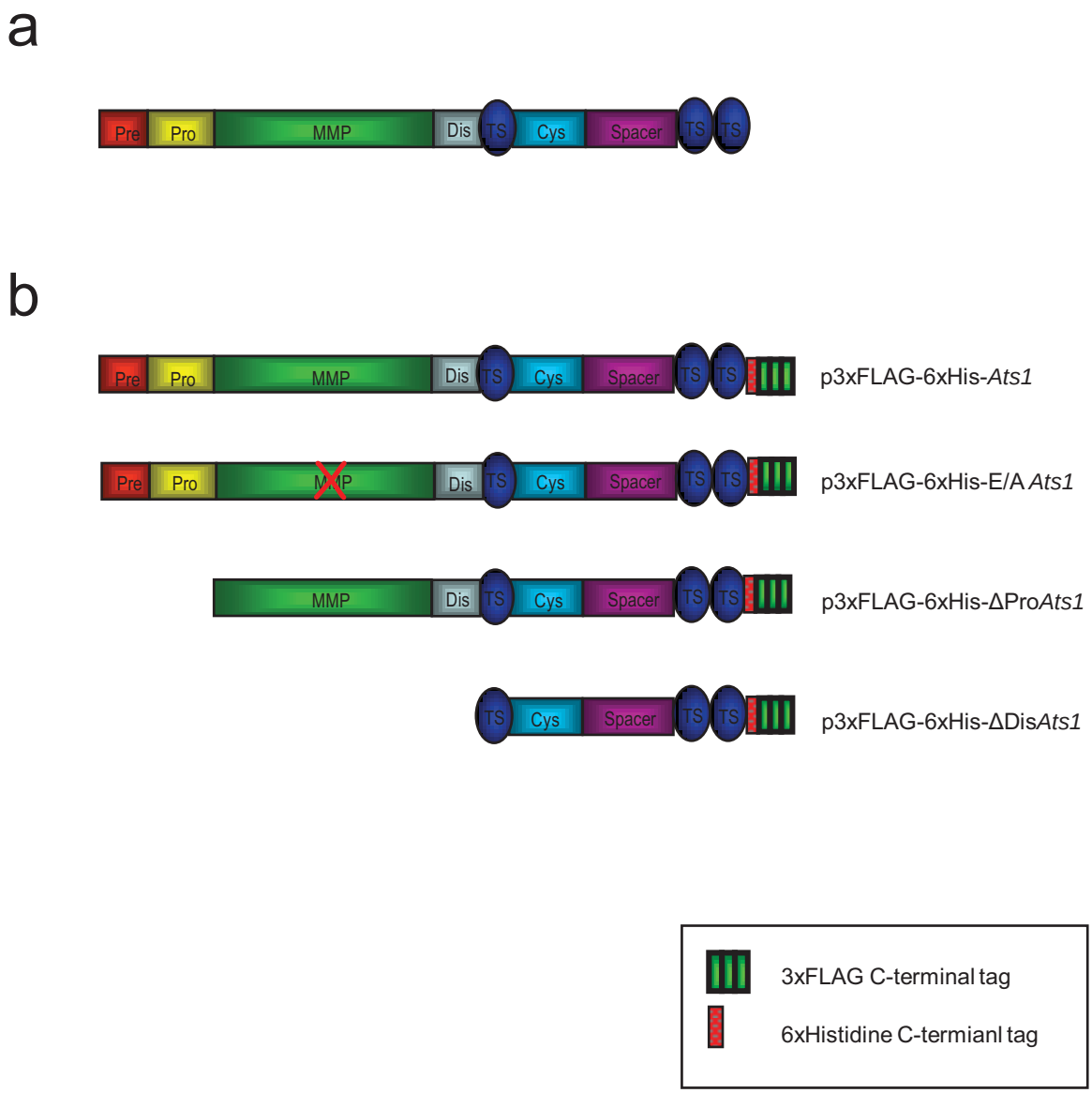

Figure 5.1 Schematic representation of *Adamts1* domain structure and generated recombinant *Adamts1* constructs.

Schematic representation of the configuration of Adamts1 domains (a). Pre, signal peptide; Pro, prodomain; MMP, metalloprotease catalytic domain; Dis, disintegrin like; Cys, cysteine rich domain; TS, thrombospondin type I repeat; Spacer, spacer domain. Constructs were generated to assess the functional importance of different domains (b). Full length and serially truncated constructs of *Adamts1* were amplified by gene specific primer based polymerase chain reaction (PCR) and sub-cloned into mammalian expression vector p3xFLAG-CMV13 (Sigma-Aldrich). Generation of a catalytically inactive construct of *Adamts1* was achieved by PCR based mutagenesis of the zinc binding domain as described previously (p3xFLAG-6xHis-E/A *Ats1*; Kuno et al. 1999). A 6x Histidine tag was also introduced at the C-terminus of the *Adamts1* constructs, upstream of the FLAG tag present in the p3xFLAG-CMV13 vector. Designated names of each construct are found to the right of each schematic.

Table 5.1 Primers utilised in the construction of *Adamts1* and *Versican* expression plasmids.

Sequences homologous to the murine *Adamts1* and *Versican* sequence are shown in italics. Letters in bold signify conserved Kozak sequence. Underlined sequence indicates restriction sites for cloning purposes. Letters in red signify introduced 6 x histidine tag.

Construct	Forward primer	Sequence 5'-3'	Introduced Restriction site (underlined sequence)	Reverse primer	Sequence 5'-3'	Introduced Restriction site (underlined sequence)
P3xFLAG*ats1*	Pro*Adamts1*(F)	GGGCCC*GCTAGC*ATGCAGCCAAAAGTCCC	NheI	Pro*Adamts1*(R)	GGGCCC*GCTCTGGATCC*CGGTCAC TG	BamHI
P3xFLAGΔPro*Ats1*	ΔPro*Adamts1*(F)	GGGCCC*GCTAGC*ATG**G**TCGTGGCTGACCAGTC	NheI	ΔPro*Adamts1*(R)	GGGCCC*AAGCTT*GCACTGTGTCAGTGTGCAAAAGTC	HindIII
P3xFLAGΔDis*Ats1*	ΔDis*Adamts1*(F)	GGGCCC*GCTAGC*ATG**G**AGCATTTTGCTACT	NheI	ΔDis*Adamts1*(R)	GGGCCC*AAGCTT*GCACTGTGTCAGTGTGCAAAAGTC	HindIII
P3xFLAG-G1	*Versican* G1 (F)	AT*GCGGCCGC*TTCCAAGGCC**A**AGATG**G**TC	*NotI*	*Versican* G1 (F)	TA*GGATCC***ATGATGATGATGATGATG***AGCTTCTGCAGCT TCTGGGTC*	BamHI
P3xFLAG-G3	*Versican* G3 (F)	TA*GCGGCCGC***A**AG**C**ATG**G**CAATCTATTTAC	*NotI*	*Versican* G3 (F)	TA*GGATCC***ATGATGATGATGATGATG***GCGCCTCGACTCC*	BamHI

was subcloned into pCR®II-TOPO®II (Invitrogen Australia Pty. Ltd., Mt Waverley, VIC, Australia) as per manufacturers' instructions. Briefly, to a 6μl reaction the following was added, 2μl of PCR product, 1μl of Salt solution (200mM NaCl, 10mM $MgCl_2$), 1μl of TOPO vector and 2μl H_2O. The reaction was mixed gently and incubated at room temperature for 5 minutes. The reaction was then incubated on ice and transformed into OneShot® MARCH1TM_T1R Competent E.coli (Invitrogen Australia Pty. Ltd., Mt Waverley, VIC, Australia). Transformation involved adding 2μl of the TOPO cloning reaction to a vial of OneShot® E. coli, gently mixing and incubating for 5 minutes on ice. Cells were then heat shocked for 30 seconds in a 42°C water bath and transferred to ice. To each tube 250μl of SOC was added and the tubes shaken horizontally (200rpm) at 37°C for 1 hour. The transformed bacteria were plated and plasmid preparations performed as per section 5.1.1.1.8.

ProAdamts1 was subsequently subloned into NheI and BamHI sites of p3XFLAG-ΔPro*Ats*1 to generate an expression vector containing the complete coding sequence of murine Adamts1. This expression vector was termed p3XFLAG-*Ats*1 and is depicted in Figure 5.1.

The ΔDis*Ats*1 construct containing Adamts1 coding sequence downstream of the disintegrin domain of Adamts1 (Figure 5.1 b), was amplified using ΔDisAdamts1(F) and ΔDisAdamts1(R) primers (Table 5.1). The gel purified PCR product was subcloned into NheI and HindIII sites of pcDNA™3.1/myc-His(-) A (Invitrogen Australia Pty. Ltd., Mt Waverley, VIC, Australia). The ΔDis*Ats*1 sequence was then subcloned from pcDNA™3.1/myc-His(-) A into p3xFLAG-CMV™-13 mammalian expression vector (Sigma-Aldrich Pty. Ltd, Castle Hill, NSW, Australia) in an identical manner to that used for ΔPro*Ats*1 (see above). The cloned ΔDis*Ats*1 fragment was termed p3XFLAG-ΔDis*Ats*1 and sequenced to confirm homology with the published *Adamts1* sequence.

To p3XFLAG-*Ats*1, p3XFLAG-ΔPro*Ats*1 and p3XFLAG-ΔDis*Ats*1 vectors, a C-terminal 6x histidine tag was added upstream and adjacent to the 3XFLAG fusion tag (Figure 5.1, b). This was introduced for purification purposes. The addition of this tag involved the following; complementary oligonucleotides, containing 6 histidine codons and overhanging XbaI sites, were hybridised in a reaction containing 100ng/μl of each oligonucleotide, 6xHis Linker (F) 5' *CTAGA*TCATCATCATCATCATCAT*T* 3' and 6xHis Linker (R) 5' *CTAGA*ATGATGATGATGATGATG*A T* 3' (letters in italics indicate XbaI restriction overhangs), 10μl 20X SSC (3M NaCl, 0.3M Sodium Citrate, pH 7.0) and H_2O to 100μl and incubation at 100°C in a dry block for 10 minutes followed by incubation at room temperature for 16 hours. The

hybridised 6XHis tag, containing XbaI restriction overhangs, was ligated into XbaI digested p3XFLAG-*Ats*1, p3XFLAG-ΔPro*Ats*1 and p3XFLAG-ΔDis*Ats*1 vectors treated with Alkaline phosphatase and precipitated (2.2.7.3 and 2.2.7.4 respectively). The resulting vectors were termed p3XFLAG-6XHis-*Ats*1, p3XFLAG-6XHis-ΔPro*Ats*1 and p3XFLAG-6XHis-ΔDis*Ats*1 (Figure 5.1 b).

Generation of a catalytically inactive construct of *Adamts1* was achieved by a PCR based mutagenesis of the zinc binding domain as described previously (Kuno *et al.* 1999). A single point mutation (GAA → CAA, Guanine → Cytosine, E → Q) at nucleotide 1596-1598 (NM_009621) and corresponding residue 403 (NP_033751) was introduced using the GeneTailor® Site Directed Mutagenesis System (Invitrogen Australia Pty. Ltd., Mt Waverley, VIC, Australia) as per the manufacturers' instructions. Primers utilised were as follows, (F) 5' ACCACAGCCCAC**C**AATTGGGCCATGTG 3' and (R) 5' TGGTGTCGGGTGGTTAACCCGGTACAC 3' (the bold residue indicates the point mutation introduced at nucleotide 1596). The template plasmid p3XFLAG-6XHis-*Ats*1 (100ng) was first incubated at 37°C for 1 hour in a reaction containing, 1.6μl Methylation buffer, 1.6μl 10X S-adenosylmethionine (SAM), 4 units of DNA methylase and H_2O to 16μl. This reaction methylates the central cytosine residue found with in the sequence CAGCTG. A PCR was performed in a 50μl volume containing 1.0 unit of Platinum® Taq, 5μl 10X High Fidelity PCR Buffer, 0.3mM each dNTP, 1mM $MgSO_4$, 0.3μM each primer, 12.5ng of methylated template DNA and H_2O to 50μl. Cycling conditions were as follows, 94°C 2 minutes (1 cycle), 94°C, 30 seconds; 55°C 30 seconds; 68°C, 4 minutes (20 cycles), 68°C, 10 minutes (1 cycle). PCR cycling was performed on a Gene Amp® ABI 9700 thermal cycler. The mutagenesis reaction was transformed into DH5α™ -T1R E. Coli (Invitrogen Australia Pty. Ltd., Mt Waverley, VIC, Australia) as per manufacturer's instruction. Briefly, 2μl of the mutagenesis reaction was transformed into 50μl of E. Coli and mixed gently. The tubes were incubated on ice for 10 minutes then heat-pulsed in a 42°C water bath for 30 seconds followed by incubation for 1 minute on ice. The cells were resuspended in 200μl of 42°C SOC (20g/L tryptone, 5g/L yeast extract, 0.5g/L NaCl, 10mM MgCl2, 20mM glucose). The resuspended cells were allowed to recover by incubating at 37°C for 1 hour with aeration (230rpm). The transformation was plated on LB-Agar plates (10g/L tryptone, 5g/L yeast extract, 5g/L NaCl, 15g/L agar) containing ampicillin (100μg/ml, Sigma-Aldrich Pty. Ltd, Castle Hill, NSW, Australia) and incubated at 37°C for 16 hours. Single clones were used to inoculate cultures for plasmid preparations (Section 2.2.7.7) and sequenced (Section 2.2.7.9) using a primer approximately 250bp

downstream of the single nucleotide change (5' GGAAGATCAGAAGGGAGCTTGA 3') to determine that the point mutation was successfully introduced (Figure 5.2).

5.2.1.1.2 p3xFLAG-6XHis-G1 and p3xFLAG-6XHis-G3

The generation of expression constructs containing the two globular domains of human *VERSICAN*, G1 and G3 were amplified by PCR using pECE-V1 (contained the coding sequence for V1 isoform of *Versican*) as a template (kind donation from John Sandy, Figure 5.3 b). Amplification of the G1 domain utilised the primers Versican G1 (F) and Versican G1 (R) and amplification of G3, primers Versican G3 (F) and Versican G3 (R) (Table 5.1). The gel purified PCR products were cloned into NotI and BamHI sites of p3xFLAG-CMV™-13. The reverse primers for the amplification of G1 and G3, Versican G3 (R) and Versican G1 (R), incorporated a C-terminal 6X histidine tag for purification purposes (Table 5.1, Figure 5.3 b). The resulting constructs were termed p3XFLAG-6XHis-G1 and p3XFLAG-6XHis-G3 and were sequenced to confirm their homology with the published sequence.

5.2.1.2 Cell Culture

Mammalian 293T, NIH3T3 and CHOK1 cell lines were maintained in T75 flasks (Corning Life Sciences, Crown Scientific, Minto, NSW, Australia) containing 12ml of Dulbecco's Modified Eagle Medium (DMEM) or alpha Minimal Essential Media (αMEM) supplemented with 10% (v/v) fetal calf serum (complete DMEM/αMEM). Cells were incubated at 37°C with 5% CO_2 in a humidified incubator. All manipulations were conducted using aseptic technique in a biohazard hood. Media was changed twice a week. Cells were harvested by aspiration of media, washing with PBS and trypsinising with 2ml of 0.25% (w/v) Trypsin 0.38 g/L of EDTA•4Na (Gibco, Invitrogen Australia Pty. Ltd., Mt Waverley, VIC, Australia). The resuspended monolayer was washed in 12 ml of complete media then plated at the required density in additional tissue culture flasks or plates. Twenty four hours prior to transfection cells were plated at a density such that the cells reached 90-95% confluency at the time of transfection.

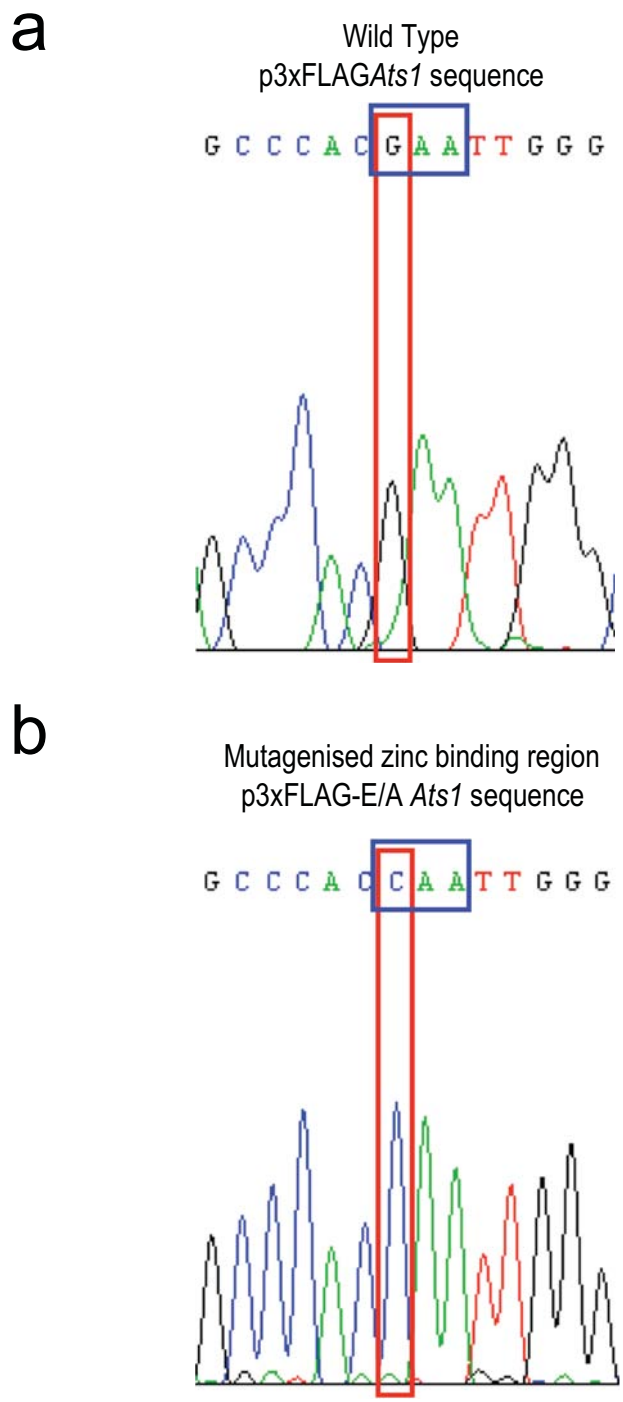

Figure 5.2 Mutation of the Adamts1 zinc binding region.

Generation of a catalytically inactive construct of Adamts1 was achieved by PCR based mutagenesis of the zinc binding domain as described previously (Kuno et al. 1999). A single point mutation of Guanine (a, *red box*) to Cytosine (b, *red box*) at nucleotide 1596-1598 (NM_009621) and corresponding residue 403 (NP_033751) was introduced. This missense mutation resulted in a GAA → CAA codon change (a and b respectively, *blue boxes*) and a Guanine (E) → Cytosine (Q) amino acid substitution.

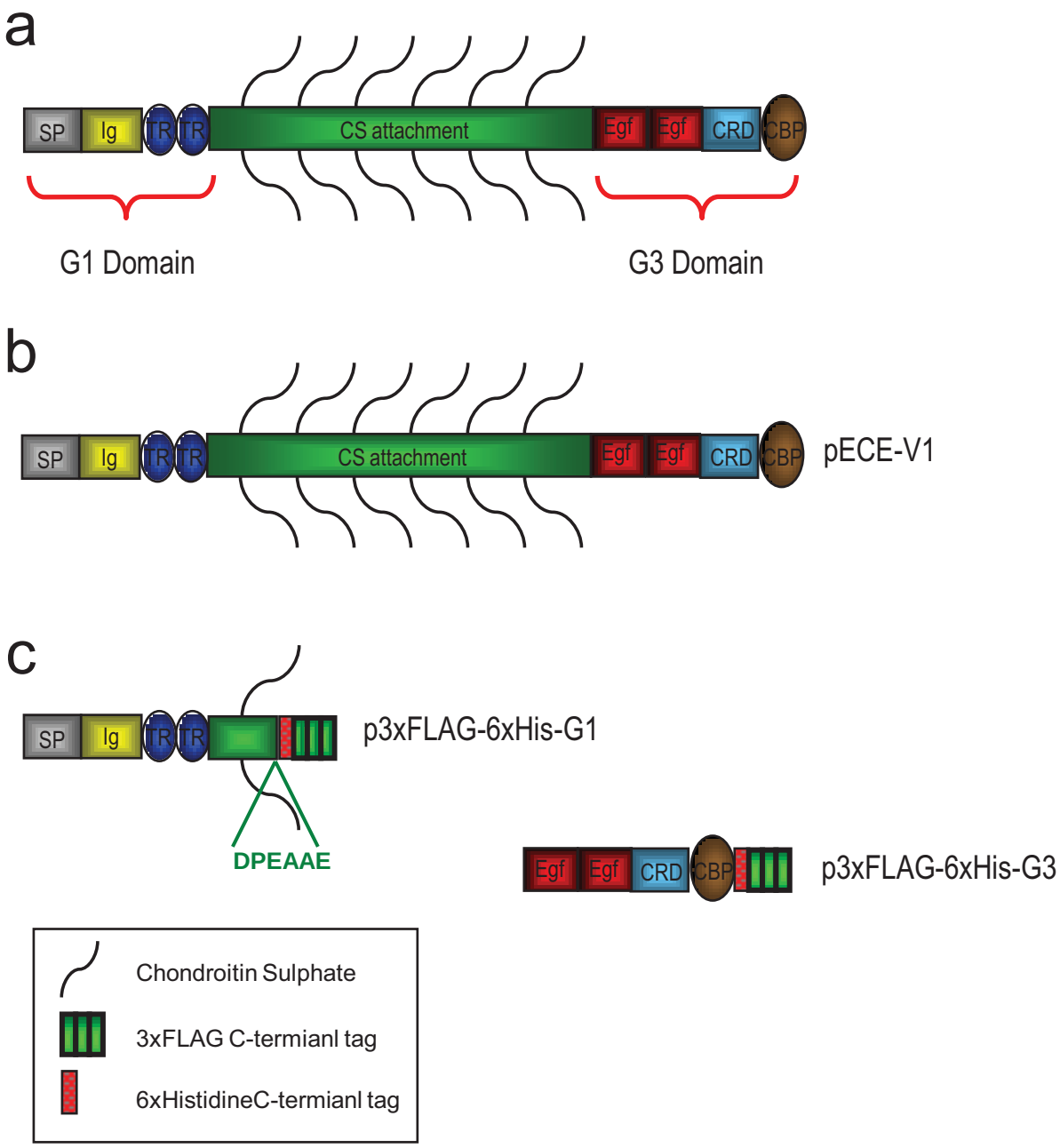

Figure 5.3 Schematic representation of the domain organization of Versican and generated *Versican* constructs.

Schematic of Versican domain organization (a). *SP*, signal peptide; *Ig*, immunoglobulin-like; *TR*, Tandem repeat, *Egf*, epidermal growth factor-like; *CRD*, carbohydrate recognition domain; *CBP*, complement binding protein. Constructs were generated to assess the functional importance of different domains (c). Designated names of each construct are found to the right of each schematic. The pECE-V1 contained the entire coding sequence of the V1 isoform of *Versican* and was a kind donation from John Sandy (b). The G1 and G3 domains of *Versican* were amplified by gene specific primer based polymerase chain reaction (PCR) and sub-cloned into mammalian expression vector p3xFLAG-CMV13 (Sigma-Aldrich) (c). The amplified G1 domain terminated at the DPEAAE amino acid sequence normally generated by Adamts1 cleavage. A 6x Histidine tag was also introduced at the C-terminus of the G1 and G3 constructs, upstream of the FLAG tag present in the p3xFLAG-CMV13 vector.

5.2.1.3 Transient and Stable Expression of recombinant proteins in mammalian cells

Expression vectors containing the various forms of *Adamts1* and *Verscian* (Figure 5.1 and Figure 5.3) were transiently transfected into 293T cells plated in 6 well plates (Corning Life Sciences, Crown Scientific, Minto, NSW, Australia), in 2ml of complete media. Transient transfections were performed using Lipofectamine™ 2000 (Invitrogen Australia Pty. Ltd., Mt Waverley, VIC, Australia) as per the manufacturers' instructions. Briefly, 4μg of plasmid DNA was added to 250μl serum-free media in one tube and 10μl Lipofecatmine™ 2000 was added to 250μl of serum-free media in a separate tube. The tubes were incubated for 5 minutes at room temperature; the solutions were then combined and allowed to incubate at room temperature for a further 20 minutes. The DNA/Lipofectamine™ 2000 solution was then pipetted onto cells in a drop wise manner. Media was replaced 5 hours post transfection with serum free DMEM containing a 1x solution of ITS (insulin, transferrin and selenium, Sigma-Aldrich Pty. Ltd, Castle Hill, NSW, Australia). For transfections involving *Adamts1* constructs, Heparin (5ug/ml) was included to enable collection of recombinant protein from the media (Kuno and Matsushima 1998). Media and cell layers were harvested 48 hours post transfection. The media was cleared of cellular debris by centrifugation, 1100rpm 10 minutes and supernatant was transferred to a new tube. Cell layers were washed with sterile PBS (0.137M NaCl, 0.0027M KCl, 0.0043 Na_2HPO_4, 0.00147M KH_2PO_4) and harvested by cell scraping followed by centrifugation, 1100rpm 5 minutes. Cell pellets were resuspended in 100μl RIPA buffer (150mM NaCl, 1% (v/v) NP-40, 0.5% (w/v) Deoxycholate, 0.1% (w/v) SDS, 50mM Tris-HCl pH8); non-soluble cellular debris was removed by centrifugation at 13,000rpm for 1 minute and supernatants were frozen for Western blot analysis.

We obtained a CHO-K1 cell line stably transfected with an expression vector for V1 *VERSICAN* (pECE-V1) termed CHO-V1 (Figure 5.3 b, kind donation from Prof. R. LeBaron, Division of Life Science, University of Texas at San Antonio). Versican expressing CHO-V1 cells were regularly placed under selection (3μM Methotrexate in complete αMEM) in order to maintain stable expression. Stable transfection of the p3xFLAG-6xHis-*Ats*1 plasmid into the CHO-V1 cell line involved plating and transfection of the cells using Lipofectamine® 2000 (Invitrogen Australia Pty. Ltd., Mt Waverley, VIC, Australia) as described above for transient transfection. Stable transfectants were selected using

400μg/ml G418 (in complete αMEM) until there were no surviving cells in duplicate wells that were not transfected. High Adamts1 expression was confirmed in the resulting cell line, which was termed CHO-V1-*Ats*1.

5.2.1.4 Purification of recombinant proteins

Purification of 6xHis tagged recombinant proteins was performed using ProBond™ Resin (Invitrogen Australia Pty. Ltd., Mt Waverley, VIC, Australia). One ml of resin was resuspended in 6ml of sterile H_2O followed by two washes using 2 x 6ml of wash/equilibration buffer (40mM Hepes pH 7.0, 1M NaCl, 10mM imidazole). Four millilitres of conditioned media (cleared of cellular debris and equilibrated to a final concentration of 20mM Hepes pH 7.0, 0.5M NaCl) was mixed with the resin at room temperature for 30 minutes. The resin and media were loaded onto a chromatography column (Bio-Rad Laboratories Pty. Ltd., Gladesville, NSW, Australia) and the flowthrough collected. The washing conditions were optimised by testing increasing concentration of imidazole in the wash buffer (40mM Hepes pH 7.0, 1M NaCl, 10-500mM imidazole) to remove of contaminating proteins but not elute the recombinant protein of interest. Optimised buffer compositions and conditions for the purification of recombinant Adamts1 proteins were; wash/equilibration buffer (40mM Hepes pH 7.0, 1M NaCl, 50mM imidazole) using 2 x 4 ml washes following binding of 4ml of conditioned media and 4 x 500μl fractions using elution buffer (40mM Hepes pH 7.0, 1M NaCl, 250 or 500mM imidazole). Optimised buffer compositions and conditions for the purification of recombinant G1 protein was; wash/equilibration buffer (40mM Hepes pH 7.0, 1M NaCl, 30mM imidazole) using 2 x 4 ml washes following binding of 4ml of conditioned media and 4 x 500μl fractions using elution buffer (40mM Hepes pH 7.0, 1M NaCl, 250mM imidazole). To purify recombinant G3 protein, which contained an additional Histidine residue in the poly-histidine tag the following conditions were used; wash/equilibration buffer (40mM Hepes pH 7.0, 1M NaCl, 100mM imidazole) using 2 x 4 ml washes following binding of 4ml of conditioned media and 4 x 500μl fractions using elution buffer (40mM Hepes pH 7.0, 1M NaCl, 50mM EDTA).

Purified full length Versican was a kind donation from Dr Carmela Ricciardelli (University of Adelaide, Australia). Recombinant Versican was purified from CHO-V1 conditioned media as described previously (Ricciardelli *et al.* 2007) using a combination of anion exchange and gel filtration chromatography. Briefly, conditioned media was batch-adsorbed to Q-Sepharose (10 ml/liter of medium, Amersham

Biosciences, GE Healthcare Bio-Sciences Pty. Ltd., Rydalmere NSW, Australia) at 4°C for 24-48 h in the presence of protease inhibitor tablets (Roche Applied Science, Castle Hill, NSW, Australia). Versican was eluted using 2M NaCl in PBS, pH 7.4 and purified by gel chromatography on a Sephacryl S400 (15 x 650-mm column, Amersham Biosciences, GE Healthcare Bio-Sciences Pty. Ltd., Rydalmere NSW, Australia) as described previously (Sakko *et al.* 2003). The elutions containing Versican were then concentrated 10-20-fold using Centriprep centrifugal filters (Amicon Bioseparations, Bedford, MA) and Nanosep™ microconcentrators (Pall Australia, Cheltneham, VIC, Australia) with M_r 50,000 and 300,000 cut-offs, respectively. The molecular integrity of the purified Versican samples was determined by Western blot using the α-Vc antibody against recombinant human Versican provided by Prof. LeBaron as previously described (du Cros *et al.* 1995).

5.2.1.5 Anti-Flag Immunohistochemistry and Western blotting

Pure recombinant proteins were identified by Western blot analysis for the Flag tag. Proteins were separated by 12% SDS-PAGE and transferred to PVDF membrane (as per section 2.2.5). Membranes were blocked with a solution of 5% (w/v) non-fat milk in PBS (80mM Na_2HPO_4, 20mM NaH_2PO_4, 100mM NaCl) for 1 hour at room temperature. The membrane was washed three times in PBS containing 0.05% Tween 20 (PBST). The primary antibody, Rabbit ANTI-FLAG® Polyclonal Antibody (Sigma-Aldrich Pty. Ltd, Castle Hill, NSW, Australia) was used at the recommended concentration of 2.5μg/ml in PBS containing 1% BSA (Sigma-Aldrich Pty. Ltd, Castle Hill, NSW, Australia) at room temperature for 2 hours. Blots were then washed in PBST and incubated with horseradish peroxidase-linked anti-rabbit IgG at 1:5000 (Millipore, North Ryde, NSW, Australia). Enhanced chemiluminescence detection was used as per manufacturer's instructions (Amersham Biosciences, GE Healthcare Bio-Sciences Pty. Ltd., Rydalmere NSW, Australia).

Anti-Flag immunohistochemistry was performed on cells grown and transfected on sterile coverslips. Immunohistochemistry was performed 24 hours post transfection. Cells were washed briefly in PBS and fixed with methanol and acetone for 10 and 1 minute(s) respectively at -20°C. Cells were subsequently washed twice with PBS. Cells were blocked in 1% BSA/PBS for 10 minutes at room temperature. The primary Rabbit ANTI-FLAG® Polyclonal Antibody (Sigma-Aldrich Pty. Ltd, Castle Hill, NSW, Australia) was incubated with cells at 5μg/ml in PBS for 1 hour at room temperature. Cells were washed and

incubated with the secondary antibody, Alexa Fluor® 488-linked anti-rabbit IgG at 1:500 (Molecular Probes, Invitrogen Australia Pty. Ltd., Mt Waverley, VIC, Australia) in PBS containing 1% BSA for 30 minutes at room temperature. Cells were washed and counter stained with 300nM DAPI (Molecular Probes, Invitrogen Australia Pty. Ltd., Mt Waverley, VIC, Australia).

5.2.1.6 Silver nitrate staining of SDS-PAGE gels

Silver staining of SDS-PAGE gels was performed using the Silver stain Plus kit (Bio-Rad Laboratories Pty. Ltd., Gladesville, NSW, Australia) as per the manufacturers' instructions. Briefly, following electrophoresis, SDS-PAGE gels were fixed in Fixative Enhancer Solution (50% methanol (v/v), 10% acetic acid (v/v), 10% Fixative Enhancer concentrate (v/v) and 30% MilliQ H_2O (v/v) for 20 minutes with agitation. Gels were washed twice in MilliQ H_2O for 10 minutes. Staining and developing was performed by incubation for 15-20 minutes, with agitation, in a solution of 5% Silver Complex Solution (v/v), 5% Reduction Moderator solution (v/v), 5% Image Development reagent (v/v), 50% Development Accelerator solution (v/v) and 35% H_20 (v/v). The staining process was stopped by washing gels in a solution of 5% acetic acid (v/v) for 15 minutes followed by rinsing in MilliQ H_2O for 5 minutes. Gels were photographed on a transilluminator (DC120 Kodak).

5.2.1.7 In vitro *oocyte maturation in the presence of recombinant Versican and Adamts1*

Hormonal stimulation of mice, isolation of cumulus oocyte complexes and *in* vitro maturation conditions used were as previously described (Section 3.2.1). In order to assess the effect of Versican on cumulus expansion *in vitro*, IVM media was supplemented with purified recombinant full length Versican (Section 5.2.1.4, using an arbitrary 1:20 dilution), 50mIU/ml recombinant human FSH (Sigma-Aldrich Pty. Ltd, Castle Hill, NSW, Australia) or 3ng/ml Egf (Sigma-Aldrich Pty. Ltd, Castle Hill, NSW, Australia). Following a culture period of 20 h the degree of cumulus expansion was assessed as described in section 2.2.2 by a trained observer who was blind to the treatment conditions, which were randomly organised to ensure no bias in the assessments.

To determine the impact of full-length Versican and Adamts1-cleaved Versican on cumulus expansion *in vitro*, conditioned media was collected from CHO-K1 control cells, CHO-V1 and CHO-V1-*Ats*1 cells. Briefly, all cell lines were plated at equal density in a T75 cell culture flask (Corning Life Sciences, Crown Scientific, Minto, NSW, Australia) in alpha Minimal Essential Media (αMEM) supplemented with 10% (v/v) fetal calf serum. Cells were allowed to adhere to the flask for 24 h at 37°C with 5% CO_2 in a humidified incubator. The cells were washed and the media changed to serum free αMEM supplemented with 1x solution of ITS (insulin, transferrin and selenium, Sigma-Aldrich Pty. Ltd, Castle Hill, NSW, Australia) and incubated for a further 48 h prior to the collection of conditioned media. The effect of CHO-K1, CHO-V1 and CHO-V1-*Ats*1 conditioned media on cumulus expansion *in vitro* was assessed by supplementation of IVM media with 50, 30, 10 or 3% (v/v) from each cell line or 50mIU/ml recombinant human FSH for comparison.

5.3 RESULTS

5.3.1 Immunolocalisation and Western blot analysis of recombinant Adamts1 proteins

Following the construction of *Adamts1* expression plasmids, p3Xflag-*Ats*1, p3xFLAG-ΔPro*Ats*1, p3xFLAG-ΔDis*Ats*1 and catalytically inactive p3xFLAG-E/A *Ats*1 (Figure 5.1 b and Section 5.2.1.1.1) the production and secretion of recombinant protein was confirmed by immunolocalisation of the FLAG tag in cell monolayers and Western blot of media and cell extracts of transiently transfected into 293T cells (Figure 5.4). Immunohistochemistry showed strong FLAG positive staining in cells transfected with p3xFLAG*Ats*1, p3xFLAG-ΔPro*Ats*1, p3xFLAG-ΔDis*Ats*1 or p3xFLAG E/A *Ats*1 (Figure 5.4 a-d). Interestingly cells transfected with p3xFLAG*Ats*1, p3xFLAG-ΔDis*Ats*1 or p3xFLAG-E/A *Ats*1, showed punctuate staining in the extracellular matrix surrounding cells (Figure 5.4 a, b and d, *white arrows*) indicative of secretion and binding of these proteins to the local ECM. This punctuate staining was not detected in cells transfected with p3xFLAG-ΔPro*Ats*1 (Figure 5.4 c) suggesting it is not secreted or does not bind ECM.

Western blot analysis of cellular extracts and media of cells transfected with p3xFLAG*Ats*1 and p3xFLAG E/A *Ats*1 showed strong α-FLAG immunoreactive bands at approximately 110kDa and 85kDa

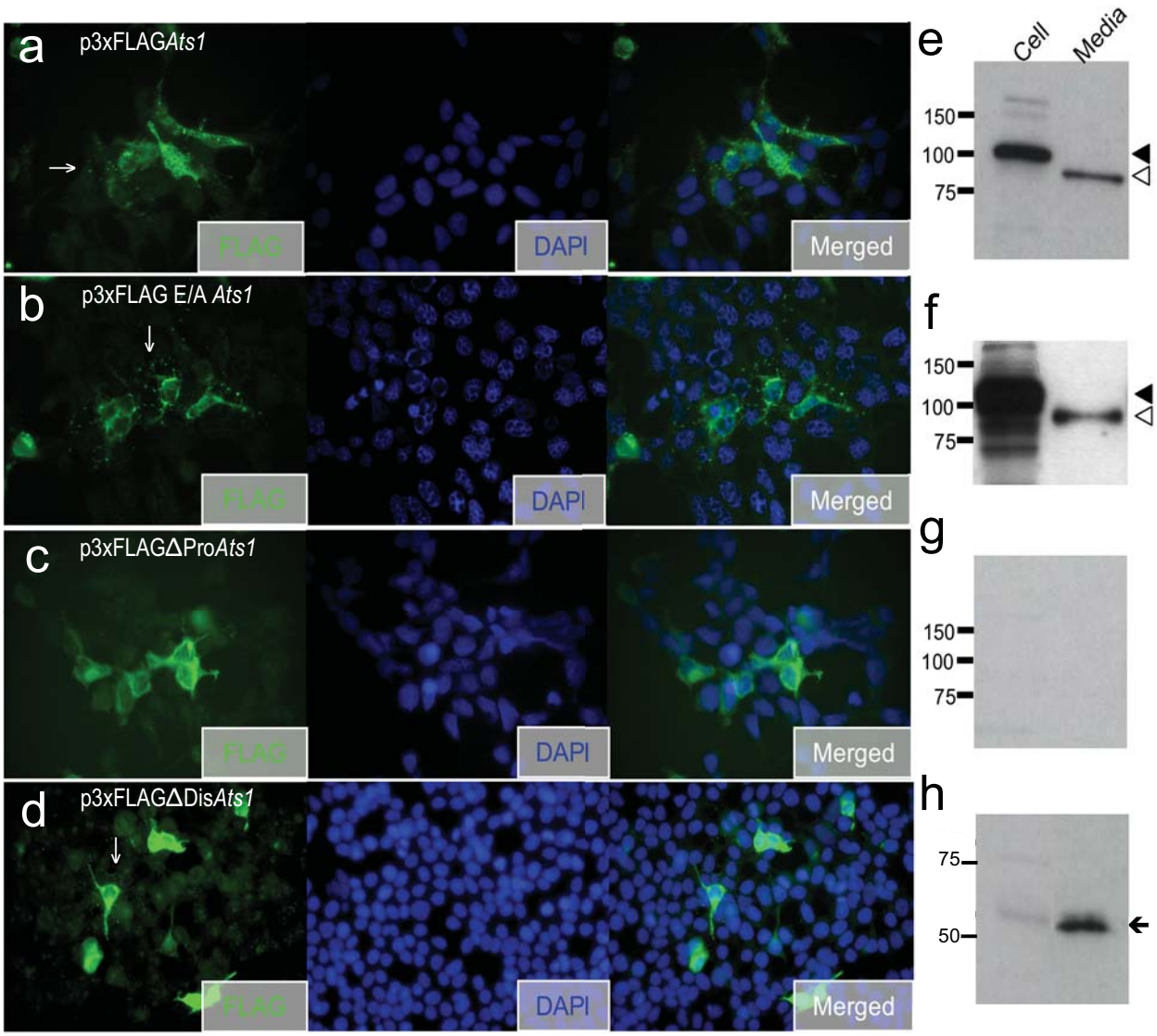

Figure 5.4 Immunolocalisation and Western blot analysis of recombinant Adamts1 proteins.

p3xFLAG constructs containing *Adamts1* were transfected into 293T cells and their expression analysed by immunohistochemistry using α-FLAG antibody (Sigma-Aldrich) and DAPI nuclear stain (a-d). Cell lysates and media were analysed by Western blot using α-FLAG antibody (e-h). Successful detection of FLAG immunoreactive proteins was seen for full length Adamts1 (p3xFLAG*Ats1*) (a); catalytically inactive Adamts1 (p3xFLAG-E/A-*Ats1*) (b); ΔproAdamts1 (p3xFLAGΔpro*Ats1*) (c) and Δ DisintegrinAdamts1 (p3xFLAGΔDis*Ats1*) (d) transfected cells. A band corresponding to a recombinant pro form of Adamts1, ~110kDa (*black arrow heads*, Russell et al, 2003), was present in the cell layer of p3xFLAG*Ats1* and p3xFLAG-E/A-*Ats1* transfected cells (e and f respectively). These transfectants also produced a band corresponding to a mature recombinant Adamts1 (~85kDa, *open arrowheads*, Russell et al 2003) present in the media. Anti-FLAG immunoreactive protein was detected within cells of p3xFLAGΔpro*Ats1* (c) however, no bands of predicted size were detected in either media or cell layers by Western blot (g). A band corresponding to the predicted size of 56kDa (calculated using bioinformatics) was present in both cell and media layers of p3xFLAGΔDis*Ats1* transfected cells (arrow, h).

in the cell and media layers respectively (Figure 5.4 e and f). These bands correspond to sizes expected for pro- and mature mouse Adamts1, respectively (Russell *et al.* 2003a) and indicate that Pro-Adamts1 is found mainly in cells while the active form is secreted into media. The p3xFLAG-ΔPro*Ats*1 construct was intended to produce constitutively active recombinant Adamts1 protease predicted to be of similar size to mature Adamts1 activated after transfection with p3xFLAG*Ats*1 (Figure 5.1 b). Repeated attempts to detect recombinant protein in either the cell or media layers of p3xFLAG-ΔPro*Ats*1 transfected cells by Western blot were unsuccesful despite the detection of α-FLAG positive protein within transfected cells by immunohistochemistry (Figure 5.4 g and c, respectively). It was concluded that overexpression of the active protease results in rapid degradation either by autolytic action or through cellular editing of the misfolded protein.

The expression plasmid, p3xFLAG-ΔDis*Ats*1, was constructed to produce recombinant Adamts1 protein containing only the TSP1 and spacer domains downstream of the disintegrin domain (Figure 5.1 b). *In silico* analysis predicted the recombinant p3xFLAG-ΔDis*Ats*1 protein to be 56kDa in size. Anti-FLAG Western blot analysis of p3xFLAG-ΔDis*Ats*1 transfected cells showed a strong band in the media layer that was approximately the predicted size (56kDa, Figure 5.4 h, *Media*). A band of similar size, but of lesser intensity, was also detected in the cell layer (Figure 5.4 h, *Cell*).

The identity of recombinant full length Adamts1 proteins detected by α–FLAG Western blot (Figure 5.4 e) were confirmed with an Adamts1 antibody directed against the metalloprotease domain of Adamts1 (α-Adamts1-MMP, formerly termed α-Adamts1-MP) (Russell *et al.* 2003a). In parallel Western blots using α-FLAG and α-Adamts1-MMP antibodies the 110 and 85kDa bands were detected in the cell and media layers respectively (Figure 5.5 a/b, lanes 1 and 2, *black* and *open arrowhead*) but not in cells transfected with p3xFLAG-EV control (Figure 5.5 a/b, lanes 3 and 4 respectively). Thus the flag positive 110 and 85kDa bands are identified as the pro- and mature forms of Adamts1 respectively. An additional α-Adamts1-MMP immunoreactive band, approximately 55-60kDa in size, was present in the cell extracts of both p3xFLAG-*Ats*1 and p3xFLAG-EV transfected cells and has been detected previously using this antibody and thought to be non-specific (Russell *et al.* 2003a). As no endogenous pro- or mature Adamts1 immunoreactive protein was detected in 293T cells using the α-Adamts1-MMP antibody in the empty vector transfected cells (Figure 5.5 b, lanes 3 and 4) the 55-60kDa protein is almost certainly non-specific.

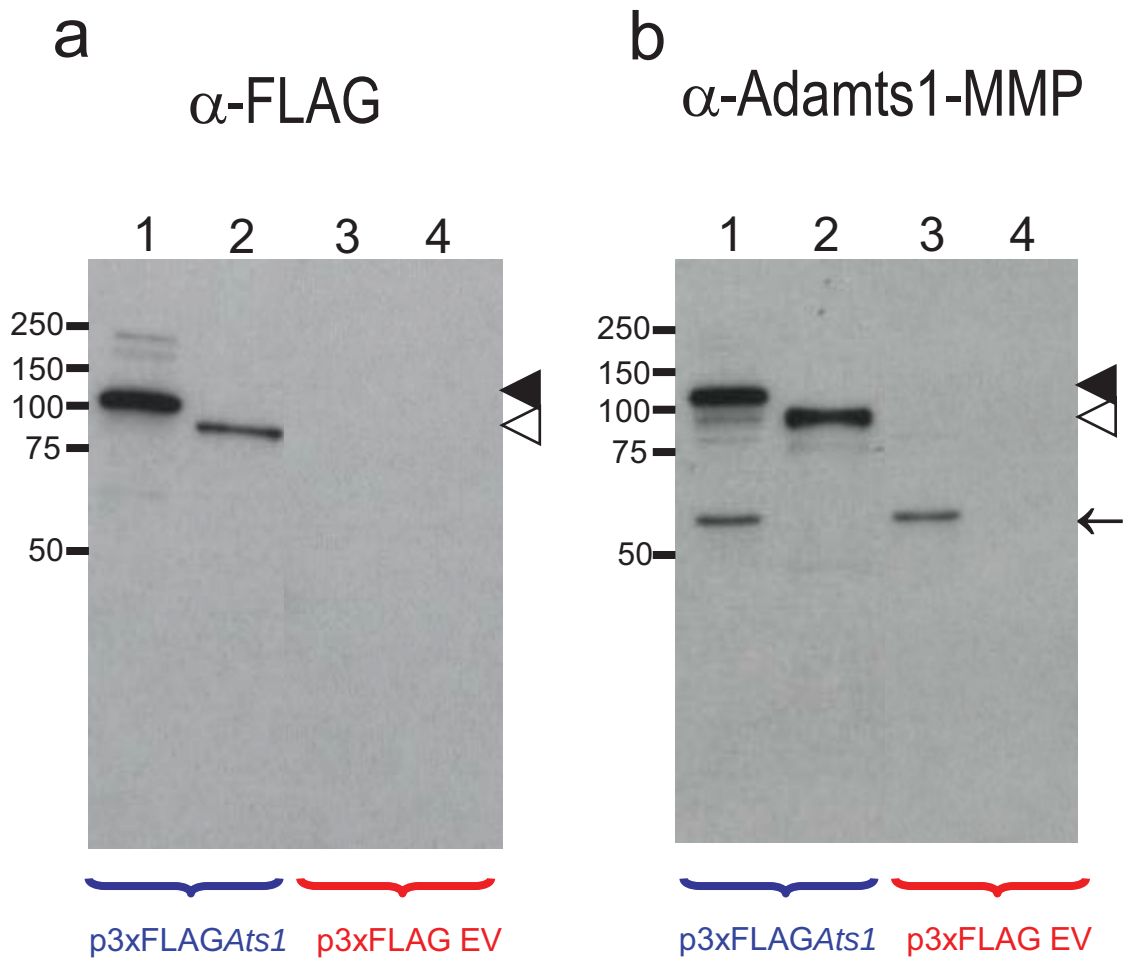

Figure 5.5 FLAG tagged recombinant Adamts1 protein is immunoreactive with both α-FLAG and α-Adamts1 antibodies.

p3xFLAG vector containing the entire coding sequence of *Adamts1* (p3xFLAG*Ats1*) or no insert (p3xFLAG EV; empty vector) were transfected into 293T cells and cell lysates (a and b, Lanes 1 & 3) and media (a and b, lanes 2 & 4) were analysed by Western blot using both α-FLAG (Sigma-Aldrich) (a) and α-Adamts1-MMP (b) antibodies. A band corresponding to a FLAG immunoreactive pro Adamts1, ~110kDa (*black arrow head*), was present in the cell layer of p3xFLAG*Ats1* transfected cells (a, lane 1) and a mature Adamts1 band present in the media (~85kDa, *open arrowhead*, a, lane 2) . Bands of similar size were detected in the cell layer and media extract using the anti-Adamts1-MMP antibody (formally termed Anti-MP-ADAMTS-1, Russell et al, 2003). Similar sized bands were not detected using either antibody in either the cell or media layer of empty vector transfected cells (a and b, lanes 3 and 4 respectively). Anti-Adamts1-MMP also detected a non-specific band of ~60kDa in the cell layer of both Adamts1 and empty vector transfected cells as seen previously (b, lanes 1 and 3, *black arrow*, Russell et al 2003).

These results show that recombinant forms of full length and protease inactive mutant Adamts1 as well as the C-terminal region are succesfully produced in transiently transfected 293T cells and can be detected by their FLAG tag, or immunodetection of the metalloprotease domain in all but the truncated protein form.

5.3.2 Assessment of recombinant Adamts1 catalytic activity

The catalytic activity of the recombinant mature Adamts1 protein was confirmed by stably transfecting CHO-V1 cells with the p3xFLAG-6xHis-*Ats*1 plasmid. These cells already express the V1 isoform of Versican (5.2.1.3). Full length recombinant Versican and mature recombinant Adamts1 were successfully detected in the media of the CHO-V1-*Ats*1 cell line, using the α-Versican and α-FLAG antibodies (Figure 5.6 a and b). The epitope, DPEAAE, generated by Adamts1 cleavage of Versican was also detected in the media of the CHO-V1-*Ats*1 cell line (Figure 5.6 c), demonstrating the successful proteolytic cleavage of Versican by recombinant Adamts1.

5.3.3 Optimisation of recombinant Adamts1 purification

To enable the purification of the recombinant proteins a 6x Histidine recombinant tag was incorporated into the p3xFLAG-*Ats1* constructs facillitating purification by nickel affinity chromatography (Figure 5.1 b, Section 5.2.1.1.1). Optimisation of the purification procedure for all recombinant Adamts1 proteins was determined using expression of the p3xFLAG-6xHis-ΔDis*Ats1* construct (Figure 5.1 b). Serial elutions from Ni-resin with increasing concentrations of imidazole, contained the ~56kDa α-FLAG positive band corresponding to the size of recombinant ΔDis*Ats1* protein in the conditioned media (Figure 5.7 a, *media*) and this band was depleted from conditioned media after interaction with Ni-resin. Strong solitary bands were detected in both 250mM and 500mM imidazole elutions (Figure 5.7 a, *E4 250mM imidazole* and *E5 500mM imidazole*, respectively). Fractions that were shown to contain strong bands corresponding to recombinant ΔDis*Ats1* protein by Western blot (Figure 5.7 a, *E4 250mM imidazole* and *E5 500mM imidazole*) additionally contained many contaminating proteins as determined by silver stain (Figure 5.7 b, *E4 250mM imidazole* and *E5 500mM imidazole*). However the number and intensity of contaminating proteins detected in E4 and E5 was less 10% than that seen in the input

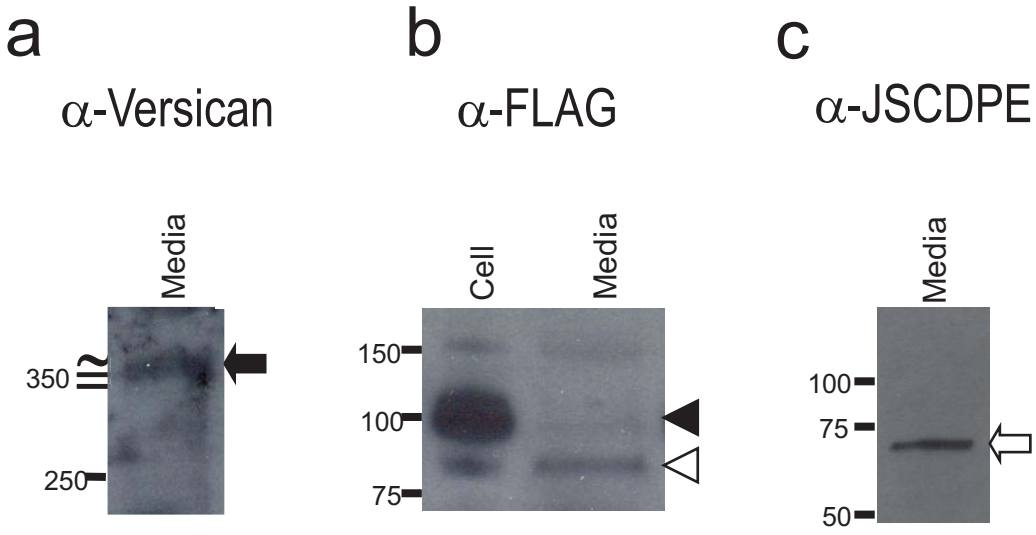

Figure 5.6 Recombinant Adamts1 is catalytically active.

p3xFLAG vector containing the entire coding sequence of *Adamts1* (p3xFLAG-6xHis-*Ats1*) was stably transfected into a CHO-K1 cell line already stably expressing the V1 isoform of *VERSICAN* (Kind donation by Prof. R. LeBaron. Cell lysates and/or Media were analysed by Western blot for full length Versican (a) using α-Versican antibody (Sandy et al. 2001); the pro and mature forms of recombinant Adamts1 using α-FLAG antibody (Sigma-Aldrich) (b); and the ectodomain DPEAAE generated by Adamts1 cleavage of VERSICAN using α-JSCDPE (previously termed anti-DPEAAE, Sandy *et al.* 2001) (c). A band, approximately 350kDa in size, corresponding to full length Versican was detected in the media (a, *black arrow*). The pro (~110kDa, *black arrow head*) and mature (~85kDa, *open arrowhead*) forms of recombinant flag tagged Adamts1 were present in the cell layer and media respectively (b). The ectodomain DPEAAE generated by Adamts1 cleavage of Versican was detected in the media (c, ~70kDa, *open arrow*).

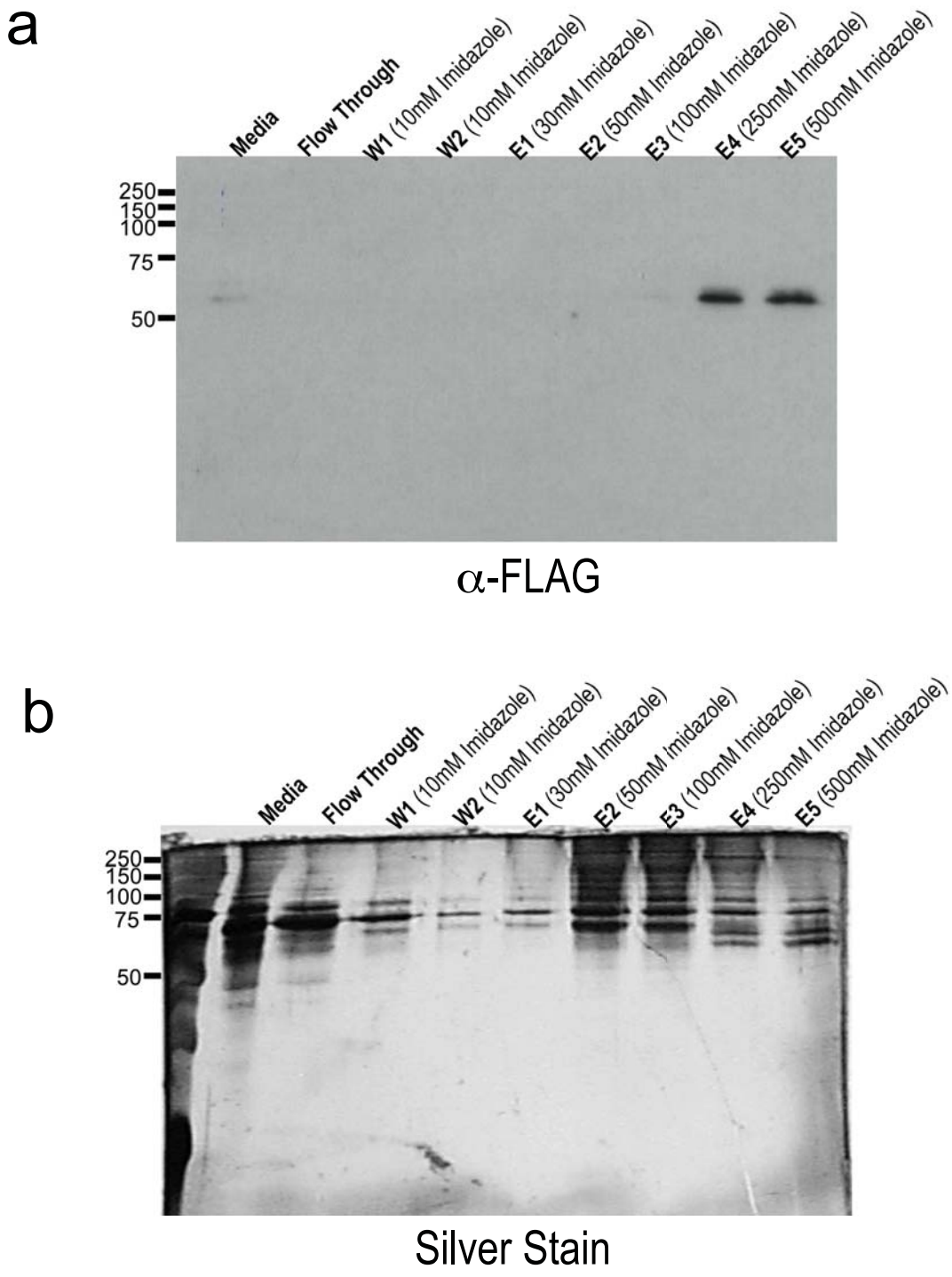

Figure 5.7 Optimisation of recombinant Adamts1 protein purification.

p3xFLAG-6xHis-ΔDis*Ats1* was transfected into 293T cells and the media collected for purification. Purification was carried out by nickel affinity chromatography utilising the introduced C-terminal 6xHistidine tag. Optimisation of purification involved binding of the recombinant protein present in the conditioned media, 2 washes of the resin with buffer containing 10mM imidazole (W1 and W2) followed by serial elutions with increasing concentrations of imidazole (E1-E5). Anti-FLAG Western blotting was used to determine which fraction the recombinant Adamts1 began to elute in (a) and an identical silver stained SDS-PAGE gel to determine the purity of each fraction (b).

conditioned media (Figure 5.7 b, *E4 250mM imidazole*, *E5 500mM imidazole* and *media* respectively) indicating that the recombinant protein was isolated from most contaminants in neat conditioned media. As recombinant ΔDis*Ats1* protein eluted only weakly in 100mM imidazole and not at all in 50mM (Figure 5.7 a), while contaminating proteins were effectively washed from the column in 50mM imidazole this was used in a refinement of the purification method for equilibration of the resin and washing steps resulting in further removal of contaminant proteins.

An example of the purification of recombinant Adamts1 using the optimised conditions is shown in Figure 5.8. Conditioned media and eluted fractions from cells expressing p3xFLAG-6xHis-*Ats1*, were compared in α-FLAG immunoblotting and silver stain (Figure 5.8 a and b, respectively, as described in Sections 5.2.1.5 and 5.2.1.6). A faint band corresponding to mature Adamts1 (~85kda) was present in the media collected from the transfected cells (Figure 5.8 a, *media*). A single band of similar size was present in the first but not the second column wash, but it was highly enriched in elutions 1-3 (Figure 5.8 a, *W1* and *E1-E3*). Single bands detected in elutions 1-3 using α-FLAG immunoblotting were also detected by silver stain (Figure 5.8 a and b, *E1-E3*) demonstrating very high purity of recombinant mature Adamts1.

5.3.4 Optimised purification of recombinant Versican proteins

Optimisation of the purification procedure for recombinant G1 Versican was carried out as described above for Adamts1. The optimised buffer compositions varied slightly from that used for Adamts1; as recombinant G1 began to elute at a concentration of 50mM imidazole, hence 30mM was used for washing and equilibration steps (5.2.1.4). An example of the optimised purification of Versican G1 is shown in Figure 5.9. The recombinant G1 fragment was engineered to mimic the Versican fragment generated by Adamts1 cleavage which *in vivo* generates a fragment of ~70kDa (Sandy *et al.* 2001; Russell *et al.* 2003a). We predicted that the recombinant G1 protein would be approximately 3.5kDa larger due to the introduction of the carboxy terminal 6xHistidine and 3xFLAG tags (ie ~74kDa). By Western blot, two α-FLAG immunoreactive proteins were detected in the conditioned media that were approximately 75-80kDa and 65-70kDa in size (Figure 5.9 a, *media*). The G1 recombinant protein contained a single chondroitin sulphate attachment site, thus the larger of the two proteins is assumed to be recombinant G1 with chondoitin sulphate attachments and the lower of the two bands (~65-

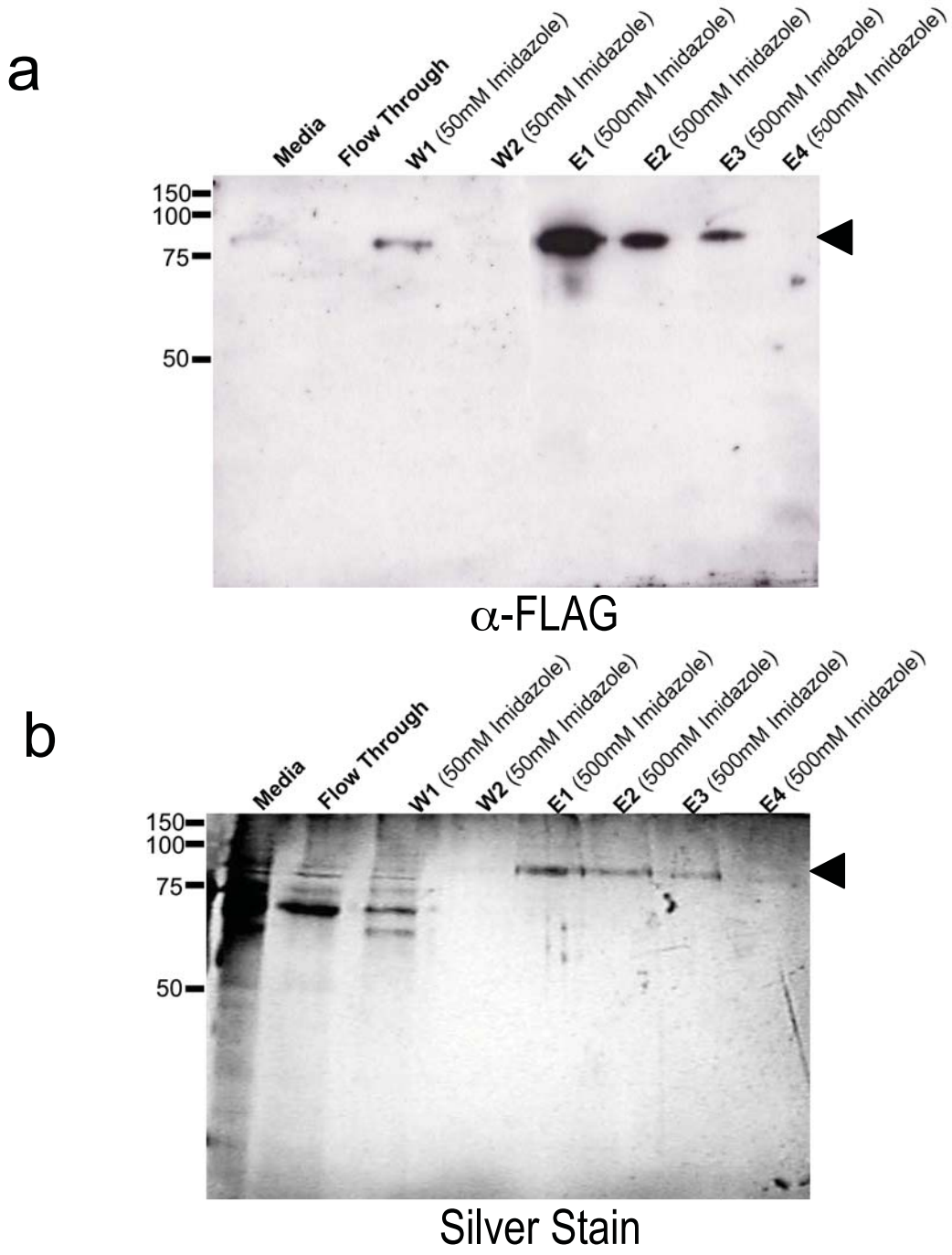

Figure 5.8 Optimised purification of recombinant Adamts1 protein.

p3xFLAG vector containing the entire coding sequence of Adamts1 (p3xFLAG-6xHis-*Ats1*) was transfected into 293T cells and the media collected for purification of mature recombinant Adamts1. Purification was carried out by nickel affinity chromatography utilising an introduced C-terminal 6x histidine tag and optimised washing and elution conditions as determined by Figure 5.7. Anti-Flag Western blotting was used to verify that a protein of approximate predicted size was eluted (a) and an identical silver stained SDS-PAGE gel to determine the purity of each elution (b). An α-FLAG immunoreactive band corresponding to the approximate predicted size of mature Adamts1 protein (~85kDa) was detected in elutions 1, 2 and 3 (a, E1-E3, *black arrowhead*). A protein of similar size, presumed to be mature Adamts1, was the predominant band detected by silver stain in these same elutions (b, E1-E3, *black arrowhead*).

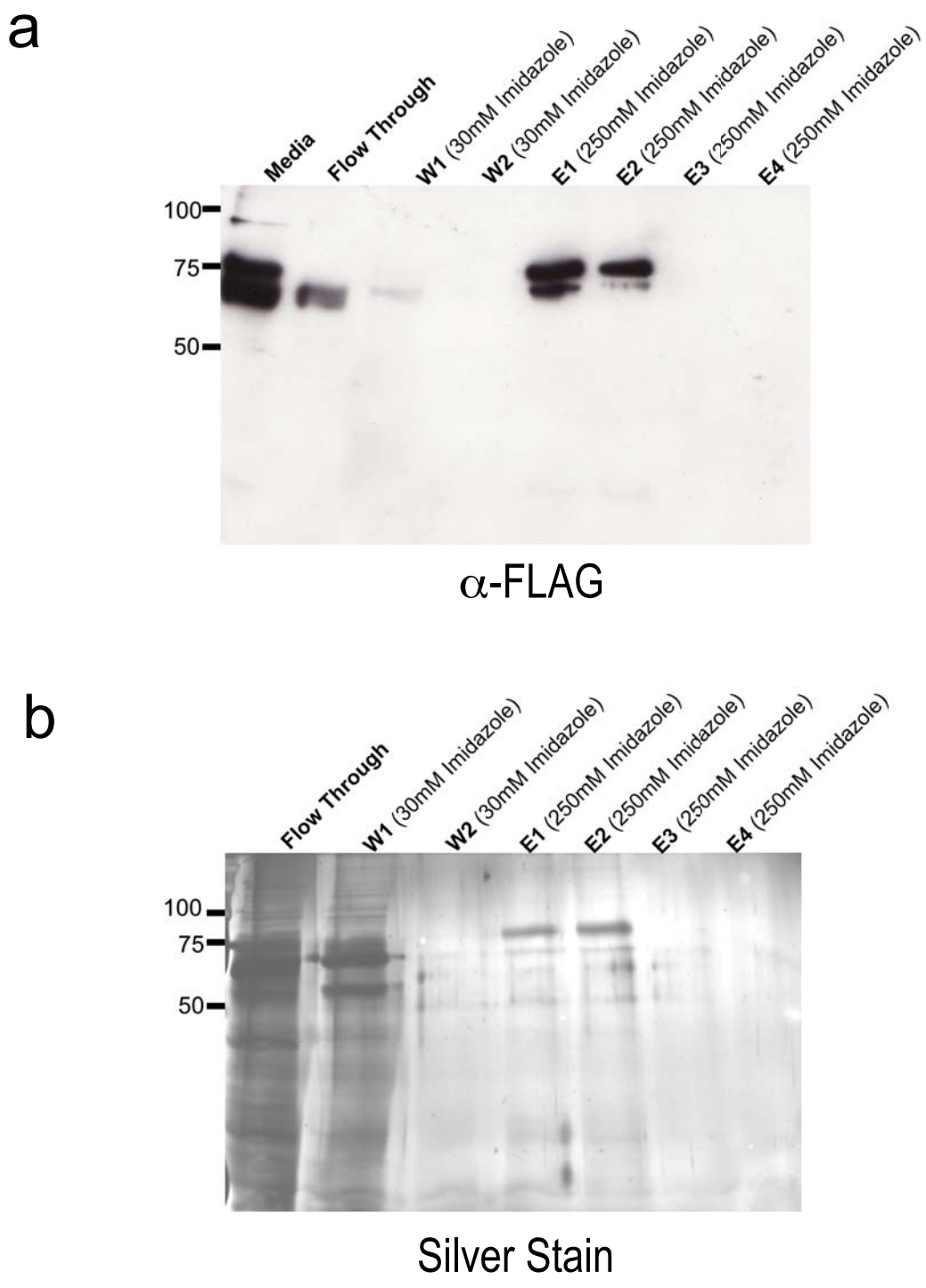

Figure 5.9 Optimised Purification of Recombinant Versican G1 protein.

p3xFLAG vector containing the coding sequence of the G1 domain of *Versican* (p3xFLAG-6xHis-G1) was transfected into CHO-KI cells and the media collected for purification of the recombinant protein. Purification was carried out by nickel affinity chromatography utilising the introduced C-terminal 6x histidine tag and optimised washing conditions. Anti-Flag Western blotting was used to verify that a protein of approximate predicted size was eluted (a) and an identical silver stained SDS-PAGE gel to determine the purity of each elution (b). A strong band was detected in elutions 1 and 2 (a, E1 and E2). A predominant band of similar size was detected by silver stain in these same elutions (b, E1 and E2).

70kDa) without. The unsulphated G1 was additionally detected in the flow through fraction indicating that it had a lesser affinity for the resin than sulphated G1 however the reason for the decreased affinity is unknown (Figure 5.9 a, *Flow Through*). These same two bands were detected in elutions 1 and 2, however the sulphated G1 protein was of much greater intensity in both elutions (Figure 5.9 a, *E1* and *E2*). By silver stain, elutions 1 and 2 contained a predominant band at approximately 75-80kDa corresponding to the recombinant sulphated G1 fragment detected by immunoblotting (Figure 5.9 b, *E1* and *E2*). Additional protein bands were detected in these elutions but at much lower intensities, demonstrating that recombinant G1 was the predominant protein present in these fractions.

The optimised purification procedure used for Versican G1 protein was not suitable for the purification of recombinant Versican G3. The purification conditions used for G1 did not result in the elution of an α-FLAG immunoreactive protein of the predicted size for G3 (data not shown). Analysis of the sequence of the construct revealed that an additional histidine residue had been incorporated into the polyhistidine tag, which was most probably due to an error in the synthesis of the reverse oligonucleotide used to amplify the G3 construct. The additional histidine tag presumably resulted in a much higher binding affinity for the nickel resin that was not out competed by imidazole. EDTA is a metal chelator able to elute strongly bound proteins by stripping the nickel from the purification resin. When the elution buffer contained 50mM EDTA a protein of the approximate predicted size (41kDa) was detected in the first two elutions by α-FLAG immunoblotting (Figure 5.10 a, *E1* and *E2* and as per Section 5.2.1.4). A band of similar size was detected by silver stain in these same two elutions (Figure 5.10 b, *E1* and *E2*, *black arrowhead*). However the band corresponding to the recombinant G3 protein was not the predominant band present in these fractions with additional larger bands of equal intensities detected demonstrating that the purification method was not applicable for this recombinant protein (Figure 5.10 b, *E1* and *E2*).

5.3.4.1 Versican induced cumulus expansion

Treatment of COCs in IVM culture with recombinant Versican purified from CHO-V1 cells expressing the full length proteoglycan resulted in a significant increase in the cumulus expansion index (CEI +/- S.E.M.) compared to culture with the solvent (PBS, *None*). The mean CEI was significantly less than that seen when COCs were cultured in the presence of Egf or FSH ($p<0.05$, Figure 5.11 a), however, the doses could not be equilibrated. When individual cumulus expansion scores were plotted, COCs

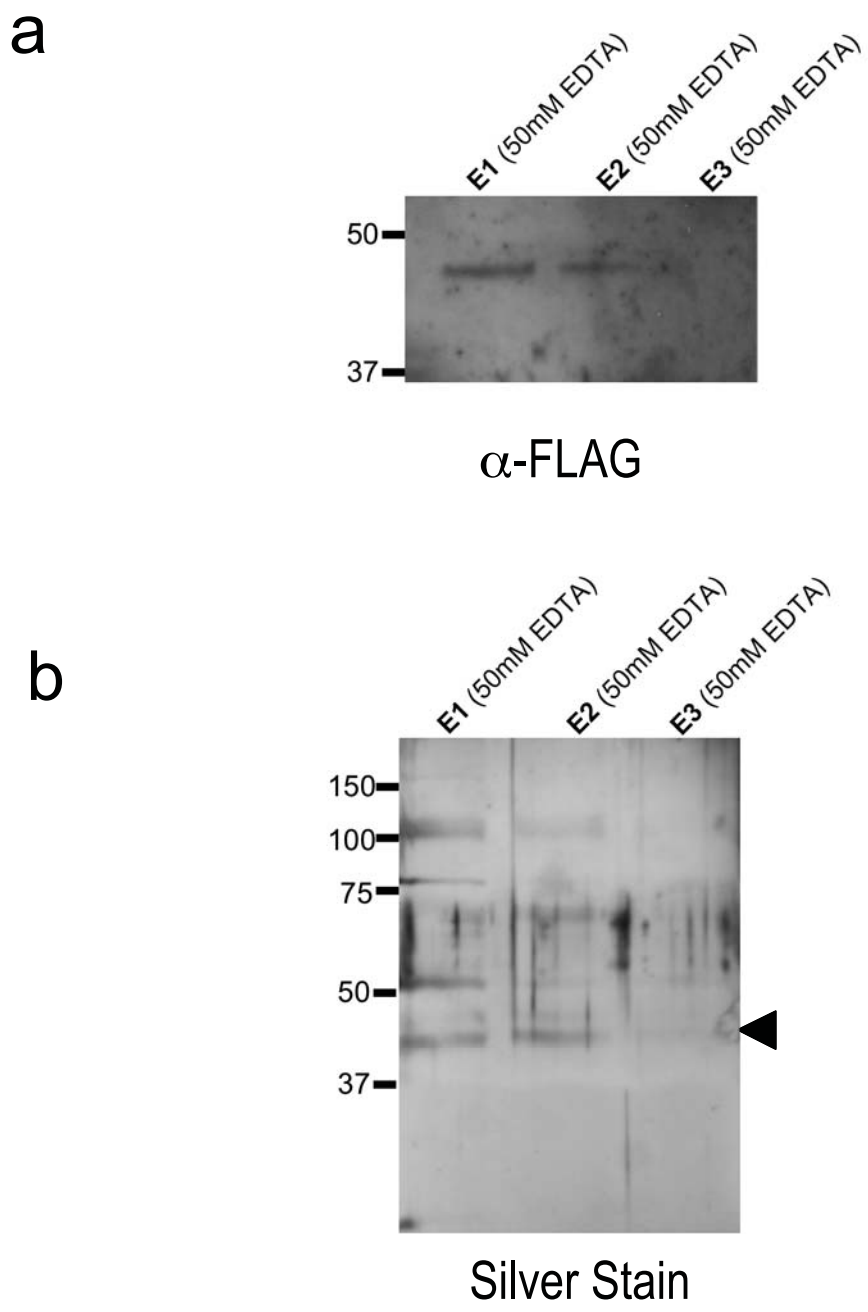

Figure 5.10 Purification of recombinant Versican G3 protein.

p3xFLAG vector containing the coding sequence of the G3 domain of *Versican* (p3xFLAG-6xHis-G3) was transfected into 293T cells and the media collected for purification of the recombinant protein. Purification was carried out by nickel affinity chromatography. Sequencing revealed the C-terminal histidine tag coded for 7 and not 6 histidine amino acids due to a nucleotide error in the reverse primer, resulting in strong affinity for and binding to the nickel resin. Elution of recombinant G3 was achieved using 50mM EDTA. Anti-Flag Western blotting was used to verify that a protein of approximate predicted size was eluted (a) and an identical silver stained SDS-PAGE gel to determine the purity of each elution (b). A band of approximate predicted size (~41kDa, predicted using bioinformatics) was detected in elutions 1 and 2 (a, E1 and E2). A band of similar size was detected by silver stain in these same elutions (b, *black arrowhead*, E1 and E2). Other contaminating proteins of similar intensities were also present in these fractions.

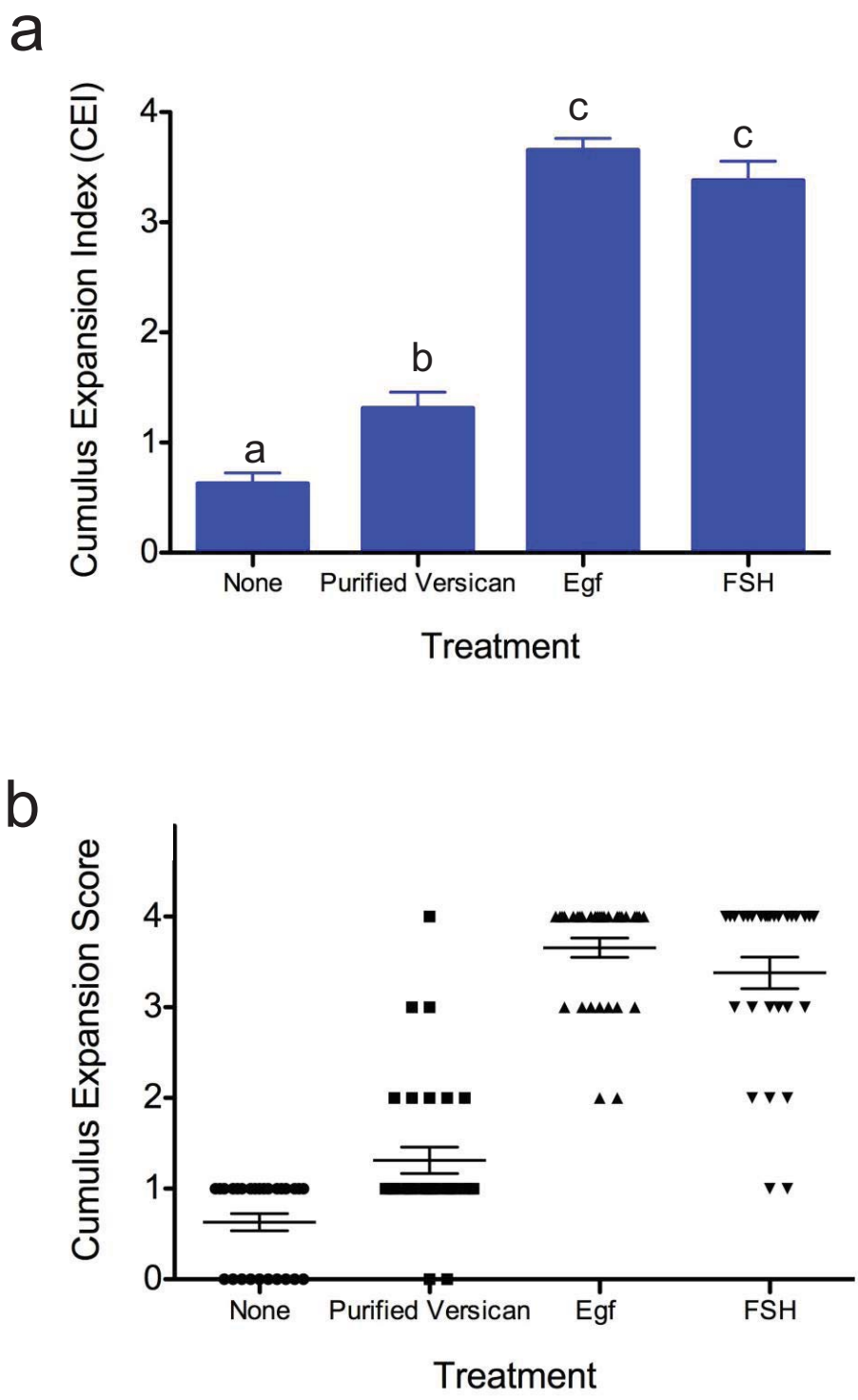

Figure 5.11 Purified Versican induces cumulus oocyte complex expansion.

Degree of cumulus expansion (+/-SEM) scored following 20 h of *in vitro* maturation. Cumulus oocyte complexes (COCs) were cultured in the presence of no stimulus (*None*), a 1:20 dilution of Versican (purified by size exclusion chromatography), Egf (3ng/ml) or FSH (50mIU/ml) (a). In b, individual COC scores were graphed for each of the treatments. Data is expressed as mean +/- S.E.M. ($n \geq 27$ COCs). Significant difference ($P<0.05$) represented by different characters.

cultured without a stimulus scored only either 0, indicating that the cumulus cells no longer surrounded the oocyte, or 1, demonstrating that no expansion had occurred and cumulus cells were tightly packed around the oocyte (Figure 5.11 b, *None*). A different pattern of individual cumulus expansion scores was seen for COCs cultured with Versican; only 2 COCs received a 0 score, most COCs scored a 1, while 8 COCs scored 2 or greater (Figure 5.11 b). This mode of analysis showed that immature COCs treated with recombinant Versican were able to induce cumulus expansion *in vitro*, but also emphasises that the increased mean CEI results from a dramatic shift in the morphology of COCs cultured with pure Versican, with several individual COCs achieving a high degree of expansion.

Cumulus expansion *in vitro* was also significantly increased by culturing unexpanded COCs in conditioned media (CM) containing full length recombinant Versican from the CHO-V1 cell line compared to the CEI of COCs cultured with an equal volume of conditioned media from the parental CHO-K1 cell line. This approach allowed for a larger concentration range of intact Versican treatment to be analysed. Treatment with 50, 30 or 10% CM resulting in significantly increased CEI compared to control CHO-K1 CM treatment and the mean CEI for each concentration of Versican was not significantly different from that seen in FSH treated positive control IVM cultures. Furthermore, recombinant Versican expressed in combination with Adamts1 to generate cleaved Versican (Figure 5.6) in the same concentrations also significantly increased CEI compared to control CHO-K1 CM. As with Versican alone, the CEI increase by 50, 30 or 10% Versican+Adamts1 conditioned media was equivalent to that induced by 50mIU FSH ($p<0.05$, Figure 5.12). The CEI seen at 50% Versican+Adamts1 conditioned media was significantly greater than that induced by the same volume of Versican alone. Individual CEI scores were plotted to compare the range of responses of COCs to FSH and the 50% CM treatments. Treatment with 50mIU FSH induced expansion in all COCs with a broad range of responses while treatment with 50% CHO-K1 CM from the control cell line resulted in slight stabilisation of the COCs (Figure 5.12 b) compared to the effect of treatment without stimulus (Figure 5.11, *None*). Treatment with Versican resulted in consistent CEI scores around 3 while the presence of Adamts1 cleaved Versican (Figure 5.12 b) resulted in equally consistent maximal CEI scores of 4.

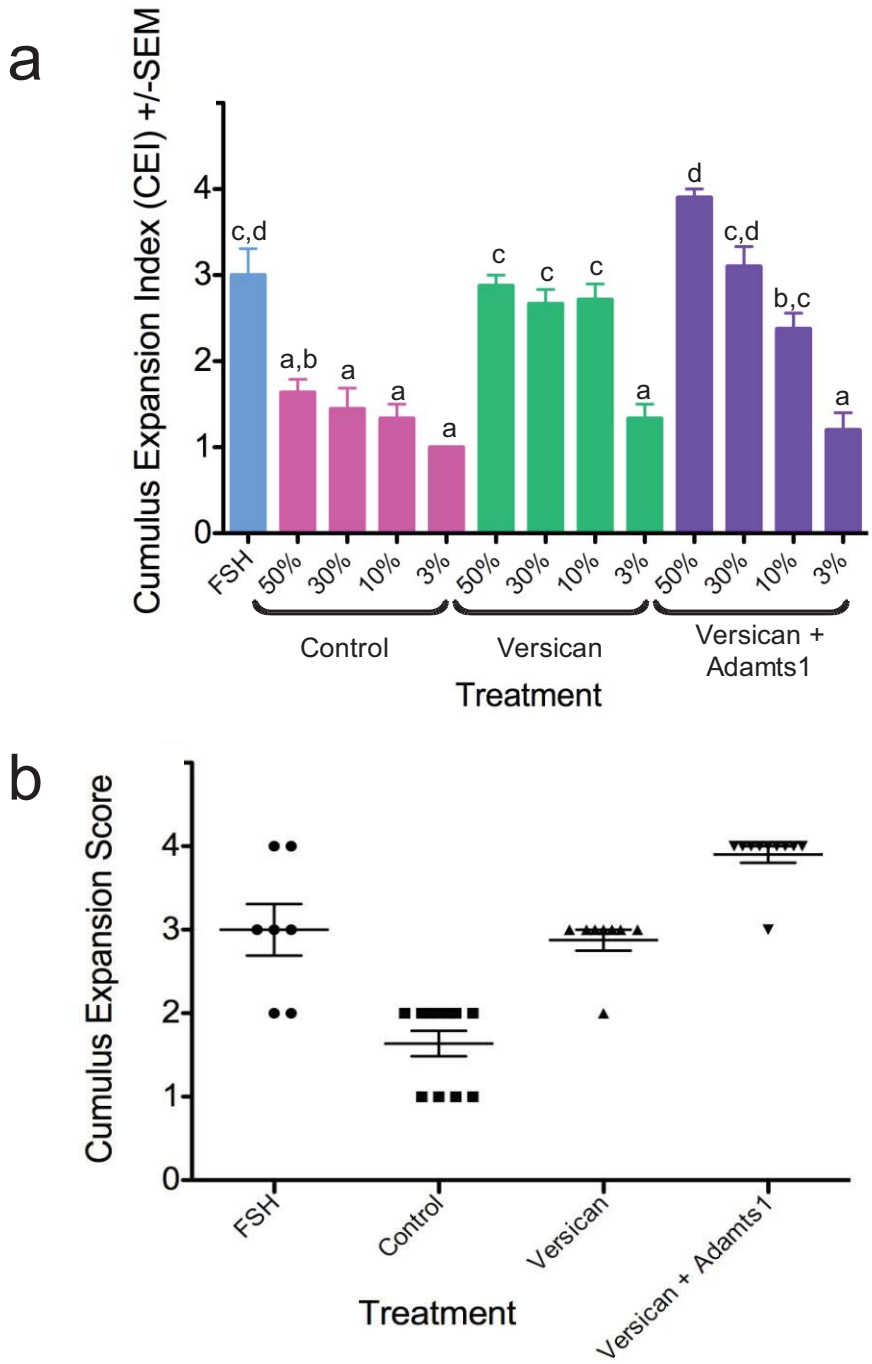

Figure 5.12 Recombinant Versican and Adamts1 cleaved Versican are able to induce cumulus oocyte expansion.

Degree of cumulus expansion scored following 20 h of *in vitro* maturation. (a) Cumulus oocyte complexes (COCs) were cultured in the presence of FSH (50mIU/ml) or media supplemented with 50, 30, 10 or 3% conditioned media from untransfected CHO-KI (*Control*), or CHO-KI cells stably transfected with Versican alone (pECE-V1) or Versican (pECE-V1) and full length Adamts1 (p3xFLAG*Ats1, Versican* + *Adamts1*). In b, individual COC scores were graphed for the FSH treatment and the Control, Versican and Adamts1 + Versican treatments of 50% conditioned media supplementation. Data is expressed as mean +/-S.E.M. (n= 5-11 COCs). Significant difference (P<0.05) represented by different characters.

5.4 DISCUSSION

The functional role of the cumulus matrix during oocyte maturation is poorly characterised. I have shown that the matrix of cumulus oocyte complexes (COCs) matured *in vitro* (IVM) is devoid of Adamts1 and Versican, normally abundant in *in vivo* matured COCs (Dunning *et al.* 2007 and Chapter 3). Adamts1 and Versican are composed of numerous domains, with potential functions that could influence cumulus expansion or oocyte maturation. In order to study the role of these functionally different motifs, I generated a series full length or modified Adamts1 and Versican expression constructs and optimised their expression and purification in a mammalian cell culture system.

5.4.1 Expression and purification of recombinant Adamts1 and Versican

Truncation of the pro-domain of Adamts1 in an attempt to produce constitutively active protease (p3xFLAG-6xHIS-ΔPro*Ats1)* resulted in no intact protein production (Figure 5.4 g). It is concluded that the pro- domain of Adamts1 is required keeping the protease in a latent state during synthesis or for correct folding and secretion as reported for other enzymes (Milla *et al.* 1999; Cao *et al.* 2000; Porter *et al.* 2005). It has subsequently been shown that the secretion of recombinant ADAMTS9 is prevented following the removal of its pro- domain (Koo *et al.* 2007). The failure of secretion of Δ Pro*Ats1* shown here is in agreement with the ADAMTS9 study, however, ADAMTS9 protein was detected in cell extracts, which did not occur with Δ Pro*Ats1* (Figure 5.4 g) (Koo *et al.* 2007). Thus while ADAMTS9 pro-domain appears necessary for secretion my results suggest that the pro- domain of Adamts1 is essential for enzyme latency preventing autolytic degradation. In support of this I found that expression of the truncated expression construct ΔDis*Ats1*, which did not contain the metalloprotease domain resulted in successful protein assembly and secretion (Figure 5.4 h). In the case of Adamts1, it appears that the pro- domain is essential for correct processing and maintenance of appropriate proteolytic latency until suitable activation.

Conditioned media of cells transfected with full length Adamts1 (p3xFLAG-6xHis-*Ats1*) contained only mature/active Adamts1 with the pro form constrained to the cell extract (Figure 5.5). This conditioned media was used as a source of active Adamts1. Purification of C-terminally 6x histidine tagged

recombinant proteins from the media of transfected cells was optimised such that the elutions contained a high purity of the desired recombinant protein (Figure 5.8 and Figure 5.9). Successful purification was achieved for all expression constructs with the exception of the Versican G3 (p3xFLAG-6xHis-G3) which contained artifactual introduction of an additional histidine residue, resulting in a excessive affinity of the recombinant protein for the nickel resin. Elution could only be achieved by the removal of the nickel ions from the purification resin with the use of a strong chelator, EDTA (Figure 5.10). The generation of a second Versican G3 construct containing 6 histidine residue at its C-terminus did not improve the purification, in fact only minimal recombinant protein was detected in the media following transfection and could not be purified under the conditions used here (data not shown). It was concluded that the G3 domain of Versican bound strongly to ECM proteins and/or cell surface integrins as has been previously reported (Aspberg *et al.* 1997; Olin *et al.* 2001; Wu *et al.* 2002; Wu *et al.* 2005). The numerous binding partners of G3 results in the recombinant fragment localising to both the ECM and to the surface of cells (Wu *et al.* 2005b) and could account for the low levels of recombinant protein detected in the media. Future improvements of the yield of recombinant G3 protein may be achieved through establishment of a stably transfected cell line facillitating saturation of binding sites resulting in the release of protein into the media. Alternatively, the binding of G3 to the ECM and cell surface could perhaps be prevented through inclusion of soluble factors that interrupt the interaction of G3 with ECM motifs such as heparin. Alternatively an altered purification protocol could be developed to extract the recombinant protein from its ECM binding partners or the protein could be produced in an alternative system such as bacterial or baculoviral production, the former of which has previously shown success (Wu *et al.* 2002). Due to time constraints in these studies I was unable to continue to assess activity of recombinant G3 Versican.

5.4.2 Active role of Versican and Adamts1 in cumulus expansion

As we were able to successfully generate recombinant Versican and Adamts1 that was catalytically active, and produced cleaved Versican in culture (Figure 5.6), we assessed the function of these products during cumulus expansion *in vitro.* Cultured COCs were treated by supplementation with recombinant Adamts1 and Versican otherwise deficient in IVM conditions (Chapter 3). Versican indeed induced cumulus expansion *in vitro* when supplied either in highly pure form or in conditioned medium. Further, cleavage of Versican by co-expressed Adamts1 further increased this response. The dilution of purified Versican chosen in this study was limited by the availability of this very difficult to purify large

proteoglycan. As a result the concentration in culture most likely did not reach concentrations similar to that seen in the follicle *in vivo*. Interestingly, it has been shown that the binding of Versican to HA as occurs in the expanding COC (Russell *et al.* 2003b), is not independent at the molecular level, but is enhanced by cooperative intermolecular interactions (Seyfried *et al.* 2006). Binding to HA is greatly enhanced when sufficient numbers of Versican molecules permit cooperative interaction. In COC cultures where the induction of HA is dependent on Egf-like signalling of Versican, this property would result in a positive feed forward relationship with a few COCs that induce HA first absorbing all available Versican if the concentration provided was not sufficient to achieve saturation in all COCs thus amplifying the expansion signal in those few COCs. The observed distribution of responses to pure Versican was consistent with this property. Sufficient binding conditions were met for Versican incorporation into the matrix of a few COCs and that this enabled cumulus expansion to proceed effectively while others failed to respond.

Under *in vivo* conditions a stimulus initiates *Has2* expression by cumulus cells and COC expansion simultaneously with Vcan expression in mural cells. Subsequently Versican becomes incorporated into the COC matrix and may activate signal transduction. Thus the activation of EgfRs by Versican may be important in latter stages of cumulus expansion and oocyte maturation following initiation by the LH surge and very rapid induction of Amphiregulin, Epiregulin and Betacellulin.

Cleavage of Versican by Adamts1 occurs in the COC (Russell 2003) and here I found that cleaved Versican further enhanced cumulus expansion compared to Versican alone. Interestingly, the response of COCs to Versican was not concentration dependent (Fig 5.12a) while Adamts1 cleaved Versican did show concentration dependent effects on COC expansion. This is also consistent with a cooperative binding effect of Versican whereby interaction with HA determines the local Versican signal within each COC, while the cleaved Versican showed characteristics of a ligand not influenced by HA interactions as expected after the HA-binding and Egf-like regions become separated.

The ability of Versican to induce cumulus expansion confirms work in other systems showing that the C-terminal Egf-like motifs of Versican activate Egf receptors (EgfRs) (Xiang *et al.* 2006). Thus Versican may cooperate with other Egf-like ligand that acts on the cumulus cells *in vivo* to mediate cumulus expansion and oocyte maturation. Adamts1 may participate in the activity of Versican, and has also been proposed to be one metalloprotease that activates other Egf-like ligands (Assidi *et al.* 2008).

Versicans activation of EgfRs and participation in the organisation of COC matrix structure, and its associated functions, are predicted to collectively promote oocyte developmental competence.

Further experiments were designed and intended to confirm that the G3 domain of Versican was responsible for the induction of cumulus expansion by utilising purified G3 recombinant protein; however due to the difficulties discussed previously in purifying this recombinant protein, this was not possible. Further refinements of the purification of G3 Versican and assessment of its action in COC expansion and induction of EgfR signal transduction are essential future directions for this research.

In summary, the results shown here indicate that the incorporation of Versican and Adamts1 into the matrix of the expanding COC *in vivo* contribute to inducing cumulus expansion. Thus it is likely that Adamts1 and Versican mediate changes in cumulus gene expression and cumulus matrix structure/composition that are linked to optimal oocyte developmental competence. As COCs matured *in vitro* do not contain Adamts1 or Versican protein (Chapter 3), and since the combination of Versican and Adamts1 promoted cumulus expansion (and presumably oocyte maturation), the absence of these matrix proteins may be (at least in part) responsible for the lower developmental competence of IVM oocytes. In addition *in vitro* matured COCs are not exposed to the stimulatory action of cleaved Versican, which appears to have a unique and specific role, presumably via activation of the EgfR pathway, in the maturation of oocytes *in vivo*.

A greater understanding of the role that Versican and Adamts1 play in the activation of oocyte maturation could be translated into improved IVM conditions. Supplementation of current IVM media with recombinant Versican and possibly Adamts1 may promote obligatory gene expression changes in cumulus cells as well as helping to recapitulate the normal matrix structure and function.

Chapter 6

Conclusions and Future Directions

6.1 SIGNIFICANCE AND CLINICAL RELEVANCE

It is widely acknowledged that mammalian oocytes matured *in vitro* are of lower quality than those matured *in vivo*, however with improvements, IVM could provide a promising therapy for patients. In particular IVM may improve the efficiency of artificial reproductive technologies (ART) for patients with conditions that cause oocyte developmental blocks, as occurs with polycystic ovarian syndrome (PCOS). Additionally, when male factor infertility is the cause of treatment, IVM reduces the risk of gonadotropin administration and is a cost effective alternative. However, due to the lower developmental potential of IVM oocytes compared to their *in vivo* matured counterparts, IVM is not routinely used in fertility clinics. Previous studies attempting to improve IVM conditions through modulating meiotic resumption, optimising nutrient supply or supplementation with antioxidants have led to minimal improvements or, in fact have had detrimental effects (Dalvit *et al.* 2005; Coy *et al.* 2005; Sutton-McDowall *et al.* 2005; Romar and Funahashi 2006; Ozawa *et al.* 2008). Normally, oocytes are matured in a highly specific 'niche' environment established and maintained by the follicular cells enclosing the oocyte. However, no previous study has examined whether factors derived from the mural granulosa cell layer are absent during IVM when the oocyte or COC, is matured in the absence of granulosa cells and the normal follicular environment. The studies described here are the first to show that standard IVM conditions result in altered gene expression profiles and matrix composition in cumulus cells compared to *in vivo* matured controls. These experiments also assessed biomechanical function of the intact COC matrix. The ability of the cumulus matrix to act as a biological barrier to diffusion of solutes and the alteration to this capacity after IVM are profound and novel outcomes of this project. This work furthers our understanding of the role of the COC matrix during oocyte maturation and identifies areas of potential improvements in IVM procedures.

6.2 MATRIX DEFICIENCIES IN THE IN VITRO CUMULUS OOCYTE COMPLEX

Expression of *Adamts1* and *Versican* mRNA and protein abundance were greatly reduced in IVM, yet maximal signal transduction response in cumulus cells was confirmed by robust induction of *Has2*.

While *in vivo* matured complexes treated with hCG showed significant induction of *Has2*, *Adamts1* and *Versican* at 6 h post hCG, and reach maximal levels after 6 to 12 h, only *Has2* was induced in IVM cultures. In agreement with our study, a subsequent microarray analysis of gene expression in IVM and *in vivo* matured COCs also identified *Adamts1* and *Versican* among the most under expressed genes after IVM (Banwell *et al* manuscript in preparation). In human follicles, *ADAMTS1* and *VERSICAN* are strongly expressed in both cumulus and mural granulosa cells, demonstrating their potential involvement in human cumulus expansion and oocyte maturation. Whether *ADAMTS1* and *VERSICAN* are induced during human IVM requires further investigation. Such experiments were not possible in our laboratory as IVM is not offered as a treatment by our clinical collaborators. It was previously thought that the expression of *Adamts1* and *Versican in vivo* were restricted to the mGC layer and not expressed by the COC (Robker *et al.* 2000; Russell *et al.* 2003b). We did find that the expression of these genes is highest in mGC, but that COCs do express both *Adamts1* and *Versican* in response to an ovulatory stimulus *in vivo*. Thus, we conclude that Adamts1 and Versican are derived predominantly from the mGCs but are also expressed in COCs *in vivo*. More importantly, these matrix components are absent following IVM. This demonstrated that COCs matured *in vitro* do not respond to maturation stimuli as they do *in vivo* and that they lack matrix components that may contribute key roles in oocyte maturation.

6.3 ALTERED BARRIER FUNCTIONS IN THE IN VITRO MATURED CUMULUS OOCYTE COMPLEX

Functional qualities of the matrix may contribute to the maturation of COCs. Following expansion COCs were able to impede the diffusion of small molecules into the oocyte, thus acting as a regulator of the immediate oocyte environment. In so doing, the COC matrix may limit the rate of supply to the oocyte of glucose and cholesterol and/or other hydrophilic and lipophilic molecules. Prior to cumulus expansion, the diffusion and uptake of glucose and cholesterol by the oocyte was rapid and linear with time of exposure. However, after COC expansion solute transport became markedly impeded and uptake by the oocyte significantly reduced, suggesting that the matrix presents a resistant barrier to glucose and cholesterol compared to unexpanded COCs. After IVM, there was a clear difference in the capacity of COC matrix to prevent the absorption of both glucose and cholesterol by the oocyte compared to *in vivo*

matured controls. As a matrix deficient in Adamts1 and Versican, the difference in solute transport after IVM implicates these two matrix components specifically in this property.

Detrimental effects of exposing oocytes to high glucose during maturation are well known and since sterols, steroids and lipids are also known to be important for oocyte maturation, our experiments reveal that the COC matrix may contribute to sustaining a niche environment around oocytes that promotes maturation. The role of Adamts1 in this function was investigated by comparing glucose and cholesterol uptake in COCs isolated from *Adamts1* null females. Solute transport properties were similar in Adamts$^{-/-}$ COCs to those isolated from heterozygous littermates indicating Adamts1 is probably not an essential contributor in this function. However, the greater barrier capacity of *in vivo* matured compared to IVM COCs demonstrated that this function is not solely due to Hyaluronan synthesis but that it is also dependent on the composition and perhaps, organisation of this matrix. Versican is likely to be a key, but not necessarily the only contributor in the observed molecular filtration property of the *in vivo* matured matrix. This should be further investigated by future experiments supplementing IVM cultures with Versican.

This is the first evidence demonstrating a potential role of the cumulus matrix during oocyte maturation through an ability to control supply of metabolites to the oocyte. The combination of limited diffusion through the matrix and rapid glycolysis by cumulus cells is expected to establish a gradient of glucose concentration allowing efficient metabolism of glucose by cumulus cells to generate substrates for cumulus energy production and HA synthesis while metabolites of glucose are supplied for oxidative phosphorylation in oocytes and limiting glucose exposure of the oocyte. Likewise, steroid, sterols and lipid supply gradients can also be established. Loss of this gradient arises in IVM COCs, which permit more rapid solute diffusion, and may account for the poor developmental competence of IVM oocytes. This function may also be particularly important in the case of hormones or growth factors. Emerging studies demonstrate that an important paracrine signalling loop is established within COCs after the initial ovulatory trigger. Local production of Egf-L and oocyte secreted growth factors are particular examples that may have select roles in inducing gene expression in the cumulus cells. Furthermore, it is not known how a unique expression pattern arises from the G-protein/PKA coupled signalling system activated by autocrine/paracrine action of PGE_2 that is not qualitatively different from FSH/LH signalling. The capacity of the COC matrix to retard diffusion may also enable retention of locally produced factors such as Prostaglandin E2 causing them to accumulate in very high concentrations and establish specific

signalling effects. The hypothesised capacity of the COC matrix to enhance responses to local signalling factors requires further investigation.

6.4 RESTORING THE DEFICIENT IN VITRO MATURED MATRIX WITH VERSICAN AND ADAMTS1

Recombinant Versican was capable of inducing cumulus expansion *in vitro* with preliminary evidence suggesting that this is enhanced following cleavage by Adamts1. Studies in several other cell systems demonstrate the ability of the C-terminal Egf-like domains of Versican to activate Egf receptors (Xiang *et al.* 2006). Thus Versican may act in a similar manner to the Egf-like ligands which induce COC expansion and oocyte maturation *in vivo* through activating Egf-R. Cleavage of Versican by Adamts1 within the expanding COC matrix may enhance interaction of its Egf-like domains with cell surface receptors. That Versican is strongly and selectively incorporated into the COC matrix and may activate Egf-R suggests that it may be a relevant activator of oocyte maturation and potentially required for the full specific response of cumulus cells after the ovulatory stimulus including transducing gene expression changes. Collectively, these functions may promote oocyte developmental competence and supplementation of IVM cultures with Adamts1 and Versican or factors promoting their expression may improve IVM success.

6.5 ADDITIONAL POTENTIAL ACTIONS OF VERSICAN AND ADAMTS1 DURING OOCYTE MATURATION

Additional known functions of Adamts1 and Versican may also be important during maturation. Versican modulates growth factor-receptor interactions (Wu *et al.* 2004), while Adamts1 modulates the activity of growth factors including VEGFs, FGFs and Egf-like factors (Luque *et al.* 2003; Liu *et al.* 2005; Suga *et al.* 2006). Pericellular Versican protects cells from oxidative stress in the presence of reactive oxygen species (ROS) in culture (Wu *et al.* 2005). To determine whether Versican is capable of protecting cumulus cells and the oocyte from oxidative damage during IVM, future experiments are necessary to assess whether recombinant Versican supplementation is able to protect COCs from ROS induced apoptosis.

6.6 SUMMARY AND FUTURE DIRECTIONS

The direct comparison of *in vivo* and *in vitro* matured mouse COCs used here to determine differences and insufficiencies of the complexes has proven to be highly useful. Results shown here demonstrate that IVM complexes show altered gene expression profiles, matrix composition, molecular filtration and cell signalling properties which may explain, in part, why IVM oocytes are of poorer quality. Similar experiments in the human, assessing IVM and *in vivo* matured complexes, by gene array and perhaps, a proteomics approach, would lead to a greater understanding of how they differ and inform how IVM could be improved. It is widely accepted that cumulus expansion and the correct formation of this matrix is critical for fertility, however few functions of the matrix have been determined. Our work has furthered our understanding of the role of the cumulus matrix during oocyte maturation and is the first to show that this matrix is altered both in composition and function following IVM.

Chapter 7

Bibliography

Albertini DF, Combelles CM, Benecchi E, Carabatsos MJ (2001) Cellular basis for paracrine regulation of ovarian follicle development. *Reproduction* **121**, 647-53.

Allworth AE, Albertini DF (1993) Meiotic maturation in cultured bovine oocytes is accompanied by remodeling of the cumulus cell cytoskeleton. *Dev Biol* **158**, 101-12.

Ang LC, Zhang Y, Cao L, Yang BL, Young B, Kiani C, Lee V, Allan K, Yang BB (1999) Versican enhances locomotion of astrocytoma cells and reduces cell adhesion through its G1 domain. *J Neuropathol Exp Neurol* **58**, 597-605.

Ashkenazi H, Cao X, Motola S, Popliker M, Conti M, Tsafriri A (2005) Epidermal growth factor family members: endogenous mediators of the ovulatory response. *Endocrinology* **146**, 77-84.

Aspberg A, Miura R, Bourdoulous S, Shimonaka M, Heinegard D, Schachner M, Ruoslahti E, Yamaguchi Y (1997) The C-type lectin domains of lecticans, a family of aggregating chondroitin sulfate proteoglycans, bind tenascin-R by protein-protein interactions independent of carbohydrate moiety. *Proc Natl Acad Sci U S A* **94**, 10116-21.

Assidi M, Dufort I, Ali A, Hamel M, Algriany O, Dielemann S, Sirard MA (2008) Identification of Potential Markers of Oocyte Competence Expressed in Bovine Cumulus Cells Matured with Follicle-Stimulating Hormone and/or Phorbol Myristate Acetate In Vitro. *Biol Reprod*.

Atef A, Francois P, Christian V, Marc-Andre S (2005) The potential role of gap junction communication between cumulus cells and bovine oocytes during in vitro maturation. *Mol Reprod Dev* **71**, 358-67.

Baird DT, Brown A, Cheng L, Critchley HO, Lin S, Narvekar N, Williams AR (2003) Mifepristone: a novel estrogen-free daily contraceptive pill. *Steroids* **68**, 1099-105.

Ball GD, Leibfried ML, Lenz RW, Ax RL, Bavister BD, First NL (1983) Factors affecting successful in vitro fertilisation of bovine follicular oocytes. *Biol Reprod* **28**, 717-25.

Barnes FL, Kausche A, Tiglias J, Wood C, Wilton L, Trounson A (1996) Production of embryos from in vitro-matured primary human oocytes. *Fertil Steril* **65**, 1151-6.

Biggers JD, Whittingham DG, Donahue RP (1967) The pattern of energy metabolism in the mouse oocyte and zygote. *Proc Natl Acad Sci U S A* **58**, 560-7.

Blasiole DA, Davis RA, Attie AD (2007) The physiological and molecular regulation of lipoprotein assembly and secretion. *Mol Biosyst* **3**, 608-19.

Boerboom D, Russell DL, Richards JS, Sirois J (2003) Regulation of transcripts encoding ADAMTS-1 (a disintegrin and metalloproteinase with thrombospondin-like motifs-1) and progesterone receptor by human chorionic gonadotropin in equine preovulatory follicles. *J Mol Endocrinol* **31**, 473-85.

Borman SM, Chaffin CL, Schwinof KM, Stouffer RL, Zelinski-Wooten MB (2004) Progesterone promotes oocyte maturation, but not ovulation, in nonhuman primate follicles without a gonadotropin surge. *Biol Reprod* **71**, 366-73.

Bottazzi B, Vouret-Craviari V*, et al.* (1997) Multimer formation and ligand recognition by the long pentraxin PTX3. Similarities and differences with the short pentraxins C-reactive protein and serum amyloid P component. *J Biol Chem* **272**, 32817-23.

Brown HM, Dunning KR, Robker RL, Pritchard M, Russell DL (2006) Requirement for ADAMTS-1 in extracellular matrix remodeling during ovarian folliculogenesis and lymphangiogenesis. *Dev Biol* **300**, 699-709.

Bruckner G, Brauer K*, et al.* (1993) Perineuronal nets provide a polyanionic, glia-associated form of microenvironment around certain neurons in many parts of the rat brain. *Glia* **8**, 183-200.

Bruckner G, Grosche J, Hartlage-Rubsamen M, Schmidt S, Schachner M (2003) Region and lamina-specific distribution of extracellular matrix proteoglycans, Hyaluronan and tenascin-R in the mouse hippocampal formation. *J Chem Neuroanat* **26**, 37-50.

Buccione R, Schroeder AC, Eppig JJ (1990) Interactions between somatic cells and germ cells throughout mammalian oogenesis. *Biol Reprod* **43**, 543-7.

Bukovsky A, Chen TT, Wimalasena J, Caudle MR (1993) Cellular localisation of luteinizing hormone receptor immunoreactivity in the ovaries of immature, gonadotropin-primed and normal cycling rats. *Biol Reprod* **48**, 1367-82.

Cao J, Hymowitz M, Conner C, Bahou WF, Zucker S (2000) The propeptide domain of membrane type 1-matrix metalloproteinase acts as an intramolecular chaperone when expressed in trans with the mature sequence in COS-1 cells. *J Biol Chem* **275**, 29648-53.

Carrette O, Nemade RV, Day AJ, Brickner A, Larsen WJ (2001) TSG-6 is concentrated in the extracellular matrix of mouse cumulus oocyte complexes through Hyaluronan and inter-alpha-inhibitor binding. *Biol Reprod* **65**, 301-8.

Castillo GM, Templeton DM (1993) Subunit structure of bovine ESF (extracellular-matrix stabilizing factor(s)). A chondroitin sulfate proteoglycan with homology to human I alpha i (inter-alpha-trypsin inhibitors). *FEBS Lett* **318**, 292-6.

Cavilla JL, Kennedy CR, Byskov AG, Hartshorne GM (2008) Human immature oocytes grow during culture for IVM. *Hum Reprod* **23**, 37-45.

Chen L, Mao SJ, Larsen WJ (1992) Identification of a factor in fetal bovine serum that stabilizes the cumulus extracellular matrix. A role for a member of the inter-alpha-trypsin inhibitor family. *J Biol Chem* **267**, 12380-6.

Chen L, Mao SJ, McLean LR, Powers RW, Larsen WJ (1994) Proteins of the inter-alpha-trypsin inhibitor family stabilize the cumulus extracellular matrix through their direct binding with hyaluronic acid. *J Biol Chem* **269**, 28282-7.

Chen L, Russell PT, Larsen WJ (1993) Functional significance of cumulus expansion in the mouse: roles for the preovulatory synthesis of hyaluronic acid within the cumulus mass. *Mol Reprod Dev* **34**, 87-93.

Chen L, Zhang H, Powers RW, Russell PT, Larsen WJ (1996) Covalent linkage between proteins of the inter-alpha-inhibitor family and hyaluronic acid is mediated by a factor produced by granulosa cells. *J Biol Chem* **271**, 19409-14.

Cherr GN, Yudin AI, Katz DF (1990) Organization of the Hamster Cumulus Extracellular Matrix: A Hyaluronate-Glycoprotein Gel which Modulates Sperm Access to the Oocyte. *Develop. Growth & Differ.* **32**, 353-365.

Cillo F, Brevini TA, Antonini S, Paffoni A, Ragni G, Gandolfi F (2007) Association between human oocyte developmental competence and expression levels of some cumulus genes. *Reproduction* **134**, 645-50.

Colton SA, Pieper GM, Downs SM (2002) Altered meiotic regulation in oocytes from diabetic mice. *Biol Reprod* **67**, 220-31.

Combelles CM, Cekleniak NA, Racowsky C, Albertini DF (2002) Assessment of nuclear and cytoplasmic maturation in in-vitro matured human oocytes. *Hum Reprod* **17**, 1006-16.

Combelles CM, Fissore RA, Albertini DF, Racowsky C (2005) In vitro maturation of human oocytes and cumulus cells using a co-culture three-dimensional collagen gel system. *Hum Reprod* **20**, 1349-58.

Corps AN, Robinson AH, Movin T, Costa ML, Ireland DC, Hazleman BL, Riley GP (2004) Versican splice variant messenger RNA expression in normal human Achilles tendon and tendinopathies. *Rheumatology (Oxford)* **43**, 969-72.

Coy P, Romar R, Payton RR, McCann L, Saxton AM, Edwards JL (2005) Maintenance of meiotic arrest in bovine oocytes using the S-enantiomer of roscovitine: effects on maturation, fertilisation and subsequent embryo development in vitro. *Reproduction* **129**, 19-26.

Cross NA, Chandrasekharan S, Jokonya N, Fowles A, Hamdy FC, Buttle DJ, Eaton CL (2005) The expression and regulation of ADAMTS-1, -4, -5, -9, and -15, and TIMP-3 by TGFbeta1 in prostate cells: relevance to the accumulation of Versican. *Prostate* **63**, 269-75.

Cukurcam S, Betzendahl I, Michel G, Vogt E, Hegele-Hartung C, Lindenthal B, Eichenlaub-Ritter U (2007) Influence of follicular fluid meiosis-activating sterol on aneuploidy rate and precocious chromatid segregation in aged mouse oocytes. *Hum Reprod* **22**, 815-28.

Dalvit G, Llanes SP, Descalzo A, Insani M, Beconi M, Cetica P (2005) Effect of alpha-tocopherol and ascorbic acid on bovine oocyte in vitro maturation. *Reprod Domest Anim* **40**, 93-7.

Davis BJ, Lennard DE, Lee CA, Tiano HF, Morham SG, Wetsel WC, Langenbach R (1999) Anovulation in cyclooxygenase-2-deficient mice is restored by prostaglandin E2 and interleukin-1beta. *Endocrinology* **140**, 2685-95.

De La Fuente R, O'Brien MJ, Eppig JJ (1999) Epidermal growth factor enhances preimplantation developmental competence of maturing mouse oocytes. *Hum Reprod* **14**, 3060-8.

Delvigne A, Rozenberg S (2002) Epidemiology and prevention of ovarian hyperstimulation syndrome (OHSS): a review. *Hum Reprod Update* **8**, 559-77.

Dong J, Opresko LK, Dempsey PJ, Lauffenburger DA, Coffey RJ, Wiley HS (1999) Metalloprotease-mediated ligand release regulates autocrine signaling through the epidermal growth factor receptor. *Proc Natl Acad Sci U S A* **96**, 6235-40.

Dours-Zimmermann MT, Zimmermann DR (1994) A novel glycosaminoglycan attachment domain identified in two alternative splice variants of human Versican. *J Biol Chem* **269**, 32992-8.

Downs SM (1989) Specificity of epidermal growth factor action on maturation of the murine oocyte and cumulus oophorus in vitro. *Biol Reprod* **41**, 371-9.

Doyle KM, Russell DL, Sriraman V, Richards JS (2004b) Coordinate transcription of the ADAMTS-1 gene by luteinizing hormone and progesterone receptor. *Mol Endocrinol* **18**, 2463-78.

Dragovic RA, Ritter LJ, Schulz SJ, Amato F, Armstrong DT, Gilchrist RB (2005) Role of oocyte-secreted growth differentiation factor 9 in the regulation of mouse cumulus expansion. *Endocrinology* **146**, 2798-806.

du Cros DL, LeBaron RG, Couchman JR (1995) Association of Versican with dermal matrices and its potential role in hair follicle development and cycling. *J Invest Dermatol* **105**, 426-31.

Dunning KR, Lane M, Brown HM, Yeo C, Robker RL, Russell DL (2007) Altered composition of the cumulus-oocyte complex matrix during in vitro maturation of oocytes. *Hum Reprod* **22**, 2842-50.

Eisenbach M, Tur-Kaspa I (1999) Do human eggs attract spermatozoa? *Bioessays* **21**, 203-10.

Elvin JA, Clark AT, Wang P, Wolfman NM, Matzuk MM (1999) Paracrine actions of growth differentiation factor-9 in the mammalian ovary. *Mol Endocrinol* **13**, 1035-48.

Eppig J (2005) Mouse oocytes control metabolic co-operativity between oocytes and cumulus cells. *Reprod Fertil Dev* **17**, 1-2.

Eppig JJ (1979a) FSH stimulates hyaluronic acid synthesis by oocyte-cumulus cell complexes from mouse preovulatory follicles. *Nature* **281**, 483-4.

Eppig JJ (1979b) Gonadotropin stimulation of the expansion of cumulus oophori isolated from mice: general conditions for expansion in vitro. *J Exp Zool* **208**, 111-20.

Eppig JJ (1980) Regulation of cumulus oophorus expansion by gonadotropins in vivo and in vitro. *Biol Reprod* **23**, 545-52.

Eppig JJ (2001) Oocyte control of ovarian follicular development and function in mammals. *Reproduction* **122**, 829-38.

Eppig JJ, Freter RR, Ward-Bailey PF, Schultz RM (1983) Inhibition of oocyte maturation in the mouse: participation of cAMP, steroid hormones, and a putative maturation-inhibitory factor. *Dev Biol* **100**, 39-49.

Eppig JJ, Wigglesworth K, Pendola F, Hirao Y (1997) Murine oocytes suppress expression of luteinizing hormone receptor messenger ribonucleic acid by granulosa cells. *Biol Reprod* **56**, 976-84.

Espey LL, Yoshioka S, Russell DL, Robker RL, Fujii S, Richards JS (2000) Ovarian expression of a disintegrin and metalloproteinase with thrombospondin motifs during ovulation in the gonadotropin-primed immature rat. *Biol Reprod* **62**, 1090-5.

Evanko SP, Angello JC, Wight TN (1999) Formation of Hyaluronan- and Versican-rich pericellular matrix is required for proliferation and migration of vascular smooth muscle cells. *Arterioscler Thromb Vasc Biol* **19**, 1004-13.

Faerge I, Strejcek F, Laurincik J, Rath D, Niemann H, Schellander K, Rosenkranz C, Hyttel PM, Grondahl C (2006) The effect of FF-MAS on porcine cumulus-oocyte complex maturation, fertilisation and pronucleus formation in vitro. *Zygote* **14**, 189-99.

Familiari G, Verlengia C, Nottola SA, Renda T, Micara G, Aragona C, Zardi L, Motta PM (1996) Heterogeneous distribution of fibronectin, tenascin-C, and laminin immunoreactive material in the cumulus-corona cells surrounding mature human oocytes from IVF-ET protocols--evidence that they are composed of different subpopulations: an immunohistochemical study using scanning confocal laser and fluorescence microscopy. *Mol Reprod Dev* **43**, 392-402.

Fraser JR, Laurent TC, Laurent UB (1997) Hyaluronan: its nature, distribution, functions and turnover. *J Intern Med* **242**, 27-33.

Freimann S, Ben-Ami I, Dantes A, Ron-El R, Amsterdam A (2004a) EGF-like factor epiregulin and amphiregulin expression is regulated by gonadotropins/cAMP in human ovarian follicular cells. *Biochem Biophys Res Commun* **324**, 829-34.

Freimann S, Ben-Ami I, Hirsh L, Dantes A, Halperin R, Amsterdam A (2004b) Drug development for ovarian hyper-stimulation and anti-cancer treatment: blocking of gonadotropin signaling for epiregulin and amphiregulin biosynthesis. *Biochem Pharmacol* **68**, 989-96.

Fulop C, Kamath RV, Li Y, Otto JM, Salustri A, Olsen BR, Glant TT, Hascall VC (1997a) Coding sequence, exon-intron structure and chromosomal localisation of murine TNF-stimulated gene 6 that is specifically expressed by expanding cumulus cell-oocyte complexes. *Gene* **202**, 95-102.

Fulop C, Salustri A, Hascall VC (1997b) Coding sequence of a Hyaluronan synthase homologue expressed during expansion of the mouse cumulus-oocyte complex. *Arch Biochem Biophys* **337**, 261-6.

Fulop C, Szanto S*, et al.* (2003) Impaired cumulus mucification and female sterility in tumor necrosis factor-induced protein-6 deficient mice. *Development* **130**, 2253-61.

Gaytan F, Bellido C, Gaytan M, Morales C, Sanchez-Criado JE (2003) Differential effects of RU486 and indomethacin on follicle rupture during the ovulatory process in the rat. *Biol Reprod* **69**, 99-105.

Gershon E, Plaks V, Aharon I, Galiani D, Reizel Y, Sela-Abramovich S, Granot I, Winterhager E, Dekel N (2008) Oocyte-directed depletion of connexin43 using the Cre-LoxP system leads to subfertility in female mice. *Dev Biol* **313**, 1-12.

Gilchrist RB, Thompson JG (2007) Oocyte maturation: emerging concepts and technologies to improve developmental potential in vitro. *Theriogenology* **67**, 6-15.

Gill A, Jamnongjit M, Hammes SR (2004) Androgens promote maturation and signaling in mouse oocytes independent of transcription: a release of inhibition model for mammalian oocyte meiosis. *Mol Endocrinol* **18**, 97-104.

Gilula NB, Epstein ML, Beers WH (1978) Cell-to-cell communication and ovulation. A study of the cumulus-oocyte complex. *J Cell Biol* **78**, 58-75.

Gosden RG (2002) Oogenesis as a foundation for embryogenesis. *Mol Cell Endocrinol* **186**, 149-53.

Goud PT, Goud AP, Qian C, Laverge H, Van der Elst J, De Sutter P, Dhont M (1998) In-vitro maturation of human germinal vesicle stage oocytes: role of cumulus cells and epidermal growth factor in the culture medium. *Hum Reprod* **13**, 1638-44.

Goudet G, Belin F, Bezard J, Gerard N (1999) Intrafollicular content of luteinizing hormone receptor, alpha-inhibin, and aromatase in relation to follicular growth, estrous cycle stage, and oocyte competence for in vitro maturation in the mare. *Biol Reprod* **60**, 1120-7.

Goueffic Y, Guilluy C, Guerin P, Patra P, Pacaud P, Loirand G (2006) Hyaluronan induces vascular smooth muscle cell migration through RHAMM-mediated PI3K-dependent Rac activation. *Cardiovasc Res* **72**, 339-48.

Granot I, Dekel N (1994) Phosphorylation and expression of connexin-43 ovarian gap junction protein are regulated by luteinizing hormone. *J Biol Chem* **269**, 30502-9.

Greve T, Xu KP, Callesen H, Hyttel P (1987) In vivo development of in vitro fertilised bovine oocytes matured in vivo versus in vitro. *J In Vitro Fert Embryo Transf* **4**, 281-5.

Grondahl C, Hansen TH, Marky-Nielsen K, Ottesen JL, Hyttel P (2000) Human oocyte maturation in vitro is stimulated by meiosis-activating sterol. *Hum Reprod* **15 Suppl 5**, 3-10.

Hamamah S (2005) [Oocyte and embryo quality: is their morphology a good criterion?]. *J Gynecol Obstet Biol Reprod (Paris)* **34**, 5S38-5S41.

Hamilton SR, Fard SF*, et al.* (2007) The Hyaluronan receptors CD44 and Rhamm (CD168) form complexes with ERK1,2 that sustain high basal motility in breast cancer cells. *J Biol Chem* **282**, 16667-80.

Harris SE, Adriaens I, Leese HJ, Gosden RG, Picton HM (2007) Carbohydrate metabolism by murine ovarian follicles and oocytes grown in vitro. *Reproduction* **134**, 415-24.

Hartig W, Derouiche A, Welt K, Brauer K, Grosche J, Mader M, Reichenbach A, Bruckner G (1999) Cortical neurons immunoreactive for the potassium channel Kv3.1b subunit are predominantly surrounded by perineuronal nets presumed as a buffering system for cations. *Brain Res* **842**, 15-29.

Hashimoto S, Minami N, Yamada M, Imai H (2000) Excessive concentration of glucose during in vitro maturation impairs the developmental competence of bovine oocytes after in vitro fertilisation: relevance to intracellular reactive oxygen species and glutathione contents. *Mol Reprod Dev* **56**, 520-6.

Hernandez-Gonzalez I, Gonzalez-Robayna I, Shimada M, Wayne CM, Ochsner SA, White L, Richards JS (2006) Gene expression profiles of cumulus cell oocyte complexes during ovulation reveal cumulus cells express neuronal and immune-related genes: does this expand their role in the ovulation process? *Mol Endocrinol* **20**, 1300-21.

Hess KA, Chen L, Larsen WJ (1998) The ovarian blood follicle barrier is both charge- and size-selective in mice. *Biol Reprod* **58**, 705-11.

Hickey TE, Marrocco DL, Amato F, Ritter LJ, Norman RJ, Gilchrist RB, Armstrong DT (2005) Androgens augment the mitogenic effects of oocyte-secreted factors and growth differentiation factor 9 on porcine granulosa cells. *Biol Reprod* **73**, 825-32.

Hinkle CL, Sunnarborg SW, Loiselle D, Parker CE, Stevenson M, Russell WE, Lee DC (2004) Selective roles for tumor necrosis factor alpha-converting enzyme/ADAM17 in the shedding of the epidermal growth factor receptor ligand family: the juxtamembrane stalk determines cleavage efficiency. *J Biol Chem* **279**, 24179-88.

Hizaki H, Segi E*, et al.* (1999) Abortive expansion of the cumulus and impaired fertility in mice lacking the prostaglandin E receptor subtype EP(2). *Proc Natl Acad Sci U S A* **96**, 10501-6.

Hong SJ, Chiu PC, Lee KF, Tse JM, Ho PC, Yeung WS (2004) Establishment of a capillary-cumulus model to study the selection of sperm for fertilisation by the cumulus oophorus. *Hum Reprod* **19**, 1562-9.

Host E, Gabrielsen A, Lindenberg S, Smidt-Jensen S (2002) Apoptosis in human cumulus cells in relation to zona pellucida thickness variation, maturation stage, and cleavage of the corresponding oocyte after intracytoplasmic sperm injection. *Fertil Steril* **77**, 511-5.

Hsieh M, Conti M (2005) G-protein-coupled receptor signaling and the EGF network in endocrine systems. *Trends Endocrinol Metab* **16**, 320-6.

Hu YC, Wang PH*, et al.* (2004) Subfertility and defective folliculogenesis in female mice lacking androgen receptor. *Proc Natl Acad Sci U S A* **101**, 11209-14.

Humzah MD, Soames RW (1988) Human intervertebral disc: structure and function. *Anat Rec* **220**, 337-56.

Iruela-Arispe ML, Carpizo D, Luque A (2003) ADAMTS1: a matrix metalloprotease with angioinhibitory properties. *Ann N Y Acad Sci* **995**, 183-90.

Itano N, Kimata K (1996) Molecular cloning of human Hyaluronan synthase. *Biochem Biophys Res Commun* **222**, 816-20.

Itano N, Sawai T*, et al.* (1999) Three isoforms of mammalian Hyaluronan synthases have distinct enzymatic properties. *J Biol Chem* **274**, 25085-92.

Ito K, Shinomura T, Zako M, Ujita M, Kimata K (1995) Multiple forms of mouse PG-M, a large chondroitin sulfate proteoglycan generated by alternative splicing. *J Biol Chem* **270**, 958-65.

Jansen E, Laven JS, Dommerholt HB, Polman J, van Rijt C, van den Hurk C, Westland J, Mosselman S, Fauser BC (2004) Abnormal gene expression profiles in human ovaries from polycystic ovary syndrome patients. *Mol Endocrinol* **18**, 3050-63.

Jeansson M, Granqvist AB, Nystrom JS, Haraldsson B (2006) Functional and molecular alterations of the glomerular barrier in long-term diabetes in mice. *Diabetologia* **49**, 2200-9.

Jeansson M, Haraldsson B (2003) Glomerular size and charge selectivity in the mouse after exposure to glucosaminoglycan-degrading enzymes. *J Am Soc Nephrol* **14**, 1756-65.

Jessen TE, Odum L (2003) Role of tumour necrosis factor stimulated gene 6 (TSG-6) in the coupling of inter-alpha-trypsin inhibitor to Hyaluronan in human follicular fluid. *Reproduction* **125**, 27-31.

Joyce IM, Pendola FL, O'Brien M, Eppig JJ (2001) Regulation of prostaglandin-endoperoxide synthase 2 messenger ribonucleic acid expression in mouse granulosa cells during ovulation. *Endocrinology* **142**, 3187-97.

Kahmann JD, O'Brien R, Werner JM, Heinegard D, Ladbury JE, Campbell ID, Day AJ (2000) Localisation and characterisation of the Hyaluronan-binding site on the link module from human TSG-6. *Structure* **8**, 763-74.

Kaneko T, Saito H, Toya M, Satio T, Nakahara K, Hiroi M (2000) Hyaluronic acid inhibits apoptosis in granulosa cells via CD44. *J Assist Reprod Genet* **17**, 162-7.

Katayama T, Kusanagi Y, Kiyomura M, Ochi H, Ito M (2003) Leukocyte behaviour and permeability in the rat mesenteric microcirculation following induction of ovulation. *Hum Reprod* **18**, 1179-84.

Kawashima H, Hirose M, Hirose J, Nagakubo D, Plaas AH, Miyasaka M (2000) Binding of a large chondroitin sulfate/dermatan sulfate proteoglycan, Versican, to L-selectin, P-selectin, and CD44. *J Biol Chem* **275**, 35448-56.

Kern CB, Norris RA, Thompson RP, Argraves WS, Fairey SE, Reyes L, Hoffman S, Markwald RR, Mjaatvedt CH (2007) Versican proteolysis mediates myocardial regression during outflow tract development. *Dev Dyn* **236**, 671-83.

Kim BK, Lee SC, Kim KJ, Han CH, Kim JH (2000) In vitro maturation, fertilisation, and development of human germinal vesicle oocytes collected from stimulated cycles. *Fertil Steril* **74**, 1153-8.

Kimura N, Hoshino Y, Totsukawa K, Sato E (2007) Cellular and molecular events during oocyte maturation in mammals: molecules of cumulus-oocyte complex matrix and signalling pathways regulating meiotic progression. *Soc Reprod Fertil Suppl* **63**, 327-42.

Kimura N, Konno Y, Miyoshi K, Matsumoto H, Sato E (2002) Expression of Hyaluronan synthases and CD44 messenger RNAs in porcine cumulus-oocyte complexes during in vitro maturation. *Biol Reprod* **66**, 707-17.

Knudson CB, Knudson W (1993) Hyaluronan-binding proteins in development, tissue homeostasis, and disease. *Faseb J* **7**, 1233-41.

Kobayashi H, Sun GW, Hirashima Y, Terao T (1999) Identification of link protein during follicle development and cumulus cell cultures in rats. *Endocrinology* **140**, 3835-42.

Koo BH, Longpre JM, Somerville RP, Alexander JP, Leduc R, Apte SS (2007) Regulation of ADAMTS9 secretion and enzymatic activity by its propeptide. *J Biol Chem* **282**, 16146-54.

Koos RD (1995) Increased expression of vascular endothelial growth/permeability factor in the rat ovary following an ovulatory gonadotropin stimulus: potential roles in follicle rupture. *Biol Reprod* **52**, 1426-35.

Krisher RL (2004) The effect of oocyte quality on development. *J Anim Sci* **82 E-Suppl**, E14-23.

Kuno K, Kanada N, Nakashima E, Fujiki F, Ichimura F, Matsushima K (1997) Molecular cloning of a gene encoding a new type of metalloproteinase-disintegrin family protein with thrombospondin motifs as an inflammation associated gene. *J Biol Chem* **272**, 556-62.

Kuno K, Matsushima K (1998) ADAMTS-1 protein anchors at the extracellular matrix through the thrombospondin type I motifs and its spacing region. *J Biol Chem* **273**, 13912-7.

Kuno K, Okada Y, Kawashima H, Nakamura H, Miyasaka M, Ohno H, Matsushima K (2000) ADAMTS-1 cleaves a cartilage proteoglycan, aggrecan. *FEBS Lett* **478**, 241-5.

Kuno K, Terashima Y, Matsushima K (1999) ADAMTS-1 is an active metalloproteinase associated with the extracellular matrix. *J Biol Chem* **274**, 18821-6.

Lam X, Gieseke C, Knoll M, Talbot P (2000) Assay and importance of adhesive interaction between hamster (Mesocricetus auratus) oocyte-cumulus complexes and the oviductal epithelium. *Biol Reprod* **62**, 579-88.

LaPierre DP, Lee DY, Li SZ, Xie YZ, Zhong L, Sheng W, Deng Z, Yang BB (2007) The ability of Versican to simultaneously cause apoptotic resistance and sensitivity. *Cancer Res* **67**, 4742-50.

Larsen WJ, Wert SE, Brunner GD (1986) A dramatic loss of cumulus cell gap junctions is correlated with germinal vesicle breakdown in rat oocytes. *Dev Biol* **113**, 517-21.

Laurent TC (1995) An early look at macromolecular crowding. *Biophys Chem* **57**, 7-14.

Laurent TC, Fraser JR (1992) Hyaluronan. *Faseb J* **6**, 2397-404.

Le Du A, Kadoch IJ*, et al.* (2005) In vitro oocyte maturation for the treatment of infertility associated with polycystic ovarian syndrome: the French experience. *Hum Reprod* **20**, 420-4.

LeBaron RG, Zimmermann DR, Ruoslahti E (1992) Hyaluronate binding properties of Versican. *J Biol Chem* **267**, 10003-10.

Lee D, Pearsall RS, Das S, Dey SK, Godfrey VL, Threadgill DW (2004) Epiregulin is not essential for development of intestinal tumors but is required for protection from intestinal damage. *Mol Cell Biol* **24**, 8907-16.

Lee KS, Joo BS, Na YJ, Yoon MS, Choi OH, Kim WW (2001) Cumulus cells apoptosis as an indicator to predict the quality of oocytes and the outcome of IVF-ET. *J Assist Reprod Genet* **18**, 490-8.

Leese HJ, Barton AM (1985) Production of pyruvate by isolated mouse cumulus cells. *J Exp Zool* **234**, 231-6.

Lesley J, English NM, Gal I, Mikecz K, Day AJ, Hyman R (2002) Hyaluronan binding properties of a CD44 chimera containing the link module of TSG-6. *J Biol Chem* **277**, 26600-8.

Lim H, Paria BC, Das SK, Dinchuk JE, Langenbach R, Trzaskos JM, Dey SK (1997) Multiple female reproductive failures in cyclooxygenase 2-deficient mice. *Cell* **91**, 197-208.

Liu YJ, Xu Y, Yu Q (2005) Full-length ADAMTS-1 and the ADAMTS-1 fragments display pro- and antimetastatic activity, respectively. *Oncogene*.

Liu YJ, Xu Y, Yu Q (2006) Full-length ADAMTS-1 and the ADAMTS-1 fragments display pro- and antimetastatic activity, respectively. *Oncogene* **25**, 2452-67.

Livak KJ, Schmittgen TD (2001) Analysis of relative gene expression data using real-time quantitative PCR and the 2(-Delta Delta C(T)) Method. *Methods* **25**, 402-8.

Luetteke NC, Qiu TH, Fenton SE, Troyer KL, Riedel RF, Chang A, Lee DC (1999) Targeted inactivation of the EGF and amphiregulin genes reveals distinct roles for EGF receptor ligands in mouse mammary gland development. *Development* **126**, 2739-50.

Luque A, Carpizo DR, Iruela-Arispe ML (2003) ADAMTS1/METH1 inhibits endothelial cell proliferation by direct binding and sequestration of VEGF165. *J Biol Chem* **278**, 23656-65.

Luvoni GC, Keskintepe L, Brackett BG (1996) Improvement in bovine embryo production in vitro by glutathione-containing culture media. *Mol Reprod Dev* **43**, 437-43.

Lydon JP, DeMayo FJ, Funk CR, Mani SK, Hughes AR, Montgomery CA, Jr., Shyamala G, Conneely OM, O'Malley BW (1995) Mice lacking progesterone receptor exhibit pleiotropic reproductive abnormalities. *Genes Dev* **9**, 2266-78.

Madan P, Bridges PJ, Komar CM, Beristain AG, Rajamahendran R, Fortune JE, MacCalman CD (2003) Expression of messenger RNA for ADAMTS subtypes changes in the periovulatory follicle after the gonadotropin surge and during luteal development and regression in cattle. *Biol Reprod* **69**, 1506-14.

Marin Bivens CL, Grondahl C, Murray A, Blume T, Su YQ, Eppig JJ (2004) Meiosis-activating sterol promotes the metaphase I to metaphase II transition and preimplantation developmental competence of mouse oocytes maturing in vitro. *Biol Reprod* **70**, 1458-64.

Matsumoto K, Shionyu M, Go M, Shimizu K, Shinomura T, Kimata K, Watanabe H (2003) Distinct interaction of Versican/PG-M with Hyaluronan and link protein. *J Biol Chem* **278**, 41205-12.

Mayer G, Hamelin J, Asselin MC, Pasquato A, Marcinkiewicz E, Tang M, Tabibzadeh S, Seidah NG (2008) The regulated cell surface zymogen activation of the proprotein convertase PC5A directs the processing of its secretory substrates. *J Biol Chem* **283**, 2373-84.

McCabe M (1972) The diffusion coefficient of caffeine through agar gels containing a hyaluronic acid-protein complex. A model system for the study of the permeability of connective tissues. *Biochem J* **127**, 249-53.

McKenzie LJ, Pangas SA, Carson SA, Kovanci E, Cisneros P, Buster JE, Amato P, Matzuk MM (2004) Human cumulus granulosa cell gene expression: a predictor of fertilisation and embryo selection in women undergoing IVF. *Hum Reprod* **19**, 2869-74.

Meyer K, Palmer JW (1934) The polysaccharide of the vitreous humor. *J Biol Chem* **107**, 629-634.

Milla ME, Leesnitzer MA*, et al.* (1999) Specific sequence elements are required for the expression of functional tumor necrosis factor-alpha-converting enzyme (TACE). *J Biol Chem* **274**, 30563-70.

Mittaz L, Russell DL, Wilson T, Brasted M, Tkalcevic J, Salamonsen LA, Hertzog PJ, Pritchard MA (2004) Adamts-1 is essential for the development and function of the urogenital system. *Biol Reprod* **70**, 1096-105.

Miura R, Aspberg A, Ethell IM, Hagihara K, Schnaar RL, Ruoslahti E, Yamaguchi Y (1999) The proteoglycan lectin domain binds sulfated cell surface glycolipids and promotes cell adhesion. *J Biol Chem* **274**, 11431-8.

Mjaatvedt CH, Yamamura H, Capehart AA, Turner D, Markwald RR (1998) The Cspg2 gene, disrupted in the hdf mutant, is required for right cardiac chamber and endocardial cushion formation. *Dev Biol* **202**, 56-66.

Morawski M, Bruckner MK, Riederer P, Bruckner G, Arendt T (2004) Perineuronal nets potentially protect against oxidative stress. *Exp Neurol* **188**, 309-15.

Mueckler M (1994) Facilitative glucose transporters. *Eur J Biochem* **219**, 713-25.

Mukhopadhyay D, Asari A, Rugg MS, Day AJ, Fulop C (2004) Specificity of the tumor necrosis factor-induced protein 6-mediated heavy chain transfer from inter-alpha-trypsin inhibitor to Hyaluronan: implications for the assembly of the cumulus extracellular matrix. *J Biol Chem* **279**, 11119-28.

Mukhopadhyay D, Hascall VC, Day AJ, Salustri A, Fulop C (2001) Two distinct populations of tumor necrosis factor-stimulated gene-6 protein in the extracellular matrix of expanded mouse cumulus cell-oocyte complexes. *Arch Biochem Biophys* **394**, 173-81.

Nagyova E, Camaioni A, Prochazka R, Salustri A (2004) Covalent transfer of heavy chains of inter-alpha-trypsin inhibitor family proteins to Hyaluronan in in vivo and in vitro expanded porcine oocyte-cumulus complexes. *Biol Reprod* **71**, 1838-43.

Ochsner SA, Russell DL, Day AJ, Breyer RM, Richards JS (2003) Decreased expression of tumor necrosis factor-alpha-stimulated gene 6 in cumulus cells of the cyclooxygenase-2 and EP2 null mice. *Endocrinology* **144**, 1008-19.

Odor DL, Blandau RJ (1973) EGG transport over the fimbrial surface of the rabbit oviduct under experimental conditions. *Fertil Steril* **24**, 292-300.

Ogston AG, Sherman TF (1961) Effects of hyaluronic acid upon diffusion of solutes and flow of solvent. *J Physiol* **156**, 67-74.

Ohta N, Saito H, Kuzumaki T, Takahashi T, Ito MM, Saito T, Nakahara K, Hiroi M (1999) Expression of CD44 in human cumulus and mural granulosa cells of individual patients in in-vitro fertilisation programmes. *Mol Hum Reprod* **5**, 22-8.

Olin AI, Morgelin M, Sasaki T, Timpl R, Heinegard D, Aspberg A (2001) The proteoglycans aggrecan and Versican form networks with fibulin-2 through their lectin domain binding. *J Biol Chem* **276**, 1253-61.

Ozawa M, Nagai T*, et al.* (2008) Comparison between effects of 3-isobutyl-1-methylxanthine and FSH on gap junctional communication, LH-receptor expression, and meiotic maturation of cumulus-oocyte complexes in pigs. *Mol Reprod Dev* **75**, 857-66.

Papanikolaou EG, Pozzobon C, Kolibianakis EM, Camus M, Tournaye H, Fatemi HM, Van Steirteghem A, Devroey P (2006) Incidence and prediction of ovarian hyperstimulation syndrome in women undergoing gonadotropin-releasing hormone antagonist in vitro fertilisation cycles. *Fertil Steril* **85**, 112-20.

Park JY, Su YQ, Ariga M, Law E, Jin SL, Conti M (2004) EGF-like growth factors as mediators of LH action in the ovulatory follicle. *Science* **303**, 682-4.

Paulson S, Sylven B, Hirsch C, Snellman O (1951) Biophysical and physiological investigations on cartilage and other mesenchymal tissues. III. The diffusion rate of various substances in normal bovine Nucleus Pulposus. *Biochim Biophys Acta* **7**, 207-13.

Pelletier G (2000) Localisation of androgen and estrogen receptors in rat and primate tissues. *Histol Histopathol* **15**, 1261-70.

Peng XR, Hsueh AJ, LaPolt PS, Bjersing L, Ny T (1991) Localisation of luteinizing hormone receptor messenger ribonucleic acid expression in ovarian cell types during follicle development and ovulation. *Endocrinology* **129**, 3200-7.

Pfaff M, McLane MA, Beviglia L, Niewiarowski S, Timpl R (1994) Comparison of disintegrins with limited variation in the RGD loop in their binding to purified integrins alpha IIb beta 3, alpha V beta 3 and alpha 5 beta 1 and in cell adhesion inhibition. *Cell Adhes Commun* **2**, 491-501.

Philipson LH, Schwartz NB (1984) Subcellular localisation of hyaluronate synthetase in oligodendroglioma cells. *J Biol Chem* **259**, 5017-23.

Porter S, Clark IM, Kevorkian L, Edwards DR (2005) The ADAMTS metalloproteinases. *Biochem J* **386**, 15-27.

Powers RW, Chen L, Russell PT, Larsen WJ (1995) Gonadotropin-stimulated regulation of blood-follicle barrier is mediated by nitric oxide. *Am J Physiol* **269**, E290-8.

Protin U, Schweighoffer T, Jochum W, Hilberg F (1999) CD44-deficient mice develop normally with changes in subpopulations and recirculation of lymphocyte subsets. *J Immunol* **163**, 4917-23.

Recklies AD, White C, Melching L, Roughley PJ (2001) Differential regulation and expression of Hyaluronan synthases in human articular chondrocytes, synovial cells and osteosarcoma cells. *Biochem J* **354**, 17-24.

Reinblatt SL, Buckett W (2008) In vitro maturation for patients with polycystic ovary syndrome. *Semin Reprod Med* **26**, 121-6.

Reitsma S, Slaaf DW, Vink H, van Zandvoort MA, oude Egbrink MG (2007) The endothelial glycocalyx: composition, functions, and visualization. *Pflugers Arch* **454**, 345-59.

Relucenti M, Heyn R, Correr S, Familiari G (2005) Cumulus oophorus extracellular matrix in the human oocyte: a role for adhesive proteins. *Ital J Anat Embryol* **110**, 219-24.

Ricciardelli C, Russell DL, Ween MP, Mayne K, Suwiwat S, Byers S, Marshall VR, Tilley WD, Horsfall DJ (2007) Formation of Hyaluronan- and Versican-rich pericellular matrix by prostate cancer cells promotes cell motility. *J Biol Chem* **282**, 10814-25.

Richards JS, Hernandez-Gonzalez I*, et al.* (2005) Regulated expression of ADAMTS family members in follicles and cumulus oocyte complexes: evidence for specific and redundant patterns during ovulation. *Biol Reprod* **72**, 1241-55.

Richards JS, Russell DL, Ochsner S, Espey LL (2002) Ovulation: new dimensions and new regulators of the inflammatory-like response. *Annu Rev Physiol* **64**, 69-92.

Rienzi L, Ubaldi FM*, et al.* (2008) Significance of metaphase II human oocyte morphology on ICSI outcome. *Fertil Steril*.

Rizos D, Ward F, Duffy P, Boland MP, Lonergan P (2002) Consequences of bovine oocyte maturation, fertilisation or early embryo development in vitro versus in vivo: implications for blastocyst yield and blastocyst quality. *Mol Reprod Dev* **61**, 234-48.

Robert C, Gagne D, Lussier JG, Bousquet D, Barnes FL, Sirard MA (2003) Presence of LH receptor mRNA in granulosa cells as a potential marker of oocyte developmental competence and characterisation of the bovine splicing isoforms. *Reproduction* **125**, 437-46.

Robker RL, Russell DL, Espey LL, Lydon JP, O'Malley BW, Richards JS (2000) Progesterone-regulated genes in the ovulation process: ADAMTS-1 and cathepsin L proteases. *Proc Natl Acad Sci U S A* **97**, 4689-94.

Rodriguez-Manzaneque JC, Milchanowski AB, Dufour EK, Leduc R, Iruela-Arispe ML (2000) Characterisation of METH-1/ADAMTS1 processing reveals two distinct active forms. *J Biol Chem* **275**, 33471-9.

Romar R, Funahashi H (2006) In vitro maturation and fertilisation of porcine oocytes after a 48 h culture in roscovitine, an inhibitor of p34cdc2/cyclin B kinase. *Anim Reprod Sci* **92**, 321-33.

Rugg MS, Willis AC, Mukhopadhyay D, Hascall VC, Fries E, Fulop C, Milner CM, Day AJ (2005) Characterisation of complexes formed between TSG-6 and inter-alpha-inhibitor that act as intermediates in the covalent transfer of heavy chains onto Hyaluronan. *J Biol Chem* **280**, 25674-86.

Ruoslahti E, Yamaguchi Y (1991) Proteoglycans as modulators of growth factor activities. *Cell* **64**, 867-9.

Russell DL, Doyle KM, Ochsner SA, Sandy JD, Richards JS (2003a) Processing and localisation of ADAMTS-1 and proteolytic cleavage of Versican during cumulus matrix expansion and ovulation. *J Biol Chem* **278**, 42330-9.

Russell DL, Ochsner SA, Hsieh M, Mulders S, Richards JS (2003b) Hormone-regulated expression and localisation of Versican in the rodent ovary. *Endocrinology* **144**, 1020-31.

Russell DL, Pritchard M, Brown H (2005) Oocyte ovulation and oviductal transport: The importance of extracellular, matrix and proteolytic activity in the cumulus complex. *Biol Reprod*, **Sp. Iss. SI**, 110-110.

Russell DL, Robker RL (2007) Molecular mechanisms of ovulation: co-ordination through the cumulus complex. *Hum Reprod Update* **13**, 289-312.

Russell DL, Salustri A (2006) Extracellular matrix of the cumulus-oocyte complex. *Semin Reprod Med* **24**, 217-27.

Sadler SE, Jacobs ND (2004) Stimulation of Xenopus laevis oocyte maturation by methyl-beta-cyclodextrin. *Biol Reprod* **70**, 1685-92.

Saito H, Kaneko T, Takahashi T, Kawachiya S, Saito T, Hiroi M (2000) Hyaluronan in follicular fluids and fertilisation of oocytes. *Fertil Steril* **74**, 1148-52.

Saito T, Hiroi M, Kato T (1994) Development of glucose utilization studied in single oocytes and preimplantation embryos from mice. *Biol Reprod* **50**, 266-70.

Sakko AJ, Ricciardelli C, Mayne K, Suwiwat S, LeBaron RG, Marshall VR, Tilley WD, Horsfall DJ (2003) Modulation of prostate cancer cell attachment to matrix by Versican. *Cancer Res* **63**, 4786-91.

Salier JP, Rouet P, Raguenez G, Daveau M (1996) The inter-alpha-inhibitor family: from structure to regulation. *Biochem J* **315 (Pt 1)**, 1-9.

Salustri A, Garlanda C*, et al.* (2004) PTX3 plays a key role in the organization of the cumulus oophorus extracellular matrix and in in vivo fertilisation. *Development* **131**, 1577-86.

Salustri A, Yanagishita M, Hascall VC (1989) Synthesis and accumulation of hyaluronic acid and proteoglycans in the mouse cumulus cell-oocyte complex during follicle-stimulating hormone-induced mucification. *J Biol Chem* **264**, 13840-7.

Salustri A, Yanagishita M, Underhill CB, Laurent TC, Hascall VC (1992) Localisation and synthesis of hyaluronic acid in the cumulus cells and mural granulosa cells of the preovulatory follicle. *Dev Biol* **151**, 541-51.

Sandy JD, Westling J*, et al.* (2001) Versican V1 proteolysis in human aorta in vivo occurs at the Glu441-Ala442 bond, a site that is cleaved by recombinant ADAMTS-1 and ADAMTS-4. *J Biol Chem* **276**, 13372-8.

Sanggaard KW, Karring H, Valnickova Z, Thogersen IB, Enghild JJ (2005) The TSG-6 and I alpha I interaction promotes a transesterification cleaving the protein-glycosaminoglycan-protein (PGP) cross-link. *J Biol Chem* **280**, 11936-42.

Sato H, Kajikawa S*, et al.* (2001) Impaired fertility in female mice lacking urinary trypsin inhibitor. *Biochem Biophys Res Commun* **281**, 1154-60.

Scarchilli L, Camaioni A*, et al.* (2007) PTX3 interacts with inter-alpha-trypsin inhibitor: implications for Hyaluronan organization and cumulus oophorus expansion. *J Biol Chem* **282**, 30161-70.

Schmits R, Filmus J*, et al.* (1997) CD44 regulates hematopoietic progenitor distribution, granuloma formation, and tumorigenicity. *Blood* **90**, 2217-33.

Schoenfelder M, Einspanier R (2003) Expression of Hyaluronan synthases and corresponding Hyaluronan receptors is differentially regulated during oocyte maturation in cattle. *Biol Reprod* **69**, 269-77.

Sekiguchi T, Mizutani T, Yamada K, Kajitani T, Yazawa T, Yoshino M, Miyamoto K (2004) Expression of epiregulin and amphiregulin in the rat ovary. *J Mol Endocrinol* **33**, 281-91.

Sela-Abramovich S, Chorev E, Galiani D, Dekel N (2005) Mitogen-activated protein kinase mediates luteinizing hormone-induced breakdown of communication and oocyte maturation in rat ovarian follicles. *Endocrinology* **146**, 1236-44.

Seyfried NT, Day AJ, Almond A (2006) Experimental evidence for all-or-none cooperative interactions between the G1-domain of Versican and multivalent Hyaluronan oligosaccharides. *Matrix Biol* **25**, 14-9.

Sheng W, Wang G*, et al.* (2005) The roles of Versican V1 and V2 isoforms in cell proliferation and apoptosis. *Mol Biol Cell* **16**, 1330-40.

Shimada M, Yanai Y, Okazaki T, Noma N, Kawashima I, Mori T, Richards JS (2008) Hyaluronan fragments generated by sperm-secreted hyaluronidase stimulate cytokine/chemokine production via the TLR2 and TLR4 pathway in cumulus cells of ovulated COCs, which may enhance fertilisation. *Development*.

Shindo T, Kurihara H*, et al.* (2000) ADAMTS-1: a metalloproteinase-disintegrin essential for normal growth, fertility, and organ morphology and function. *J Clin Invest* **105**, 1345-52.

Shinomura T, Nishida Y, Ito K, Kimata K (1993) cDNA cloning of PG-M, a large chondroitin sulfate proteoglycan expressed during chondrogenesis in chick limb buds. Alternative spliced multiforms of PG-M and their relationships to Versican. *J Biol Chem* **268**, 14461-9.

Shinomura T, Zako M, Ito K, Ujita M, Kimata K (1995) The gene structure and organization of mouse PG-M, a large chondroitin sulfate proteoglycan. Genomic background for the generation of multiple PG-M transcripts. *J Biol Chem* **270**, 10328-33.

Shyjan AM, Heldin P, Butcher EC, Yoshino T, Briskin MJ (1996) Functional cloning of the cDNA for a human Hyaluronan synthase. *J Biol Chem* **271**, 23395-9.

Sirard MA, Richard F, Blondin P, Robert C (2006) Contribution of the oocyte to embryo quality. *Theriogenology* **65**, 126-36.

Sirois J, Richards JS (1992) Purification and characterisation of a novel, distinct isoform of prostaglandin endoperoxide synthase induced by human chorionic gonadotropin in granulosa cells of rat preovulatory follicles. *J Biol Chem* **267**, 6382-8.

Smith DM, Tenney DY (1980) Effects of steroids on mouse oocyte maturation in vitro. *J Reprod Fertil* **60**, 331-8.

Somfai T, Kikuchi K, Onishi A, Iwamoto M, Fuchimoto D, Papp AB, Sato E, Nagai T (2004) Relationship between the morphological changes of somatic compartment and the kinetics of nuclear and cytoplasmic maturation of oocytes during in vitro maturation of porcine follicular oocytes. *Mol Reprod Dev* **68**, 484-91.

Spicer AP, McDonald JA (1998) Characterisation and molecular evolution of a vertebrate Hyaluronan synthase gene family. *J Biol Chem* **273**, 1923-32.

Spicer AP, Seldin MF*, et al.* (1997) Chromosomal localisation of the human and mouse Hyaluronan synthase genes. *Genomics* **41**, 493-7.

Spivak-Kroizman T, Lemmon MA*, et al.* (1994) Heparin-induced oligomerization of FGF molecules is responsible for FGF receptor dimerization, activation, and cell proliferation. *Cell* **79**, 1015-24.

Su YQ, Sugiura K, Wigglesworth K, O'Brien MJ, Affourtit JP, Pangas SA, Matzuk MM, Eppig JJ (2008) Oocyte regulation of metabolic cooperativity between mouse cumulus cells and oocytes: BMP15 and GDF9 control cholesterol biosynthesis in cumulus cells. *Development* **135**, 111-21.

Su YQ, Wu X, O'Brien MJ, Pendola FL, Denegre JN, Matzuk MM, Eppig JJ (2004) Synergistic roles of BMP15 and GDF9 in the development and function of the oocyte-cumulus cell complex in mice: genetic evidence for an oocyte-granulosa cell regulatory loop. *Dev Biol* **276**, 64-73.

Suga A, Hikasa H, Taira M (2006) Xenopus ADAMTS1 negatively modulates FGF signaling independent of its metalloprotease activity. *Dev Biol* **295**, 26-39.

Sugiura K, Pendola FL, Eppig JJ (2005) Oocyte control of metabolic cooperativity between oocytes and companion granulosa cells: energy metabolism. *Dev Biol* **279**, 20-30.

Sun GW, Kobayashi H, Suzuki M, Kanayama N, Terao T (2002) Link protein as an enhancer of cumulus cell-oocyte complex expansion. *Mol Reprod Dev* **63**, 223-31.

Sun GW, Kobayashi H, Suzuki M, Kanayama N, Terao T (2003) Follicle-stimulating hormone and insulin-like growth factor I synergistically induce up-regulation of cartilage link protein (Crtl1) via activation of phosphatidylinositol-dependent kinase/Akt in rat granulosa cells. *Endocrinology* **144**, 793-801.

Sutton ML, Gilchrist RB, Thompson JG (2003) Effects of in-vivo and in-vitro environments on the metabolism of the cumulus-oocyte complex and its influence on oocyte developmental capacity. *Hum Reprod Update* **9**, 35-48.

Sutton-McDowall ML, Gilchrist RB, Thompson JG (2004) Cumulus expansion and glucose utilisation by bovine cumulus-oocyte complexes during in vitro maturation: the influence of glucosamine and follicle-stimulating hormone. *Reproduction* **128**, 313-9.

Sutton-McDowall ML, Gilchrist RB, Thompson JG (2005) Effect of hexoses and gonadotrophin supplementation on bovine oocyte nuclear maturation during in vitro maturation in a synthetic follicle fluid medium. *Reprod Fertil Dev* **17**, 407-15.

Sutton-McDowall ML, Mitchell M, Cetica P, Dalvit G, Pantaleon M, Lane M, Gilchrist RB, Thompson JG (2006) Glucosamine supplementation during in vitro maturation inhibits subsequent embryo development: possible role of the hexosamine pathway as a regulator of developmental competence. *Biol Reprod* **74**, 881-8.

Szoltys M, Slomczynska M, Tabarowski Z (2003) Immunohistochemical localisation of androgen receptor in rat oocytes. *Folia Histochem Cytobiol* **41**, 59-64.

Sztrolovics R, Grover J, Cs-Szabo G, Shi SL, Zhang Y, Mort JS, Roughley PJ (2002) The characterisation of Versican and its message in human articular cartilage and intervertebral disc. *J Orthop Res* **20**, 257-66.

Tanaka Y, Adams DH, Hubscher S, Hirano H, Siebenlist U, Shaw S (1993) T-cell adhesion induced by proteoglycan-immobilized cytokine MIP-1 beta. *Nature* **361**, 79-82.

Thompson JG, Gardner DK, Pugh PA, McMillan WH, Tervit HR (1995) Lamb birth weight is affected by culture system utilized during in vitro pre-elongation development of ovine embryos. *Biol Reprod* **53**, 1385-91.

Thompson JG, Lane M, Gilchrist RB (2007) Metabolism of the bovine cumulus-oocyte complex and influence on subsequent developmental competence. *Soc Reprod Fertil Suppl* **64**, 179-90.

Tirone E, D'Alessandris C, Hascall VC, Siracusa G, Salustri A (1997) Hyaluronan synthesis by mouse cumulus cells is regulated by interactions between follicle-stimulating hormone (or epidermal growth factor) and a soluble oocyte factor (or transforming growth factor beta1). *J Biol Chem* **272**, 4787-94.

Tolg C, Hamilton SR, Nakrieko KA, Kooshesh F, Walton P, McCarthy JB, Bissell MJ, Turley EA (2006) Rhamm-/- fibroblasts are defective in CD44-mediated ERK1,2 motogenic signaling, leading to defective skin wound repair. *J Cell Biol* **175**, 1017-28.

Trounson A, Anderiesz C, Jones G (2001) Maturation of human oocytes in vitro and their developmental competence. *Reproduction* **121**, 51-75.

Tullet JM, Pocock V, Steel JH, White R, Milligan S, Parker MG (2005) Multiple signaling defects in the absence of RIP140 impair both cumulus expansion and follicle rupture. *Endocrinology* **146**, 4127-37.

Ujita M, Shinomura T, Ito K, Kitagawa Y, Kimata K (1994) Expression and binding activity of the carboxyl-terminal portion of the core protein of PG-M, a large chondroitin sulfate proteoglycan. *J Biol Chem* **269**, 27603-9.

Usami Y, Fujimura Y, Miura S, Shima H, Yoshida E, Yoshioka A, Hirano K, Suzuki M, Titani K (1994) A 28 kDa-protein with disintegrin-like structure (jararhagin-C) purified from Bothrops jararaca venom inhibits collagen- and ADP-induced platelet aggregation. *Biochem Biophys Res Commun* **201**, 331-9.

Van Soom A, Tanghe S, De Pauw I, Maes D, de Kruif A (2002) Function of the cumulus oophorus before and during mammalian fertilisation. *Reprod Domest Anim* **37**, 144-51.

Vanderhyden BC, Caron PJ, Buccione R, Eppig JJ (1990) Developmental pattern of the secretion of cumulus expansion-enabling factor by mouse oocytes and the role of oocytes in promoting granulosa cell differentiation. *Dev Biol* **140**, 307-17.

Varani S, Elvin JA, Yan C, DeMayo J, DeMayo FJ, Horton HF, Byrne MC, Matzuk MM (2002) Knockout of pentraxin 3, a downstream target of growth differentiation factor-9, causes female subfertility. *Mol Endocrinol* **16**, 1154-67.

Vazquez F, Hastings G, Ortega MA, Lane TF, Oikemus S, Lombardo M, Iruela-Arispe ML (1999) METH-1, a human ortholog of ADAMTS-1, and METH-2 are members of a new family of proteins with angio-inhibitory activity. *J Biol Chem* **274**, 23349-57.

Wang Q, Sun QY (2007) Evaluation of oocyte quality: morphological, cellular and molecular predictors. *Reprod Fertil Dev* **19**, 1-12.

Wang WH, Gill J (2004) In vitro maturation and in vitro fertilisation of human oocytes. *Methods Mol Biol* **253**, 235-53.

Weigel PH, Hascall VC, Tammi M (1997) Hyaluronan synthases. *J Biol Chem* **272**, 13997-4000.

Weissman B, Meyer K (1954) The structure of hyalobiuronic acid and of hyaluronic acid from umbilical cord. *J Am Chem Soc* **76**, 1753-1757.

White R, Leonardsson G, Rosewell I, Ann Jacobs M, Milligan S, Parker M (2000) The nuclear receptor co-repressor nrip1 (RIP140) is essential for female fertility. *Nat Med* **6**, 1368-74.

Wight TN, Merrilees MJ (2004) Proteoglycans in atherosclerosis and restenosis: key roles for Versican. *Circ Res* **94**, 1158-67.

Wolfsberg TG, White JM (1996) ADAMs in fertilisation and development. *Dev Biol* **180**, 389-401.

Wong WY, Richards JS (1992) Induction of prostaglandin H synthase in rat preovulatory follicles by gonadotropin-releasing hormone. *Endocrinology* **130**, 3512-21.

Wu Y, Chen L, Cao L, Sheng W, Yang BB (2004) Overexpression of the C-terminal PG-M/Versican domain impairs growth of tumor cells by intervening in the interaction between epidermal growth factor receptor and beta1-integrin. *J Cell Sci* **117**, 2227-37.

Wu Y, Chen L, Zheng PS, Yang BB (2002) beta 1-Integrin-mediated glioma cell adhesion and free radical-induced apoptosis are regulated by binding to a C-terminal domain of PG-M/Versican. *J Biol Chem* **277**, 12294-301.

Wu Y, Wu J, Lee DY, Yee A, Cao L, Zhang Y, Kiani C, Yang BB (2005a) Versican protects cells from oxidative stress-induced apoptosis. *Matrix Biol* **24**, 3-13.

Wu Y, Zhang Y*, et al.* (2001) Identification of the motif in Versican G3 domain that plays a dominant-negative effect on astrocytoma cell proliferation through inhibiting Versican secretion and binding. *J Biol Chem* **276**, 14178-86.

Wu YJ, La Pierre DP, Wu J, Yee AJ, Yang BB (2005b) The interaction of Versican with its binding partners. *Cell Res* **15**, 483-94.

Xiang YY, Dong H, Wan Y, Li J, Yee A, Yang BB, Lu WY (2006) Versican G3 domain regulates neurite growth and synaptic transmission of hippocampal neurons by activation of epidermal growth factor receptor. *J Biol Chem* **281**, 19358-68.

Yamagata M, Saga S, Kato M, Bernfield M, Kimata K (1993) Selective distributions of proteoglycans and their ligands in pericellular matrix of cultured fibroblasts. Implications for their roles in cell-substratum adhesion. *J Cell Sci* **106 (Pt 1)**, 55-65.

Yamagata M, Suzuki S, Akiyama SK, Yamada KM, Kimata K (1989) Regulation of cell-substrate adhesion by proteoglycans immobilized on extracellular substrates. *J Biol Chem* **264**, 8012-8.

Yamaguchi Y (2000) Lecticans: organizers of the brain extracellular matrix. *Cell Mol Life Sci* **57**, 276-89.

Yang BL, Zhang Y, Cao L, Yang BB (1999) Cell adhesion and proliferation mediated through the G1 domain of Versican. *J Cell Biochem* **72**, 210-20.

Yokoo M, Miyahayashi Y, Naganuma T, Kimura N, Sasada H, Sato E (2002) Identification of hyaluronic acid-binding proteins and their expressions in porcine cumulus-oocyte complexes during in vitro maturation. *Biol Reprod* **67**, 1165-71.

Yoshioka S, Ochsner S, Russell DL, Ujioka T, Fujii S, Richards JS, Espey LL (2000) Expression of tumor necrosis factor-stimulated gene-6 in the rat ovary in response to an ovulatory dose of gonadotropin. *Endocrinology* **141**, 4114-9.

Yuan YQ, Van Soom A, Leroy JL, Dewulf J, Van Zeveren A, de Kruif A, Peelman LJ (2005) Apoptosis in cumulus cells, but not in oocytes, may influence bovine embryonic developmental competence. *Theriogenology* **63**, 2147-63.

Yudin AI, Cherr GN, Katz DF (1988) Structure of the cumulus matrix and zona pellucida in the golden hamster: a new view of sperm interaction with oocyte-associated extracellular matrices. *Cell Tissue Res* **251**, 555-64.

Zako M, Shinomura T, Ujita M, Ito K, Kimata K (1995) Expression of PG-M(V3), an alternatively spliced form of PG-M without a chondroitin sulfate attachment in region in mouse and human tissues. *J Biol Chem* **270**, 3914-8.

Zhang X, Jafari N, Barnes RB, Confino E, Milad M, Kazer RR (2005) Studies of gene expression in human cumulus cells indicate pentraxin 3 as a possible marker for oocyte quality. *Fertil Steril* **83 Suppl 1**, 1169-79.

Zhang Y, Cao L, Yang BL, Yang BB (1998) The G3 domain of Versican enhances cell proliferation via epidermial growth factor-like motifs. *J Biol Chem* **273**, 21342-51.

Zhao M, Yoneda M, Ohashi Y, Kurono S, Iwata H, Ohnuki Y, Kimata K (1995) Evidence for the covalent binding of SHAP, heavy chains of inter-alpha-trypsin inhibitor, to Hyaluronan. *J Biol Chem* **270**, 26657-63.

Zhuo L, Yoneda M, Zhao M, Yingsung W, Yoshida N, Kitagawa Y, Kawamura K, Suzuki T, Kimata K (2001) Defect in SHAP-Hyaluronan complex causes severe female infertility. A study by inactivation of the bikunin gene in mice. *J Biol Chem* **276**, 7693-6.

Zimmermann DR, Ruoslahti E (1989) Multiple domains of the large fibroblast proteoglycan, Versican. *Embo J* **8**, 2975-81.

Chapter 8

Publication arising from this thesis

Dunning, K.R., Lane, M., Brown, H.M., Yeo, C., Robker, R.L. and Russell, D.L. (2007) Altered composition of the cumulus-oocyte complex matrix during in vitro maturation of oocytes.
Human Reproduction, v.22 (11) pp. 2842-2850, November 2007